SEISMIC ANALYSIS OF CAST-IN-SITU CONCRETE DIAPHRAGM WITH OPENING ADJACENT TO SHEAR WALL IN WALL-FRAME STRUCTURAL SYSTEM

A.K.M.MAHMUD-UL-HASAN

MASTER OF SCIENCE IN CIVIL ENGINEERING (STRUCTURAL)

DEPARTMENT OF CIVIL ENGINEERING
BANGLADESH UNIVERSITY OF ENGINEERING AND TECHNOLOGY
DHAKA, BANGLADESH

MARCH, 2019

SEISMIC ANALYSIS OF CAST-IN-SITU CONCRETE DIAPHRAGM WITH OPENING ADJACENT TO SHEAR WALL IN WALL-FRAME STRUCTURAL SYSTEM

by

A.K.M.MAHMUD-UL-HASAN
Student No. 0413042311 P

A thesis submitted to the Department of Civil Engineering, Bangladesh University of Engineering and Technology (BUET), Dhaka in partial fulfillment of the requirements for the degree of

MASTER OF SCIENCE IN CIVIL ENGINEERING (STRUCTURAL)

DEPARTMENT OF CIVIL ENGINEERING
BANGLADESH UNIVERSITY OF ENGINEERING AND TECHNOLOGY
DHAKA, BANGLADESH

MARCH, 2019

The thesis titled "**SEISMIC ANALYSIS OF CAST-IN-SITU CONCRETE DIAPHRAGM WITH OPENING ADJACENT TO SHEAR WALL IN WALL-FRAME STRUCTURAL SYSTEM**" submitted by A.K.M.Mahmud-Ul-Hasan, Roll No.0413042311P, Session: April 2013, has been accepted as satisfactory in partial fulfillment of the requirement for the degree of **Master of Science in Civil Engineering (Structural)** on 28th March, 2019.

BOARD OF EXAMINERS

Dr. Raquib Ahsan — **Chairman**
Professor (Supervisor)
Department of Civil Engineering,
BUET, Dhaka.

Dr. Ahsanul Kabir — **Member**
Professor and Head (Ex-officio)
Department of Civil Engineering,
BUET, Dhaka.

Dr. Khan Mahmud Amanat — **Member**
Professor
Department of Civil Engineering,
BUET, Dhaka.

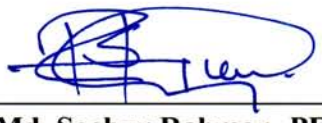

Dr. Md. Soebur Rahman, PEng — **Member**
Major & Associate Professor (External)
Department of Civil Engineering,
MIST, Mirpur Cantonment, Dhaka

DECLARATION

It is hereby declared that except for the contents where specific references have been made to the work of others, the study contained in this thesis is the result of investigation carried out by the author. No part of this thesis has been submitted to any other University or other educational establishment for a Degree, Diploma or other qualification.

Signature of the Candidate

A.K.M.MAHMUD-UL-HASAN

DEDICATION

This thesis is dedicated to my parents and teachers

ACKNOWLEDGMENT

Alhamdulillah. All praises to Allah (SWT) who bestowed His Mercy upon me to complete this work successfully.

I would like to take this opportunity to express my profound gratitude and deep regard to my thesis supervisor Professor Dr. Raquib Ahsan, Department of Civil Engineering, Bangladesh University of Engineering and Technology (BUET) for his exemplary guidance, quick response and constant encouragement throughout the duration of the research. His valuable suggestions and enthusiastic supervision were of immense help throughout my research work. Working under him was an extremely knowledgeable experience for me.

I wish to express my gratitude and heartiest thanks to respected defense committee members Prof. Dr. Ahsanul Kabir, Prof. Dr. Khan Mahmud Amanat and Associate Prof. Dr. Md. Soebur Rahman for their valuable advice and help in reviewing this thesis.

A very special debt of deep gratitude is offered to the author's parents and sisters for their continuous encouragement and cooperation during this study.

ABSTRACT

Opening in cast-in-situ concrete diaphragm such as stairs, elevator cores, atriums, skylights, etc are very common in reinforced concrete buildings. Diaphragm opening adjacent to shear wall can cause high in-plane stress concentration around diaphragm opening during earthquake.

The purpose of this research is to examine the limit of extent of diaphragm opening adjacent to shear wall with respect to diaphragm discontinuity criteria of ASCE 7-10 for wall-frame structural system for some specific layouts of shear walls in a 3-storied building. The worst orientation of diaphragm opening adjacent to shear wall which have the most adverse effect on local seismic demands of diaphragm locations near diaphragm opening is to be determined with the help of in-plane stress analyses of diaphragm for some specific cases. Possible locations near diaphragm opening adjacent to shear wall where cracking and yielding of diaphragm occur during seismic loading is to be identified in this research work.

3D FEM models of dual system buildings are adopted where diaphragm is modeled with nonlinear layer shell elements. Equivalent lateral force analysis, modal response spectrum analysis, modal linear response history analysis, diaphragm design force procedure as per section 12.10.1.1 of ASCE 7-10 and pushover analysis as per ASCE 41-13 have been performed by considering unidirectional and orthogonal application of seismic loading in order to extract in-plane force/stress data from nonlinear layered shells. In-plane stress data have been analyzed statistically with standard deviation and Z-score using the concept of Gaussian distribution.

In-plane stresses in diaphragm around diaphragm opening adjacent to shear wall form pushover analyses as per ASCE 41-13 are higher than linear elastic and linear dynamic diaphragm design force procedures of ASCE 7-10. Statistical analyses shows that the building model with diaphragm opening adjacent to an interior shear wall experiences high in-plane stress around diaphragm discontinuity compared to other building models. Although open areas in diaphragm (11% or 14% of the diaphragm gross area) of models are not considered as diaphragm discontinuity according to ASCE 7-10, linear elastic diaphragm design force procedures as per ASCE 7-10 underestimates in-plane shear forces in diaphragm locations around diaphragm opening adjacent to shear wall compared to in-plane shear forces from pushover analyses according to ASCE 41-13. Hence pushover analysis should be performed when diaphragm opening is present adjacent to shear wall. Diaphragm thickness determined from regular design procedure in these locations may be suitable for gravity load transfer but may not be suitable to transfer in-plane shear stress to the seismic force resisting vertical elements. Guidelines and seismic requirements should be developed for structures with diaphragm opening adjacent to shear wall assigned to Seismic Design Categories C.

Table of Contents

NOTATION

A_{cv} Gross area of concrete section of diaphragms in the direction of shear force

A_g Gross cross sectional area of chord or collector

A_s Tension reinforcement of chord or collector

C_d Deflection Amplification Factor

C_u Compressive force in collector

F_{11} Direct force per unit length acting at the mid-surface of the element on the positive and negative 1 faces in the 1-axis direction

F_{22} Direct force per unit length acting at the mid-surface of the element on the positive and negative 2 faces in the 2-axis direction

F_{12} Shearing force per unit length acting at the mid-surface of the element on the positive and negative 1 faces in the 2-axis direction

Fa Short Period Site Coefficient

F_{px} Diaphragm design force

F_i Design force from Equivalent lateral force analysis applied to level i

Fv Long Period Site Coefficient

F_x Story shear at story level from seismic forces

f_c' specified compressive strength of concrete

f_y yield strength of Reinforcing bar

f_r the modulus of rupture

I_e Seismic Importance Factor

M_{11} Direct moment per unit length acting at the mid-surface of the element on the positive and negative 1 faces about the 2-axis.

M_{22} Direct moment per unit length acting at the mid-surface of the element on the positive and negative 2 faces about the 1-axis.

M_{12} Twisting moment per unit length acting at the mid-surface of the element on the positive and negative 1 faces about the 1-axis, and acting on the positive and negative 2 faces about the 2-axis

P_0 Compressive strength of collector

R Response Modification Factor

S_s Short Period Acceleration

S_{11} the direct stress (force per unit area) acting on the positive and negative 1 faces in the 1-axis direction

S_{22} the direct stress (force per unit area) acting on the positive and negative 2 faces in the 2-axis direction

S_{33} the direct stress (force per unit area) acting on the positive and negative 3 faces in the 3-axis direction

S_{12} the shearing stress (force per unit area) acting on the positive and negative 1 faces in the 2-axis direction and acting on the positive and negative 2 faces in the 1-axis direction

S_l Long Period Acceleration

S_{DS} Short Period Spectral Response Acceleration

S_{Dl} Long Period Spectral Response Acceleration

Ta Fundamental Period of Structure

T_u Flexural Tension force for chord and collector

V_{13} Out-of-plane shear per unit length acting at the mid-surface of the element on the positive and negative 1 faces in the 3-axis direction

V_{23} Out-of-plane shear per unit length acting at the mid-surface of the element on the positive and negative 2 faces in the 3-axis direction

V_n Nominal shear strength

w_i the weight tributary to level i

w_{px} the weight tributary to the diaphragm at level x

x the value to be standardized

z z-score (Standard Score)

φ Strength reduction factor for tension member

ϕ the strength reduction factor for diaphragm shear

λ the modification factor to reflect the reduced mechanical properties of lightweight concrete relative to normal weight concrete of the same compressive strength

ρ_t the ratio of area of distributed transverse reinforcement to gross concrete area perpendicular to that reinforcement

Ωo Over-strength Factor

μ the mean of data

σ the standard deviation of data

n	the number of data sets
σ_{11}	the direct stress (force per unit area) acting on the positive and negative 1 faces in the 1-axis direction
σ_{22}	the direct stress (force per unit area) acting on the positive and negative 2 faces in the 2-axis direction
σ_{12}	the shearing stress (force per unit area) acting on the positive and negative 1 faces in the 2-axis direction and acting on the positive and negative 2 faces in the 1-axis direction
σ_{13}	Out-of-plane shearing stress (force per unit area) acting on the positive and negative 1 faces in the 3-axis direction
σ_{23}	Out-of-plane shearing stress (force per unit area) acting on the positive and negative 2 faces in the 3-axis direction
ε_{11}	the direct strain measure the change in length along the material local 1 axis
ε_{22}	the direct strain measure the change in length along the material local 2 axis
γ_{12}	The engineering shear strains measure the change in angle in the material local 1-2 planes
γ_{13}	The engineering shear strains measure the change in angle in the material local 1-3 planes
γ_{23}	The engineering shear strains measure the change in angle in the material local 2-3 planes

LIST OF ABBREVIATION

ACI	American Concrete Institute
ATC	Applied Technology Council
ASCE	American Society of Civil Engineers
BNBC	Bangladesh National Building Code
EC	Eurocodes
FEMA	Federal Emergency Management Agency
ELFA	Equivalent Lateral Force Analysis
FEM	Finite Element Method
IS	Indian Standard
LEP	Linear Elastic Procedures
LDP	Linear Dynamic Procedure
MRHA	Modal Response History Analysis
NSP	Nonlinear Static Procedure
RC	Reinforced Concrete
RSA	Response Spectrum Analysis
TEC	Turkish Earthquake Code
3D	Three Dimensional
2D	Two Dimensional

Chapter 1

INTRODUCTION

1.1 General

Now-a-days diaphragm opening is a common architectural feature in RC residential buildings, commercial buildings and industrial buildings to meet functional requirements of the building such as stairways, elevator shafts, escalators and architectural beautification of structure. A diaphragm carries gravity loads and distributes lateral forces induced by earthquake to the seismic force resisting vertical elements in proportion to their own rigidities. Opening in diaphragm can reduce the stiffness of the diaphragm and increase the in-plane deformability of the diaphragm. Reinforced floor systems may face in-plane slab yielding and cracking at the presence diaphragm opening. Structural members such as beam, column and shear walls can be overloaded then design force when base shear redistribution occurs due to slab in-plane cracking and yielding which can lead to local or global collapse of building.

The shear wall attracts more seismic force than column in a wall frame structural system because its in-plane stiffness is more than that of the column. Opening in diaphragm adjacent to a shear wall jeopardizes safe transfer of diaphragm forces to the shear wall. As a result diaphragm faces stress concentration around opening near shear wall which can cause diaphragm yielding and cracking during earthquake. It is thus, of the utmost importance, that they must be provided with sufficient in-plane stiffness and strength, together with efficient connection with the vertical structural elements

In this paper, seismic analysis of cast in situ concrete diaphragm with opening adjacent to shear wall in wall-frame structural system (Dual system with intermediate moment resisting frames capable of resisting at least 25% of the prescribed seismic force) is performed. The buildings assumed to be located in Dhaka, Bangladesh. The various analytical approaches are adopted to identify the seismic demand of concrete diaphragm with diaphragm opening adjacent to shear wall. Effort has been made in this study to find out the worst orientation of diaphragm opening adjacent to end shear wall and intermediate shear wall in Dual system buildings by stress analyses of diaphragm.

Global behaviors of structure and local behavior of diaphragm near diaphragm opening adjacent to shear wall are explained with evidence.

Most of the past researches were focused on the global behavior of moment resisting RC building with diaphragm openings. Very few researches are found dealing with global and local behavior of structures with diaphragm openings adjacent to shear walls. Harash (2011) performed comparative analysis of the seismic response of three storied RC buildings with shear walls and moment resisting frames which are oriented with diaphragm openings. Structural systems of these buildings were building frame system with ordinary reinforced concrete shear walls. However diaphragm forces and stress concentration around diaphragm opening adjacent to shear wall is not yet investigated to capture the local seismic demand and behavior of diaphragm.

Researches were also not conducted for dual system with intermediate moment resisting frames (capable of resisting at least 25% of the prescribed seismic force) which are oriented with diaphragm openings adjacent to shear wall.

Previous researchers analyzed the diaphragm considering only unidirectional seismic forces but diaphragm should be analyzed for orthogonal seismic loadings. The diaphragm should be analyzed and designed for orthogonal loading to capture the full behavior of diaphragm during earthquake. In this thesis we have analyzed and designed diaphragm for orthogonal seismic loadings to fulfill this knowledge gap.

Most of the time, diaphragms with openings are analyzed without stress calculation and there is less confidence about the analysis and design of cast in situ diaphragm with diaphragm openings adjacent to shear wall in wall frame structural systems (Dual system with intermediate moment resisting frames). Proper in-plane stress analyses for diaphragm subjected to orthogonal seismic force are not performed in the previous researches. So this thesis will help professional engineers to understand seismic demand of diaphragm around diaphragm openings adjacent to shear walls.

Nine building models were analyzed with diaphragm openings adjacent to end shear walls and intermediate shear walls. The shear wall aspect ratio is 1.95 in the buildings models. So shear walls in the buildings models are squat type shear walls. The squat shear walls are generally failed in racking/shear mode which is not desirable for earthquake resistant structures. Squat type shear walls also experience the racking

deformation. In the present study, it is of particular interest to examine diaphragm forces/stresses of diaphragm locations near diaphragm openings adjacent to squat type shear walls. Although Harash (2011) used similar kind of models that are adopted in the present study, structural system of his models were however building frame system (where ordinary reinforced concrete shear wall carried the entire seismic base shear and frames carried the gravity loads), structural system of building models to be analyzed in this study are on the other hand Dual system (a kind of wall-frame structural system with ordinary reinforced concrete shear walls and intermediate moment resisting frames capable of resisting at least 25% of the prescribed seismic force). The building models are designed and analyzed considering the seismic zone and soil type of Dhaka, Bangladesh.

1.2 Objectives with Specific Aims

i. To compare diaphragm forces/stresses of diaphragm locations around diaphragm opening adjacent to shear wall from LEP, LDP and Pushover analyses for providing design recommendations.

ii. To find out the worst orientation of diaphragm opening adjacent to shear wall and most highly stressed locations of diaphragm around diaphragm opening in Dual system buildings.

iii. To examine the limit of diaphragm opening in building plan with respect to diaphragm discontinuity criteria of ASCE 7-10 (ASCE, 2010) for wall-frame structural system having diaphragm opening adjacent to shear wall.

1.3 Scope

3D FEM models of 3-storied dual system buildings are adopted where diaphragm is modeled with nonlinear layer shell elements. Soil-structure interaction and nonlinear dynamic analysis are not considered in the study. Symmetric buildings are considered for analysis without any kind of vertical irregularity.

1.4 Methodology of the Study

Following steps will be adopted to conduct the present research:

i. FEM Modeling: Different 3D FEM models of regular shaped wall-frame buildings are prepared with different positions of shear wall and different positions of diaphragm opening adjacent to shear wall.

ii. Diaphragm Modeling:

Building models with plan aspect ratio of 4:1 with diaphragm opening of 11% of the diaphragm gross area and building models with plan aspect ratio of 3:1 with diaphragm opening of 11% of the diaphragm gross area were analyzed with LEP, LDP and Pushover analyses in this research work. Opening in diaphragm can significantly reduce the in-plane rigidity of diaphragm. The diaphragm of Models with plan aspect ratio of 3:1 without horizontal irregularity are allowed to model as rigid diaphragm as per Section 12.3.1.2 of ASCE 7-10 (ASCE, 2010). However, Saffarini and Qudaimat (1992) found that rigid-floor assumption is accurate for buildings without shear walls, but it can cause errors for building system with shear walls. According to Section 12.3.1.2 of ASCE 7-10, the diaphragm of Models with plan aspect ratio of 4:1 are not allowed to model as rigid diaphragm. Section 12.3.1 of ASCE 7-10 specifies that the diaphragm should be modeled as semi-rigid diaphragm where the diaphragm cannot be idealized as rigid or flexible diaphragm. Semi-rigid diaphragm in ETABS 2016 (CSI, 2017) accounts actual in-plan stiffness properties and behavior of diaphragm. Moreover, Semi-rigid diaphragm can help to determine force acting between diaphragm and vertical elements of seismic force resisting system through section cuts. Where the diaphragm is modeled as rigid, section cuts through the diaphragm cannot be used to determine diaphragm forces. Therefore, diaphragm of Models were modeled as semi-rigid diaphragm.

The diaphragm of building models are modeled with Nonlinear layered shell element to collect in-plane stress/force data. 2-D modified Darwin-Pecknold concrete model has been added to the nonlinear layered shell which represents concrete compression, cracking, and shear behavior under both monotonic and cyclic loading,

iii. Methods of analysis: The following types of analyses are performed to determine diaphragm forces. Both unidirectional and orthogonal seismic loading as per ASCE 7-10 (ASCE, 2010) and ASCE 41-13 (ASCE, 2014) are applied to structure.

a. Equivalent static force method: Equivalent static force method of analysis is a linear static procedure, in which the response of the building is assumed as linear elastic manner. The Equivalent static analysis of FEM models is carried out as per section 12.8 of ASCE 7-10 (ASCE, 2010).

b. Response spectrum analysis method: Properly combined accelerations are scaled in Modal Response Spectrum Analysis to get diaphragm design forces as per section 12.9 of ASCE 7-10 (ASCE, 2010).

c. Modal linear response history analysis: A linear response history analysis consists of an analysis of a linear mathematical model of the structure to determine its response, through methods of numerical integration, to suites of ground motion acceleration histories compatible with the design response spectrum for the site as per chapter 16 of ASCE 7-10 (ASCE, 2010). Maximum diaphragm stress/forces are computed from Modal linear response history analyses.

d. Pushover analyses: Diaphragm forces/stresses for the selected seismic hazard level from pushover analyses as per ASCE 41-13 (ASCE, 2014) are examined.

e. Diaphragm force as per section 12.10.1.1 of ASCE 7-10 (ASCE, 2010): Diaphragm forces as per section 12.10.1.1of ASCE 7-10 are applied to 3D building models to determine in-plane flexural and shear stress around diaphragm opening adjacent to shear wall.

1.5 Organization of the Thesis

The whole thesis is organized into six chapters. Chapter 1 is the current chapter. It sets objective, methodology of the thesis. It establishes the knowledge gaps which need to be fulfilled regarding diaphragm opening adjacent to shear walls.

Chapter 2 concentrates on all the previous literature to-date about analysis procedures, modeling and design of cast-in-situ concrete diaphragms with opening adjacent to shear wall. This chapter also presented on Earlier Research on Diaphragm opening in Building Plan.

Chapter 3 describes the assumption and modeling procedures of structural components in ETABS 2016 (CSI, 2017). It describes about the geometry of the models and seismic

parameters considered for seismic analyses of models. It also describes how to perform Equivalent lateral force procedure, Response spectrum analysis, Modal linear response history analysis, Diaphragm design force procedure as per eq.12.10-1 of ASCE 7-10 (ASCE, 2010) and Pushover analysis in ETABS 2016 (2017) for collecting in-plane stress/force data from nonlinear layer shell.

Chapter 4 presents the results of the analytical investigation described in Chapter 3 regarding the seismic response of the building models with diaphragm openings adjacent to shear walls. This chapter also provides and compares in-plane flexural stress data and in-plane shear stress data of the diaphragm from diaphragm design force procedures described in Chapter 3 through bar charts and statistical analyses. Maximum story displacement at target displacement from pushover analyses are also compared in this chapter. This chapter will also provide the discussion on all the obtained results.

Chapter 5 presents design guidelines for design of collector, chord and shear reinforcement as per ACI 318-14 (ACI, 2014) code. This chapter compares in plane shear force data of diaphragm locations near diaphragm opening adjacent to shear wall of Model-2 from LEP, LDP and Pushover analyses with bar charts and contour diagram to provide design recommendations. This chapter also compares chords and collectors force around diaphragm opening adjacent to shear wall of Model-2 from LEP, LDP and Pushover analyses.

Chapter 6 presents the conclusions of this research and also provides recommendations for future study.

Finally, in text quoted references are listed.

Chapter 2

LITERATURE REVIEW

2.1 Introduction

In this chapter, available literatures regarding seismic analysis of cast-in-situ concrete diaphragm with diaphragm openings will be reviewed. This chapter focuses on recent contributions related to analysis and design of cast-in-situ concrete diaphragm with diaphragm openings and past efforts most closely related to the needs of the present work.

2.2 Behavior of Diaphragm Under Seismic loading

Earthquake loads at any level of a building is distributed to the lateral load–resisting vertical elements through the floor and roof slabs. The primary function of diaphragm is to interconnect all lateral-force-resisting components through large in-plane stiffness. The function of a floor or roof, acting as a diaphragm, is to transmit inertia forces generated by earthquake accelerations of the floor mass at a given level to all horizontal-force-resisting elements. Vertical elements such as walls and frames will thus contribute to the total lateral force resistance, in proportion to their own stiffness.

According to Gardiner et al. (2008), the frame will primarily deform in shear mode when frame will subjected to lateral forces and the wall will deform in a bending mode when wall will subjected to lateral forces. The connection of the frames and walls to a diaphragm requires deformation compatibility for the entire structure. This compatibility restraint alters the overall deformation of the structure forming a combination of shear deformation mode in upper stories and flexural deformation mode in lower stories. Wall-frame interaction causes an increase in forces that are present in the floor diaphragm which have been found to be many times larger than the inertia forces in the diaphragms. The forces that develop from this wall-frame interaction action are referred to as transfer or compatibility forces. **Figure 2-1** shows deformation patterns for frame and wall elements. For analytical purpose, these are assumed to behave as deep beams. The slab is the web of the beam carrying the shear, and the perimeter spandrel or wall, if any, is the flange of the beam-resisting bending.

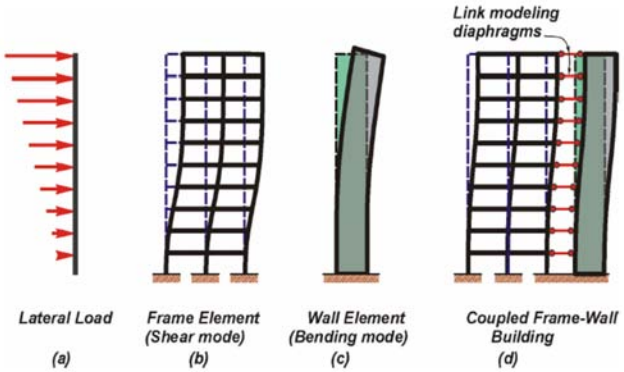

Figure 2-1 Deformation patterns for frame and wall elements (Gardiner et al., 2008)

Diaphragms are thus an essential part of the seismic force-resisting system and require design attention by the structural engineer to ensure the structural system performs adequately during earthquake shaking. Diaphragm action may be jeopardized if openings significantly reduce the ability of the diaphragm to resist in-plane flexure and shear. Inappropriate location or large-size openings for stairs or elevator cores, atriums, skylights, etc. create problems similar to those related to cutting the flanges and holes in the web of a steel beam adjacent to the flange, which is shown in **Figure 2-2**. This reduces the ability of the diaphragm to transfer the chord forces and may cause rupture in the web.

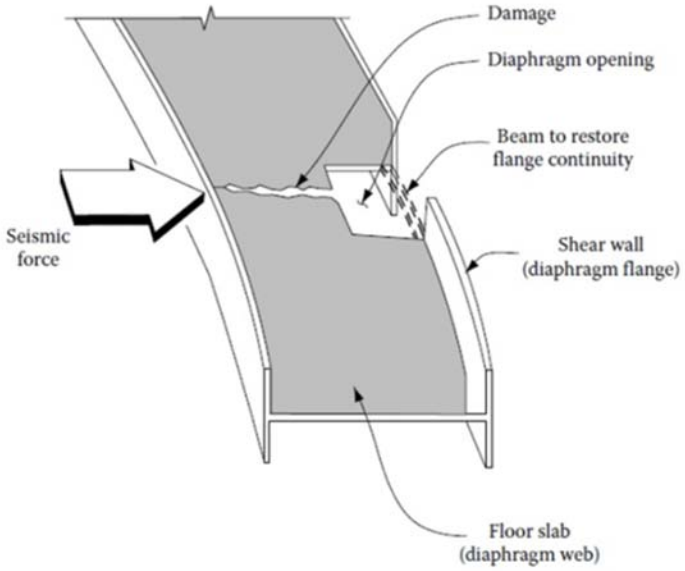

Figure 2-2 Diaphragms with openings (Taranath, 2010**).**

2.3 Situations Where Diaphragm Opening Adjacent to Shear Wall is Required

Shear walls are widely used for both tall buildings and low-rise buildings. They are important structural members used in the lateral force resisting system. Sometimes shear walls are used in low-rise buildings and industrial buildings to resist seismic forces and to control story drifts so that structural and nonstructural damages are less during earthquake. Lift shafts or service ducts is often used as the main horizontal load carrying member which is known as a core wall. Diaphragm opening is present in core wall. Sometimes stair is located near shear wall or lift core which is considered as diaphragm opening adjacent to shear wall. Sometimes diaphragm opening in cast-in-situ concrete diaphragm adjacent to shear wall is suggested by architecture to meet functional or aesthetic requirements for residential and industrial buildings. However, diaphragm opening should be avoided near shear wall as it jeopardizes safe transfer of in-plane shear force to shear wall during earthquake.

2.4 Buildings with Diaphragm Opening Adjacent to Shear Wall

In this section, real life examples of building with diaphragm opening adjacent to shear wall are presented. **Figure 2-3** shows perspective view of City Centre and Doreen Tower in Dhaka.

City Centre is a high-rise building that was constructed in the Motijheel Business District of Dhaka. City Centre is comprises of 37 floors and its height is 118.98 m (390.4 ft). It has 4-nos RC central core (Lift cores) and RC Shear walls which are connected with RC floor beams. **Figure 2-4** shows floor plan of City Center. Diaphragm openings are present in lift cores. Diaphragm opening such as stair is also located adjacent to shear wall in this building. Service ducts (diaphragm openings) are also present adjacent to lift cores.

Doreen Tower is located at 6-A North Avenue, Gulshan-2, the literal heart of Dhaka, at the confluence of Gulshan Avenue and Kemal Ataturk Avenue. The 25-storey building Trade Tower is Topped-out with a height of 92 meter (302 feet), and it is one of the tallest buildings in Bangladesh. **Figure 2-5** shows floor plan of Doreen Tower. RC lift cores, shear walls and columns are connected with RC floor beams. Diaphragm openings are present in lift cores. Diaphragm opening such as stair is also located adjacent to shear wall in this building.

Figure 2-3 Perspective view of City Centre and Doreen Tower

2.5 Diaphragm Components

Diaphragms are commonly composed of various components, including the diaphragm slab, chords, collectors (also known as drag struts or distributors), and connections to the vertical elements. **Figure 2-6** illustrates a simplified model of how a diaphragm resists in-plane loads and identifies its parts. The diaphragm could be modeled as a beam spanning between two supports, with reactions, shear and moment diagrams as shown (**Figure 2-6c**). Bending moment Mu can be resisted by a tension (Tu) and compression (Cu) couple (**Figure 2-6b**). The components at the diaphragm boundary acting in tension and compression are known as the tension chord and the compression chord, respectively.

If the diaphragm moment is resisted by tension and compression chords at the boundaries of the diaphragm as shown in **Figure 2-6a**, then equilibrium requires that the diaphragm shear be distributed uniformly along the depth of the diaphragm as shown in **Figure 2-6b**. Tension and compression elements called collectors are required to "collect" this shear and transmit it to the walls. A collector can transmit all its forces into the ends of the walls as shown on the right side of **Figure 2-7a**, or if the forces and resulting congestion are beyond practical limits, the collector can be spread into the adjacent slab as shown on the left side of **Figure 2-7a**.

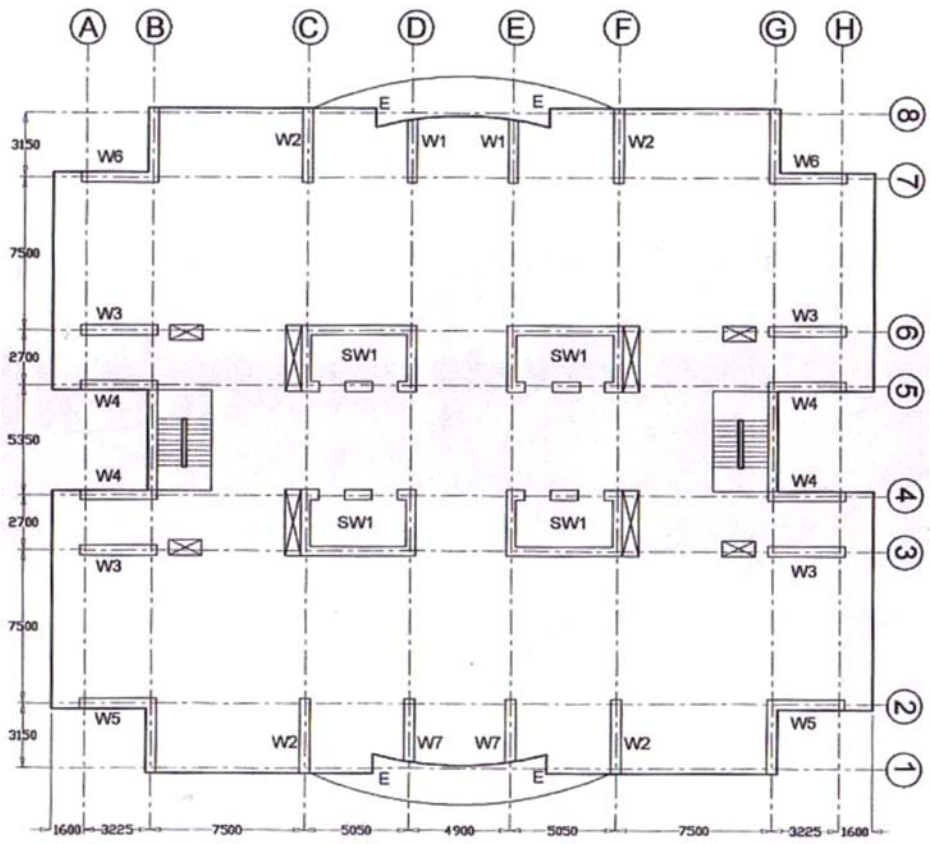

Figure 2-4 Floor plan of City Centre

2.6 Dual System

According to Section 12.2.5.1 of ASCE 7-10 (ASCE, 2010), the definition of Dual system is as follows: the Dual system takes the contribution of both moment resisting frames and shear walls for resisting seismic forces. The total seismic forces is resisted by the combination of the moment frames and the shear walls or braced frames in proportion to their rigidities where the moment frame shall be capable of resisting at least 25 percent of the design seismic forces.

Section 12.2.5.1 of FEMA P-1051-1 (FEMA, 2015) describes more elaborately the system requirements for Dual system. Section 12.2.5.1 specifies that the moment frame of a dual system must be capable of resisting at least 25% of the design seismic forces; this percentage is based on judgment.

The purpose of the 25% frame is to provide a secondary seismic force-resisting system with higher degrees of redundancy and ductility to improve the ability of the building to support the service loads (or at least the effect of gravity loads) after strong

earthquake shaking. The primary system (walls or bracing) acting together with the moment frame must be capable of resisting all of the design seismic forces. The following analyses are required for dual systems (FEMA, 2015).

Figure 2-5 Floor Plane of Doreen Tower

i. The moment frame and shear walls or braced frames must resist the design seismic forces, considering fully the force and deformation interaction of the walls or braced frames and the moment frames as a single system (FEMA, 2015). This analysis must be made in accordance with the principles of structural mechanics that consider the relative rigidities of the elements and torsion in the system (FEMA, 2015). Deformations imposed upon members of the moment frame by their interaction with the shear walls or braced frames must be considered in this analysis (FEMA, 2015).

ii. The moment frame must be designed with sufficient strength to resist at least 25% of the design seismic forces. (FEMA, 2015).

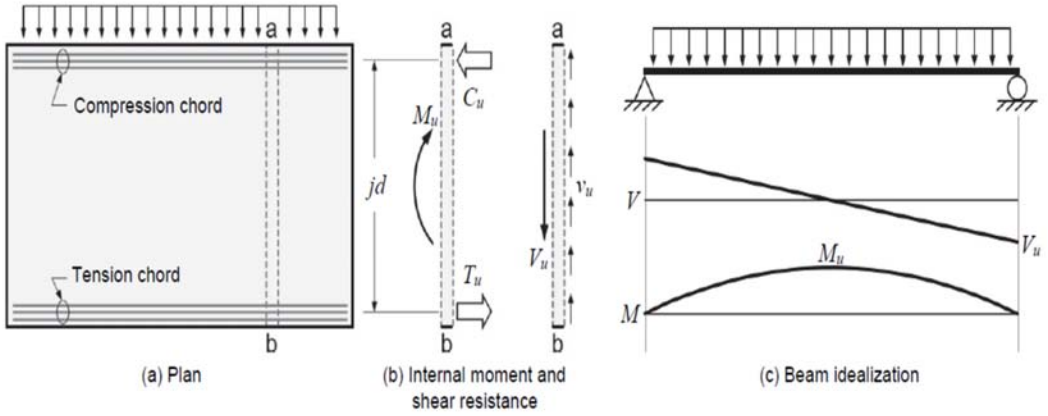

Figure 2-6 Moment and shear at a section cut (Moehle et al., 2010)

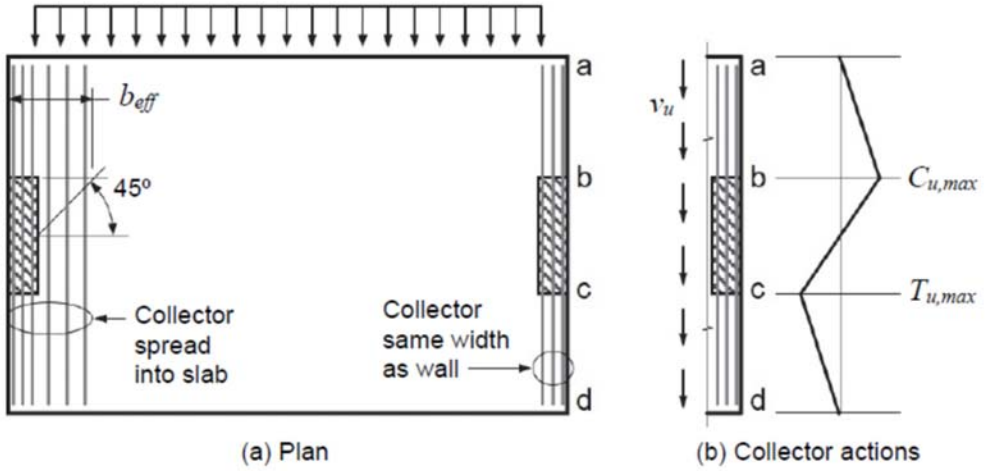

Figure 2-7 Collectors (Moehle et al., 2010).

2.7 Direction of Loading Criteria for Analysis and Design of Diaphragm

Moehle et al. (2010) specifies that "In general, diaphragms and collectors are permitted to be designed for seismic forces applied independently in each of the two orthogonal directions. For structures assigned to Seismic Design Category C, D, E, or F and having nonparallel systems (plan irregularity Type 5 per ASCE 7-10 Table 12.3-1), however, diaphragm design must consider the interaction of orthogonal loading in one of two ways. If the Equivalent Lateral Force Procedure or Modal Response Spectrum Analysis is used, 100 percent of the effects in one primary direction are to be combined with 30

percent of the effects in the other direction. If a response-history analysis is performed in accordance with ASCE 7 §16.1 or ASCE 7 §16.2, orthogonal pairs of ground motion histories are to be applied simultaneously. Though not required by ASCE 7, common practice is to consider the orthogonal combination for all diaphragm and collector design" (Moehle et al., 2010).

2.8 Design Methodology of Diaphragm with Large Opening

At diaphragm discontinuities, such as openings in diaphragm, the design shall assure that the dissipation or transfer of edge (chord) forces combined with other forces in the diaphragm is within shear and tension capacity of the diaphragm. "The principals of earthquake resistant design require the diaphragm to be stiff, damage free and capable of holding all the vertical of seismic force resisting elements together" (Moehle et al., 2010).

Moehle et al. (2010) specifies that "the small diaphragm opening having width or length on order of few thicknesses does not require special analysis. The diaphragm with large opening should have the ability to safely transfer forces (axial stress, shear stress) around it. The diaphragm may experience axial stress around the opening due to global or local behavior of structure and diaphragm. Confinement reinforcement is used when axial stress crosses permissible limit".

Moehle et al. (2010) suggested "the load path to vertical elements in diaphragm and around diaphragm opening should be clearly identified. Adequate strength should be provided to the diaphragm along these load paths at least equal to the maximum force that can be developed by the vertical elements".

2.8.1 Collector design forces as per ASCE 7-10

Collector elements shall be provided in diaphragm which are capable of transferring the seismic forces originating in other portions of the structure to the element providing the resistance to those forces.

According to Section 12.10.2.1 of ASCE 7-10 (ASCE, 2010), there are three procedures to determine forces of collectors, collector connections and collector connections with vertical elements for structure assigned to Seismic Design Category C through F. The maximum force from these three approaches is used to design

collectors, collector elements and collector connections to vertical elements. Transfer force need to be considered in collector forces as per Section 12.10.1.1 of ASCE 7-10.

i. Collector forces are determined from Equivalent lateral force procedure and Modal Response Spectrum Analysis procedure using load combination with over strength factor of section 12.4.3.2 of ASCE 7-10 (ASCE, 2010).

ii. Collector forces are determined from Diaphragm Design forces (F_{px}) as per Eq.12.10-1 using load combination with over strength factor of section 12.4.3.2 of ASCE 7-10 (ASCE, 2010).

iii. Collector forces are determined from Minimum Diaphragm Design forces ($F_{px,Min}$) as per Eq.12.10-2 using Basic load combination of section 12.4.3.2 of ASCE 7-10 (ASCE, 2010). Collector forces form the above three procedures should not exceed the maximum diaphragm design force ($F_{px,Max}$) as per Eq.12.10-3 of ASCE 7-10.

Moehle et al. (2010) mentioned that the Seismic forces (F_x) from Equivalent lateral force procedure or Modal response Spectrum Analysis are applied to the all diaphragm concurrently to determine collector forces as per procedure 1 described above. F_{px} as per procedure 2 and $F_{px,Min}$ from procedure 2 are typically applied one level at a time to the diaphragm under consideration by using overall building analysis model or by using an isolated model of individual diaphragm.

2.8.2 Design of collector

The procedures described for design of collector by Moehle et al. (2010) are described below.

$$A_s = \frac{T_u}{\varphi f_y} \qquad \text{Eq. 2-1}$$

A_s = Tension reinforcement of Collector (in^2)

T_u = Tensile force in collector (kips)

C_u = Compressive force in collector (kips)

f_y = yield strength of Reinforcing bar (ksi)

φ = Strength reduction factor for tension member ($\varphi = 0.9$)

The design compressive strength of collector element must be greater than or equal to factored compressive force in collector.

$$Cu > \varphi P_0 \quad \text{Eq. 2-2}$$

$$\varphi P_0 = \varphi\left[.085 f_c'\left(A_g - A_s\right) + f_y A_s\right] \quad \text{Eq. 2-3}$$

Where,

P_0 = Compressive strength of collector (kips)

f_c' = specified compressive strength of concrete, psi

A_g = Gross cross sectional area of collector (in^2)

A_s = Tension reinforcement of Collector (in^2)

Section 18.12.7.5 of ACI 318-14 (ACI, 2014) requires the confinement reinforcement for collector where compressive stress exceeds $0.2f_c'$ or $0.5f_c'$ where design flexural compressive forces have been amplified to account for overstrength of the vertical elements of the seismic force-resisting system. The transverse confinement reinforcement is not required where the compressive stresses in collector are below $0.15f_c'$ and $0.4f_c'$ for standard load combinations and load combinations with overstrength, respectively.

2.8.3 Diaphragm design force for chord design and shear design of diaphragm

Moehle et al. (2010) particularized that the diaphragm should be designed for the maximum of diaphragm force determined form F_x an F_{px}. Where F_x is the story shear at story level from seismic forces determined from Equivalent lateral force procedure and Modal response spectrum analysis. Although linear response history analysis and Nonlinear Dynamic analysis can also be used to determine F_x. F_x do not necessarily reflect the estimated maximum force induced at a particular diaphragm level. Therefore Section 12.10.1.1 requires the diaphragm to be designed for F_{px}. F_{px} is the diaphragm design force as per Eq.12.10-1 of ASCE 7-10 (ASCE, 2010). F_{px} must be equal or greater than $F_{px,min}$ of Eq.12.10-2 but must be less than $F_{px,max}$ of Eq.12.10-3. When F_x or F_{px} is applied at diaphragm, inertial forces develop in diaphragm and transmit to the vertical elements of seismic force resisting system. Different vertical structural members subjected to inertial forces displace differently when subjected to inertial forces. Although vertical structural members try to displace differently, the diaphragm imposes displacement compatibility. Diaphragm develops significant internal forces

due to displacement compatibility and lateral shear forces are transferred from one vertical element to other vertical elements of seismic force resisting system by frame interaction. This force is defined as transfer force. The diaphragm design force should also consider transfer forces in diaphragm.

2.8.4 Design of tension and compression chords

Moehle et al. (2010) describes that Reinforcement area of tension chord (As) is placed near the edge of diaphragm. Reinforcement area of tension chord (As) can also be placed within beam located at the edge of diaphragm. Generally reinforcement of tension chord is placed in the middle third of the slab or beam thickness to avoid interference with slab or beam longitudinal reinforcement and to reduce its contributions to slab and beam flexural strength. The design chord force should be computed for the orthogonal seismic load effects. The confinement reinforcement is required for flexural compressive zone of chord where flexural compressive stress exceeds $0.2f_c'$ or $0.5f_c'$ where design flexural compressive forces have been amplified to account for overstrength of the vertical elements of the seismic force-resisting system. The slab thickness needs to be increased because confinement reinforcement with seismic hoop may not fit in slab thickness where confinement reinforcements are placed in slab.

$$A_s = \frac{T_u}{\varphi f_y} \qquad \text{Eq. 2-4}$$

Where

A_s = Tension reinforcement of Chord

T_u = Flexural Tension force for chord

f_y = yield strength of Reinforcing bar

φ = Strength reduction factor for tension member ($\varphi = 0.9$)

2.8.5 Design of diaphragm shear reinforcements

NIST (2016) states that the shear stress distribution should be constant through the diaphragm depth where in-plan moment of diaphragm due to seismic loading is resisted by chords located at outer boundaries of diaphragm. Additional chords and collectors should be provided to the diaphragm with horizontal or vertical structural irregularities to resist nonuniform shear stress.

2.8.6 Strength reduction factor for diaphragm shear

Section 21.2.4.2 of ACI 318-14 (ACI, 2014) requires that the strength reduction factor ϕ for diaphragm shear should not exceed the minimum ϕ used for shear of the vertical components of primary seismic force-resisting system. The shear strength of a diaphragm will be less than shear strength of the vertical elements.

2.8.7 Design shear strength of diaphragm

Section 18.12.9.1 of ACI 318-14 (ACI, 2014) prescribed that V_n of diaphragm should not exceed $8A_{cv}\sqrt{f_c'}$. The design shear strength is given by ϕV_n, where $\phi = 0.6$ or 0.75.

$$V_n = A_{cv}\left(2\lambda\sqrt{f_c'} + \rho_t f_y\right) \qquad \text{Eq. 2-5}$$

V_n is nominal shear strength, lb.

ρ_t is the ratio of area of distributed transverse reinforcement to gross concrete area perpendicular to that reinforcement. ρ_t is perpendicular to the diaphragm moment reinforcement and parallel to the in-plane shear force.

A_{cv} is the gross area of concrete section of diaphragms in the direction of shear force, not to exceed the thickness times the width of the diaphragm, inch².

f_c' is the specified compressive strength of concrete, psi

f_y is the specified yield strength for nonprestressed reinforcement, psi

λ is the modification factor to reflect the reduced mechanical properties of lightweight concrete relative to normal weight concrete of the same compressive strength

ϕ = strength reduction factor for shear strength of diaphragm.

2.9 Layered Shell Modeling

Modeling Enhancements Implemented (2015) states that, “A new 2-D modified Darwin-Pecknold concrete model has been added to the nonlinear layered shell. It represents concrete compression, cracking, and shear behavior under both monotonic and cyclic loading, and accounts for crack rotation”.

The Modified Darwin-Pecknold reinforced concrete material model is a two-dimensional concrete material model that can account directly for the interaction between bending and shear in shear wall and slab structures. The shear strength of a concrete wall and slab may depend substantially on the axial forces and bending moments. The 2D concrete model attempts to model coupling between axial-bending and shear. The 2D concrete model is a coaxially rotating smeared crack concrete model. This model considers cracking and crushing of the concrete, and when it is combined with a steel material it considers yield of the steel. Compressive strength reduction based on perpendicular tensile strain is accounted with the consideration of Vecchio-Collins behavior. The model is used for reinforced concrete and does not account for the tensile strength of concrete. The bond slip and dowel action are not considered in this model (Technical note, 2015).

According to CSI Analysis Reference Manual (2016), the direction of cracking can change during the loading history, and the shear strength is affected by the tension strain in the material. The axial stress-strain stress-strain curve specified for the material is simplified to account for initial stiffness, yielding, ultimate plateau, and strength loss due to crushing. Zero tensile strength is assumed. Hysteresis is governed by the concrete hysteresis model with the energy dissipation factor equal to zero. The layered shell allows this material to be used for membrane and/or flexural behavior and to be combined with steel reinforcement placed in arbitrary directions and locations. Transverse or out-of-plane shear is assumed to be elastic and isotropic using the shear stiffness G_{13} for both σ_{13}-γ_{13} and σ_{23}- γ_{23} behavior.

Select Membrane to model only in-plane behavior, Plate to model only out-of-plane bending behavior, and Shell to model full shell behavior. The number of Integration points should be specified in the thickness direction for the layer. The locations are determined by the ETABS 2016 (CSI, 2017) using standard Guass quadrature rules. The material angle is measured counterclockwise from the local 1 axis of the shell object to the local 1 axis of the material. Choose Directional to independently control behavior for each of the three components. Choosing Coupled will force all three components to be nonlinear, using the Modified Darwin-Pecknold 2-D reinforced concrete material model (Slab, Wall Property Layer Definition Data, n.d).

Choose Linear, Nonlinear, or Inactive from the drop-down list for σ_{11}, σ_{22}, and σ_{12} components. When any of the components is set to be Linear, the layer will behave linearly in that direction in a nonlinear load case. When any of the components is set to be Nonlinear, the layer will behave nonlinearly in that direction in a nonlinear load case. When any of the components is set to Inactive, the layer will not contribute to the stiffness in that direction in a nonlinear load case. (Slab, Wall Property Layer Definition Data, n.d).

Unless all three material components are Linear, the Poisson's ratio will be taken as zero in a nonlinear load case, regardless of the value defined in the material property. Regardless of the selected behavior, all three material components will behave linearly in a linear load case. (Slab, Wall Property Layer Definition Data, n.d).

2.9.1 Layered section property

CSI Analysis Reference Manual (2016) specifies that for the layered Section property, you define how the section is built-up in the thickness direction. Any number of layers is allowed, even a single layer. Layers are located with respect to a reference surface. This reference surface may be the middle surface, the neutral surface, the top, the bot tom, or any other location you choose. By default, the reference surface contains the element nodes, although this can be changed using joint off sets. The thick-plate (Mindlin/Reissner) formulation, which includes the effects of transverse shear deformation, is always used for bending behavior the layered shell.

2.9.2 Layer name

CSI Analysis Reference Manual (2016) reports the layer name is arbitrary, but must be unique within a single Section. However, the same layer name can be used in different Sections. This can be useful because results for a given layer name can be plotted simultaneously for elements having different Sections.

2.9.3 Layer distance

CSI Analysis Reference Manual (2016) reports each layer is located by specifying the distance from the reference surface to the center of the layer, measured in the positive local-3 direction of the element which is shown in **Figure 2-9**.

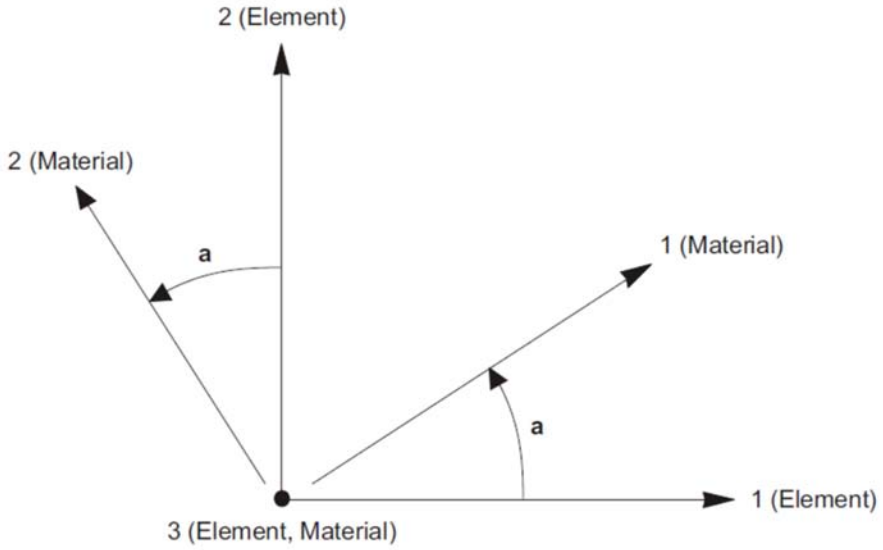

Figure 2-8 Shell Section Material Angle (CSI Analysis Reference Manual, 2016)

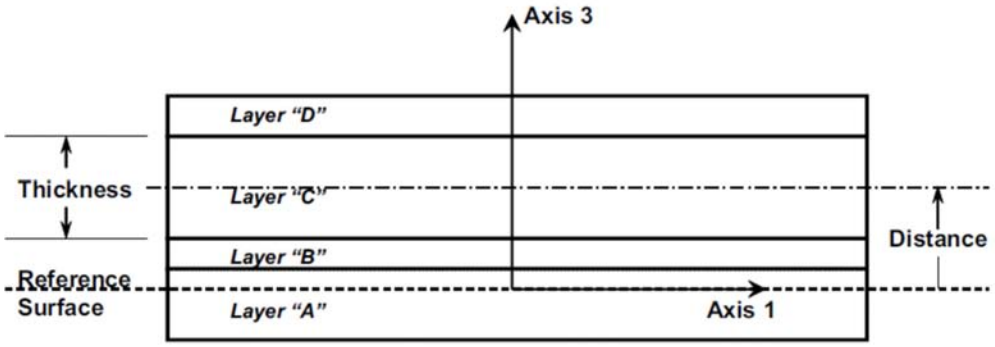

Figure 2-9 Four-Layer Shell, Showing the Reference Surface, the Names of the Layers, and the Distance and Thickness for Layer "C" (CSI Analysis Reference Manual, 2016).

2.9.4 Layer thickness

CSI Analysis Reference Manual (2016) reports each layer has a single thickness, measured in the local-3 direction of the element. For modeling rebar or material fibers, you can specify a very thin "smeared" layer that has an equivalent cross-sectional area.

2.9.5 Layer type

• **Membrane:** Strains in the layer (ε_{11}, ε_{22}, γ_{12}) are computed only from in-plane membrane displacements, and stresses in the layer (σ_{11}, σ_{22}, σ_{12}) contribute only to in-plane membrane forces (F_{11}, F_{22}, F_{12}).

• **Plate:** Strains in the layer (ε_{11} , ε_{22} , γ_{12} , γ_{13} , γ_{23}) are computed only from plate-bending rotations and trans verse displacements, and stresses in the layer (σ_{11} , σ_{22} , σ_{12} , σ_{13} , σ_{23}) contribute only to plate-bending moments and transverse shearing forces (M_{11} , M_{22} , M_{12} ,V_{13} ,V_{23}).

• **Shell**, which combines membrane and plate behavior: Strains in the layer (ε_{11} , ε_{22} , γ_{12} , γ_{13} , γ_{23}) are computed from all displacements and plate-bending rotations, and stresses in the layer (σ_{11} , σ_{22} , σ_{12} , σ_{13} , σ_{23}) contribute to all forces and plate-bending moments (F_{11} , F_{22} , F_{12} , M_{11} , M_{22} , M_{12} ,V_{13} ,V_{23}). In most applications, layers should use shell behavior.

CSI Analysis Reference Manual (2016) reports mass and weight are computed only for membrane and shell layers, not for plate layers. This prevents double-counting when independent membrane and plate layers are used for the same material.

2.9.6 Layer number of thickness integration points

According to CSI Analysis Reference Manual (2016) material behavior is integrated (sampled) at a finite number of points in the thickness direction of each layer. You may choose one to five points for each layer. The location of these points follows standard Guass integration procedures. For a single layer of linear material, one point in the thickness direction is adequate to represent membrane behavior, and two points will capture both membrane and plate behavior. If you have multiple layers, you may be able to use a single point for thinner layers. Nonlinear behavior may require more integration points or more layers in order to capture yielding near the top and bottom surfaces. Using an excessive number of integration points can increase analysis time. You may need to experiment to find a balance between accuracy and computational efficiency.

2.9.7 Layer material

CSI Analysis Reference Manual (2016) suggested the material properties for each layer are specified by reference to a previously defined Material. The material may be isotropic, uniaxial, or orthotropic. If an anisotropic material is chosen, orthotropic properties will be used.

2.9.8 Layer material angle

According to CSI Analysis Reference Manual (2016), for orthotropic and uniaxial materials, the material axes may be rotated with respect to the element axes. Each layer may have a different material angle. **Figure 2-8** shows shell section material angle.

2.9.9 Layer material behavior

CSI Analysis Reference Manual (2016) specifies that, Directional behavior can be applied to all materials. Coupled behavior is available for concrete materials only, and uses the modified Darwin-Pecknold behavior.

2.9.10 Layer material components

This option applies only to "Directional" material behavior. For each of the three membrane stress components (σ_{11}, σ_{22}, σ_{12}), you can choose whether the behavior is linear, nonlinear, or inactive. For a uniaxial material, only the two components (σ_{11}, σ_{12}) are significant, since σ_{22} =0 always. Material components are defined in the material local coordinate system, which depends on the material angle and may not be the same for every layer. If all three components are linear (two for the uniaxial material), then the linear material matrix is used for the layer. If one or more of the three components is nonlinear or inactive, then all linear components use an uncoupled isotropic linear stress-strain law, all nonlinear components use the nonlinear stress strain relationship, and all in active components assume zero stress. The components become uncoupled, and behave as if Poisson's ratio is zero (CSI Analysis Reference Manual, 2016).

2.9.11 Interaction between layers

Layers are defined in dependently, and it is permissible for layers to overlap, or for gaps to exist between the layers. It is up to you to decide what is appropriate. Layers are kinematically connected by the Mindlin/Reissner assumption that normal to the reference surface remain straight after deformation. This is the shell equivalent to the beam assumption that plane sections remain plane (CSI Analysis Reference Manual, 2016).

2.9.12 Integration in the plane

Force-deflection behavior is computed by integrating the stress-strain behavior through the thick ness and over the 1-2 plane of the element. You can specify the number of

integration points in the thickness direction of each layer. For each of these thickness locations, integration in the plane is performed at the standard 2 x 2 Gauss points (coordinates ±0.577 on a square of size ±1.0). Nonlinear behavior is sampled only at these points. This is equivalent to having two fibers, located approximately at the ¼ and ¾ points, in each of the local 1 and 2 directions. Plotted or tabulated stresses at locations other than the four Gauss points are interpolated or extrapolated, and do not necessarily represent the sampled nonlinear stresses. For this reason, stresses at the joints may sometimes appear to exceed failure stresses (CSI Analysis Reference Manual, 2016).

2.10 Diaphragm Forces from Section Cut in ETABS 2016

Forces are reported in the section-cut coordinate system which is defined by three axes (1, 2, Z). Section cut in elements is done by using draw section cut command in ETABS 2016 (2017). Section-cut 1 axis is located within the plane parallel to the global X-Y plane. Section cut 1 axis rotates counterclockwise from the global X axis according to the user-defined parameter Angle (X to 1). Section-cut 2 axis is located within the plane parallel to the global X-Y plane and it is oriented 90° counterclockwise from the section-cut 1 axis. Section-cut Z axis is parallel to the global Z axis. Integrated forces are reported either on the left or right side of the section cut according to the right-hand rule (Kalny, 2014).

2.11 Statistically Significant Data

In science, many researchers report the standard deviation of experimental data, and only effects that fall much farther than two standard deviations away from what would have been expected are considered statistically significant (Standard deviation, n.d).

2.12 Approximate Tensile Strength of Concrete

The ACI Code recommends that the modulus of rupture f_r be taken to equal $7.5\sqrt{f_c'}$ for normal weight concrete (Nilson et al., 2004).

2.13 Diaphragm Discontinuity Irregularity as per ASCE 7-10

Table 12.3-1(3) of ASCE 7-10 (ASCE, 2010) requires the diaphragm with an abrupt discontinuity or variation in stiffness, including one having a cutout or open area

greater than 50% of the gross enclosed diaphragm area, or a change in effective diaphragm stiffness of more than 50% from one story to the next should be treated as Diaphragm Discontinuity Irregularity. **Figure 2-10** shows diaphragm discontinuity criteria as per ASCE 7-10.

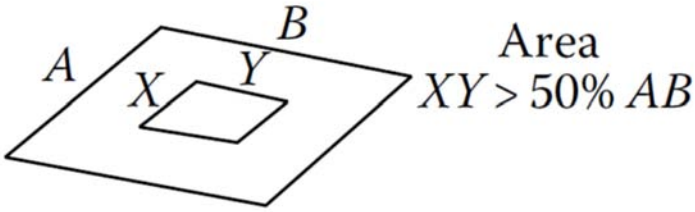

Figure 2-10 Diaphragm discontinuity irregularity (Taranath, 2010).

2.14 Literature Review on Earlier Research

Literature reviews of earlier researches on diaphragm opening in building plan and Squat shear wall are presented in this section according to chronological order.

2.14.1 Roper and Iding (1984)

Roper and Iding (1984) concluded that cracking and in-plane yielding of Reinforced concrete floor systems with the plan aspect ratio over 3:1 may occur in low-rise rectangular buildings consist of end shear walls and moment resisting interior frames.

2.14.2 Harash (2011)

Harash (2011) performed comparative analysis of the seismic response of three storied RC Building frame system buildings by distributing diaphragm opening symmetrically and non-symmetrically in the building plan. Different scenarios were created by increasing or decreasing diaphragm openings apart from code prescribed allowable percentage of opening with different diaphragm plan aspect ratios in Building frame structural system. Non-linear static (Pushover analysis) and nonlinear time history analysis are performed on these scenarios with the help of IDRC2, a non-commercial program capable of conducting nonlinear analysis of RC buildings with rigid, elastic and inelastic floor diaphragms. Then comparative studies of seismic response of above mentioned scenarios were performed. An error index was suggested for the displacement amplification factor (C_d) of ASCE 7-05 (ASCE, 2005) to account inelastic frame displacement. A three parameter hysteresis model along with an

idealized trilinear moment-curvature envelop of the slabs were used in the inelastic dynamic analysis to duplicate the various aspects reinforced concrete behavior under inelastic dynamic loading. He gave some recommendations for the design of chord of diaphragm based on the results of Pushover analysis. He concluded that the influence of inelastic inplane diaphragm deformation cannot be overlooked when diaphragm opening is located in the middle two thirds of the building plan having plan aspect ratio of 4:1. The combined effects of inelastic floor diaphragm deformation and yielding of shear wall increase the base shear of the interior frame in these buildings. However diaphragm forces and stress concentration around diaphragm opening adjacent to shear wall is not yet investigated to capture the local seismic demand and behavior of diaphragm.

2.14.3 Ozturk (2011)

Ozturk (2011) analyzed response of reinforced concrete moment resisting frame buildings having diaphragm opening of different positions and ratios under earthquake loads following the codes of IBC-2006 (ICC, 2006), Eurocode (CEN, 2004), and TEC-07 (TEC, 2007). The analysis was carried out by considering the effects of the number of story, beam continuity in diaphragm opening, different earthquake zones, different soil types and diaphragm behavior (Rigid diaphragm) on the structural system. He concluded that the maximum lateral displacement and torsional values occur for the buildings when slab opening are not symmetrical and the continuity of the beams is not enabled. The increase in number of stories, the poor nature of soils, the largeness of the earthquake zones increase the negative effects of the slab opening on the structural behavior. Although the diaphragms have diaphragm opening greater than the diaphragm opening permitted by codes, the diaphragm acts as rigid diaphragm for buildings having diaphragm openings distributed symmetrically in building plan.

2.14.4 Ravikumer et al. (2012)

Ravikumer et al. (2012) examined the performance of plan irregular (such as diaphragm opening, re-entrant corners and vertical irregularity with setback) buildings resting on sloping ground with linear analysis as per code-IS: 1893, Part-1 (BIS, 2002) and non-linear pushover analysis as per ATC-40 (ATC, 1996). Comparative studies of story displacement, Base shear and performance level were investigated for the above

mentioned irregularly configured buildings. The performances of these plans irregular buildings were also studied in terms of time period, base shear, lateral displacement, story drift and eccentricity using linear analysis. The entire modeling, analysis and design were carried out by ETABS 6.0 nonlinear version software. They showed that the building having irregular shaped diaphragm opening possessed poor performance level in pushover analysis compared to building having regular shaped diaphragm opening. This showed that there is a lack of transferring of forces to each vertical member due to presence of irregular shaped opening in building.

2.14.5 Orakcal et al. (2012)

According to Orakcal et al. (2012), an adequate design of a slender reinforced concrete shear wall requires that shear failure of wall will not occur before the wall experiences a ductile flexural response under seismic excitations. Even so, this may not be achieved when the shear wall is relatively short, and its response is governed by shear deformations. Such shear walls are subjected to predominant shear actions.

2.14.6 Baratta et al. (2012, 2013)

Squat shear walls are more vulnerable to overturning (Baratta et al., 2012, 2013).

2.14.7 Ahmed and Reza (2014)

Ahmed and Reza (2014) examined a G+9 storied building having plan irregularities like rectangular shaped, diaphragm opening, Y-shaped models in severe earthquake zone with pushover analysis to evaluate performance point, pushover curve, performance levels and hinge formations for comparative studies. They found that point displacement of roof is greater for building with diaphragm opening located in the center of that model compared to others models. Base shear for rectangular model is greater than diaphragm discontinuity and Y-shaped models. Increase in mass of rectangular building tends to increase in base shear compared to others models.

2.14.8 Ramya (2014)

According to Ramya (2014), the shear walls are classified on the basis of aspect ratio (height/width ratio). The shear walls with aspect ratio between 1 and 3 are considered to be of squat type and shear walls with aspect ratio greater than 3 are considered to be

of slender type. The squat shear walls are generally failed in racking (shear mode) whereas the slender shear walls fail in a flexural mode. In the case of low-rise shear walls, the racking deformation (a kind of shear deformation) becomes predominant and substantially contributes to the overall deformation.

2.14.9 Manira and John (2015)

Manira and John (2015) examined six types of G+7 story moment resisting frame buildings having symmetrical and non-symmetrical distribution of diaphragm opening. The linear analysis was performed to determine seismic responses of these buildings. Then Seismic performances of these buildings were compared based on their natural time period, stiffness, base shear and modal mass participation. They concluded that the behavior of buildings is better when the diaphragm opening is close to the center of the building.

2.14.10 Sahu and Dwivedi (2017)

Sahu and Dwivedi (2017) analyzed various square shaped models of RC framed multistoried buildings having various percentages (0%,4%,16%,24% and 36%) of diaphragm openings by Earthquake Static Analysis and Response Spectrum analysis using a commercial software STAAD Pro. Earthquake Static Analysis and Response Spectrum analysis were performed for models by following IS: 1893, part-1 (BIS, 2002). They concluded that increase in the opening percentage of diaphragm, increase the story drift and decrease the base shear in all the models. Story drift and base shear calculated from the earthquake static analysis are higher than the response spectrum analysis. Shear force, bending moment and Axial Force obtained from the earthquake static analysis are also higher as compared to response spectrum analysis.

2.14.11 Vinod and Pramod (2017)

Vinod and Pramod (2017) studied the effect of discontinuities in the diaphragm (0%, 10%, 20%, and 30% openings) on the seismic behavior of four and eight story RC moment resisting frame buildings. Parameters such as Natural Time Period, Base Shear, Mode shape, Drift and Displacements and internal forces in members are used to compare the seismic performance of four and eight story building. The buildings were modeled with ETABS 2015 software. The Equivalent lateral force analysis as per the

seismic code IS: 1893, Part-1 (BIS, 2002) and Response Spectrum Analysis as per IS 1893, Part-1 were used to compare seismic performance of these buildings. The diaphragms in these buildings are modeled as rigid diaphragm. They concluded that seismic behavior of diaphragm with 20% of opening is the better one when compared to other conditions for RC multistory buildings in seismic prone areas, even the number of story height increases.

Most of the past researches were focused on the global behavior of moment resisting RC building with diaphragm openings. Very few researches are found dealing with global and local behavior of structures with diaphragm openings adjacent to shear walls. Diaphragm forces and stress concentration around diaphragm opening adjacent to shear wall is not yet investigated to capture the local seismic demand and behavior of diaphragm. Researches were also not conducted for dual system with intermediate moment resisting frames, which are oriented with diaphragm openings adjacent to shear wall. Previous researchers analyzed the diaphragm considering only unidirectional seismic forces but diaphragm should be analyzed for orthogonal seismic loadings. The diaphragm should be analyzed and designed for orthogonal loading to capture the full behavior of diaphragm during earthquake. In this thesis, diaphragm of models are analyzed and designed for orthogonal seismic loadings to fulfill these knowledge gaps.

2.15 Summary

This chapter presented all the previous literature to-date about analysis procedures, modeling and design of cast-in-situ concrete diaphragms with opening. This chapter presents on Earlier Research on Diaphragm opening in Building Plan. This chapter briefly describes about nonlinear layer shell. This chapter describes about requirements of dual system buildings and design methodology of diaphragm with large opening. This chapter also describes about direction of loading criteria for analysis and design of diaphragm.

Chapter 3

ANALYSIS PROCEDURES OF RC BUILDINGS WITH DIAPHRAGM OPENINGS

3.1 Introduction

In this research, nine building Models are investigated. All buildings are 3-storied buildings having story height of 13 ft. The total height of the building is 39 ft. It is considered that all the buildings are situated in Dhaka city, Bangladesh. The lateral force resisting system in both directions consist of Dual systems with ordinary shear walls and Intermediate moment frames capable of resisting at least 25% of prescribed seismic forces. All structural elements are designed and detailed as per ACI 318-14 (ACI, 2014) and ASCE 7-10 (ASCE, 2010) prescribed forces.

3.2 Justification for the Models

According to Orakcal et al. (2012), an adequate design of a slender reinforced concrete shear wall requires that shear failure of wall will not occur before the wall experiences a ductile flexural response under seismic excitations. Even so, this may not be achieved when the shear wall is relatively short, and its response is governed by shear deformations. Such shear walls are subjected to predominant shear actions (Orakcal et al., 2012). According to Ramya (2014), the shear walls are classified on the basis of aspect ratio (height/width ratio). The shear walls with aspect ratio between 1 and 3 are considered to be of squat type and shear walls with aspect ratio greater than 3 are considered to be of slender type. The squat shear walls are generally failed in racking (shear mode) whereas the slender shear walls fail in a flexural mode. In the case of low-rise shear walls, the racking deformation (a kind of shear deformation) becomes predominant and substantially contributes to the overall deformation (Ramya. 2014). Squat shear walls are more vulnerable to overturning (Baratta et al.,2012, 2013).

Roper and Iding (1984) concluded that cracking and in-plane yielding of Reinforced concrete floor systems with the plan aspect ratio over 3:1 may occur in low-rise rectangular buildings consist of end shear walls and moment resisting interior frames. Harash (2011) stated that the combined effects of inelastic floor diaphragm deformation and yielding of shear wall shifts the base shear to the interior frames of the building up

to thirty percent when diaphragm opening is located in the middle two thirds of the building plan having plan aspect ratio of 4:1.

Nine (09) building models were analyzed with diaphragm openings adjacent to end shear walls and intermediate shear walls. The shear wall aspect ratio is 1.95 in the buildings models. So shear walls in the buildings models are squat type shear walls. The squat shear walls are generally failed in racking/shear mode which is not desirable for earthquake resistant structures. Squat type shear walls also experience the racking deformation. We are particularly interested to examine diaphragm forces/stresses of diaphragm locations near diaphragm openings adjacent to squat type shear walls. Although Harash (2011) used similar kind of models that we are using in our study but structural system of his models were building frame system (where ordinary reinforced concrete shear wall carried the entire seismic base shear and frames carried the gravity loads) but structural system of building models to be analyzed in this study are Dual system (a kind of wall-frame structural system with ordinary reinforced concrete shear walls and intermediate moment resisting frames capable of resisting at least 25% of the prescribed seismic force). Harash (2011) used eight inch thick shear walls in his models but ten inch thick shear walls are considered in building models in this study for detailing of chords and collectors.

3.3 Geometry of Building Models

The structural system of all buildings is Dual systems with Intermediate moment Frames capable of Resisting at least 25% of Prescribed seismic forces as per Table 12.2-1, E (8) of ASCE 7-10 (ASCE, 2010) and as per Table 6.2.19, E(4) of BNBC-2017 (HBRI & BRTC, 2017) in both directions. The shear walls of these buildings are ordinary reinforced concrete shear wall. Occupancy type of these buildings is Residential Building and Risk category of is I as per Table 1.5-1 of ASCE 7-10. Seismic Importance Factor (I_e) is 01 as per Table 1.5-2 of ASCE 7-10. Occupancy category of these buildings is I as per Table 6.1.1 of BNBC -2017. Importance factor is 01 as per Table 6.2.17 of BNBC-2017 for buildings to be investigated. It is assumed that 3-storied buildings are situated on deep deposits of dense or medium dense sand gravel or stiff clay with thickness from several tens to many hundreds of meters so site class is SC as per Table 6.2.13 of BNBC-2017. Site location for these buildings is Dhaka (Bangladesh) so seismic zone for these buildings is zone-2 as per Table 6.2.14

of BNBC-2017. So using the above-mentioned information the Seismic Design Category of buildings is determined. The Seismic Design Category of buildings is C as per Table 6.2.13 and Table 6.2.18 of BNBC-2017. It is assumed that compressive strength fc' for walls, columns, beams and slabs of these buildings is 4000 psi. The rebar yield strength of rebar used in structural elements in these buildings is 60000 psi. **Figure 3-1** shows nonlinear material data (stress vs strain) for the 4000 psi concrete and **Figure 3-2** shows nonlinear material data (stress vs strain) for rebar of 60000 psi. The nonlinear material data was used for nonlinear layered shell at the time of performing nonlinear static analysis.

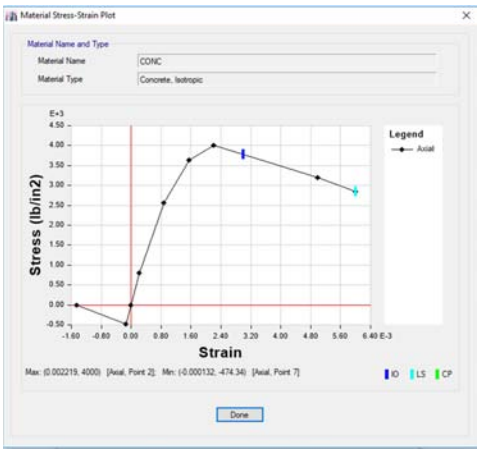

Figure 3-1 Nonlinear Material data (Stress vs Strain) for the Concrete

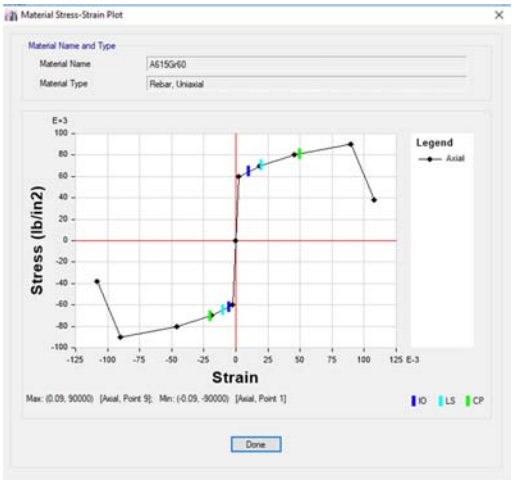

Figure 3-2 Nonlinear Material data (Stress vs Strain) for Rebar

It is considered that gravity loads such as live load (uniform) is 50 psf and super imposed dead load (uniform) is 20 psf for 3-storied buildings to be investigated. **Table 3-1** shows the dimensions of building plan and shear wall location. All the buildings

models are located in moderate seismic intensity area as per Table 6.2.14 of BNBC-2017 (HBRI & BRTC, 2017). Structural configurations of Building models are presented in **Table 3-1**. Seismic parameters for the buildings to be investigated are summarized in **Table 3-2**. Lay-out plan of building models are shown in **Figures 3-3** to **3-11**.

Table 3-1 Structural configurations of Building models

Model ID	Length (ft)	Width (ft)	Number of Bays along the length of Model	Number of Bays along the width of Model	Shear wall location along length of Model	Shear wall location along width of Model	Plan Aspect Ratio	Openings in Diaphragm
Model-1	240	60	12 Nos @ 20 ft	6 Nos @ 20 ft	End shear wall	End shear wall	4:1	None
Model-2	240	60	12 Nos @ 20 ft	6 Nos @ 20 ft	End shear wall	End shear wall	4:1	At end
Model-3	240	60	12 Nos @ 20 ft	6 Nos @ 20 ft	End shear wall	End shear wall	4:1	Interior
Model-4	180	60	9 Nos @ 20 ft	6 Nos @ 20 ft	End shear wall	End shear wall	3:1	None
Model-5	180	60	9 Nos @ 20 ft	6 Nos @ 20 ft	End shear wall	End shear wall	3:1	At end
Model-6	180	60	9 Nos @ 20 ft	6 Nos @ 20 ft	End shear wall	End shear wall	3:1	Interior
Model-7	240	60	12 Nos @ 20 ft	6 Nos @ 20 ft	End shear wall	Interior shear wall	4:1	None
Model-8	240	60	12 Nos @ 20 ft	6 Nos @ 20 ft	End shear wall	Interior shear wall	4:1	Middle
Model-9	240	60	12 Nos @ 20 ft	6 Nos @ 20 ft	End shear wall	Interior shear wall	4:1	Interior

Table 3-2 Seismic Parameters per ASCE 7-10 and BNBC-2017

Parameters	Value
Short Period Acceleration as per Table 6.C.1,Appendix C,BNBC -2017, S_s	0.5
Long Period Acceleration as per Table 6.C.1,Appendix C, BNBC-2017, S_l	0.2
Short Period Site Coefficient as per Table 6.C.2,Appendix C, BNBC-2017, Fa	1.15
Long Period Site Coefficient as per Table 6.C.3,Appendix C, BNBC-2017, Fv	1.725
Short Period Spectral Response Acceleration Parameter Table 6.C.4,Appendix C, BNBC-2017, S_{DS}	0.383
Long Period Spectral Response Acceleration Parameter Table 6.C.5,Appendix C, BNBC-2017, S_{Dl}	0.23
Response Modification Factor, R,N-S & R,E-W	5.5
Over-strength Factor, Ωo, N-S & Ωo, E-W	2.5
Deflection Amplification Factor, Cd, N-S & Cd, E-W	4.5
Fundamental Period of Structure, Ta, N-S as per Equation 12.8-7 of ASCE 7-10	0.31
Fundamental Period of Structure, Ta, E-W as per Equation 12.8-7 of ASCE 7-10	0.31

The slab is one-way slab having thickness of 5 inch. The slab thickness is calculated based on minimum thickness of one-way slab as per Table 7.3.1.1 of ASCE 318-14 (ACI, 2014). The floor slab diaphragm, it is a one-way 5 in. slab spanning across the frames with intermediate B4 (14in.X14in.) supporting beams, i.e., 10 ft slab span. All the vertical seismic force resisting elements in the models has fixed support in the foundation level. Reinforced Concrete Elements of these buildings are designed

considering seismic load from Equivalent lateral force procedure as per ASCE 7-10 (ASCE, 2010) and Reinforced Concrete Elements of these building models are detailed as per ACI 318-14 (ACI, 2014) which are summarized in **Tables 3-3 to 3-5**.

3.4 Modeling of Column, Shear wall and Beam in ETABS 2016

The columns and beams are modeled as frame element in ETABS 2016 (CSI, 2017). The shear walls are modeled as shell element in ETABS 2016. The moment of inertia of columns, beams and shear walls in models for elastic analysis at factored load level is taken as per Table 6.6.3.1.1(a) of ACI 318-14 (ACI, 2014). The shear walls in models are considered to be uncracked section in factored load level for elastic analysis.

3.5 Modeling of Slab

In this section, considerations for modeling slab for Models in ETABS 2016 (CSI, 2017) are discussed.

3.5.1 Modeling of slab as nonlinear layer shell element

The slabs in the buildings are modeled as nonlinear layer shell element. Coupled material behavior is considered for concrete materials of slab. The coupled material behavior of concrete forces all the in-plane stress components (S_{11}, S_{22}, and S_{33}) of the concrete to be nonlinear. **Figure 3-12** shows direct and shearing stress components of shell elements in ETABS 2016 (CSI, 2017). The coupled behavior of concrete uses the modified Darwin-Pecknold behavior which represents concrete compression, cracking, and shear behavior under both monotonic and cyclic loading, and accounts for crack rotation. The directional material behavior is considered for reinforcement in slab. The directional material behavior is used to independently control the behavior of three stress component. The S_{11} and S_{12} component of reinforcement are considered to behave nonlinearly. The S_{22} component of reinforcement is chosen to be inactive. We have considered that the reinforcement of slab will take shear after the cracking of concrete. Therefore we have chosen S_{12} component of reinforcement to be nonlinear instead of inactive.

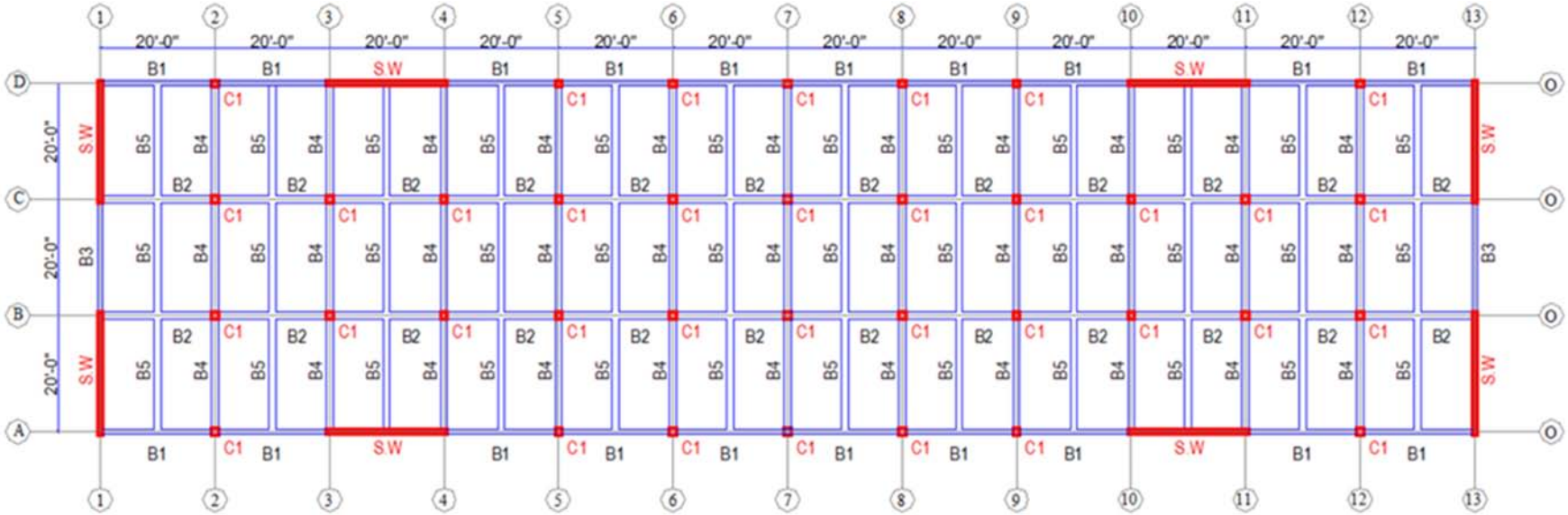

Figure 3-3 Layout Plan of Model-1

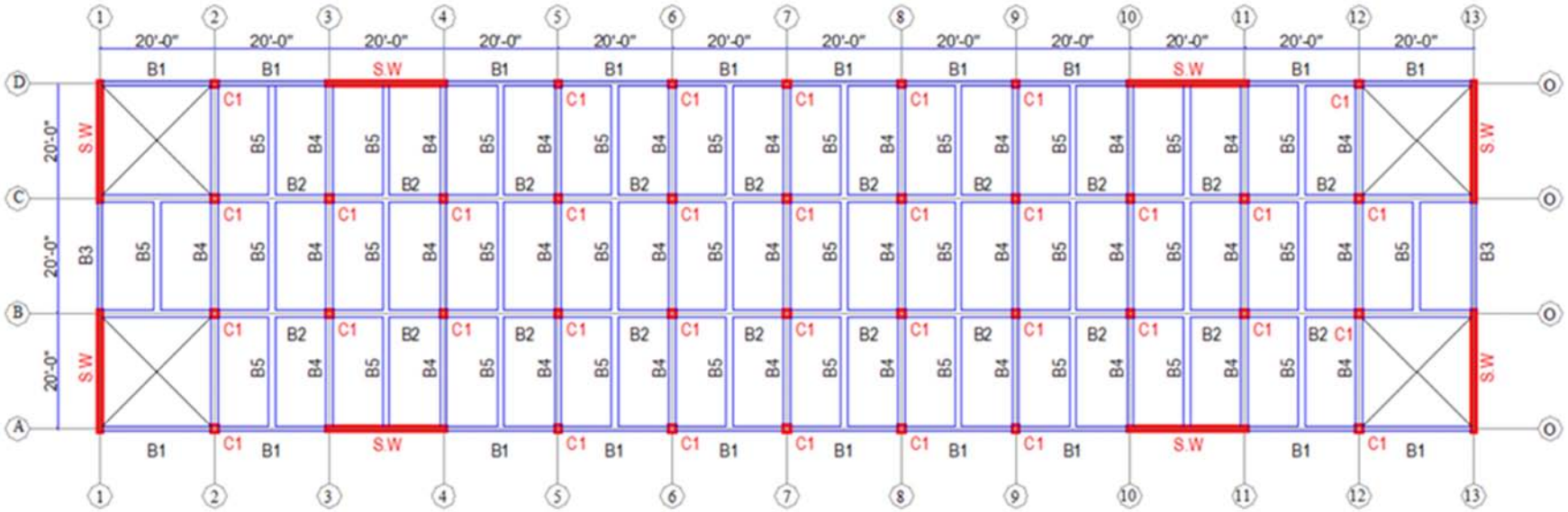

Figure 3-4 Layout Plan of Model-2

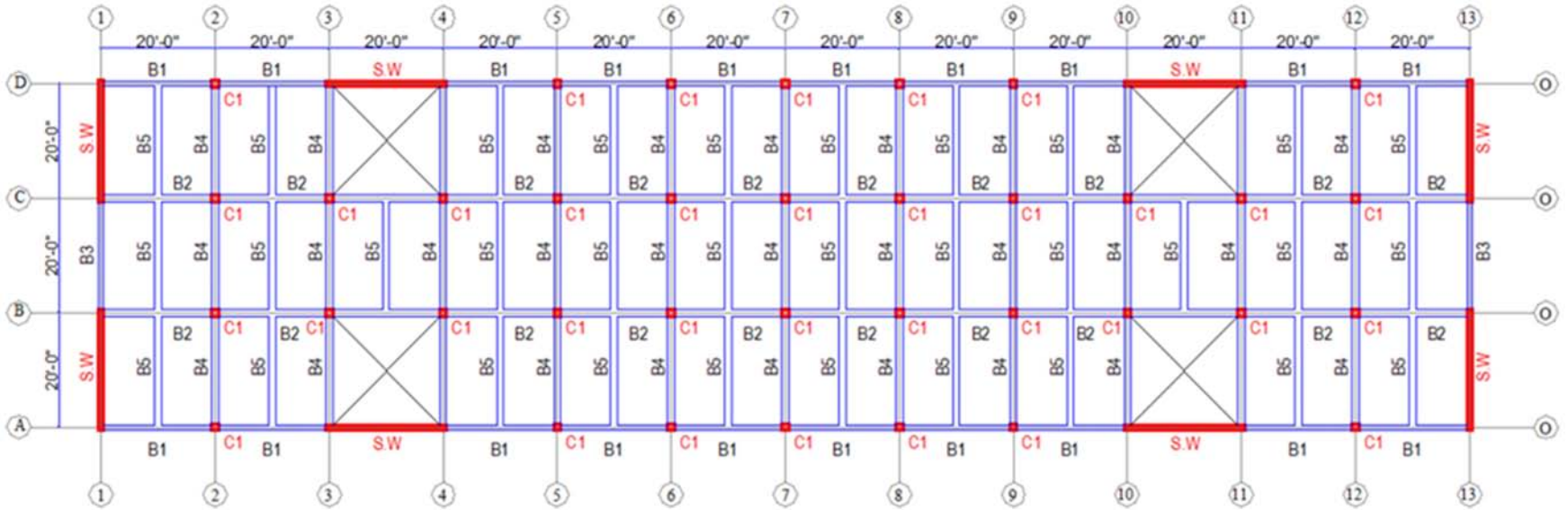

Figure 3-5 Layout Plan of Model-3

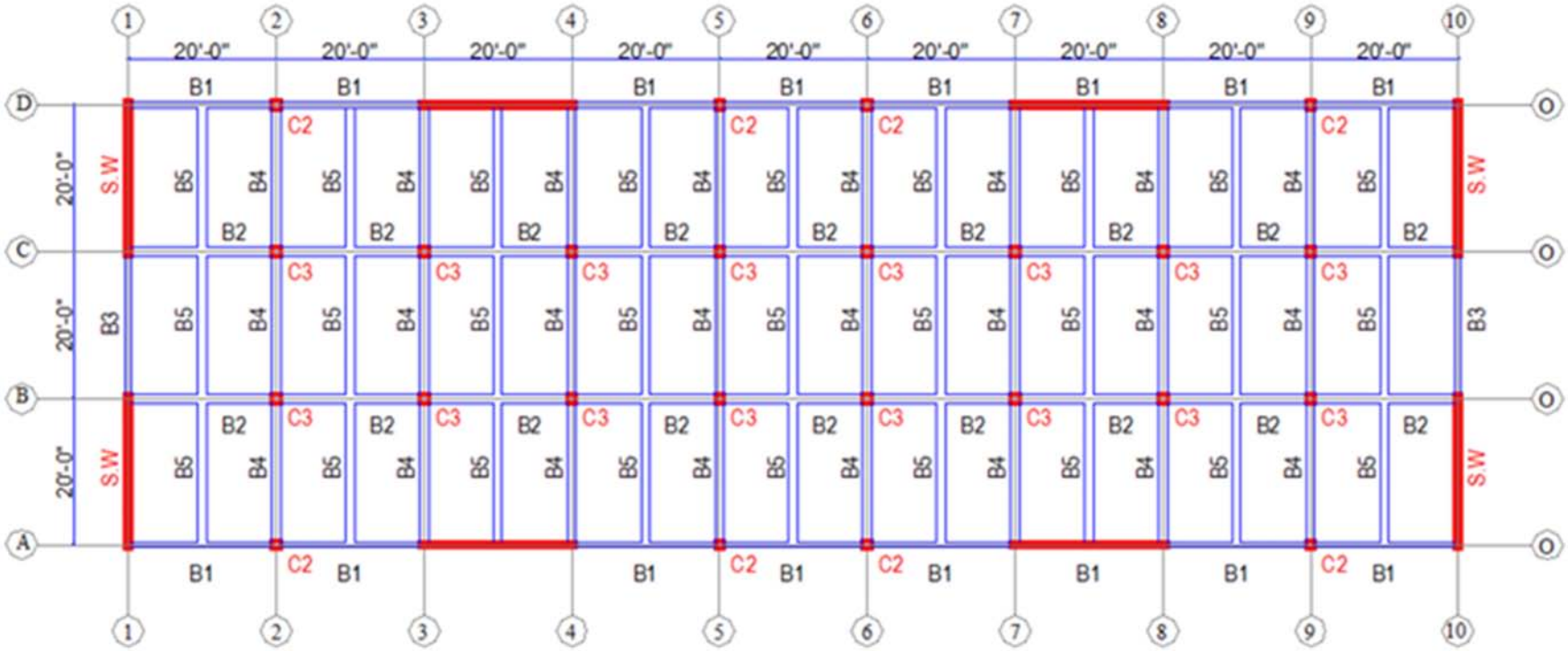

Figure 3-6 Layout Plan of Model-4

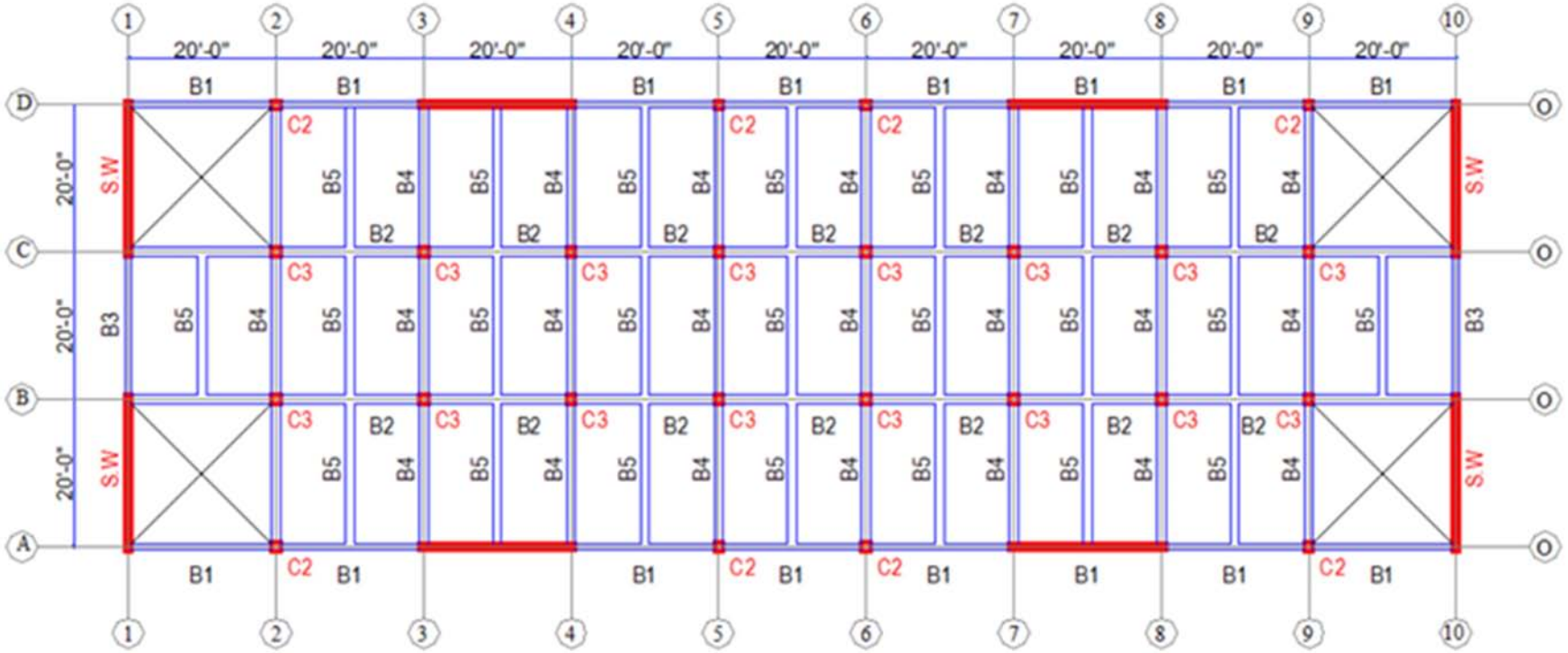

Figure 3-7 Layout Plan of Model-5

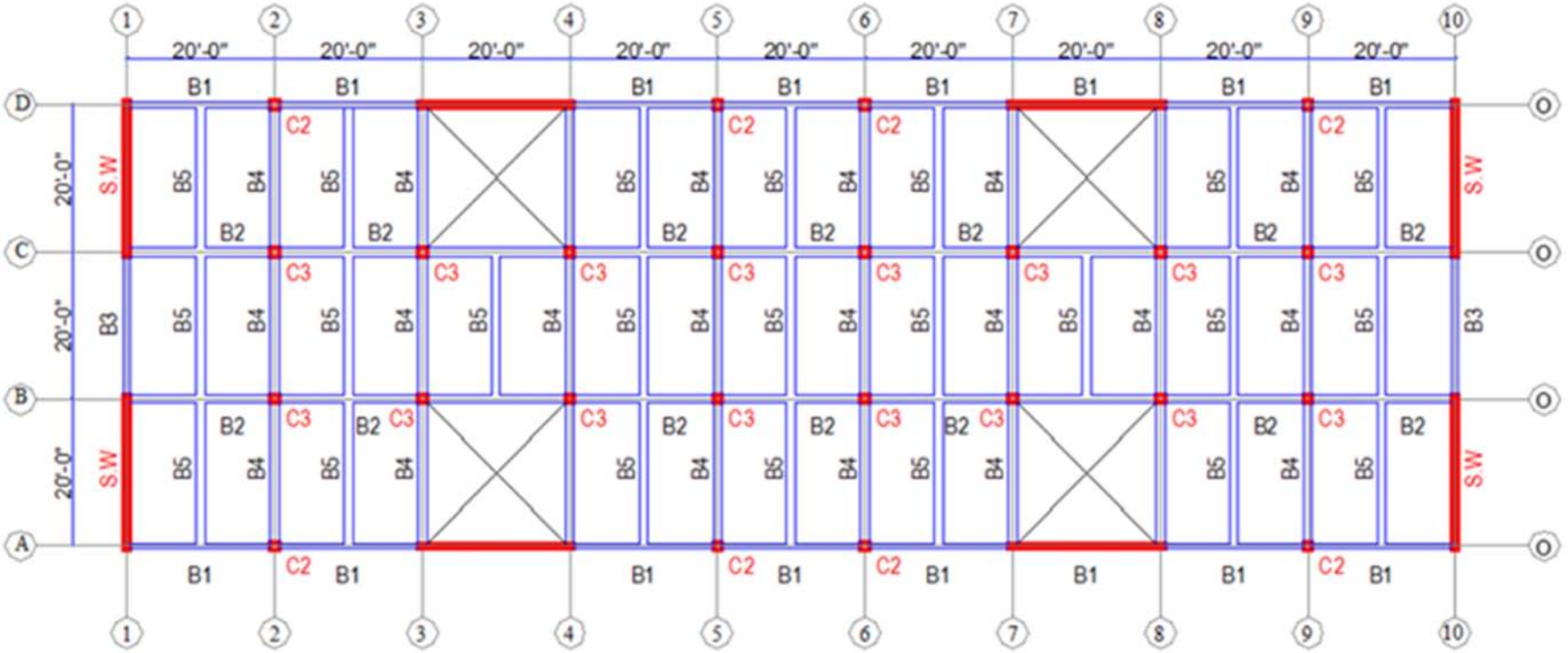

Figure 3-8 Layout Plan of Model-6

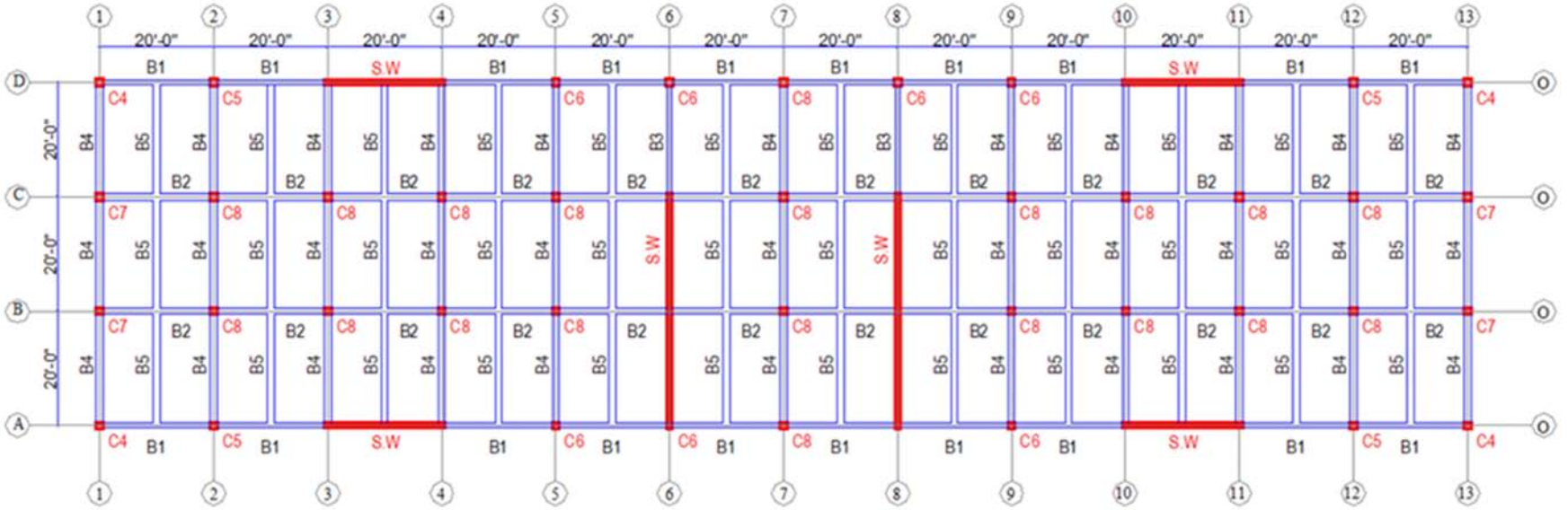

Figure 3-9 Layout Plan of Model-7

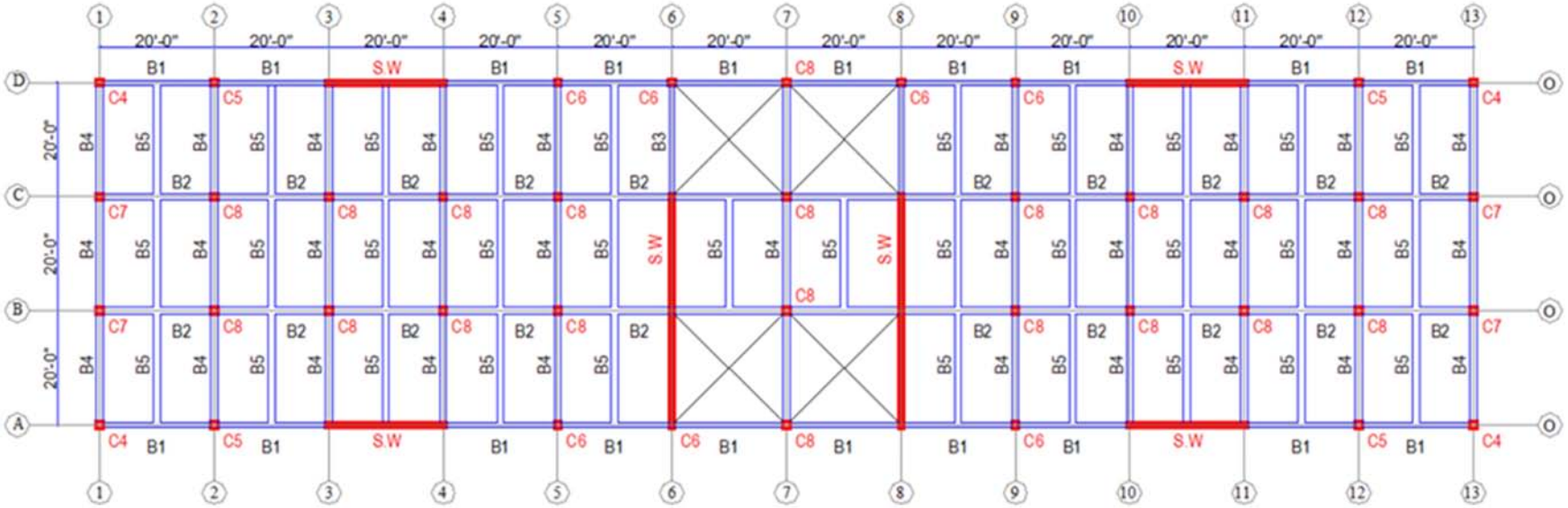

Figure 3-10 Layout Plan of Model-8

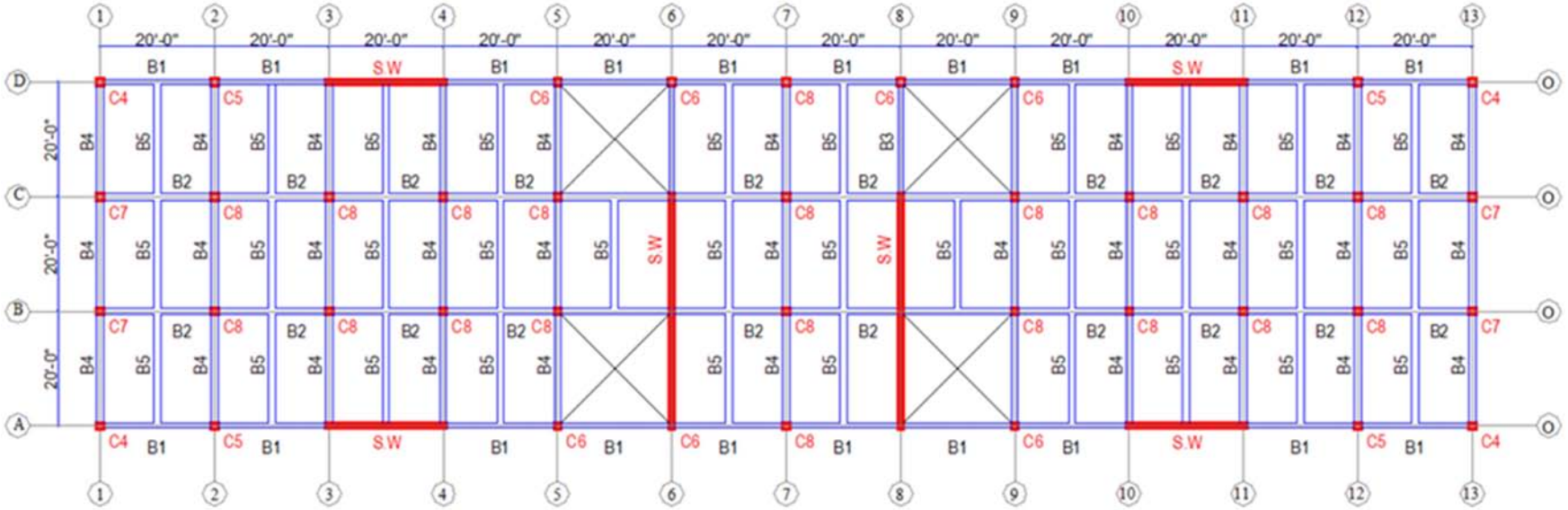

Figure 3-11 Layout Plan of Model-9

Table 3-3 Reinforced Concrete Elements Details per ACI 318-14 for Model-1, 2, 3

Element Type	Element Size	Reinforcement details
Slab	5 inch	10mm @ 12 inch c/c
Beam (B1)	10 in.X24 in.	Top= 3-16mm + 2-20mm (2-layer)
		Bottom=3-16mm + 2-20mm (2-layer)
		Stirrups=10mm @10inch c/c (2-leg)
Beam (B2)	14 in.X24 in.	Top= 2-16mm + 1-20mm
		Bottom=2-16mm + 1-20mm
		Stirrups=10mm @10inch c/c (2-leg)
Beam (B3)	10 in.X24 in.	Top= 2-16mm + 1-20mm
		Bottom=2-16mm + 1-20mm
		Stirrups=10mm @10inch c/c (2-leg)
Beam (B4)	14 in.X24 in.	Top= 2-16mm + 1-20mm
		Bottom=2-16mm + 1-20mm
		Stirrups=10mm @10inch c/c (2-leg)
Beam (B5)	14 in.X14 in.	Top= 2-16mm
		Bottom=2-16mm
		Stirrups=10mm @6 inch c/c (2-leg)
Column (C1)	14 in.X14 in.	4-16mm + 2-20mm
		Stirrups=10mm @7 inch c/c
Shear wall	10 inch	Vertical =16mm @ 18 inch c/c (at each face)
		Horizontal =12mm@14 inch (at each face)

Table 3-4 Reinforced Concrete Elements Details per ACI 318-14 for Model-4, 5, 6

Element Type	Element Size	Reinforcement details
Slab	5 inch	10mm @ 12 inch c/c
Beam (B1)	10 in.X24 in.	Top= 2-16mm + 4-20mm (2-layer)
		Bottom=2-16mm + 4-20mm (2-layer)
		Stirrups=10mm @10inch c/c (2-leg)
Beam (B2)	14 in.X24 in.	Top= 2-16mm + 1-20mm
		Bottom=2-16mm + 1-20mm
		Stirrups=10mm @10inch c/c (2-leg)
Beam (B3)	10 in.X24 in.	Top= 4-16mm + 1-20mm (2-layer)
		Bottom=4-16mm + 1-20mm (2-layer)
		Stirrups=10mm @10inch c/c (2-leg)
Beam (B4)	14 in.X24 in.	Top= 2-16mm + 1-20mm
		Bottom=2-16mm + 1-20mm
		Stirrups=10mm @10inch c/c (2-leg)
Beam (B5)	14 in.X14 in.	Top= 2-16mm
		Bottom=2-16mm
		Stirrups=10mm @6 inch c/c (2-leg)
Column (C2)	14 in.X14 in.	2-16mm + 4-25mm
		Stirrups=10mm @7 inch c/c
Column (C3)	14 in.X14 in.	4-16mm + 2-20mm
		Stirrups=10mm @7 inch c/c
Shear wall	10 inch	Vertical =16mm @ 18 inch c/c (at each face)
		Horizontal =12mm @14 inch (at each face)

Ondrej (2019) specifies that "Within layered shell objects, straight normals remain straight, which enforces full composite behavior between layers. Straight normals do not necessarily remain normal to the mid-surface, which allows transverse shear

deformation. For membrane and bending behavior, quadratic displacement fields are assumed, with appropriate handling to prevent shear locking. Plane-stress behavior is assumed within each layer."

Table 3-5 Reinforced Concrete Elements Details per ACI 318-14 for Model-7, 8, 9

Element Type	Element Size	Reinforcement details
Slab	5 inch	10mm @ 12 inch c/c
Beam (B1)	10 in.X24 in.	Top= 6-20mm (2-layer)
		Bottom=6-20mm (2-layer)
		Stirrups=10mm @10inch c/c (2-leg)
Beam (B2)	14 in.X24 in.	Top= 4-20mm
		Bottom=4-20mm
		Stirrups=10mm @10inch c/c (2-leg)
Beam (B3)	10 in.X24 in.	Top= 3-20mm
		Bottom=2-20mm
		Stirrups=10mm @10inch c/c (2-leg)
Beam (B4)	14 in.X24 in.	Top= 2-16mm + 1-20mm
		Bottom=2-16mm + 1-20mm
		Stirrups=10mm @10inch c/c (2-leg)
Beam (B5)	14 in.X14 in.	Top= 2-16mm
		Bottom=2-16mm
		Stirrups=10mm @6 inch c/c (2-leg)
Column (C4)	14 in.X14 in.	4-16mm + 4-20mm
		Stirrups=10mm @7 inch c/c
Column (C5)	14 in.X14 in.	2-16mm + 4-25mm
		Stirrups=10mm @7 inch c/c
Column (C6)	14 in.X14 in.	4-16mm + 2-25mm
		Stirrups=10mm @7 inch c/c
Column (C7)	14 in.X14 in.	8-20mm
		Stirrups=10mm @7 inch c/c
Column (C8)	14 in.X14 in.	4-16mm + 2-20mm
		Stirrups=10mm @7 inch c/c
Shear wall	10 inch	Vertical =16mm @ 18 inch c/c (at each face)
		Horizontal =12mm @14 inch (at each face)

The number of Integration points should be specified in the thickness direction for the layer. Nonlinear behavior may require more integration points or more layers in order to capture yielding near the top and bottom of surfaces. Five integration points are selected for concrete along thickness of concrete to capture yielding near the top and bottom of surfaces and one integration point is selected for reinforcement along equivalent layer thickness of reinforcement. **Figure 3-13** shows nonlinear layered shell property which are assigned in nonlinear layer shell.

3.5.2 Diaphragm In-plane Stiffness Modeling

Section 12.3.1.2 of ASCE 7-10 (ASCE, 2010) allows the diaphragm to be modeled as rigid diaphragm where the diaphragm has span to depth ratio of 3 or less in structure

without horizontal structural irregularity. In-plane deformation of diaphragm affects the design displacement and internal force distribution in structure where the diaphragm has large span to depth ratio. Opening in diaphragm can significantly reduce the in-plane rigidity of diaphragm. According to Section 12.3.1 of ASCE 7-10, the stiffness of diaphragms and vertical elements of seismic force-resisting system should be incorporated in the structural model. The diaphragm should be modeled as semi-rigid diaphragm where the diaphragm cannot be idealized as rigid or flexible diaphragm.

Guzman (2016) specifies "Semi-rigid diaphragm accounts actual in-plan stiffness properties and behavior of diaphragm. Diaphragm should be modeled as Semi-rigid diaphragm when diaphragm shows significant in-plane deformation". According to Moehle et al. (2010), Semi-rigid diaphragm can help to determine force acting between diaphragm and vertical elements of seismic force resisting system. Section cuts through a group of elements including semi-rigid diaphragm can give better knowledge of load path and load values where diaphragm is modeled as semi-rigid diaphragm. Saffarini and Qudaimat (1992) found that rigid-floor assumption is accurate for buildings without shear walls, but it can cause errors for building system with shear walls.

The diaphragm of Models with plan aspect ratio of 4:1 are not allowed to model as rigid diaphragm as per Section 12.3.1.2 of ASCE 7-10. Semi-rigid diaphragm in ETABS 2016 (CSI, 2017) accounts actual in-plan stiffness properties and behavior of diaphragm. Therefore, Models having diaphragm plan aspect ratio of 4:1 are modeled as semi-rigid diaphragm. The diaphragm of Models with plan aspect ratio of 3:1 are allowed to model as rigid diaphragm as per Section 12.3.1.2 of ASCE 7-10. However, rigid floor assumption can cause errors for building system with shear walls. According to Section 12.3.1 of ASCE 7-10, the diaphragm should be modeled as semi-rigid diaphragm where the diaphragm cannot be idealized as rigid or flexible diaphragm. Semi-rigid diaphragm in ETABS 2016 (CSI, 2017) accounts actual in-plan stiffness properties and behavior of diaphragm. Therefore, Models having diaphragm plan aspect ratio of 3:1 are also modeled as semi-rigid diaphragm.

3.5.3 Meshing of diaphragm

The Finite element mesh size should be 1/5 to 1/3 of the bay length or wall length to model the diaphragm flexibility (Moehle et al., 2010). Finite element mesh size should be moderately fine when section cut is made in the diaphragm to determine load path

and shear distribution in diaphragm. The mesh size is taken 24in.X24in. for diaphragm of the models to be analyzed.

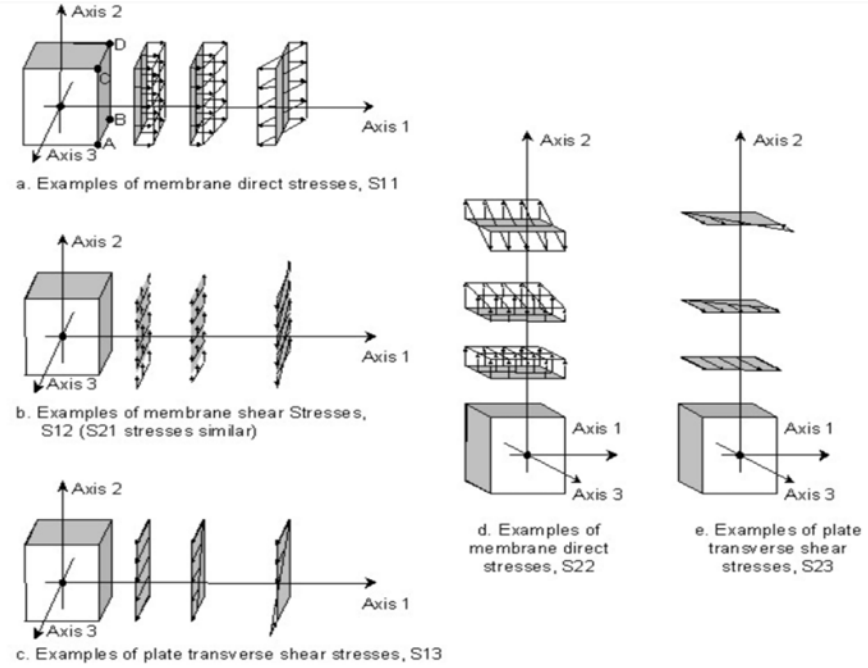

Figure 3-12 Direct and shearing stress components of shell elements in ETABS 2016 (Shell element internal stresses, n.d)

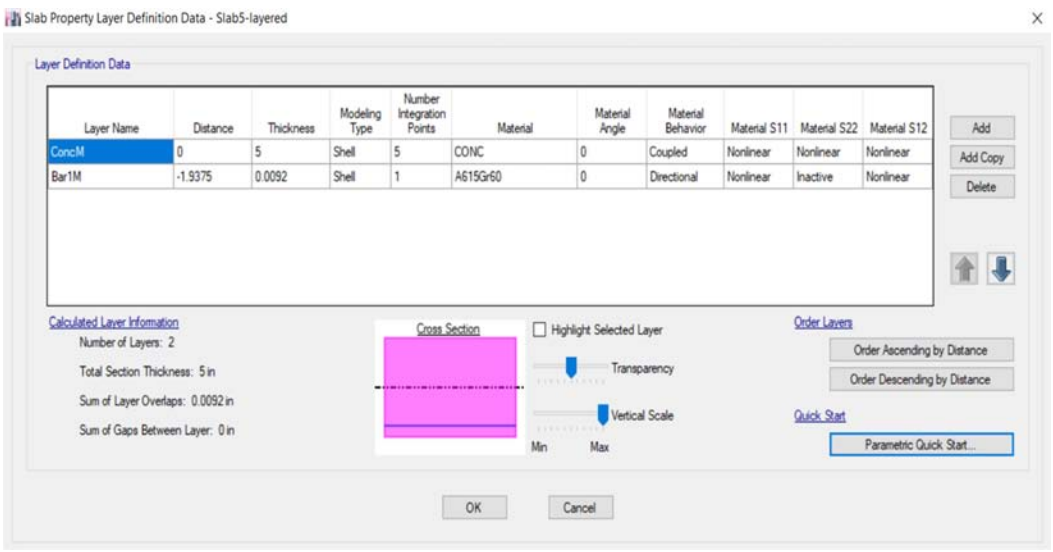

Figure 3-13 Slab modeling (Nonlinear layered shell) in ETABS 2016 (CSI, 2017)

3.6 Diaphragm Design Forces (Analytical Investigations Procedures)

Six procedures are used to determine diaphragm design forces which are described below.

ELFA Method-1: Diaphragm Design Force will be determined from Equivalent Lateral Force Procedure as per section 12.8 of ASCE 7-10 (ASCE, 2010). This is referred as ELFA Method-1 in this thesis paper.

ELFA Method-2: Diaphragm Design forces will be determined as per section 12.10.1.1 of ASCE 7-10 (ASCE, 2010). The story shear forces from equivalent lateral force analysis as per section 12.8 of ASCE 7-10 will be used in Eq. 12.10-1 of ASCE 7-10 to determine diaphragm design forces. This is referred as ELFA Method-2 in this thesis paper.

RSA Method-1: Diaphragm Design Force will be determined from Modal Response Spectrum Analysis as per section 12.9 of ASCE 7-10 (ASCE, 2010). This is referred as RSA Method-1 in this thesis paper.

RSA Method-2: Diaphragm Design forces will be determined as per section 12.10.1.1 of ASCE 7-10 (ASCE, 2010). The story shear forces from Modal Response Spectrum Analysis as per section 12.9 of ASCE 7-10 are used in Eq. 12.10-1 of ASCE 7-10 to determine diaphragm design forces. This is referred as RSA Method-2 in this thesis paper.

Linear Response History Analysis (LRHA): Diaphragm Design Forces will be determined From Linear Response History Analysis as per Chapter 16 of ASCE 7-10 (ASCE, 2010). This will be referred as LRHA in this thesis paper.

Nonlinear Static Analysis (NSP): Diaphragm Design Forces are determined From Nonlinear static procedure as per ASCE 41-13 (ASCE, 2014). Diaphragm Design Forces will be determined at 1.5 times of target displacement. The target displacement represents the maximum displacement likely to be experienced in the building for the selected Seismic hazard level. Diaphragm Design Forces are also be determined for concurrent seismic effects in nonlinear static procedure.

3.6.1 ELFA method-1

Diaphragm Design Force is determined from Equivalent Lateral Force Procedure as per section 12.8 of ASCE 7-10 (ASCE, 2010). According to Moehle et al. (2010), diaphragms and collectors are permitted to be designed for seismic forces applied independently in each of the two orthogonal directions. The structures assigned to

Seismic Design Categories C through F and having non-parallel systems or plan irregularity type 5 should consider Orthogonal Combination Procedure or Simultaneous Application of Orthogonal Ground Motion but diaphragm design must also consider the interaction of orthogonal loading. If the Equivalent Lateral Force Procedure or Modal Response Spectrum Analysis is used, 100 percent of the seismic load effects in one primary direction are to be combined with 30 percent of the seismic load effects in the other direction. Though not required by ASCE 7, common practice is to consider the orthogonal combination for all diaphragm and collector design. According to section 4.1.5.4.1 of FEMA P-751 (FEMA, 2012), the accidental torsion should be considered with orthogonal loading effects. When orthogonal load effects are included in the analysis, four directions of seismic force (+X, -X, +Y, -Y) must be considered and for each direction of force, there are two possible directions in which the accidental eccentricity can apply (causing positive or negative torsion). This requires a total of eight possible combinations of direct force plus accidental torsion. Where 100 percent of the seismic load effects in one primary direction are combined with 30 percent of the seismic load effects in the other direction, the number of load combinations increases to 16 because, for each direct application of load, a positive or negative orthogonal loading can exist. **Figure 3-14** shows orthogonal loading conditions applicable for ELFA Method-1.

We have defined six seismic loads in load pattern in ETABS 2016 (CSI, 2017) are as follows:

EQ_X = Seismic load in positive X direction.

EQ_X (+5%Y) = Seismic load in positive X direction with accidental eccentricity of 5% of building length from C.G along positive Y-direction.

EQ_X (-5%Y) = Seismic load in positive X direction with accidental eccentricity of 5% of building length from C.G along negative Y-direction.

EQ_Y = Seismic load in positive Y direction.

EQ_Y (+5%X) = Seismic load in positive Y direction with accidental eccentricity of 5% of building width from C.G along positive X-direction.

EQ_Y (-5%X) = Seismic load in positive Y direction with accidental eccentricity of 5% of building width from C.G along negative X-direction.

These six seismic loads are applied independently in each of the two orthogonal directions in the models. Then we have created 16 directional load combinations based on the defined seismic load in load patterns in ETABS 2016 (CSI, 2017) are as follows: Sixteen basic load combinations are created in ELFA Method-1 Analysis including accidental torsion and orthogonal loading effects as per FEMA P-751(FEMA, 2012) which are shown below.

[1]=100 %(+5%Y) EQ_X + 30% EQ_Y

[2]=-100%(-5%Y) EQ_X + 30% EQ_Y

[3]=30% EQ_X -+100% EQ_Y(-5%X)

[4]= 30% EQ_X -100% EQ_Y (-5%X)

[5]= 100 %(-5%Y) EQ_X + 30% EQ_Y

[6]= -100%(-5%Y) EQ_X + 30% EQ_Y

[7]= 30 % EQ_X + 100% (+5%X) EQY

[8]= 30 % EQ_X - 100% (+5%X) EQY

[9]= 100 %(+5%Y) EQ_X - 30% EQ_Y

[10]= -100 %(+5%Y) EQ_X - 30% EQ_Y

[11]= - 30% EQ_X + 100% (-5%X) EQ_Y

[12]= - 30% EQ_X - 100% (-5%X) EQ_Y

[13]= 100% (-5%Y) EQX - 30%EQ_Y

[14]= -100% (-5%Y) EQX - 30%EQ_Y

[15]= - 30% EQ_X + 100% (+5%X) EQ_Y

[16]= - 30% EQ_X - 100% (+5%X) EQ_Y

Eight extra load combinations in ELFA Method-1 Analysis excluding Accidental Torsion are shown below which are also used because the effect of accidental torsion should be ignored if it reduces shear in vertical load resisting element.

[17]= 100% EQ_X + 30% EQ_Y

[18]= 100% EQ_X - 30% EQ_Y

[19]= - 100% EQ_X + 30% EQ_Y

[20]= - 100% EQ_X - 30% EQ_Y

[21]= 30% EQ_X + 100% EQ_Y

[22]= 30% EQ_X - 100% EQ_Y

[23]= -30% EQ_X + 100% EQ_Y

[24]= -30% EQ_Y - 100% EQ_Y

The basic load combinations for strength design as per section 12.4.2.3 of ASCE 7-10 (ASCE, 2010) with orthogonal seismic loading and accidental torsion create 48 load combinations to determine diaphragm forces which are shown in **Appendix A**.

The basic load combinations with overstrength factor for strength design as per section 12.4.3.2 of ASCE 7-10 (ASCE, 2010) with orthogonal seismic loading and accidental torsion create 48 load combinations to determine collector forces and chord forces in diaphragm which are shown in **Appendix A**.

3.6.2 ELFA method-2

Diaphragm Design forces will be determined as per section 12.10.1.1 of ASCE 7-10 (ASCE, 2010). The story shear forces from equivalent lateral force analysis as per section 12.8 of ASCE 7-10 are used in Eq. 12.10-1 of ASCE 7-10 to determine diaphragm design force for each story level. The diaphragm design force from ELFA method-2 as per Eq.12.10-1 of ASCE 7-10 is as follows

$$F_{px} = \frac{\sum_{i=1}^{n} Fi}{\sum_{i=1}^{n} wi} w_{px} \qquad \text{Eq. 3-1}$$

Where

$F_{px} =$ the diaphragm design force

$F_i =$ the design force from Equivalent lateral force analysis applied to level i

$w_i =$ the weight tributary to level i

$w_{px} =$ the weight tributary to the diaphragm at level x

In here, the design force applied to level i (Fi) is the seismic story shear obtained from equivalent lateral force analysis.

The diaphragm design force from Eq.12.10-1 should not be less than diaphragm design force from Eq.12.10-2 of ASCE 7-10 (ASCE, 2010) as follows

$$F_{px} = 0.2 S_{DS} I_e w_{px} \qquad \text{Eq. 3-2}$$

The diaphragm design force from Eq.12.10-1 should not be greater than diaphragm design force from Eq.12.10-3 of ASCE 7-10 (ASCE, 2010) as follows

$$F_{px} = 0.4 S_{DS} I_e w_{px}$$ Eq. 3-3

Importance factor Ie =01 and S_{DS} = 0.383 (for seismic zone-2 and Soil type-SC as per Table 6.C.4 of BNBC (2017), Appendix C). Diaphragm design forces in X-direction as per Eq.12.10-1 of ASCE 7-10 (2010) without accidental eccentricity for Model-1 is shown in **Table 3-6.**

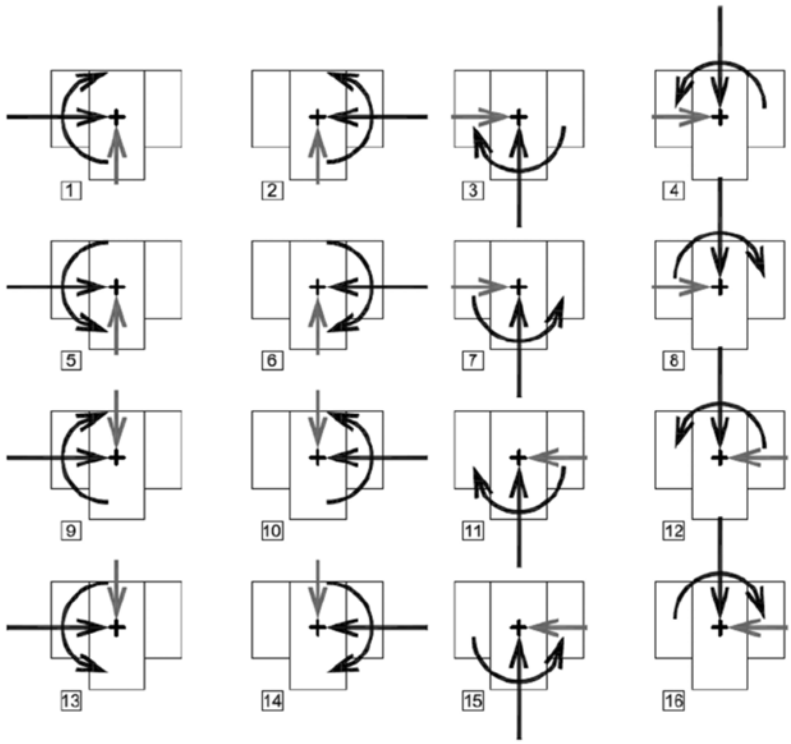

Figure 3-14 Orthogonal Loading conditions applicable for ELF analysis (FEMA, 2016)

Table 3-6. Diaphragm design forces in X-direction as per Eq.12.10-1 of ASCE 7-10 (2010) without accidental eccentricity for Model-1, EQpx

Story	Wpx(kips)	Fx(kips)	∑Fi (kips)	∑Wi (kips)	Fpx(kips)	Fpx,mim (kips)	Fpx,max(kips)	Fpx,design (kips)
Story 3	2182	241	241	2182	241	167	334	241
Story 2	2360	174	415	4542	216	181	362	216
Story 1	2360	87	502	6902	172	181	362	181

EQpx = Diaphragm design forces in X-direction as per Eq.12.10-1 of ASCE 7-10 (ASCE, 2010) without accidental eccentricity.

(+5%Y)EQpx = Diaphragm design forces in X-direction as per Eq.12.10-1 of ASCE 7-10 (ASCE, 2010) with accidental eccentricity of 5% of building length form C.G along positive Y-direction.

(-5%Y)EQpx = Diaphragm design forces in X-direction as per Eq.12.10-1 of ASCE 7-10 (ASCE, 2010) with accidental eccentricity of 5% of building length form C.G along negative Y-direction.

EQpy = Diaphragm design forces in Y-direction as per Eq.12.10-1 of ASCE 7-10 (ASCE, 2010) without accidental eccentricity.

(+5%X)EQpy = Diaphragm design forces in Y-direction as per Eq.12.10-1 of ASCE 7-10 (ASCE, 2010) with accidental eccentricity of 5% of building width form C.G along positive X-direction.

(-5%X)EQpy = Diaphragm design forces in Y-direction as per Eq.12.10-1 of ASCE 7-10 (ASCE, 2010) with accidental eccentricity of 5% of building width form C.G along negative X-direction.

These six seismic loads are applied independently in each of the two orthogonal directions in the models. Diaphragm design forces as per Eq.12.10-1 of ASCE 7-10 (ASCE, 2010) for EQpx, (+5%Y), EQpx, (-5%Y)EQpx, EQpy, (+5%X)EQpy and (-5%X)EQpy are same as accidental torsion does not change Fx (story shear from ELFA method-1).

The basic load combinations for strength design with orthogonal seismic loading and accidental torsion to determine diaphragm forces for ELFA Method-2 are as same as ELFA Method-1, which are shown in **Appendix-A**.

The basic load combinations with overstrength factor for strength design with orthogonal seismic loading and accidental torsion to determine collector forces and chord forces in diaphragm for ELFA Method-2 are as same as ELFA Method-1, which are shown in **Appendix-A**.

3.6.3 RSA method-1

Diaphragm Design Force will be determined from Modal Response Spectrum Analysis as per section 12.9 of ASCE 7-10 (ASCE, 2010). This is referred as RSA Method-1 in this thesis paper. BNBC-2017 (HBRI & BRTC, 2017) Design Acceleration Response Spectra for Seismic Zone-2 and Soil Type SC is presented in **Figure 3-15** for modal response spectrum analysis.

Sufficient numbers of modes are considered in response spectrum analysis so that combined modal mass participation of modes obtains at least 90 percent of the actual mass in each of the orthogonal horizontal directions of response considered by the model as per Section 12.9.1 of ASCE 7-10 (ASCE, 2010).The CQC technique for modal combination provides better results than the SRSS method for the case of closely spaced modes as per Section 12.9.3 of ASCE 7-10. Therefore we have selected CQC modal combination method**.**

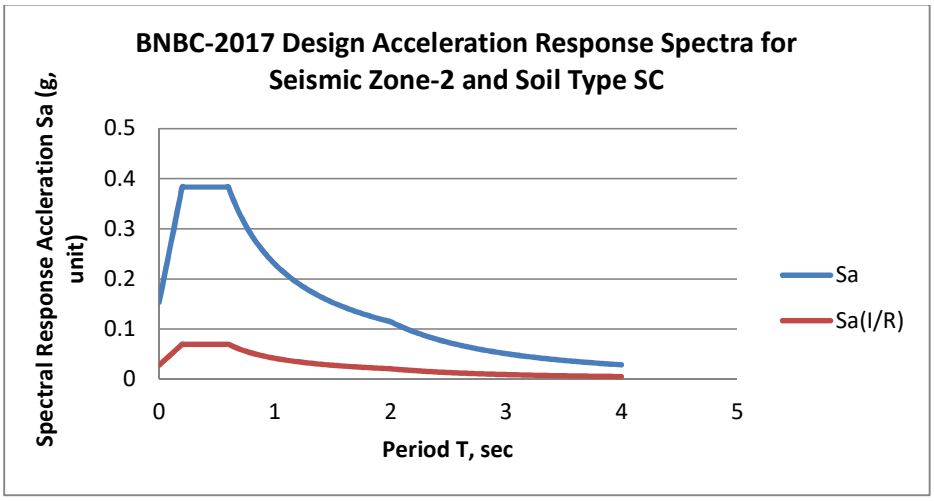

Figure 3-15 BNBC-2017 (HBRI & BRTC, 2017) Design Acceleration Response Spectra for Seismic Zone-2 and Soil Type SC.

The amplification of torsion is not required where accidental torsion effects are included in the dynamic analysis mode as per section 12.9.5 of ASCE 7-10 (ASCE, 2010). We have used this approach to include the effect of accidental torsion in modal response spectrum analysis. The details of the above mentioned approach as per section 4.1.6.3 of FEMA P-751(FEMA, 2012) is as follows:

At first center of mass of diaphragm is displaced plus or minus 5 percent of the diaphragm dimension perpendicular to the direction of the applied response spectrum. The displacement of center of mass along plus and minus 5% of the diaphragm length and width creates four mass locations. As there are four possible mass locations, this will require four separate modal analyses for torsion with each analysis using a different set of mode shapes and frequencies. Then four Modal response spectrum analyses {(+5%Y) RSX, (-5%Y) RSX, (+5%X) RSY, (-5%X) RSY} are performed using these four separate modal analyses.

Additionally two more response spectrum analyses are performed for X (RSX) and Y (RSY) directions without considering accidental torsion.

All the response quantities are scaled up to 85% of base shear from ELFA Method-1 analysis when the response quantities from modal analysis corresponding to a total base shear is less than 85% of the base shear computed from the ELFA Method-1 analysis procedure as per section 12.9.4.1 of ASCE 7-10 (ASCE, 2010).

Six basic load combinations are created in RSA Method-1 including accidental torsion and orthogonal loading effects.

[1]= RSX + 0.3RSY

[2]= 0.3RSX + RSY

[3]= (+5%Y) RSX + 0.3RSY

[4]= (-5%Y) RSX + 0.3RSY

[5]= 0.3RSX + (+5%X) RSY

[6]= 0.3RSX + (-5%X) RSY

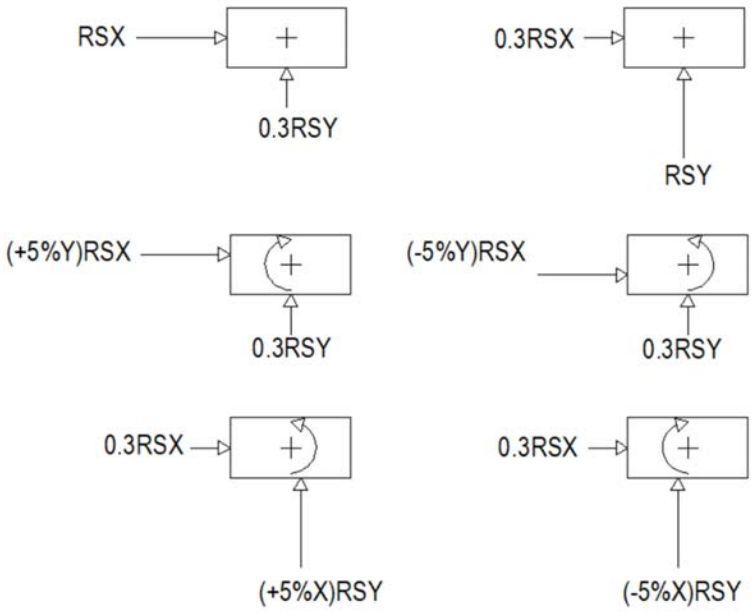

Figure 3-16 Orthogonal Loading conditions applicable for RSA analysis

Figure 3-16 shows orthogonal loading that are applicable for modal response spectrum analysis (RSA Method-1). These six load combinations are used in the basic load combinations for strength design as per section 12.4.2.3 of ASCE 7-10 (ASCE, 2010)

to determine diaphragm forces from Modal response spectrum analysis which are shown in **Appendix-B**. The basic load combinations with overstrength factor for strength design as per section 12.4.3.2 of ASCE 7-10 (ASCE, 2010) with the above mentioned six load combinations are used to determine collector forces from Modal response spectrum analysis which are shown in **Appendix-B**.

3.6.4 RSA method-2

Diaphragm Design forces are determined as per section 12.10.1.1 of ASCE 7-10 (ASCE, 2010). The story shear forces from Response spectrum analysis as per section 12.9 of ASCE 7-10 are used in Eq. 12.10-1 of ASCE 7-10 to determine diaphragm design forces for each story level. The diaphragm design force from RSA method-2 as per Eq.12.10-1 of ASCE 7-10 is as same as ELFA method-2. The only difference between ELFA method-2 and RSA method-2 is that RSA method-2 uses the design force from Response spectrum analysis (RSA Method-1) applied to level i (F_i) for calculation of diaphragm design force.

Importance factor I_e =01 and S_{DS} = 0.383 (for seismic zone-2 and Soil type-SC as per Table 6.C.4 of Appendix C of BNBC-2017 (HBRI & BRTC, 2017). The diaphragm design forces as per Eq.12.10-1 of ASCE 7-10 (2010) for Model-1 using story shear from RSA Method-1 are shown in **Tables 3-7 to 3-12**.

Table 3-7. Diaphragm design forces in X-direction as per Eq.12.10-1 of ASCE 7-10 (2010) without accidental eccentricity for Model-1, RSpx

Story	Wpx(kips)	Fx(kips)	∑Fi (kips)	∑Wi (kips)	Fpx(kips)	Fpx,mim (kips)	Fpx,max(kips)	Fpx,design (kips)
Story 3	2182	230	230	2182	230	167	334	230
Story 2	2360	139	369	4542	192	181	362	192
Story 1	2360	57	427	6902	146	181	362	181

Table 3-8. Diaphragm design forces in X-direction as per Eq.12.10-1 of ASCE 7-10 (2010) with accidental eccentricity of 5% of building length form C.G along positive Y direction for Model-1, (+5%Y)RSpx

Story	Wpx(kips)	Fx(kips)	∑Fi (kips)	∑Wi (kips)	Fpx(kips)	Fpx,mim (kips)	Fpx,max(kips)	Fpx,design (kips)
Story 3	2182	230	230	2182	230	167	334	230
Story 2	2360	139	369	4542	192	181	362	192
Story 1	2360	57	427	6902	146	181	362	181

The basic load combinations for strength design with orthogonal seismic loading and accidental torsion to determine diaphragm forces for RSA Method-2 are as same as ELFA Method-1, which are shown in **Appendix-A**.

Table 3-9. Diaphragm design forces in X-direction as per Eq.12.10-1 of ASCE 7-10 (2010) with accidental eccentricity of 5% of building length form C.G along negative Y direction for Model-1, (-5%Y)RSpx

Story	Wpx(kips)	Fx(kips)	∑Fi (kips)	∑Wi (kips)	Fpx(kips)	Fpx,mim (kips)	Fpx,max(kips)	Fpx,design (kips)
Story 3	2182	230	230	2182	230	167	334	230
Story 2	2360	139	369	4542	192	181	362	192
Story 1	2360	57	427	6902	146	181	362	181

Table 3-10. Diaphragm design forces in Y-direction as per Eq.12.10-1 of ASCE 7-10 (2010) without accidental eccentricity for Model-1, RSpy

Story	Wpx(kips)	Fx(kips)	∑Fi (kips)	∑Wi (kips)	Fpx(kips)	Fpx,mim (kips)	Fpx,max(kips)	Fpx,design (kips)
Story 3	2182	224	224	2182	224	167	334	224
Story 2	2360	139	363	4542	189	181	362	189
Story 1	2360	64	427	6902	146	181	362	181

Table 3-11. Diaphragm design forces in Y-direction as per Eq.12.10-1 of ASCE 7-10 (2010) with accidental eccentricity of 5% of building width form C.G along positive X direction for Model-1, (+5%X)RSpy

Story	Wpx(kips)	Fx(kips)	∑Fi (kips)	∑Wi (kips)	Fpx(kips)	Fpx,mim (kips)	Fpx,max(kips)	Fpx,design (kips)
Story 3	2182	224	224	2182	224	167	334	224
Story 2	2360	139	363	4542	189	181	362	189
Story 1	2360	63	427	6902	146	181	362	181

Table 3-12. Diaphragm design forces in Y-direction as per Eq.12.10-1 of ASCE 7-10 (2010) with accidental eccentricity of 5% of building width form C.G along negative X-direction for Model-1, (-5%X)RSpy

Story	Wpx(kips)	Fx(kips)	∑Fi (kips)	∑Wi (kips)	Fpx(kips)	Fpx,mim (kips)	Fpx,max(kips)	Fpx,design (kips)
Story 3	2182	224	224	2182	224	167	334	224
Story 2	2360	139	363	4542	189	181	362	189
Story 1	2360	63	427	6902	146	181	362	181

The basic load combinations with overstrength factor for strength design with orthogonal seismic loading and accidental torsion to determine collector forces and chord forces in diaphragm for RSA Method-2 are as same as ELFA Method-1, which are shown in **Appendix-A**.

3.6.5 Modal response history analysis

The number of pair of ground motions should be at least three as section 16.1.3 of ASCE 7-10 (ASCE, 2010). We have selected four (04) pair of un-scaled ground motions from PEER NGA Strong Ground Motion Database for performing Modal linear response history analysis. Ground motions used for Modal linear response history analysis are shown in **Table 3-13**. **Figures 3-17 to 3-24** shows acceleration time history of ground motions used for modal linear response history analyses.

Table 3-13 Ground motion used for Modal linear response history analysis

Earthquake Event name	Station name	Magnitude	Component source motion	PGA(g unit)	Record Name used for Analysis
Loma Prieta	Corralitos	6.93	1989-Horizontal component-1	0.64	A00
			1989-Horizontal component-2	0.48	A90
San Fernando	Pacoima Dam (upper left abut)	6.61	1971-Horizontal component-1	1.22	B00
			1971-Horizontal component-2	1.24	B90
Parkfield	Cholame - Shandon Array #5	6.19	1966-Horizontal component-1	0.44	C00
			1966-Horizontal component-2	0.37	C90
Loma Prieta	Gilroy - Historic Bldg.	6.93	1989-Horizontal component-1	0.29	D00
			1989-Horizontal component-2	0.24	D90

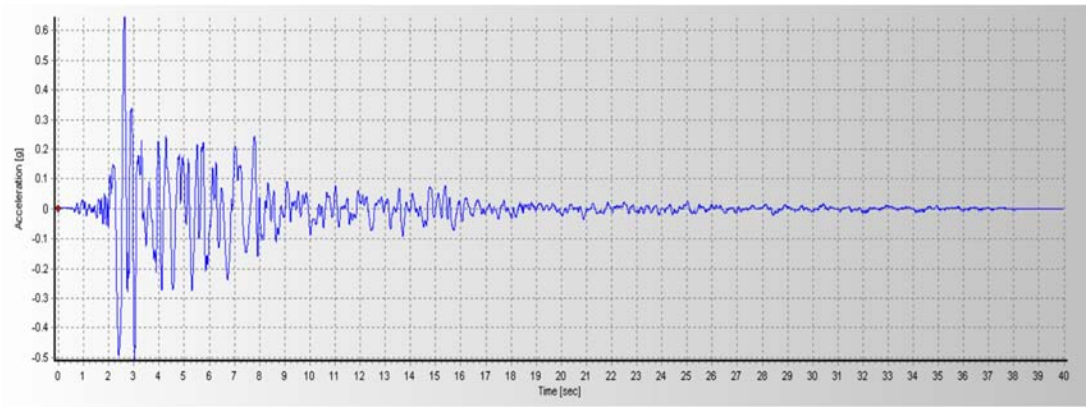

Figure 3-17 Acceleration time history of Loma Prieta - Corralitos - 1989-Horizontal component-1 from SeismoSignal (SeismoSoft, 2016)

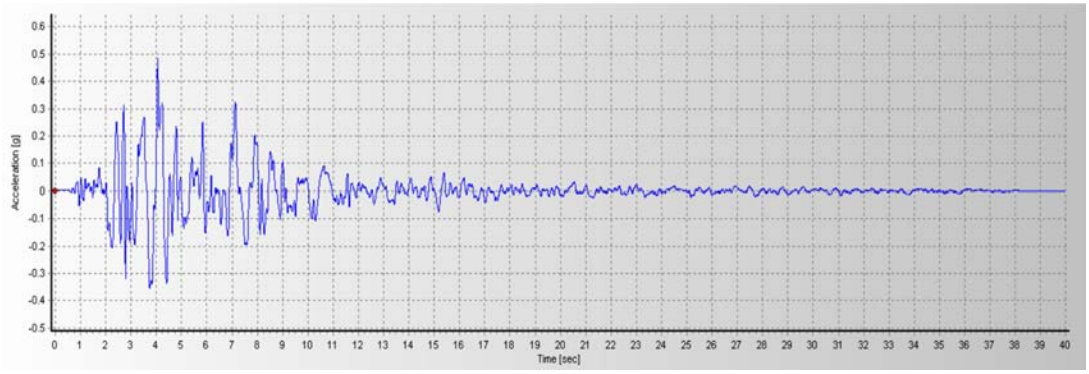

Figure 3-18 Acceleration time history of Loma Prieta - Corralitos - 1989-Horizontal component-2 from SeismoSignal (SeismoSoft, 2016)

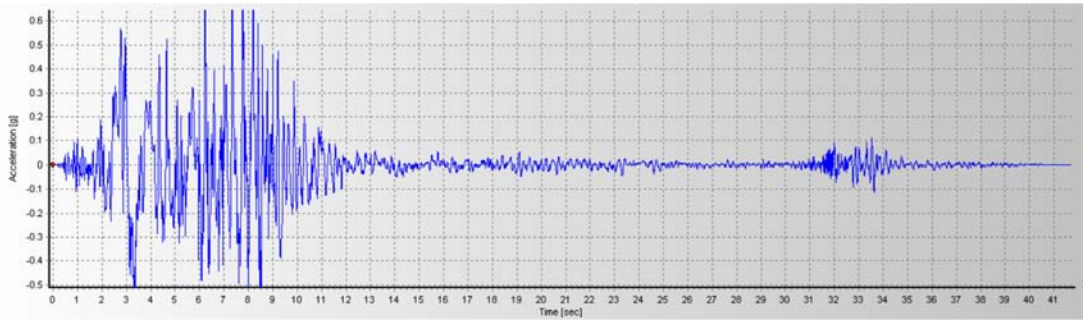

Figure 3-19 Acceleration time history of San Fernando - Pacoima -1971-Horizontal component-1 from SeismoSignal (SeismoSoft, 2016)

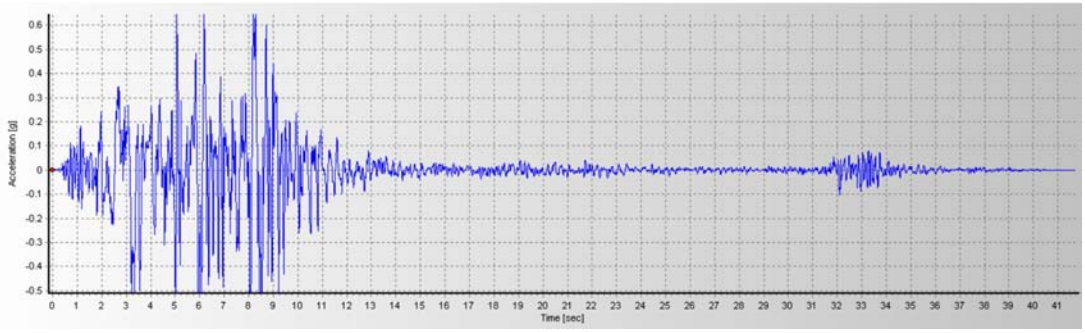

Figure 3-20 Acceleration time history of San Fernando - Pacoima -1971-Horizontal component-2 from SeismoSignal (SeismoSoft, 2016)

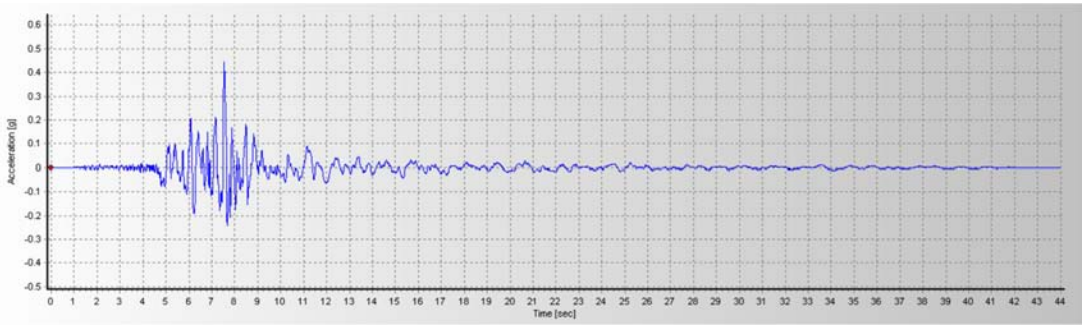

Figure 3-21 Acceleration time history of Parkfield-1966-Cholame - Shandon Array #5-Horizontal component-1 from SeismoSignal (SeismoSoft, 2016)

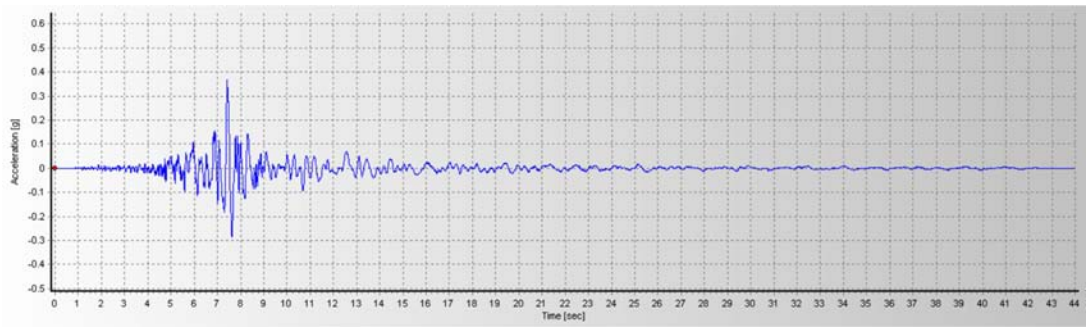

Figure 3-22 Acceleration time history of Parkfield-1966-Cholame - Shandon Array #5-Horizontal component-2 from SeismoSignal (SeismoSoft, 2016)

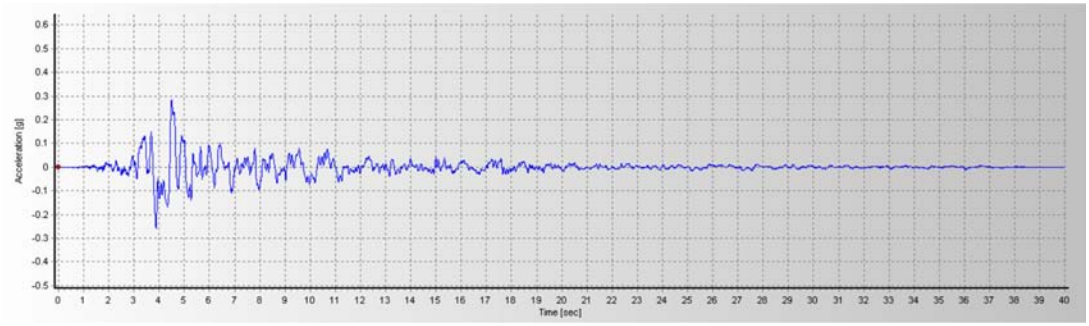

Figure 3-23 Acceleration time history of Loma Prieta - Gilroy - Historic Bldg - 1989-Horizontal component-1 from SeismoSignal (SeismoSoft, 2016)

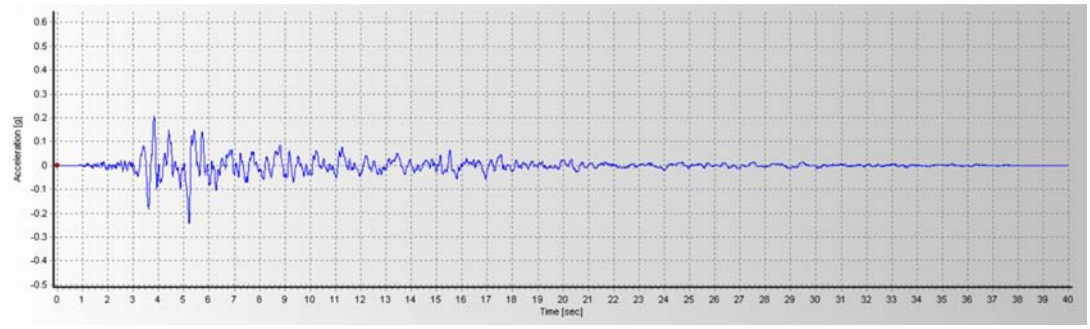

Figure 3-24 Acceleration time history of Loma Prieta - Gilroy - Historic Bldg - 1989-Horizontal component-2 from SeismoSignal (SeismoSoft, 2016)

3.6.5.i Scaling of ground motions for compatibility with the design spectrum

The ground motions must be scaled for compatibility with the design spectrum before using it in the response history analysis. The scaling procedures for three-dimensional

dynamic analysis are performed by following the procedures described in section 4.1.7.1 of FEMA P-751 (FEMA, 2012). Ground motions scaling procedures described in section 4.1.7.1 of FEMA P-751 follows the requirements of Section 16.1.3.2 of ASCE 7-10 (ASCE, 2010). Ground motion scaling is done by following six steps of section 4.1.7.1 of FEMA P-751 are described below:

Step 1: At first, 5 percent damped pseudo-acceleration spectrum for each unscaled component of each pair of ground motions is determined using SeismoSignal (SeismoSoft, 2016). The SRSS spectrum for each pair of ground motion is created using pseudo-acceleration spectrum for each unscaled component of each pair of ground motions.

Figure 3-25 shows pseudo-acceleration spectrum for Loma Prieta-Corralitos-1989-Horizontal component-1 (A00-component) and **Figure 3-26** shows pseudo-acceleration spectrum for Loma Prieta-Corralitos-1989-Horizontal component-2 (A90-component). The SRSS acceleration spectrum for Loma Prieta- Corralitos Earthquake (Earthquake A) is made using the pseudo-acceleration spectrum of A00 and A90 component of earthquake A. The unscaled SRSS acceleration spectrums for other earthquake are prepared following the same procedure. **Figure 3-27** shows unscaled SRSS spectra for the above mentioned selected earthquake. **Figure 3-28** shows unscaled SRSS acceleration spectra and target spectrum for Earthquake A, B, C and D.

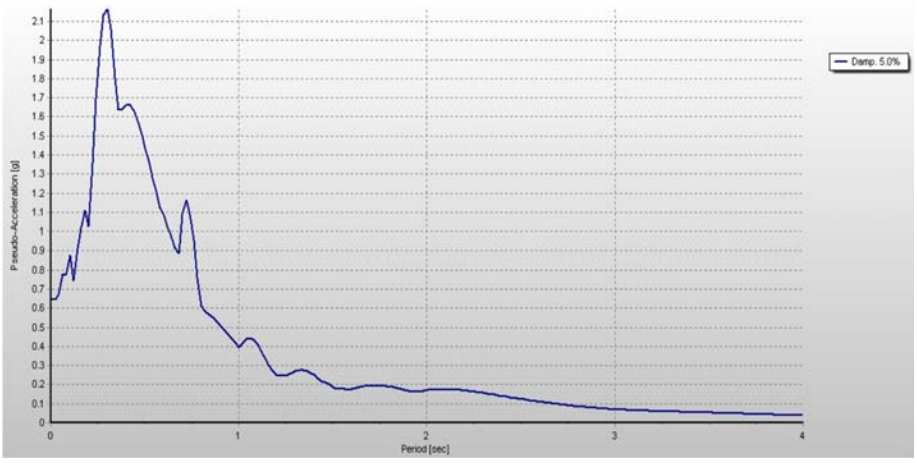

Figure 3-25 5 percent damped pseudo-acceleration spectrum for ground motions of A00 component of Earthquake A from SeismoSignal (SeismoSoft, 2016)

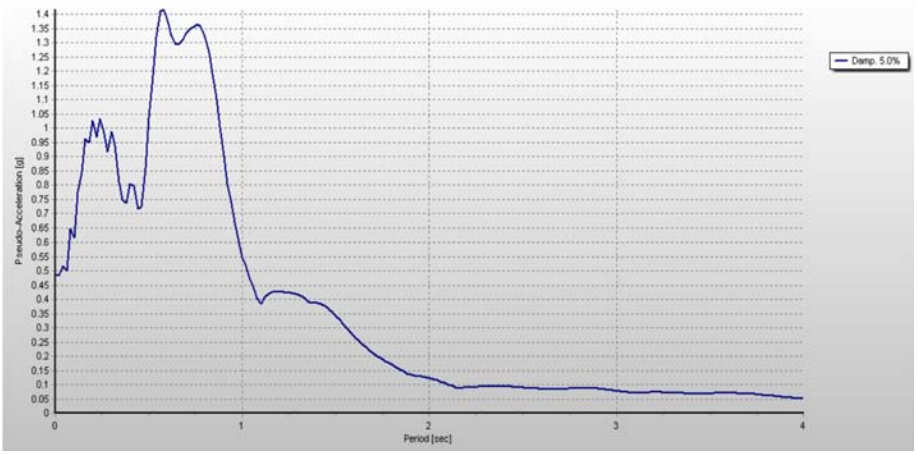

Figure 3-26 5 percent damped pseudo-acceleration spectrum for ground motions of A90 component of Earthquake A from SeismoSignal (SeismoSoft, 2016)

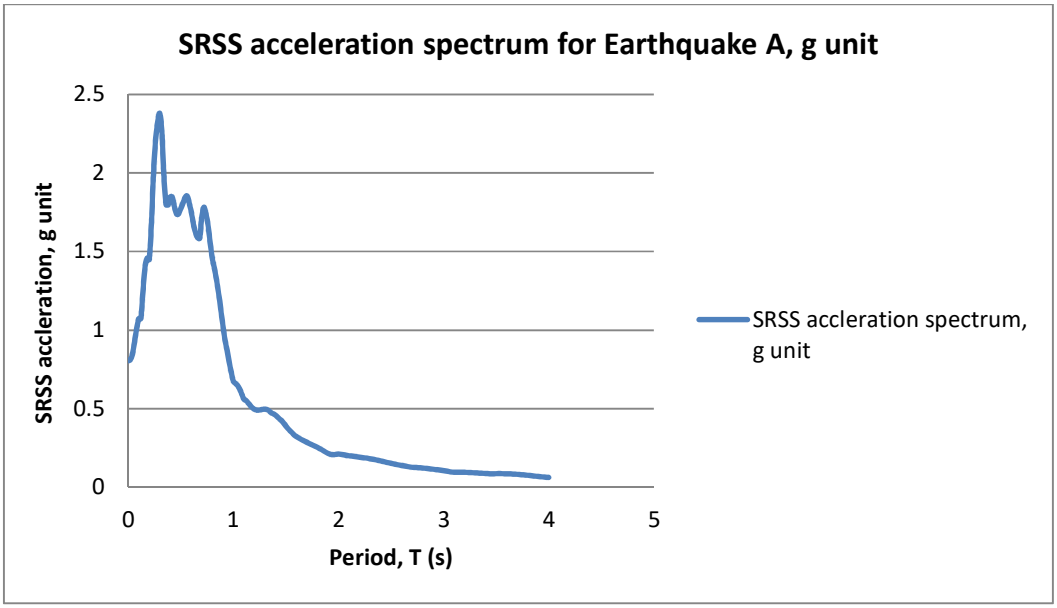

Figure 3-27 5 percent damped SRSS acceleration spectrum for ground motions Earthquake A, g unit.

According to section 4.1.7.1 of FEMA P-751 (FEMA, 2012), ASCE 7-10 (ASCE, 2010) does not provide clear guidance as to which fundamental period, T, should be used for determining 0.2T and 1.5T when the periods of vibration are different in the two orthogonal directions of analysis. This issue is resolved herein by taking T as the average of the computed periods in the two principal directions. The average period is referred to a T_{avg}.. **Table 3-14** shows how to determine T_{avg} for Model-1.

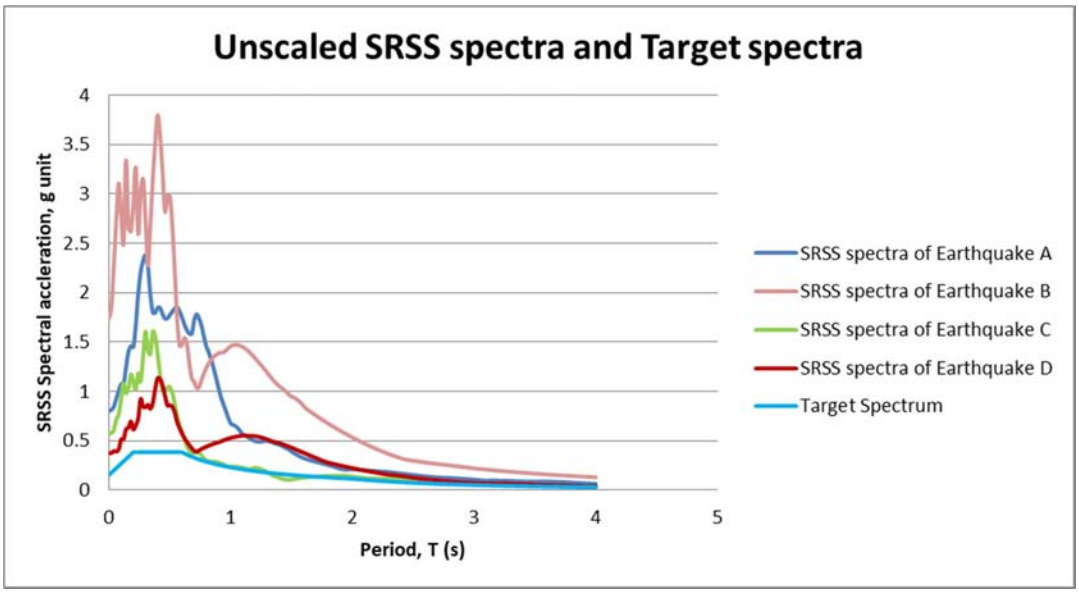

Figure 3-28 Unscaled SRSS acceleration spectra and target spectrum

Table 3-14 Tavg of Model-1

Mode number	Period (sec)	Modal Participating Mass Ratios towards UX direction	Modal Participating Mass Ratios towards UY direction
1	0.34	0	0.72
2	0.26	0.75	0
T avg=	0.30	sec	

Step 2: The design acceleration spectrum is computed for seismic zone-2 and soil type SC as per BNBC-2017 (HBRI & BRTC, 2017) is shown in **Figure 3-29**.

Step 3: Each SRSS spectrum is scaled such that the spectral ordinate of the scaled spectrum at T_{Avg} is equal to the spectral ordinate of the design spectrum at the same period. Each SRSS spectrum will have a unique scale factor, S1. S1 is the ratio of Target spectrum ordinate at T_{avg} to SRSS Spectrum ordinate at T_{avg}. T_{avg} for Model-1 is 0.305 sec. the spectral ordinate of target spectrum at T_{avg} is 0.383g, where g is the acceleration due to gravity. **Table 3-15** shows how to determine S1 scale factor for ground motions. **Table 3-15** describes S1 scaling process of SRSS spectrum.

Step 4: A new spectrum is created that is the average of the S1 scaled SRSS spectra. This spectrum is designated as the "average S1 scaled SRSS spectrum" and should have the same spectral ordinate as the target spectrum at the period T_{avg}. The average S1 scaled SRSS spectrum is created by using S1 scaled SRSS spectrums of Earthquake

A, B, C and D. **Figure 3-30** shows average S1 scaled SRSS spectrum. **Figure 3-31** shows average S1 scaled SRSS spectrum and target spectrum.

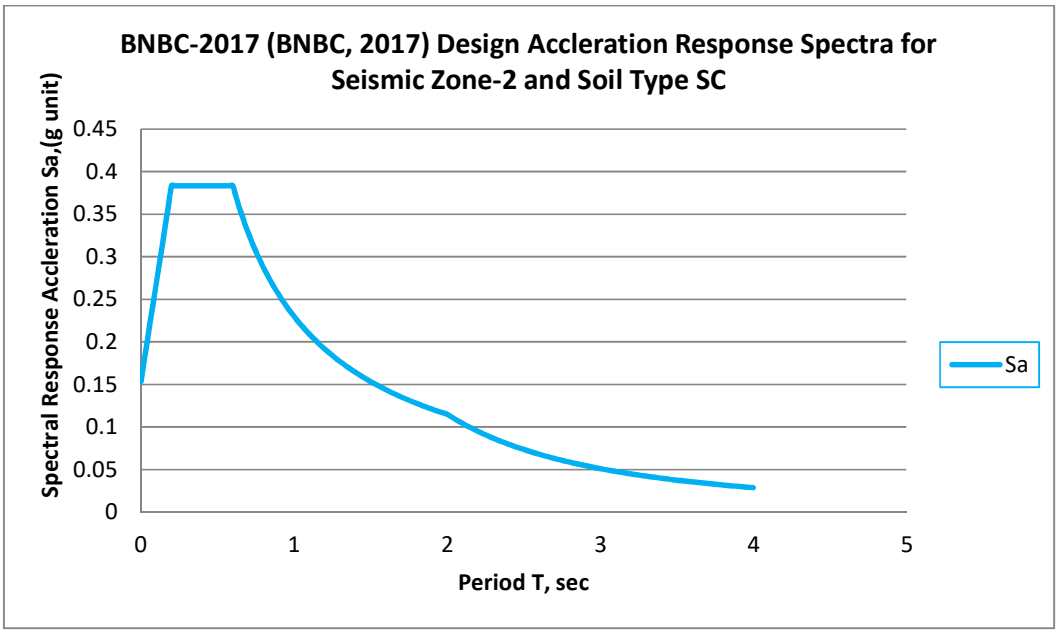

Figure 3-29 BNBC 2017 (HBRI & BRTC, 2017) Design Acceleration Response Spectra or target spectrum for Seismic Zone-2 and Soil Type SC

Table 3-15 S1 scaling process

Earthquake A	Period (sec)	SRSS spectrum ordinate, g unit	S1 Scale factor
	0.3	2.38	
	0.32	2.27	
T avg (sec)=	0.30	2.35	0.16
Earthquake D	0.3	0.84	
	0.32	0.86	
T avg (sec)=	0.30	0.85	0.45
Earthquake C	0.3	1.61	
	0.32	1.41	
T avg (sec)=	0.30	1.56	0.25
Earthquake B	0.3	2.75	
	0.32	2.27	
T avg (sec)=	0.30	2.63	0.15

Step 5: For each spectral ordinate in the period range $0.2T_{avg}$ to $1.5T_{avg}$, divide the ordinate of the target spectrum by the corresponding ordinate of the average S1 scaled SRSS spectrum, producing a set of spectral ratios over the range $0.2T_{avg}$ to $1.5T_{avg}$. The

largest value among these ratios is designated as S2. The average S1 scaled SRSS spectrum for all earthquakes are shown in **Figure 3-31**.

The largest value of ratio of target spectrum to average S1 scaled SRSS spectrum between $0.2T_{avg}$ and $1.5T_{avg}$ period is 1.27. So the value of S2 is 1.27. **Figure 3-32** shows Period vs. Ratio of target spectrum to average S1 scaled SRSS spectrum. The largest value of ratio of target spectrum to average S1 scaled SRSS spectrum between $0.2T_{avg}$ and $1.5T_{avg}$ period is shown in this **Figure 3-32**.

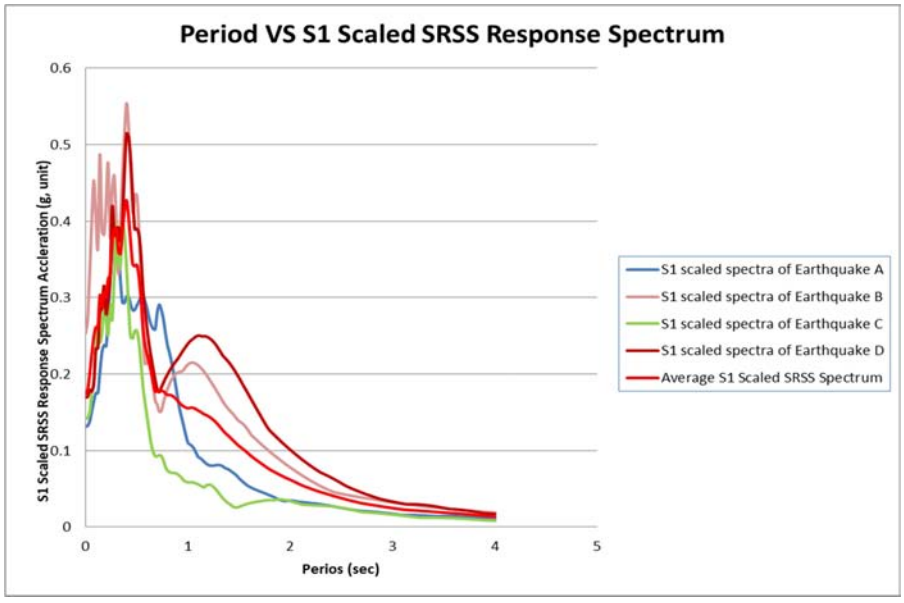

Figure 3-30 Average S1 scaled SRSS spectrum

Step 6: The factor S1 determined in Step 3 for each pair in the set is multiplied by the factor S2 determined in Step 5. This product, SS = S1 × S2 is the scale factor that should be applied to each component of ground motion in pair. Each pair of motions are scaled such that the average of the SS scaled SRSS spectra from all horizontal component pairs does not fall below the corresponding ordinate of the target response spectrum in the period range from $0.2T_{avg}$ to $1.5T_{avg}$ according to Section 16.1.3.2 of ASCE 7-10 (ASCE, 2010). The average of the SS scaled SRSS spectra is shown in **Figure 3-33**. **Figure 3-34** shows SS scale factors for Earthquake A, B, C, D. **Figure 3-35** shows the SS scaled spectra for the "00" components of each earthquake, together with the target spectrum. **Figure 3-36** shows the SS scaled spectra for the "90" components of each earthquake, together with the target spectrum.

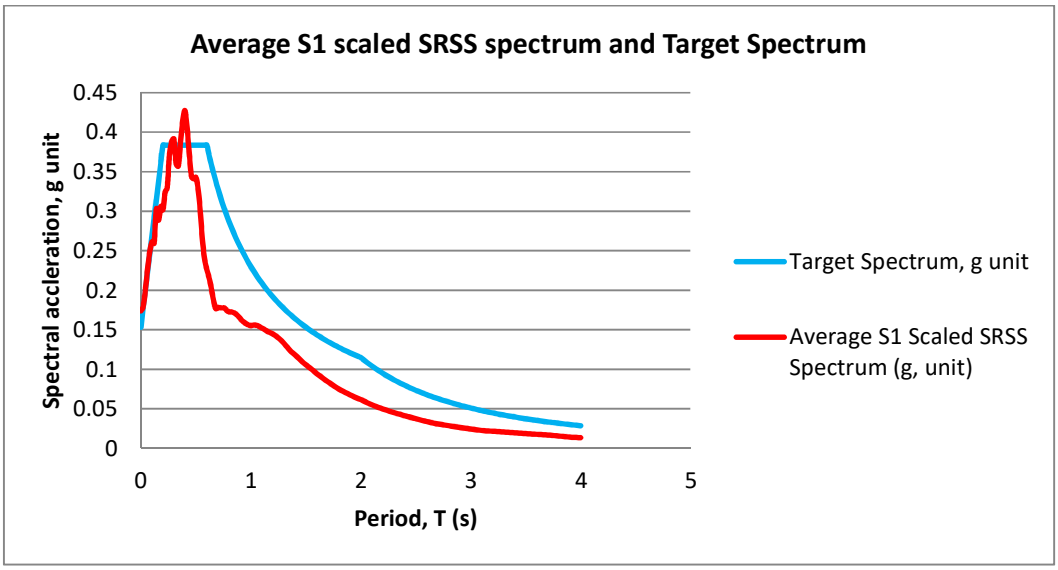

Figure 3-31 Average S1 scaled SRSS spectrum and target spectrum

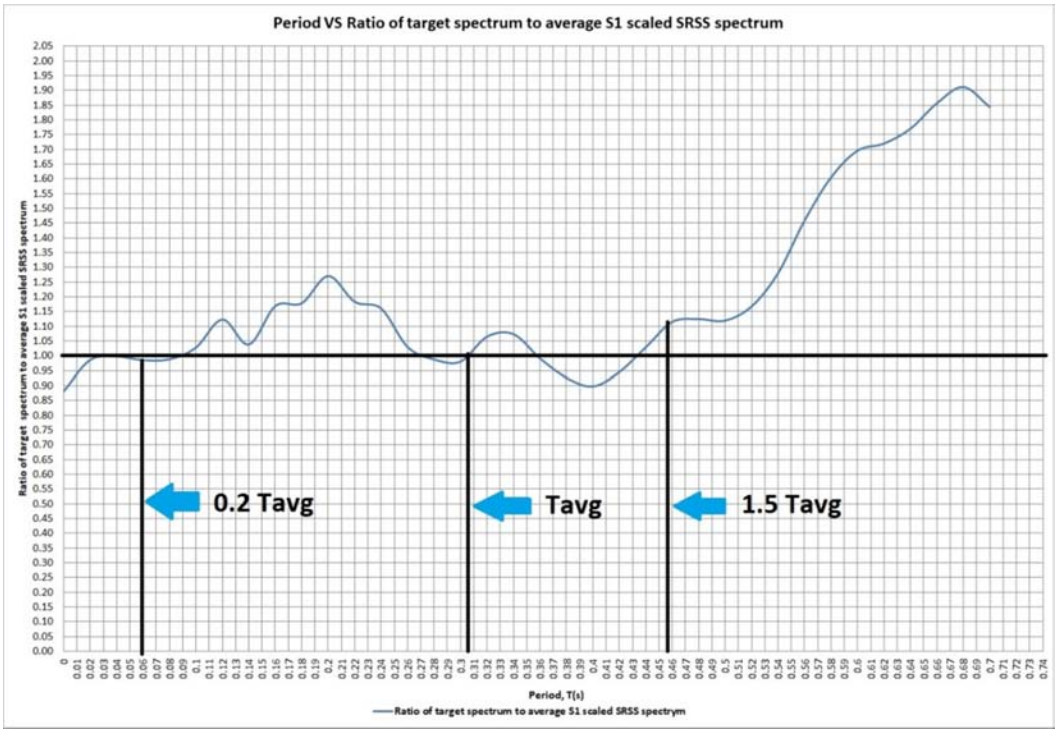

Figure 3-32 Period vs. Ratio of target spectrum to average S1 scaled SRSS spectrum

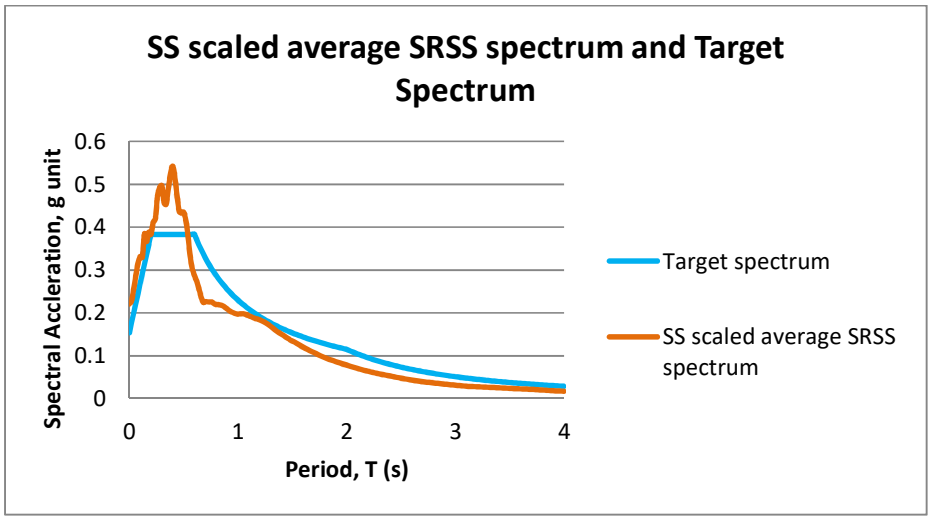

Figure 3-33 SS scaled average SRSS spectrum and target spectrum

Earthquake	S1 Scale factor	S2 Scale factor	SS scale factor
Earthquake A	0.16	1.27	0.21
Earthquake B	0.15	1.27	0.19
Earthquake C	0.25	1.27	0.31
Earthquake D	0.45	1.27	0.58

Figure 3-34 SS scale factors for Earthquakes

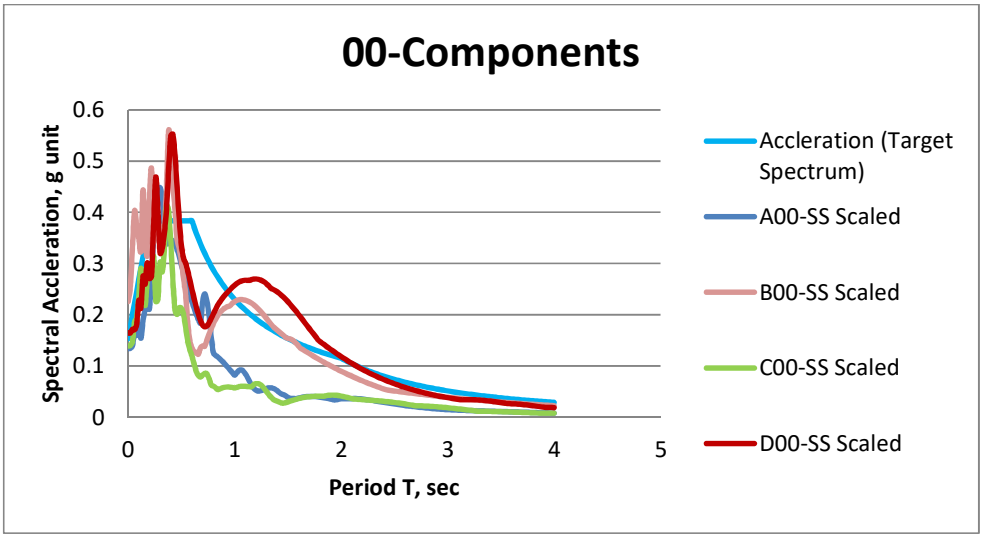

Figure 3-35 SS scaled individual spectra (00-Components) and target spectrum

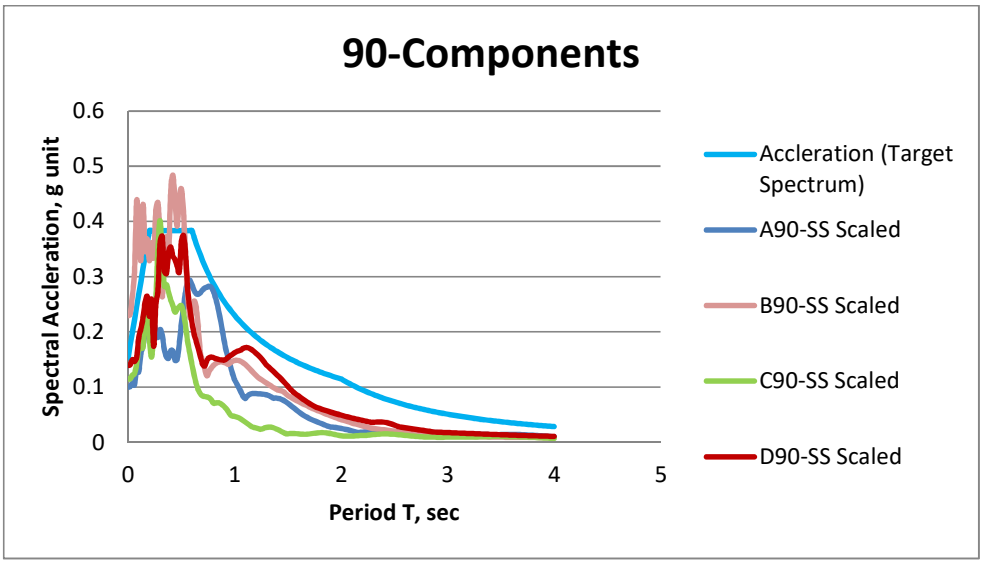

Figure 3-36 SS scaled individual spectra (90-Components) and target spectrum

16 dynamic analyses are performed with scaled ground motions applied only in one direction as per section 4.1.7.1 of FEMA P-751 (FEMA, 2012). **Figure 3-37** shows 16 dynamic analyses with scaled ground motions applied only in one direction.

Each base shear from ground motions is scaled with Ie/R as per section 16.1.4 (a) of ASCE 7-10 (ASCE, 2010). Then second scaling of base shear (Ie/R and SS scaled) is done following the requirements section 12.9.2.5.2 of ASCE 7-16 (ASCE, 2017).

3.6.5.ii Torsional and orthogonal loading for modal linear response history analysis

The amplification of torsion is not required where accidental torsion effects are included in the dynamic analysis mode as per section 12.9.5 of ASCE 7-10 (ASCE, 2010). We have used this approach to include the effect of accidental torsion in Modal linear response history analysis. The details of the above mentioned approach as per section 4.3.6.3 of FEMA P-1051 (FEMA, 2016) is as follows:

At first center of mass of diaphragm is displaced plus or minus 5 percent of the diaphragm dimension. The displacement of center of mass along plus and minus 5% of the diaphragm length and width creates four mass locations. As there are four possible mass locations, this will require four separate modal analyses for torsion with each analysis using a different set of mode shapes and frequencies.

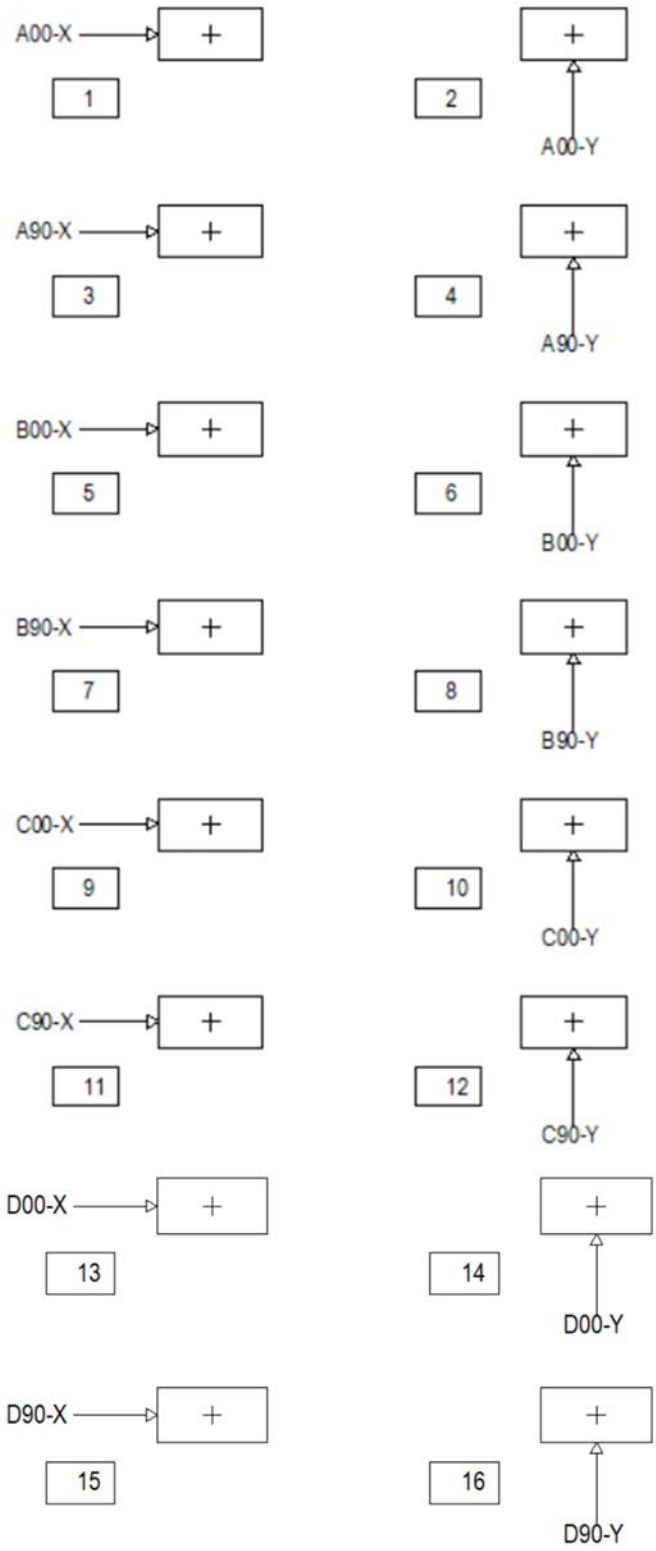

Figure 3-37 Dynamic analyses with scaled ground motions applied only in one direction as per FEMA P-751 (FEMA, 2012)

Torsional and orthogonal loading in a three dimensional structure can be applied following four configuration for each pair of ground motion as per section 4.1.7.3 of FEMA P-751 (FEMA, 2012) which are shown in **Figure 3-38**.

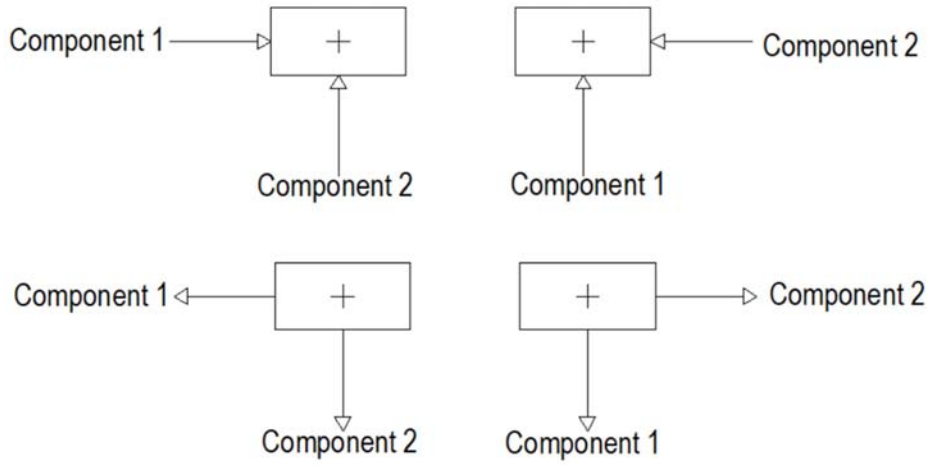

Figure 3-38 Orthogonal Loading for Linear Response History Analysis as per section 4.1.7.3 of FEMA P-751 (FEMA, 2012)

Total of 4 configurations of orthogonal loading are generated without accidental torsion which is shown in **Figure 3-38**. Total of 16 configurations are formed when accidental torsion is incorporated in each of the above mentioned orthogonal loading configuration for a single pair of ground motions. So total of 20 orthogonal loading combinations are formed for a single earthquake. The procedures of orthogonal loading with accidental torsion for Modal linear response history analysis are described in section 4.3.6.3 of FEMA P-1051 (FEMA, 2016). Twenty orthogonal loading combinations with accidental torsion for Earthquake A are shown in **Figure 3-39.**

These 20 load combinations are used in the basic load combinations for strength design as per section 12.4.2.3 of ASCE 7-10 (ASCE, 2010) to make 40 load combinations to determine maximum diaphragm design forces for Earthquake A from Modal linear response history analysis which are shown in **Appendix-C**.

The orthogonal loading effects and accidental torsion creates for a single earthquake creates 20 load combinations which are used in the basic load combinations for strength design with overstrength factor as per section 12.4.2.3 of ASCE 7-10 (ASCE, 2010) to make 40 load combinations to determine maximum collector forces and chord forces of diaphragm for Earthquake A from Modal linear response history analysis which are

shown in **Appendix-C**. The diaphragm forces from linear response history analysis for Earthquake B, C, and D are also determined following the above mentioned procedures.

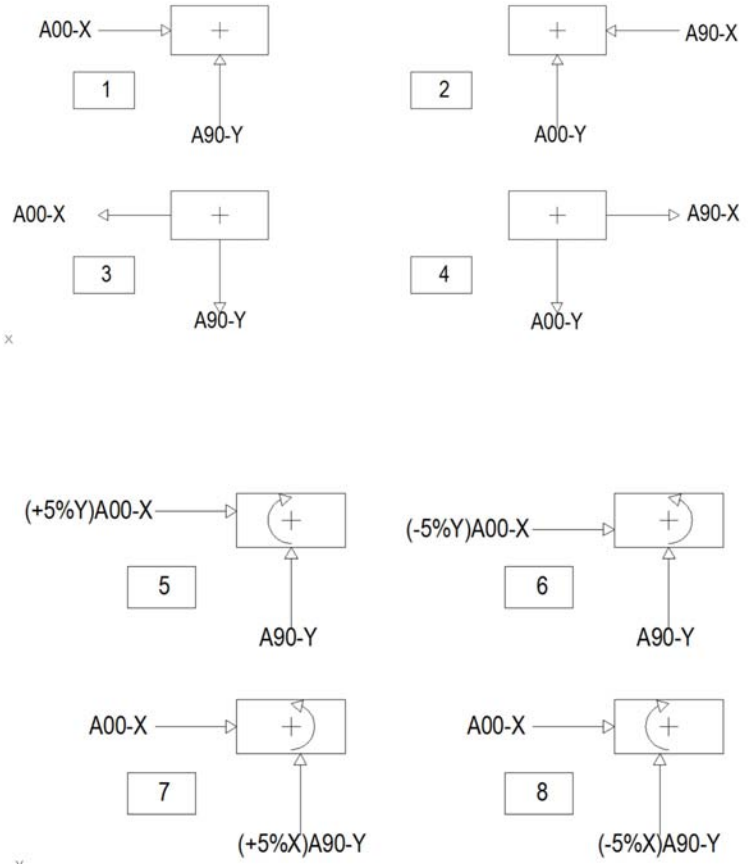

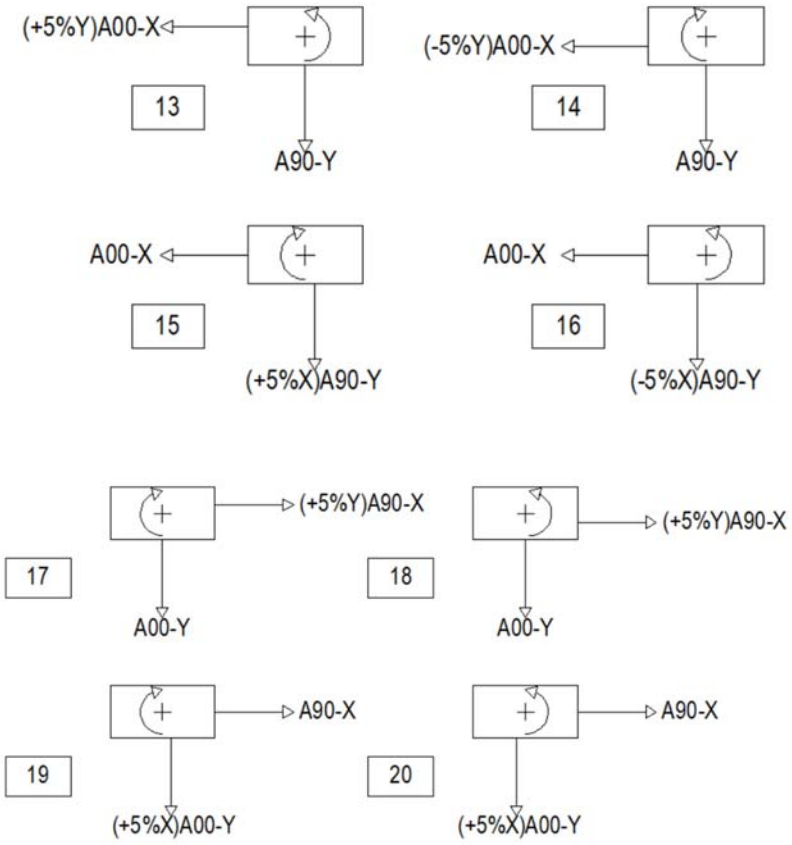

Figure 3-39 Orthogonal Loading in Linear Response History Analyses for Earthquake A

3.6.6 Nonlinear static analysis

Diaphragm Design Forces are determined From Nonlinear static procedure as per ASCE 41-13 (ASCE, 2014). Diaphragm Design Forces are determined at 1.5 times of target displacement. The target displacement represents the maximum displacement likely to be experienced in the building for the selected Seismic hazard level. Diaphragm Design Forces are also determined for orthogonal nonlinear static loadings.

3.6.6.i Assignment of auto hinges in beams, columns and shear walls

Nonlinear load deformation relationships for various reinforced components are defined in the mathematical models. Nonlinear flexural hinges (Auto M3 hinges) are assigned at the ends of beams to represent the nonlinear flexural response of beam in pushover analysis. The auto M3 hinges are generated in beams following Table 10-7 (Concrete beam-flexure, item i) of ASCE 41-13 (ASCE, 2014). Nonlinear Auto P-M2-M3 hinges are assigned at the ends of columns to represent the nonlinear response of

columns in pushover analysis. The auto P-M2-M3 hinges are generated in columns following Table 10-8 (Concrete columns) of ASCE 41-13. Auto fiber P-M3 hinges are assigned in shear walls to capture nonlinear response of shear walls in pushover analysis.

Auto hinge properties are defined by ETABS 2016 (CSI, 2017). The ETABS 2016 cannot fully define the auto properties until the section to which they apply has been identified. ETABS 2016 combines its built-in criteria with the defined section properties for beams, columns and shear walls to generate the final hinge properties (Frame/Wall Nonlinear Hinge, n.d).

Auto hinges are section dependent. So section of concrete frame elements and shear walls and their longitudinal reinforcements should be assigned based on design. If reinforcements are not assigned based on design then concrete frame design should be performed after assigning auto hinges in ETABS 2016 (CSI, 2017) so that auto hinges can get section properties from the concrete frame design. We have assigned reinforcements in beams and columns based on concrete frame design as per ACI 318-14 (ACI, 2014) so that auto hinges can generate based on designed section properties. Auto P-M3 hinges in shear walls are also section dependent. The section properties of shear walls can be assigned in several ways. The reinforcement size and reinforcement layout in shear walls based on design can be defined to generate section properties for auto P-M3 hinges. The designed section properties for shear walls can also be determined from concrete shear wall design in ETABS 2016. Assignment of vertical and horizontal reinforcement ratio for shear walls is another way of defining section properties for auto P-M3 hinges of shear walls. The vertical and horizontal reinforcement ratios of shear walls are assigned to shear walls based on shear wall design as per ACI 318-14 for pushover analysis. The auto P-M3 hinges get section properties form these reinforcement ratios.

3.6.6.ii Gravity load analysis for nonlinear static analysis

Nonlinear static load case is created for gravity load analysis using load combination defined in Eq.7-3 of ASCE 41-13 (ASCE, 2014). Full load control application is used for this load case in ETABS 2016 (CSI, 2017). P-Δ effects are also considered in this load case.

3.6.6.iii Lateral load for nonlinear static analysis

A new load case is created for lateral load analysis for nonlinear static procedure. This load case is contained from gravity load analysis. Nonlinear static analysis case with displacement control application is selected. Then modal load pattern is selected in load application. The vertical distributions of lateral loads for NSP are proportional to the shape of the fundamental mode in the direction under consideration. The control node is selected at the center of mass at the roof of a building. Then lateral load analysis for NSP is carried out to determine target displacement in capacity curve of mathematical model using ETABS 2016 (CSI, 2017). Then the lateral load analysis for NSP is carried out at least 150% of the target displacement in the direction under consideration as per Section 7.4.3.2.1 of ASCE 41-13 (ASCE, 2014). P-Δ effects are also considered in this load case.

It is not required by ASCE 41-13 (ASCE, 2014) to consider orthogonal loading for the analysis of diaphragm. However Moehle et al. (2010) requires that the diaphragm must be designed for orthogonal loading conditions. Therefore we have also used orthogonal loading in nonlinear static procedure to determine diaphragm forces. The concurrent seismic effects are performed in nonlinear static procedures following the requirements of Section 7.2.5.1 of ASCE 41-13. The orthogonal loadings for nonlinear static procedures are applied as follows:

(i) Forces and deformations associated with 100% of the target displacement in the X direction only, plus the forces (not deformations) associated with 30% of the displacements in the Y direction only.

(ii) Forces and deformations associated with 100% of the displacements in the Y direction only, plus the forces (not deformations) associated with 30% of the displacements in the X direction only.

3.6.6.iv Seismic demand in the form of an elastic response spectrum

The seismic evaluations of the mathematical models in ETABS 2016 (CSI, 2017) are done for BSE-1N (Basic Safety Earthquake-1) for use with the Basic Performance Objective Equivalent to New Building Standards which is taken as two-thirds of the BSE-2N at a site. Where BSE-2N (Basic Safety Earthquake-2) is used with the Basic

Performance Objective Equivalent to New Building Standards, taken as the ground shaking based on the Risk-Targeted Maximum Considered Earthquake (MCE_R). Our building models are located in Dhaka city, Zone-2, soil type SC as per BNBC-2017 (HBRI & BRTC, 2017). So design response spectrum was generated for Dhaka city, zone-2, soil type SC as per BNBC-2017 to define seismic demand for nonlinear static procedures. Seismic demand presented for pushover analysis conforms to the requirements of BSE-1N (Basic Safety Earthquake-1). The Risk category is I for our building models as per Table 1.5-1 of ASCE 7-10 (2010). The Basic Performance Objective Equivalent to New Building Standards (BPON) is 3-B for risk category I and BSE-1N as per Table 2-2 of ASCE 41-13 (2014). 3-B stands for Life safety structural performance as per Section 2.3.1 of ASCE 41-13 and position retention nonstructural performance as per Section 2.3.2 of ASCE 41-13.

The diaphragm forces are extracted form ETABS 2016 (CSI, 2017) at the step where control node displacement is 150% of the target displacement for pushover analysis along Y-direction. The diaphragm forces are also extracted form ETABS 2016 for concurrent seismic effects in nonlinear static procedures.

3.7 Diaphragm forces/stresses

Equivalent lateral force procedures, Response spectrum analyses, Modal linear response history analyses, Pushover analyses and diaphragm design force procedures as per section 12.10.1.1of ASCE 7-10 (ASCE, 2010) are performed in 3D building models using FEM based analytical software ETABS 2016 (CSI, 2017). Forces/stresses in diaphragm and Forces acting between diaphragm and vertical element of the seismic force resisting system are extracted from Section cuts through group of elements.

3.8 Comparison of Diaphragm forces/stresses

Diaphragm forces such as in-plane flexural stress and in-plane shear stress around diaphragm openings adjacent to shear walls are computed with the help of Equivalent lateral force procedures, Response spectrum analyses, Modal linear response history analyses, Pushover analyses and diaphragm design force procedures as per section 12.10.1.1 of ASCE 7-10 (ASCE, 2010). In-plane stress data for diaphragm design force procedures stated above are compared with bar charts and statistical analyses to find out which diaphragm force procedure is affecting the diaphragm behavior most.

Statistical analyses are also performed to find out worst orientation of diaphragm opening adjacent to shear wall. In-plane stress data of diaphragm with and without diaphragm opening in building models are also compared to find out how much stress hike up occurred due to introduction of diaphragm opening. Then Diaphragm forces/stresses are compared to review of diaphragm discontinuity irregularity criteria as per ASCE 7-10 (ASCE, 2010) when diaphragm opening is located adjacent shear wall in wall frame structural system.

3.9 Maximum displacement

Target displacement and maximum inelastic displacement at target displacement in top story of building models are determined from pushover analyses. Global behaviors of building models with and without diaphragm opening are compared with maximum displacement at top story from pushover analysis.

3.10 Data analysis

Statistical analysis of diaphragm's in-plane stress data of diaphragm locations near diaphragm opening adjacent to shear wall from LEP, LDP and Pushover analyses are performed with the help of standard deviation and Z-score to find out worst orientation of diaphragm opening adjacent to shear wall.

3.11 Summary

In this chapter geometry of models and considered seismic parameters are described. Considerations used for modeling structural members in ETABS 2016 (CSI, 2017) are presented in this chapter. Unidirectional and orthogonal seismic loading application based on LEP, LDP and Pushover analyses for analyzing diaphragm of models are also described in this chapter. Procedures for performing statistical analyses of diaphragm's in-plane stress data of diaphragm locations near diaphragm opening adjacent to shear wall are described to find out the worst orientation of diaphragm opening adjacent to shear wall and to compare in-plane stress/force data from different diaphragm design force procedures.

Chapter 4

RESULTS AND DISCUSSIONS

4.1 Introduction

In this chapter, shell layer stresses around diaphragm opening adjacent to shear wall obtained from different diaphragm design force procedures (ELFA Method-1, ELFA Method-2, RSA Method-1, RSA Method-2, LRHA and Pushover Analysis) are presented.

There are nine (09) building models, which are investigated with different diaphragm force procedures. The analysis has been carried out by ETABS 2016 (CSI, 2017) integrated civil engineering software.

The pushover analyses of building models are performed using ETABS 2016 (CSI, 2017) following ASCE 41-13 (ASCE, 2014). Target displacement of each building models are also presented in this section. Maximum displacement of top story of the building at the target displacement obtained pushover analysis as per ASCE 41-13 are also presented in this chapter.

The shell layer stresses of different diaphragm locations around diaphragm opening adjacent to shear wall are presented in bar charts. The shell layer stresses from diaphragm design force procedures for building models with and without diaphragm openings are presented in bar charts for comparisons. Different data sets for maximum and minimum shell layer stress are summarized in tables for statistical analyses (standard deviation and Z-score). The statistical analyses are performed to find out which scenario of diaphragm opening location adjacent to shear wall has profound effect on the local behavior of diaphragm.

4.2 Inelastic Total Drift from Pushover Analysis

The target displacement represents the maximum displacement likely to be experienced for the selected Seismic Hazard Level as explained in chapter 3. The control node is located at the center of mass at the roof of a building. Target displacement and capacity curve for model-2 from Pushover analyses in ETABS 2016 (CSI, 2017) are shown in the **Figures 4-1 and 4-2**. The target displacement is the maximum displacement likely to be experienced for the selected Seismic Hazard Level. In Pushover analysis, the

building is subjected to monotonically increasing lateral loads representing inertia forces in an earthquake until the target displacement is exceeded. In ETABS 2016, the monitoring of the control node (C.G of the roof top) displacement is done with corresponding base shear to draw capacity curve of the building when the building is subjected to monotonically increasing lateral loads.

For semi-rigid diaphragm sometimes the maximum story displacement may not be as same as the target displacement of control node as semi-rigid diaphragm accounts the actual in-plan stiffness properties and behavior of diaphragm. Therefore, maximum story displacement for top story is also collected at target displacement. **Figure 4-3** shows control node (c.g of the roof top) of Model-8. **Figure 4-4** shows joint-2 of Model-8 deflected more in top floor along Y-direction compared to control node of Model-8 during pushover analysis along Y-direction. Maximum displacement observed in top story at target displacement of control node and corresponding base shear from Pushover analysis along X and Y-direction are shown in **Table 4-1**.

4.3 Shell Layer Stress from Diaphragm Design Force Procedures

Shell layer stresses around diaphragm opening adjacent to shear wall are obtained from different diaphragm design force procedures (ELFA Method-1, ELFA Method-2, RSA Method-1, RSA Method-2, LRHA and Pushover Analysis). Diaphragm locations around diaphragm opening adjacent to shear wall are selected for investigation. Diaphragm locations under consideration for investigation of shell layer stress of Models are shown in **Figures 4-5 to 4-13**. Shell layer stresses (maximum S_{12} stress component at bottom of layer shell) of diaphragm locations for building models with and without diaphragm opening adjacent to shear wall are compared with bar charts in **Figures 4-14 to 4-19** with six diaphragm design force procedures discussed above**.** **Figures 4-14 to 4-19** are referred in **Tables 4-2 to 4-3**. Three in-plane stress components (S_{11}, S_{22} and S_{12}) are selected for investigation. For each diaphragm location, maximum and minimum stresses of S_{11}, S_{22} and S_{12} stress components at top and bottom of the layer shell are statically investigated in **Tables 4-4 to 4-25 of Appendix D.** Shell layer stresses of diaphragm locations for building models with and without diaphragm opening adjacent to shear wall are compared with bar charts in **Figures 4-23 to 4-122 of Appendix E** with six diaphragm design force procedures

discussed above**. Figures 4-23 to 4-122 of Appendix E** are also referred in **Tables 4-4 to 4-25 of Appendix D** for convenience.

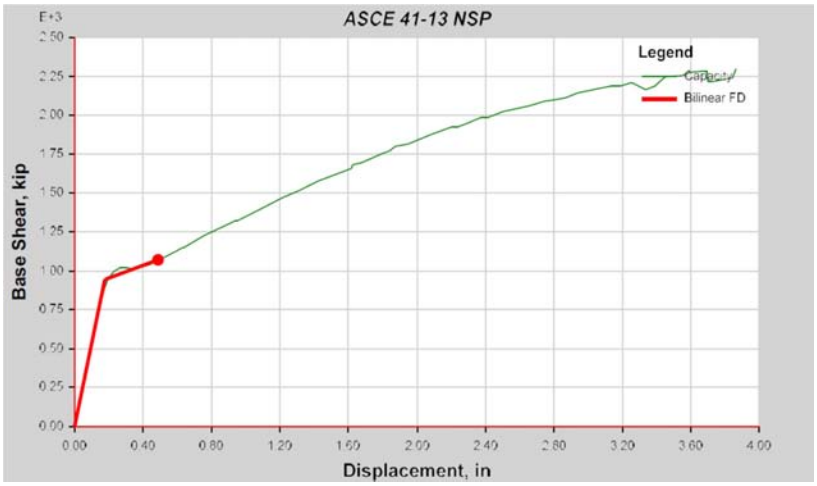

Figure 4-1 Pushover curve from Pushover along X-direction for Model-2

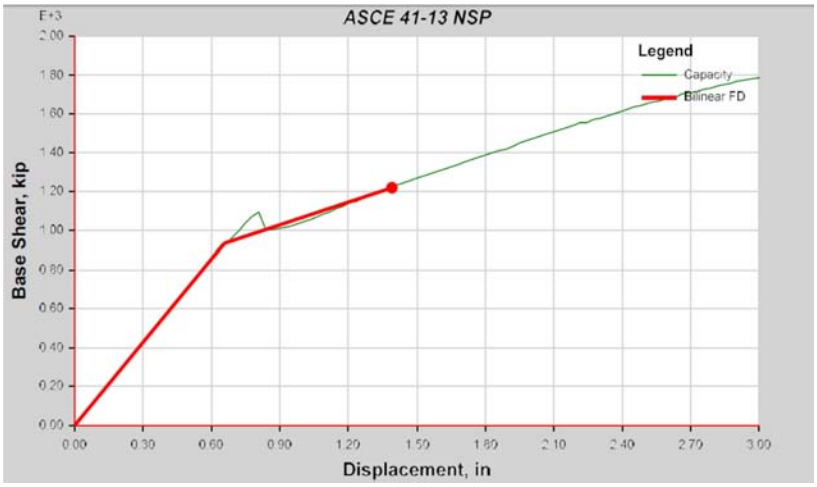

Figure 4-2 Pushover curve from Pushover along Y-direction for Model-2

Huge stress data are obtained from LEP, LDP and NSP of diaphragm design force procedures for top and bottom layer of nonlinear layer shell. Statistical analyses are performed storywise to screen out unimportant stress data and to find out most highly stressed locations of diaphragm around diaphragm opening adjacent to shear wall. Different data sets for maximum and minimum shell layer stress of S_{11}, S_{22} and S_{12} stress components are summarized in **Tables 4-4 to 4-25 of Appendix D** for statistical analyses (standard deviation and Z-score). For maximum (positive values) of shell layer stresses, stresses over mean plus one standard deviation with Z-score are summarized in the tables. For minimum (negative values) of shell layer stresses, stresses below mean minus one standard deviation with Z-score are summarized in the tables. The

statistical analyses are performed to find out which scenario of diaphragm opening location adjacent to shear wall has the most profound effect on the local behavior of diaphragm. Maximum and minimum shell layer stress in top and bottom of shell layers at different stories are summarized in **Tables 4-4 to 4-25 of Appendix D**. High in-plane stresses obtained from different analyses procedures are given in the tables with stress value for convenience.

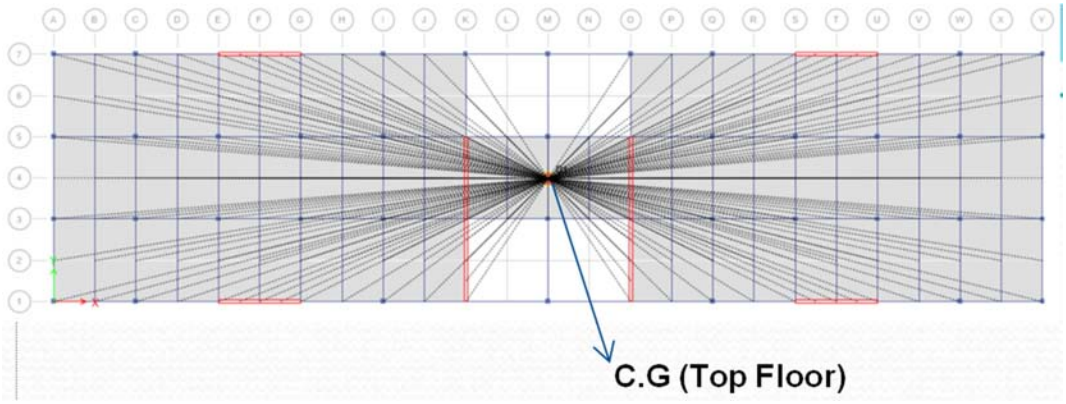

Figure 4-3 Control node (C.G of the roof top) of Model-8

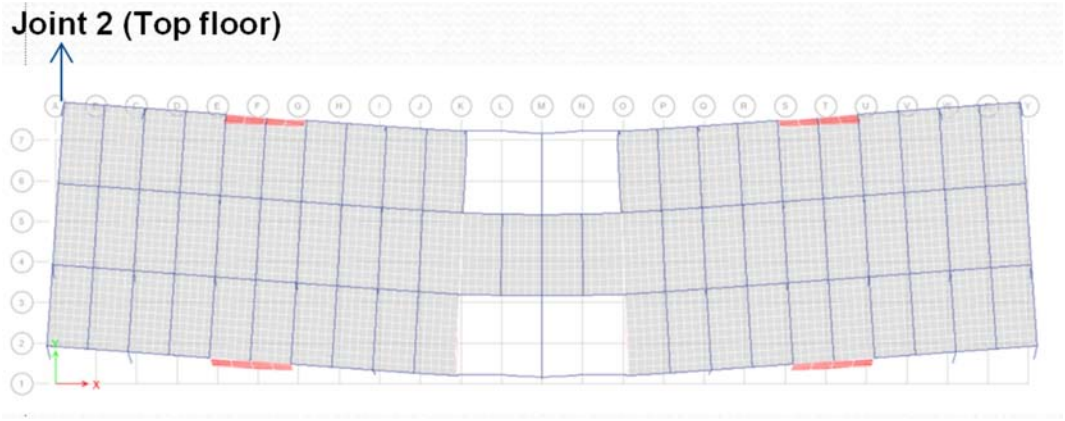

Figure 4-4 Deformed shape of Roof top of Model-8 at target displacement during pushover along Y-direction.

Diaphragm locations around diaphragm opening adjacent to shear wall experiencing high in-plane stress during earthquake are put in **Tables 4-4 to 4-25 of Appendix D**. Statistical analyses of stress data with reference figures of **Appendix E** are also shown in these tables. **Figure 4-20** shows absolute maximum shell resultant forces (F_{12}) contour diagram of Model-9 (story 3) from Pushover analysis along Y-direction up to 1.5 times target displacement. **Figure 4-21** shows contour diagram of absolute maximum shell layer stresses (S_{12}) at top of layered shell of Model-9 (story 3) from

Pushover analysis along Y-direction up to 1.5 times target displacement. **Figure 4-22** shows contour diagram of absolute maximum shell layer stresses (S_{12}) at bottom of layered shell of Model-9 (story 3) from Pushover analysis along Y-direction up to 1.5 times target displacement.

Table 4-1 Maximum displacement observed in top story at target displacement of control node (C.G of top story) and corresponding base shear from Pushover analysis along X and Y-direction.

Model ID	Pushover Direction	Base shear at Target displacement	Target displacement of control node (C.G of Top story)	Maximum displacement observed among other location of top story
		kips	inch	inch
Model-1	Along X-direction	1086	0.550	0.550
Model-1	Along Y-direction	1228	1.180	1.180
Model-2	Along X-direction	1068	0.487	0.487
Model-2	Along Y-direction	1220	1.390	1.390
Model-3	Along X-direction	968	0.542	0.542
Model-3	Along Y-direction	1175	1.218	1.218
Model-4	Along X-direction	984	0.386	0.386
Model-4	Along Y-direction	990	0.680	0.680
Model-5	Along X-direction	944	0.293	0.293
Model-5	Along Y-direction	940	0.858	0.858
Model-6	Along X-direction	889	0.364	0.364
Model-6	Along Y-direction	968	0.688	0.688
Model-7	Along X-direction	1090	0.554	0.554
Model-7	Along Y-direction	1502	0.117	0.673
Model-8	Along X-direction	1041	0.499	0.499
Model-8	Along Y-direction	1399	0.101	0.855
Model-9	Along X-direction	1058	0.498	0.498
Model-9	Along Y-direction	1489	0.116	1.013

The ACI Code recommends that the modulus of rupture f_r be taken to equal $7.5\sqrt{f_c'}$ for normal weight concrete. So the modulus of rupture f_r is 475 psi for concrete having f_c' of 4000 psi. Cracks will develop in concrete if in-plane flexural stress is over modulus of rupture. The principal of earthquake resistant building requires that the diaphragm should be damaged free during earthquake.

Diaphragm locations experiencing shear stress values over 76 psi ($\varphi 2\sqrt{fc'}$) require shear reinforcements and diaphragm location experiencing shear stress over 304 psi ($\varphi 8\sqrt{fc'}$) requires change of diaphragm section where $\varphi = 0.6$.

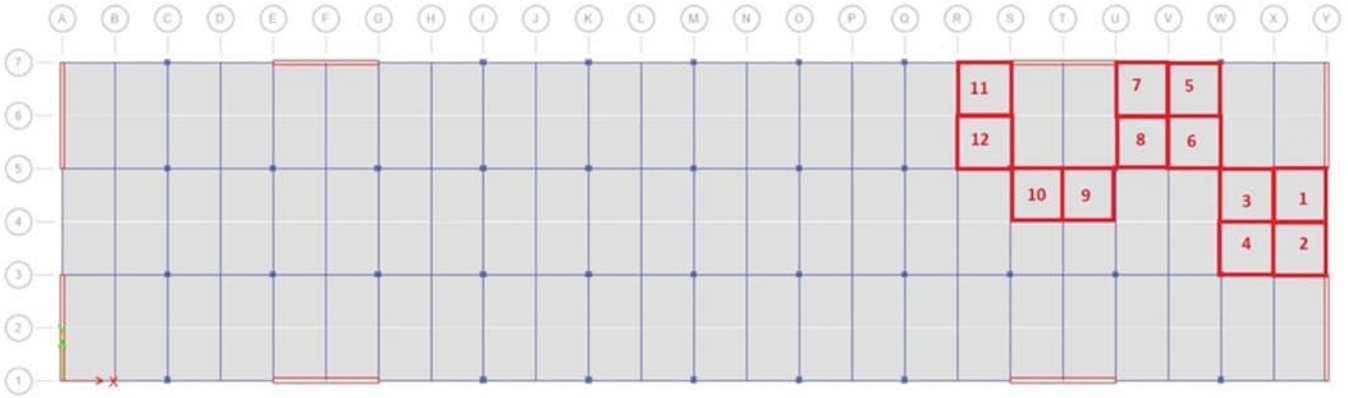

Figure 4-5 Diaphragm locations under consideration for investigation of shell layer stress of Model-1

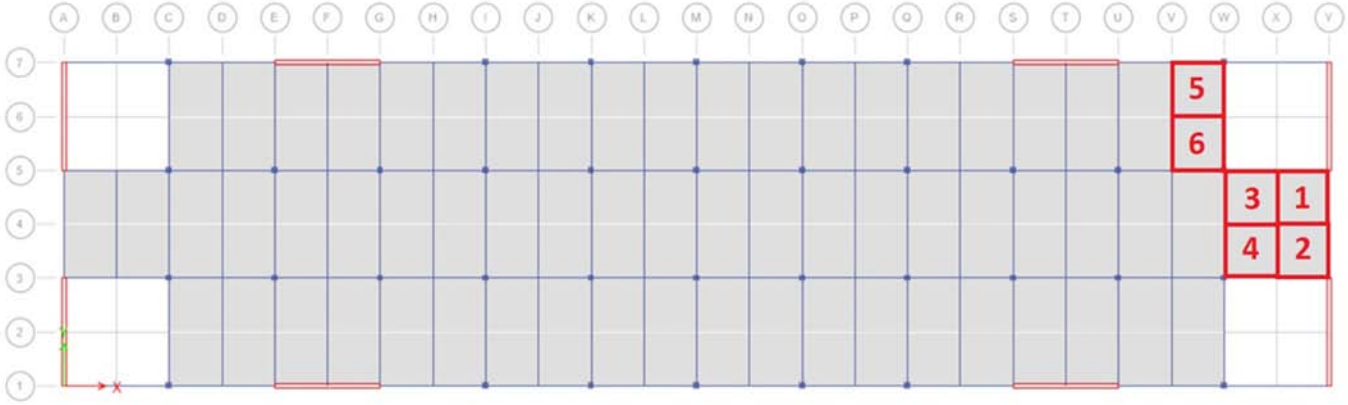

Figure 4-6 Diaphragm locations under consideration for investigation of shell layer stress of Model-2

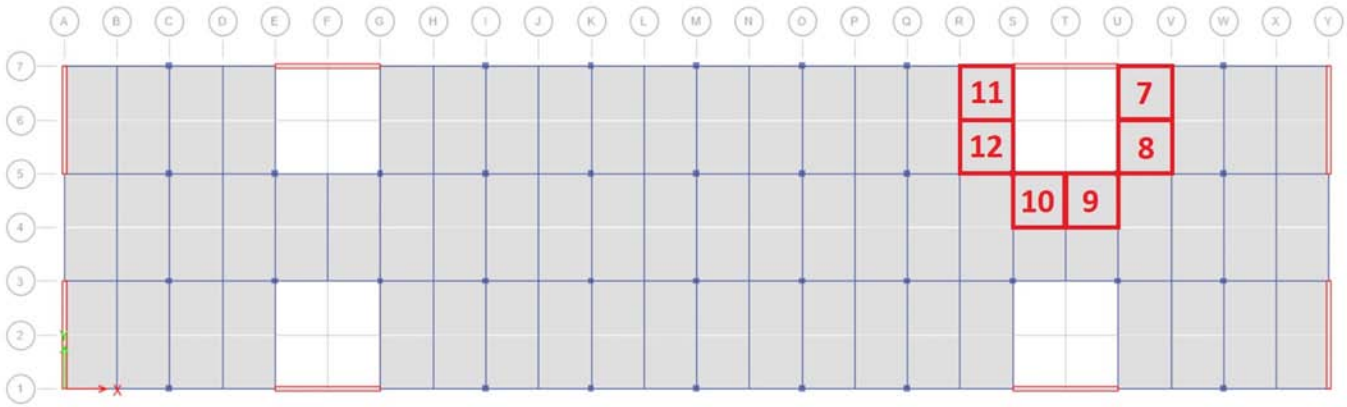

Figure 4-7 Diaphragm locations under consideration for investigation of shell layer stress of Model-3

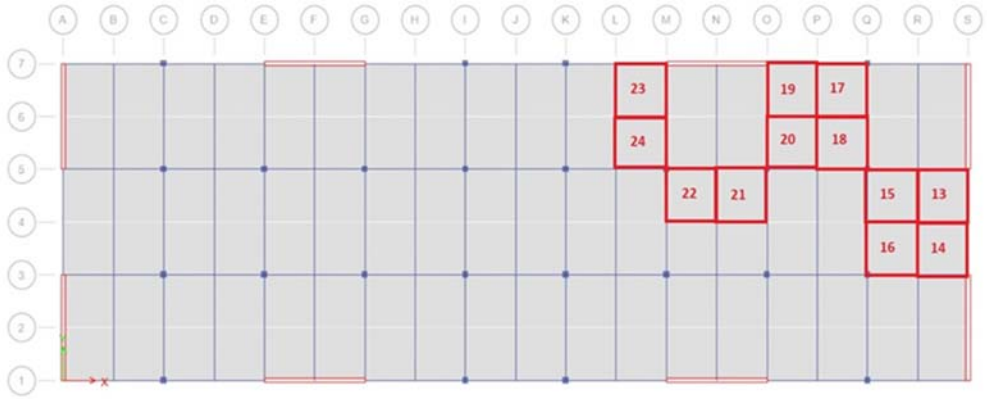

Figure 4-8 Diaphragm locations under consideration for investigation of shell layer stress of Model-4

Figure 4-9 Diaphragm locations under consideration for investigation of shell layer stress of Model-5

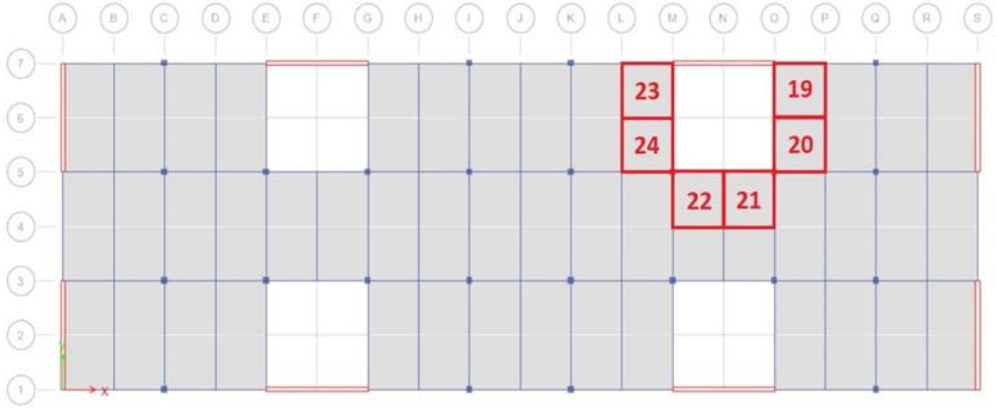

Figure 4-10 Diaphragm locations under consideration for investigation of shell layer stress of Model-6

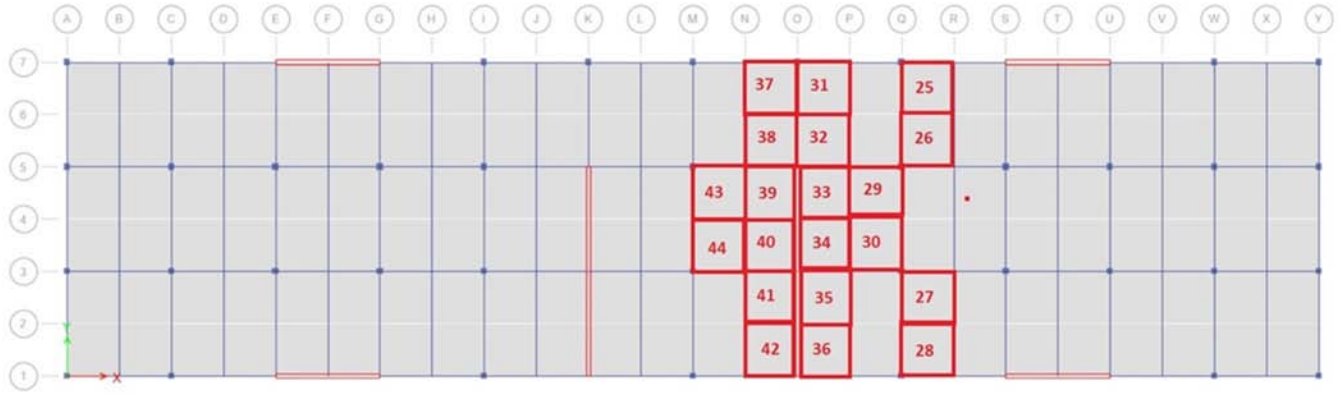

Figure 4-11 Diaphragm locations under consideration for investigation of shell layer stress of Model-7

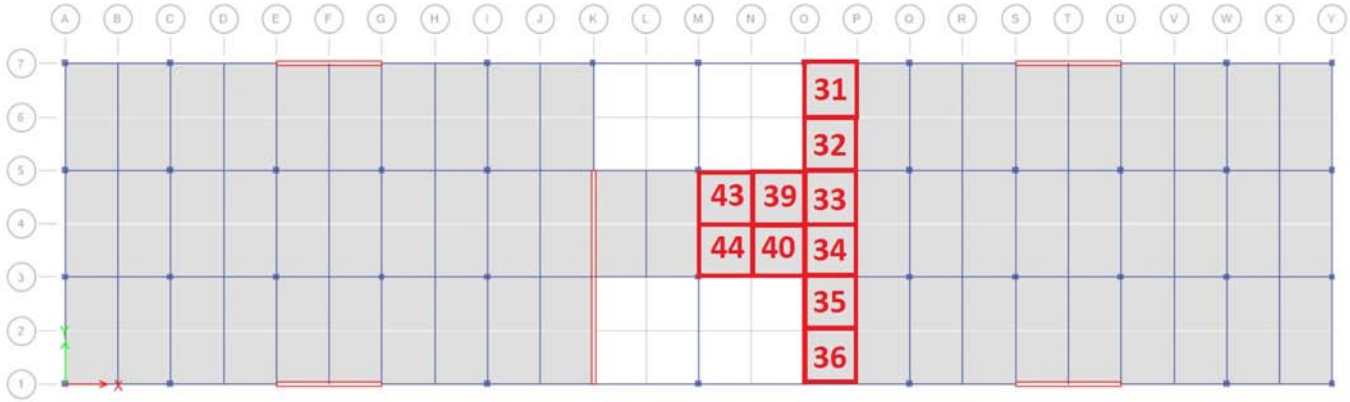

Figure 4-12 Diaphragm locations under consideration for investigation of shell layer stress of Model-8

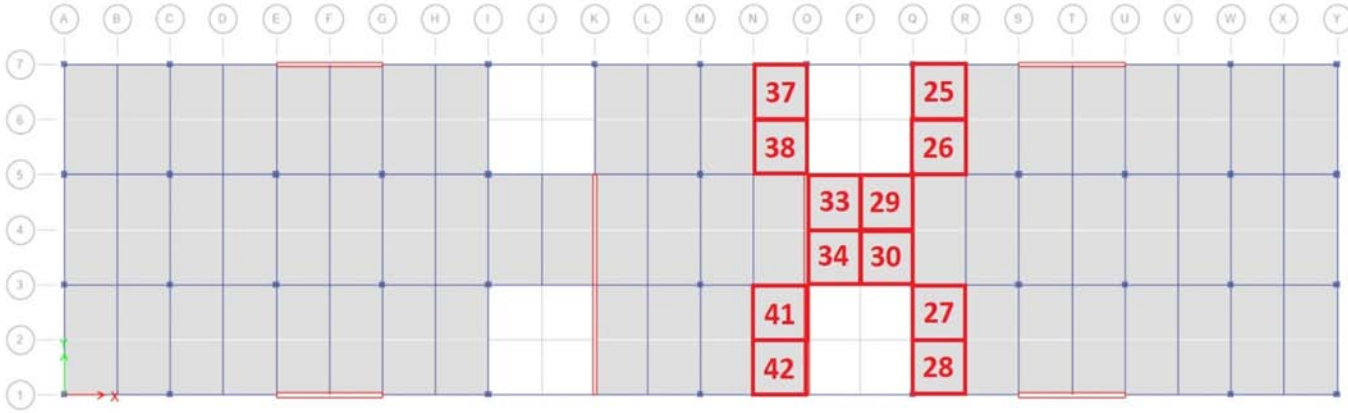

Figure 4-13 Diaphragm locations under consideration for investigation of shell layer stress of Model-9

Definition of terms and notations used in tables and discussion are described below.

First part is the name of in-plane stress component such as S_{11}, S_{22}, S_{12}.

Second part is the location of shell layer in nonlinear layer shell such as top or bottom of nonlinear layer shell.

Third part shows the stress value is maximum or minimum of the stress component.

Fourth part shows the story number.

Fifth part shows diaphragm design force procedures under consideration. LEP stands for linear elastic diaphragm design force procedures. LDP stands for linear dynamic diaphragm design force procedure. NSP stands for nonlinear static procedures or pushover analyses. Therefore, S_{11}-Top-Max-Story 3-LEP and LDP means maximum shell layer stress of S_{11} stress component in top of nonlinear layer shell at story 3 form linear elastic and linear dynamic diaphragm design force procedures.

Table 4-2 Maximum S_{12} in-plane shear stress at the bottom of layered shells from Diaphragm force procedures at Stories of models

S12-Bottom-Max-Story 3-LEP and LDP **μ = 100 psi** **σ = 91 psi**

Model Number-Diaphragm Location-Diaphragm Design Force Procedures	Stress at Story 3 (psi)	Shear reinforcement required or not	Change of Diaphragm section required or not	Location	Data points Location in Normal distribution curve/Bell curve/Gaussian distribution	Z-Score	Reference figure
M9-F42-LRHA	446	Yes	Yes	Near shear wall	Value Greater than μ +3σ	3.82	Figure 4-15
M9-F41-LRHA	440	Yes	Yes	Near shear wall	Value Greater than μ +3σ	3.76	Figure 4-14
M9-F38-LRHA	264	Yes	No	Near shear wall	Value between μ +2σ and μ +σ	1.82	N/A
M9-F33-LRHA	244	Yes	No	Near shear wall	Value between μ +2σ and μ +σ	1.60	N/A
M9-F25-LRHA	243	Yes	No	Near column	Value between μ +2σ and μ +σ	1.58	N/A
M9-F30-LRHA	197	Yes	No	Near column	Value between μ +2σ and μ +σ	1.07	N/A
M2-F6-LRHA	282	Yes	No	Near column	Value between μ +3σ and μ +2σ	2.01	Figure 4-16
M2-F2-LRHA	258	Yes	No	Near shear wall	Value between μ +2σ and μ +σ	1.75	N/A
M2-F3-LRHA	255	Yes	No	Near column	Value between μ +2σ and μ +σ	1.71	N/A
M8-F31-LRHA	280	Yes	No	Near column	Value between μ +2σ and μ +σ	1.99	Figure 4-81
M8-F40-ELFA Method-2	202	Yes	No	Near shear wall	Value between μ +2σ and μ +σ	1.13	N/A
M3-F7-LRHA	251	Yes	No	Near shear wall	Value between μ +2σ and μ +σ	1.67	N/A
M3-F12-LRHA	211	Yes	No	Near column	Value between μ +2σ and μ +σ	1.23	N/A
M3-F10-LRHA	197	Yes	No	Near column	Value between μ +2σ and μ +σ	1.07	N/A
M5-F18-LRHA	239	Yes	No	Near column	Value between μ +2σ and μ +σ	1.54	N/A
M5-F15-LRHA	221	Yes	No	Near column	Value between μ +2σ and μ +σ	1.34	N/A
M5-F14-LRHA	221	Yes	No	Near shear wall	Value between μ +2σ and μ +σ	1.33	N/A
M6-F19-LRHA	218	Yes	No	Near shear wall	Value between μ +2σ and μ +σ	1.30	N/A

S12-Bottom-Max-Story 2-LEP and LDP **μ = 96 psi** **σ = 87 psi**

Model Number-Diaphragm Location-Diaphragm Design Force Procedures	Stress at Story 2 (psi)	Shear reinforcement required or not	Change of Diaphragm section required or not	Location	Data points Location in Normal distribution curve/Bell curve/Gaussian distribution	Z-Score	Reference figure
M9-F42-LRHA	425	Yes	Yes	Near shear wall	Value Greater than μ +3σ	3.80	Figure 4-15
M9-F41-LRHA	420	Yes	Yes	Near shear wall	Value Greater than μ +3σ	3.75	Figure 4-14
M9-F25-LRHA	232	Yes	No	Near column	Value between μ +2σ and μ +σ	1.57	N/A
M9-F33-LRHA	231	Yes	No	Near shear wall	Value between μ +2σ and μ +σ	1.57	N/A
M9-F38-LRHA	229	Yes	No	Near shear wall	Value between μ +2σ and μ +σ	1.54	N/A
M9-F30-LRHA	184	Yes	No	Near column	Value between μ +2σ and μ +σ	1.02	N/A
M8-F31-LRHA	273	Yes	No	Near column	Value between μ +3σ and μ +2σ	2.04	Figure 4-81
M8-F40-ELFA Method-2	184	Yes	No	Near shear wall	Value between μ +2σ and μ +σ	1.02	N/A
M2-F6-ELFA Method-2	247	Yes	No	Near column	Value between μ +2σ and μ +σ	1.74	Figure 4-16
M2-F2-LRHA	228	Yes	No	Near shear wall	Value between μ +2σ and μ +σ	1.52	N/A
M2-F3-LRHA	216	Yes	No	Near column	Value between μ +2σ and μ +σ	1.38	N/A
M3-F7-LRHA	230	Yes	No	Near shear wall	Value between μ +2σ and μ +σ	1.55	N/A
M3-F12-ELFA Method-2	187	Yes	No	Near column	Value between μ +2σ and μ +σ	1.05	N/A
M5-F18-ELFA Method-2	220	Yes	No	Near column	Value between μ +2σ and μ +σ	1.43	N/A
M5-F14-LRHA	204	Yes	No	Near shear wall	Value between μ +2σ and μ +σ	1.25	N/A
M5-F15-LRHA	195	Yes	No	Near column	Value between μ +2σ and μ +σ	1.15	N/A
M6-F19-LRHA	199	Yes	No	Near shear wall	Value between μ +2σ and μ +σ	1.19	N/A

S12-Bottom-Max-Story 1-LEP and LDP **μ = 85 psi** **σ = 82 psi**

Model Number-Diaphragm Location-Diaphragm Design Force Procedures	Stress at Story 1 (psi)	Shear reinforcement required or not	Change of Diaphragm section required or not	Location	Data points Location in Normal distribution curve/Bell curve/Gaussian distribution	Z-Score	Reference figure
M9-F42-LRHA	416	Yes	Yes	Near shear wall	Value Greater than μ +3σ	4.04	Figure 4-15
M9-F41-LRHA	411	Yes	Yes	Near shear wall	Value Greater than μ +3σ	3.97	Figure 4-14
M9-F33-LRHA	207	Yes	No	Near shear wall	Value between μ +2σ and μ +σ	1.49	N/A
M9-F38-LRHA	200	Yes	No	Near shear wall	Value between μ +2σ and μ +σ	1.40	N/A
M9-F25-ELFA Method-2	188	Yes	No	Near column	Value between μ +2σ and μ +σ	1.26	N/A
M8-F31-LRHA	224	Yes	No	Near column	Value between μ +2σ and μ +σ	1.70	Figure 4-81
M8-F40-ELFA Method-2	175	Yes	No	Near shear wall	Value between μ +2σ and μ +σ	1.10	N/A
M2-F6-ELFA Method-2	221	Yes	No	Near column	Value between μ +2σ and μ +σ	1.65	Figure 4-16
M2-F2-ELFA Method-2	204	Yes	No	Near shear wall	Value between μ +2σ and μ +σ	1.44	N/A
M2-F3-ELFA Method-2	191	Yes	No	Near column	Value between μ +2σ and μ +σ	1.30	N/A
M5-F18-LRHA	203	Yes	No	Near column	Value between μ +2σ and μ +σ	1.44	N/A
M5--F14-ELFA Method-2	189	Yes	No	Near shear wall	Value between μ +2σ and μ +σ	1.27	N/A
M5-F15-LRHA	183	Yes	No	Near column	Value between μ +2σ and μ +σ	1.20	N/A
M3-F7-ELFA Method-2	197	Yes	No	Near shear wall	Value between μ +2σ and μ +σ	1.37	N/A
M6-F19-LRHA	185	Yes	No	Near shear wall	Value between μ +2σ and μ +σ	1.22	N/A

Table 4-3 Maximum S_{12} in-plane shear stress at the bottom of layered shells from Pushover analyses at stories of models

S12-Bottom-Max-Story 3-NSP μ = 193 psi σ = 198 psi

Model Number-Diaphragm Location-Diaphragm Design Force Procedures	Stress at Story 3 (psi)	Shear reinforcement required or not	Change of Diaphragm section required or not	Location	Data points Location in Normal distribution curve/Bell curve/Gaussian distribution	Z-Score	Reference figure
M8-F31-PushY-1.5XTg	1103	Yes	Yes	Near column	Value Greater than μ +3σ	4.59	Figure 4-17
M8-F35-PushY-1.5XTg	619	Yes	Yes	Near shear wall	Value between μ +3σ and μ +2σ	2.15	Figure 4-98
M8-F33-PushY-1.5XTg	549	Yes	Yes	Near shear wall	Value between μ +2σ and μ +σ	1.80	Figure 4-18
M8-F34-PushY-1.5XTg	495	Yes	Yes	Near shear wall	Value between μ +2σ and μ +σ	1.52	Figure 4-103
M9-F30-PushY-1.5XTg	1093	Yes	Yes	Near column	Value Greater than μ +3σ	4.54	Figure 4-19
M9-F33-PushY-1.5XTg	1085	Yes	Yes	Near shear wall	Value Greater than μ +3σ	4.50	Figure 4-18
M9-F25-PushY-1.5XTg	923	Yes	Yes	Near column	Value Greater than μ +3σ	3.68	Figure 4-101
M9-F38-PushY-1.5XTg	731	Yes	Yes	Near shear wall	Value between μ +3σ and μ +2σ	2.71	Figure 4-102
M9-F34-PushY-1.5XTg	614	Yes	Yes	Near shear wall	Value between μ +3σ and μ +2σ	2.13	Figure 4-103
M9-F27-PushY-1.5XTg	592	Yes	Yes	Near column	Value between μ +3σ and μ +2σ	2.02	Figure 4-104
M9-F29-PushY-1.5XTg	542	Yes	Yes	Near column	Value between μ +2σ and μ +σ	1.77	N/A
M9-F42-Push-100%X+30%Y	457	Yes	Yes	Near shear wall	Value between μ +2σ and μ +σ	1.34	N/A

S12-Bottom-Max-Story 2-NSP μ = 179 psi σ = 167 psi

Model Number-Diaphragm Location-Diaphragm Design Force Procedures	Stress at Story 2 (psi)	Shear reinforcement required or not	Change of Diaphragm section required or not	Location	Data points Location in Normal distribution curve/Bell curve/Gaussian distribution	Z-Score	Reference figure
M8-F31-PushY-1.5XTg	944	Yes	Yes	Near column	Value Greater than μ +3σ	4.58	Figure 4-17
M8-F35-PushY-1.5XTg	492	Yes	Yes	Near shear wall	Value between μ +2σ and μ +σ	1.88	Figure 4-98
M8-F33-PushY-1.5XTg	469	Yes	Yes	Near shear wall	Value between μ +2σ and μ +σ	1.74	Figure 4-18
M8-F34-PushY-1.5XTg	381	Yes	Yes	Near shear wall	Value between μ +2σ and μ +σ	1.21	Figure 4-103
M9-F33-PushY-1.5XTg	936	Yes	Yes	Near shear wall	Value Greater than μ +3σ	4.54	Figure 4-18
M9-F30-PushY-1.5XTg	879	Yes	Yes	Near column	Value Greater than μ +3σ	4.19	Figure 4-19
M9-F25-PushY-1.5XTg	784	Yes	Yes	Near column	Value Greater than μ +3σ	3.62	Figure 4-101
M9-F27-PushY-1.5XTg	553	Yes	Yes	Near column	Value between μ +3σ and μ +2σ	2.24	Figure 4-104
M9-F38-PushY-1.5XTg	544	Yes	Yes	Near shear wall	Value between μ +3σ and μ +2σ	2.19	Figure 4-102
M9-F42-Push-100%X+30%Y	479	Yes	Yes	Near shear wall	Value between μ +2σ and μ +σ	1.80	N/A
M9-F34-PushY-1.5XTg	431	Yes	Yes	Near shear wall	Value between μ +2σ and μ +σ	1.51	Figure 4-103
M9-F29-PushY-1.5XTg	428	Yes	Yes	Near column	Value between μ +2σ and μ +σ	1.49	N/A

S12-Bottom-Max-Story 1-NSP μ = 146 psi σ = 116 psi

Model Number-Diaphragm Location-Diaphragm Design Force Procedures	Stress at Story 1 (psi)	Shear reinforcement required or not	Change of Diaphragm section required or not	Location	Data points Location in Normal distribution curve/Bell curve/Gaussian distribution	Z-Score	Reference figure
M8-F31-PushY-1.5XTg	571	Yes	Yes	Near column	Value Greater than μ +3σ	3.69	Figure 4-17
M8-F35-PushY-1.5XTg	397	Yes	Yes	Near shear wall	Value between μ +3σ and μ +2σ	2.18	Figure 4-98
M8-F34-PushY-1.5XTg	279	Yes	No	Near shear wall	Value between μ +2σ and μ +σ	1.16	Figure 4-103
M9-F33-PushY-1.5XTg	526	Yes	Yes	Near shear wall	Value Greater than μ +3σ	3.30	Figure 4-18
M9-F25-PushY-1.5XTg	524	Yes	Yes	Near column	Value Greater than μ +3σ	3.28	Figure 4-101
M9-F30-PushY-1.5XTg	497	Yes	Yes	Near column	Value Greater than μ +3σ	3.04	Figure 4-19
M9-F42-Push-100%X+30%Y	453	Yes	Yes	Near shear wall	Value between μ +3σ and μ +2σ	2.66	N/A
M9-F27-PushY-1.5XTg	438	Yes	Yes	Near column	Value between μ +3σ and μ +2σ	2.53	Figure 4-104
M9-F38-PushY-1.5XTg	334	Yes	Yes	Near shear wall	Value between μ +2σ and μ +σ	1.63	Figure 4-102
M9-F34-PushY-1.5XTg	280	Yes	No	Near shear wall	Value between μ +2σ and μ +σ	1.16	Figure 4-103
M6-F19-PushY-1.5XTg	302	Yes	No	Near shear wall	Value between μ +2σ and μ +σ	1.35	N/A
M6-F24-PushY-1.5XTg	267	Yes	No	Near column	Value between μ +2σ and μ +σ	1.05	N/A
M3-F7-PushY-1.5XTg	292	Yes	No	Near shear wall	Value between μ +2σ and μ +σ	1.27	N/A
M3-F12-PushY-1.5XTg	266	Yes	No	Near column	Value between μ +2σ and μ +σ	1.04	N/A
M2-F2-Push-100%X+30%Y	285	Yes	No	Near shear wall	Value between μ +2σ and μ +σ	1.21	N/A
M5-F14-PushY-1.5XTg	284	Yes	No	Near shear wall	Value between μ +2σ and μ +σ	1.20	N/A

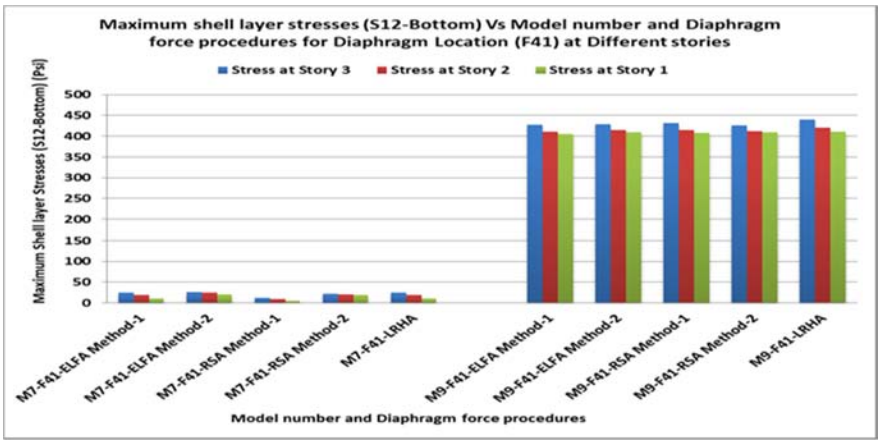

Figure 4-14 Maximum shell layer stresses (S12-Bottom) Vs Model number and Diaphragm force procedures for Diaphragm Location (F41) at Different stories

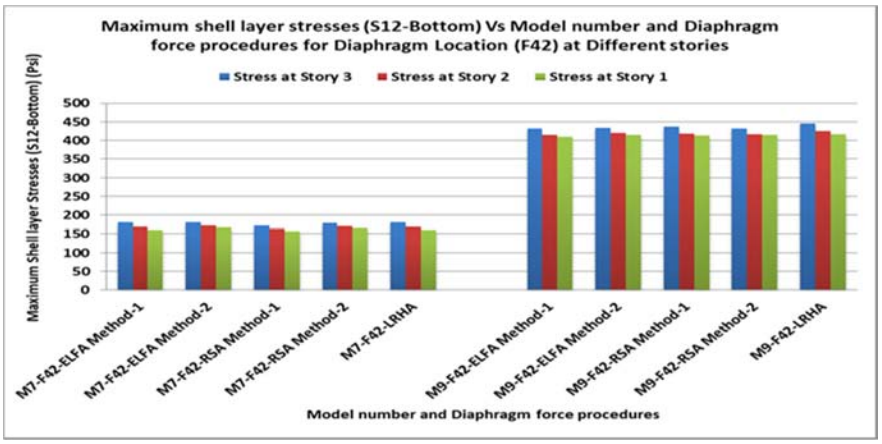

Figure 4-15 Maximum shell layer stresses (S12-Bottom) Vs Model number and Diaphragm force procedures for Diaphragm Location (F42) at Different stories

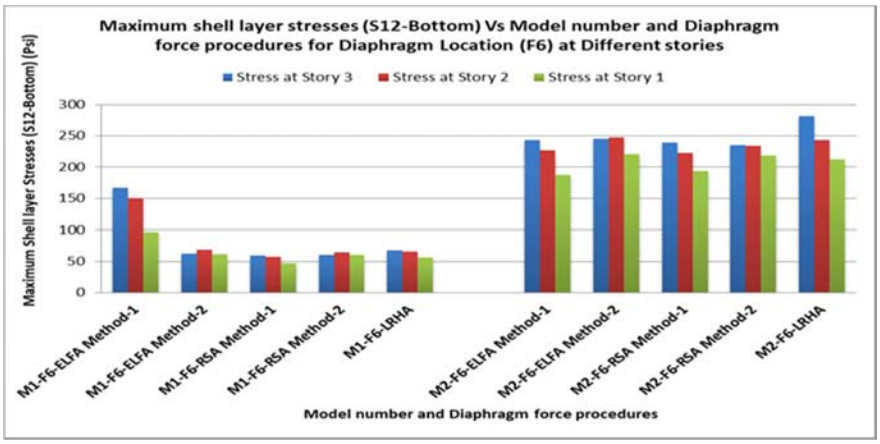

Figure 4-16 Maximum shell layer stresses (S12-Bottom) Vs Model number and Diaphragm force procedures for Diaphragm Location (F6) at Different stories

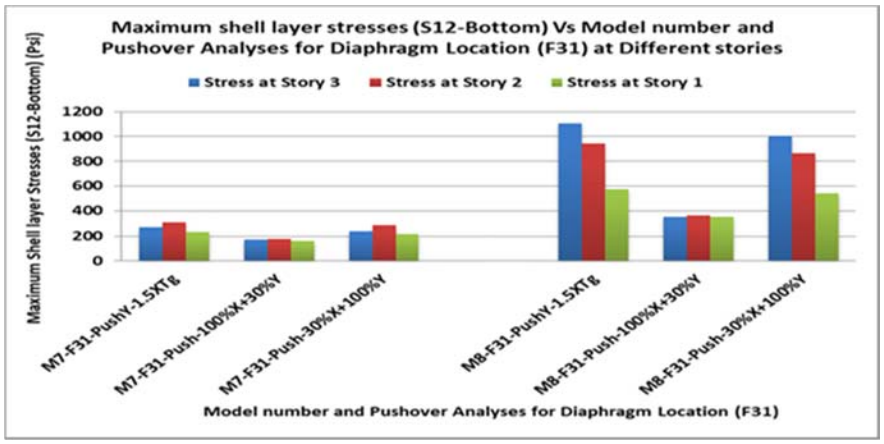

Figure 4-17 Maximum shell layer stresses (S12-Bottom) Vs Model number and Pushover Analyses for Diaphragm Location (F31) at Different stories

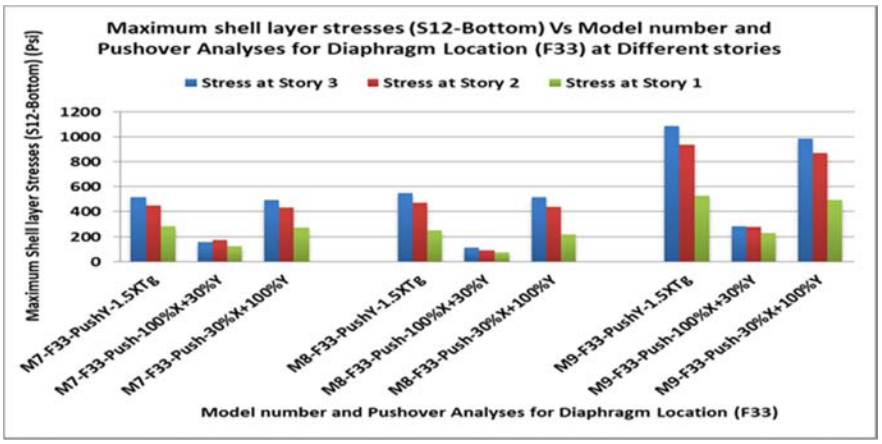

Figure 4-18 Maximum shell layer stresses (S12-Bottom) Vs Model number and Pushover Analyses for Diaphragm Location (F33) at Different stories

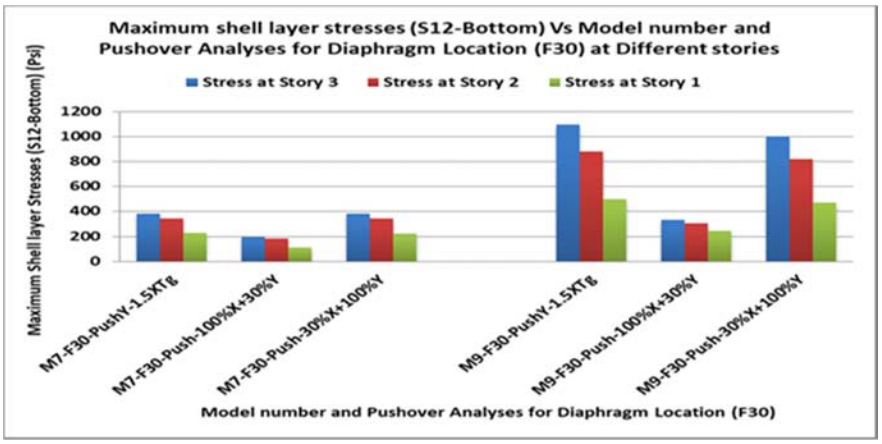

Figure 4-19 Maximum shell layer stresses (S12-Bottom) Vs Model number and Pushover Analyses for Diaphragm Location (F30) at Different stories

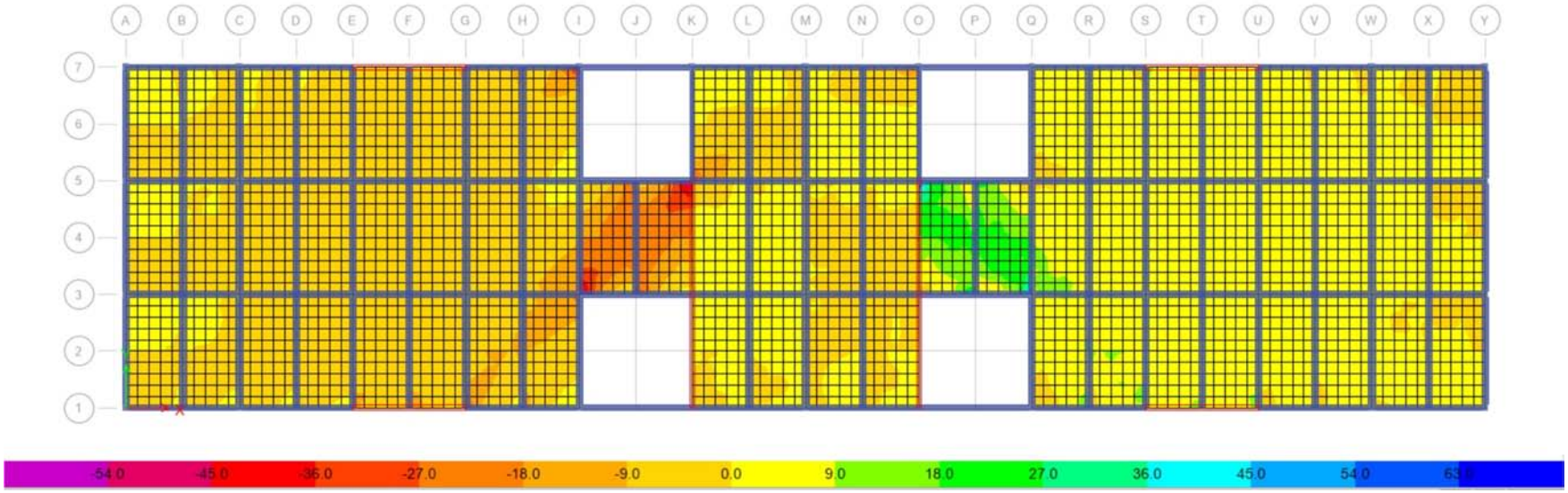

Figure 4-20 Absolute maximum shell resultant forces (F12) contour diagram of Model-9 (story 3) from Pushover analysis along Y-direction up to 1.5 times target displacement (kips/ft)

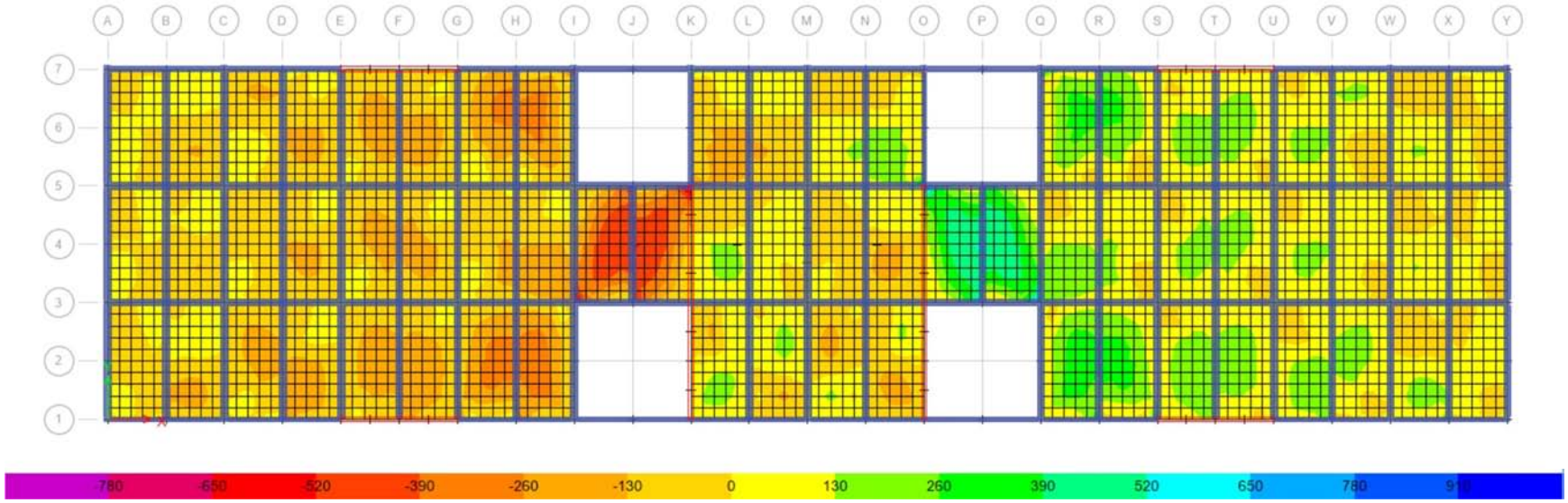

Figure 4-21 Contour diagram of absolute maximum shell layer stresses (S_{12}) at top of layered shell of Model-9 (story 3) from Pushover analysis along Y-direction up to 1.5 times target displacement (psi)

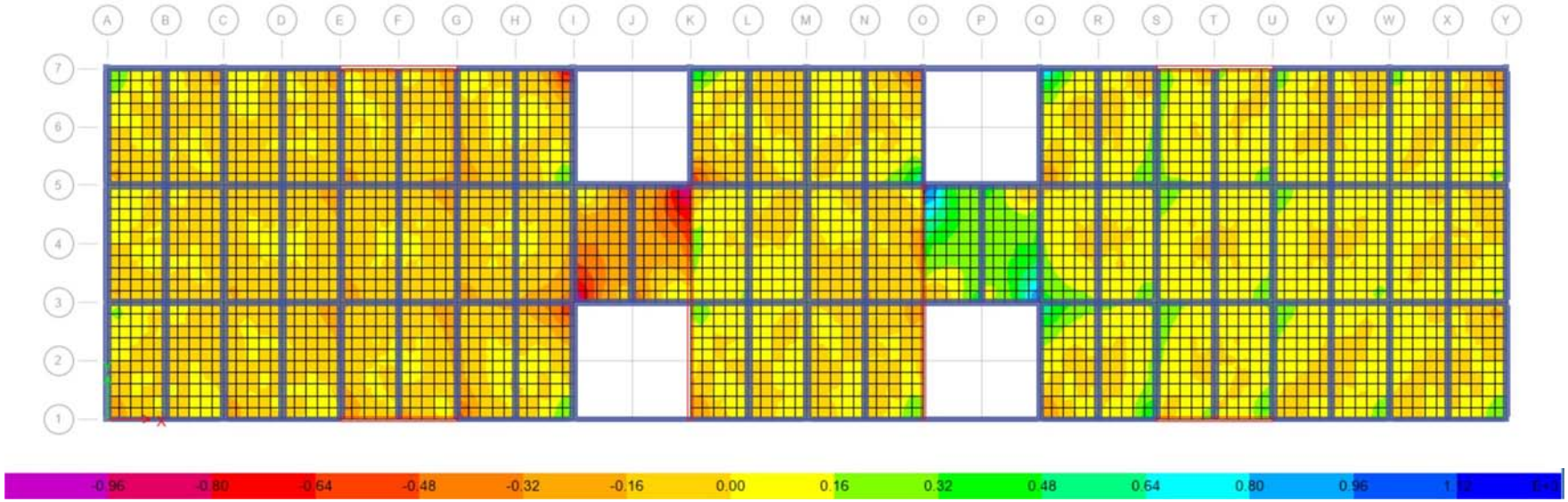

Figure 4-22 Contour diagram of absolute maximum shell layer stresses (S_{12}) at bottom of layered shell of Model-9 (story 3) from Pushover analysis along Y-direction up to 1.5 times target displacement (psi)

4.4 Discussion on results

Discussion on analytical study results are described in this section.

4.4.1 Maximum displacement observed at target displacement from Pushover analysis

Maximum displacement observed in top story along Y-direction at target displacement from pushover analyses are higher compared to maximum displacement observed in top story along X-direction at target displacement from pushover analyses for building models. Therefore all the building models are weak in Y-direction compared to X-direction. Building models experiencing maximum inelastic total drift along Y-direction at target displacement from pushover analyses are arranged in descending orders which are shown as follows: Model-2, Model-3, Model-9, Model-8, Model-5 and Model-6. These observations are made by checking maximum inelastic total drift along Y-direction at target displacement from pushover analyses. Therefore, Model-2 (Models with end shear walls) is experiencing maximum inelastic total drift along Y-direction compared to Model-9 and Model-8 (Models with intermediate shear walls).

4.4.2 Worst orientation of diaphragm opening adjacent to shear wall

Worst orientation of diaphragm opening adjacent to end shear wall and intermediate shear wall is determined based on two questions. First question: Are both top and bottom layers of nonlinear shell of the building model experiencing high in-plane flexural stress and in-plane shear stress compared to other building models. Second question: Are more diaphragm locations near diaphragm opening adjacent to shear wall are experiencing high in-plane flexural stress and in-plane shear stress compared to other building models. It is found that more diaphragm locations around diaphragm opening of Model-9 are experiencing high in-plane stress (that exceeds $\mu + \sigma$ or below $\mu - \sigma$) from S_{11}, S_{22} and S_{12} stress component compared to other models. Hence Orientation of diaphragm openings adjacent to intermediate shear walls of Model-9 is the worst scenario compared other models. Diaphragm locations near diaphragm opening adjacent to intermediate shear wall will experience high in-plane stress in both top and bottom layers of nonlinear layered shell compared to other models during earthquake.

Model-9 and Model-2 will experience high in-plane flexural and in-plane shear stress in diaphragm locations near diaphragm opening adjacent to shear wall compared to other models during earthquake. However, more diaphragm locations are affected by high in-plane stress in diaphragm locations near diaphragm opening of Model-9 compared to Model-2 during earthquake. Most of the time Model-2 will experience high in-plane stress (by S_{11}, S_{22} and S_{12} stress components that exceed $\mu + \sigma$ or below $\mu - \sigma$) only in top or bottom layer of nonlinear layered shell in diaphragm locations around diaphragm opening adjacent to shear wall but Model-9 will experience high in-plane stress in both top and bottom layer of nonlinear layered shell (by S_{11}, S_{22} and S_{12} stress components that exceeds $\mu + \sigma$ or below $\mu - \sigma$) compared to other models. Hence, orientation of diaphragm locations near diaphragm opening adjacent to shear wall of Model-9 is the worst scenario compared to other models.

Model-9 is experiencing high in-plane stress near diaphragm openings adjacent shear walls compared to all the building models. So models having diaphragm locations near diaphragm openings adjacent to intermediate shear walls are experiencing high in-plane stress compared to other models. Orientation of diaphragm openings near intermediate shear walls of Model-9 is the worst scenario as diaphragm locations near diaphragm openings adjacent to shear walls because more diaphragm locations around diaphragm opening are experiencing high in-plane stress in the both top and bottom layer of nonlinear layer shell by S_{11}, S_{22} and S_{12} stress component compared to other models. Diaphragm locations around diaphragm opening of Model-9 are experiencing high in-plane stress (that exceeds $\mu + \sigma$ or below $\mu - \sigma$) by S_{11}, S_{22} and S_{12} stress component compared to other models. These observations are made by analyzing the data of **Tables 4-2 to 4-25**.

4.4.3 Models demanding change of diaphragm section near diaphragm opening adjacent to shear wall due to high in-plane shear stress

Diaphragm locations near diaphragm openings adjacent to shear walls of Model-9 require change of diaphragm sections and shear reinforcements for safe transfer of diaphragm in-plane shear to the seismic force resisting vertical structural elements. Diaphragm locations near diaphragm openings adjacent to shear walls of Model-9, Model-8, Model-2, Model-5, Model-3 and Model-6 require change of diaphragm sections and shear reinforcements for safe transfer of diaphragm in-plane shear to the

seismic force resisting vertical structural elements. Change of diaphragm sections can be introduced by increasing the thickness of diaphragm. But thickness of diaphragm locations near diaphragm openings adjacent to shear walls of Model-9, Model-8, Model-2 and Model-5 will be high compared to Model-3 and Model-6 as in-plane shear stress is high in diaphragm of Model-9, Model-8, Model-2 and Model-5 near diaphragm openings compared to Model-3 and Model-6. These observations are made by checking the shear stress data from Pushover analyses.

4.4.4 Reduction of In-plane stress data of nonlinear layer shell for design

Plotted or tabulated stresses at locations other than the four Gauss points are interpolated or extrapolated, and do not necessarily represent the sampled nonlinear stresses. For this reason, stresses at the joints may sometimes appear to exceed failure stresses (CSI Analysis Reference Manual, 2016). In-plane stress data of nonlinear layer shell from ETABS 2016 (2017) can be reduced up to 100 to 300 psi for analyses and design of diaphragm when in-plane stress data are extracted from tables in ETABS 2016 for pushover analyses. When maximum or minimum of layer shell stress are located in diaphragm connection to beams and seismic force resisting vertical elements, ETABS 2016 gives stress data of the location where diaphragm is connected to centerline of beams and seismic force resisting vertical elements. So designer may take diaphragm's stress data between the diaphragm section and the face of beams or seismic force resisting vertical elements which is almost 100 to 300 psi less than the diaphragm's stress data of diaphragm section at the centerline of beams and seismic force resisting vertical elements.

4.4.5 Dominating diaphragm design force procedure between Linear elastic procedure and Linear dynamic procedure for in-plane stress analysis

In-plane stress of diaphragm locations near diaphragm opening adjacent to shear walls from Modal linear response history analysis dominates over other linear elastic procedures. This observation are made by analyzing the data of **Tables 4-2 to 4-25** and **Figures 4-14 to 4-122**.

4.4.6 Comparison of in-plane stress form different diaphragm design force procedures (LEP and LDP) and pushover analyses

Linear elastic and linear dynamic diaphragm design force procedures underestimates in-plane stress in diaphragm locations around diaphragm opening adjacent shear wall as in-plane stress form pushover analyses are higher than linear elastic and linear dynamic diaphragm design force procedures in these diaphragm locations. **Tables 4-2 to 4-25** presented in-plane stress data from different diaphragm force procedures and pushover analyses for diaphragm locations near diaphragm opening adjacent to shear wall. It is clear from **Tables 4-2 to 4-25** that in-plane stress form pushover analyses are higher than linear elastic and linear dynamic diaphragm design force procedures.

4.4.7 Need for development of diaphragm discontinuity criteria when diaphragm opening is adjacent to shear wall

According to ASCE 7-10 (ASCE, 2010), Diaphragm discontinuity irregularity is defined to exist where there is a diaphragm with an abrupt discontinuity or variation in stiffness, including one having a cutout or open area greater than 50% of the gross enclosed diaphragm area. We have investigated building models with plan aspect ratio of 4:1 (Model-2, Model-3, Model-7 and Model-8) having cutoff area of 11% of the gross enclosed diaphragm area and building models with plan aspect ratio of 3:1 (Model-5, and Model-6) having cutoff area of 14% of the gross enclosed diaphragm area. These models are not fulfilling the criteria of diaphragm discontinuity, as open area in diaphragm is less than 50 percent of the gross enclosed diaphragm area. Although open area in diaphragm is less than 50 percent of the gross enclosed diaphragm area, diaphragm locations near diaphragm openings adjacent to shear walls experience high in-plane flexural and in-plane shear force/stress which cannot be overlooked. Sometimes diaphragm locations near diaphragm opening adjacent to shear walls are experiencing high in-plane shear stress that requires increase of thickness of diaphragm for safe transfer of in-plane shear stress to seismic force resisting vertical elements. According to ASCE 7-10, Structures having diaphragm discontinuity irregularity assigned to the seismic design categories (SDC D, E and F) listed in Table 12.3-1 of ASCE 7-10 shall comply with the requirements in the sections 12.3.3.4 and Table 12.6-1 of ASCE 7-10. However, ASCE 7-10 does not provide any guideline or requirements for structure with diaphragm discontinuity (diaphragm opening >50% or

diaphragm opening <50% of gross enclosed diaphragm area) assigned to Seismic design category C. The building models analyzed in this thesis are assigned to Seismic design category C and diaphragm locations around diaphragm opening adjacent to shear wall of these models are subjected to high in-plane flexural stress and in-plane shear stress even though the diaphragm opening in these buildings is 11% to 14% of the gross diaphragm area. Therefore, guidelines and requirements should be developed for structures with diaphragm opening adjacent to shear wall assigned to Seismic Design Category C.

4.5 Summary

In-plane stress of diaphragm locations near diaphragm opening adjacent to shear walls from Modal linear response history analysis dominates over other linear elastic procedures but in-plane stress form pushover analyses are higher than linear elastic and linear dynamic diaphragm design force procedures in these diaphragm locations. Orientation of diaphragm openings near intermediate shear walls of Model-9 is the worst scenario because statistical analysis shows that more diaphragm locations around diaphragm opening are experiencing high in-plane stress in the both top and bottom layer of nonlinear layer shell by S_{11}, S_{22} and S_{12} stress component (that exceeds $\mu + \sigma$ or below $\mu - \sigma$) compared to other models. ASCE 7-10 (ASCE, 2010) does not provide any guideline or requirements for structure with diaphragm discontinuity (diaphragm opening >50% or diaphragm opening <50% of gross enclosed diaphragm area) assigned to Seismic design category C. Although diaphragm opening is l1% or 14% of the gross enclosed area of diaphragm of models and models are located in Seismic design category C, highly stressed diaphragm locations around diaphragm opening adjacent to shear wall are identified which cannot be overlooked. Sometimes shear reinforcements and change of diaphragm section are required in these highly stress diaphragm locations for safe transfer of diaphragm inertial and transfer force to seismic force resisting vertical elements.

Chapter 5

DESIGN OF COLLEECTOR, CHORD AND SHEAR REINFORCEMENT OF DIAPHRAGM

5.1 Introduction

In this chapter design of collector, chord and shear reinforcement are designed based on ACI 318-14 (ACI, 2014) code. Diaphragm design force are calculated and compared from ELFA Method-1, ELFA Method-2, RSA Method-1, RSA Method-2 and Pushover analyses for design of collector, chord and shear reinforcement. Both unidirectional and orthogonal applications of diaphragm design forces are applied to the diaphragm to get the maximum diaphragm design force for design of collector, chord and shear reinforcement. Over strength factor is used to the diaphragm design force of ELFA Method-1, ELFA Method-2, RSA Method-1 and RSA Method-2 to get design forces for collector, chord and shear reinforcement. In this chapter diaphragm design force from pushover analyses are used to design chord, collector and shear reinforcement of diaphragm as pushover analyses gives more realistic results compared to other diaphragm force procedures.

5.2 Design of Diaphragm for In-plane Shear Force

Diaphragm locations near diaphragm openings adjacent to end shear walls of model-2 are chosen for design of shear reinforcements which are shown in **Figure 5-1**. Contour diagrams of in-plane shear forces near diaphragm opening adjacent to shear walls form pushover analyses are shown in **Figures 5-2 to 5-6**. Contour diagram of in-plane shear forces near diaphragm opening adjacent to shear walls form ELFA Method-2 is shown in **Figures 5-7**. Comparative analysis of in-plane shear forces from different diaphragm force procedures (LEP and LDP) and pushover analyses of diaphragm locations near diaphragm opening of model-2 are shown in **Figures 5-8 to 5-31**.

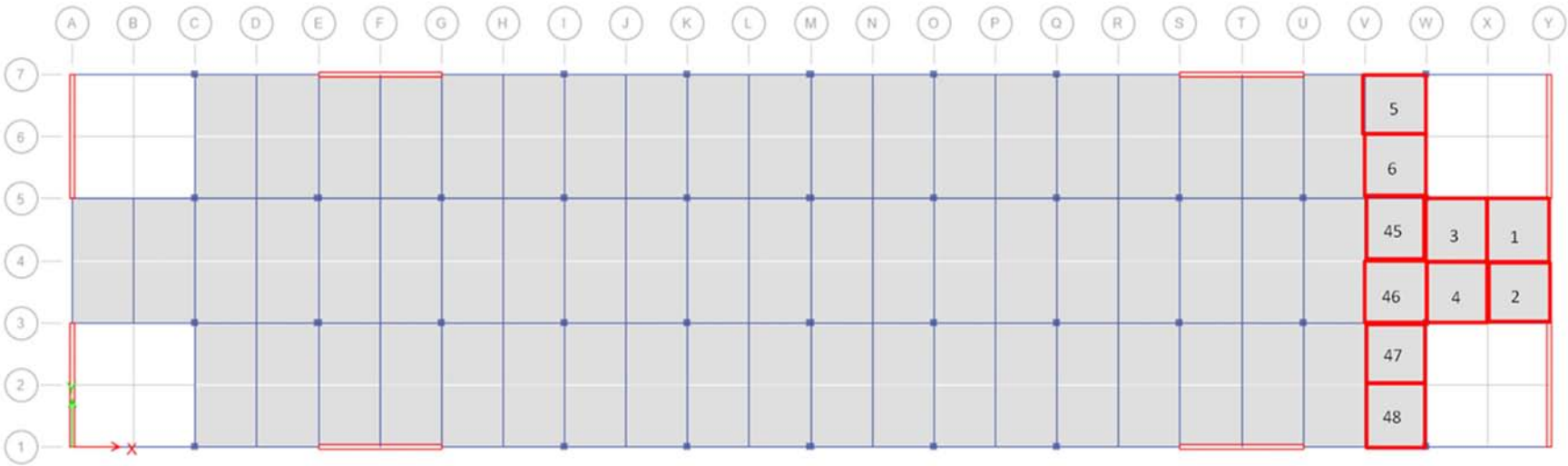

Figure 5-1 Diaphragm locations located near diaphragm opening adjacent to shear walls (Model-2).

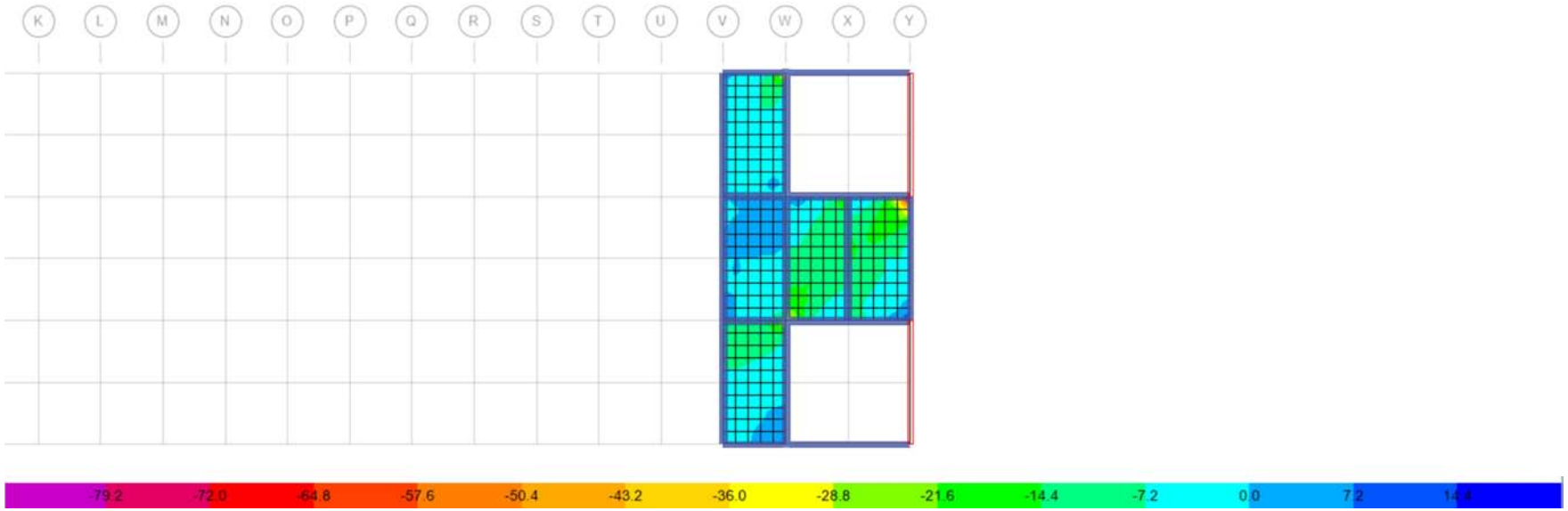

Figure 5-2 Resultant force F12 contour diagram of Diaphragm locations located near diaphragm opening adjacent to shear walls (Model-2, Story 3) from pushover analysis along Y-direction at 1.5 times the target displacement (with chord and collector reinforcement in beam near diaphragm opening)

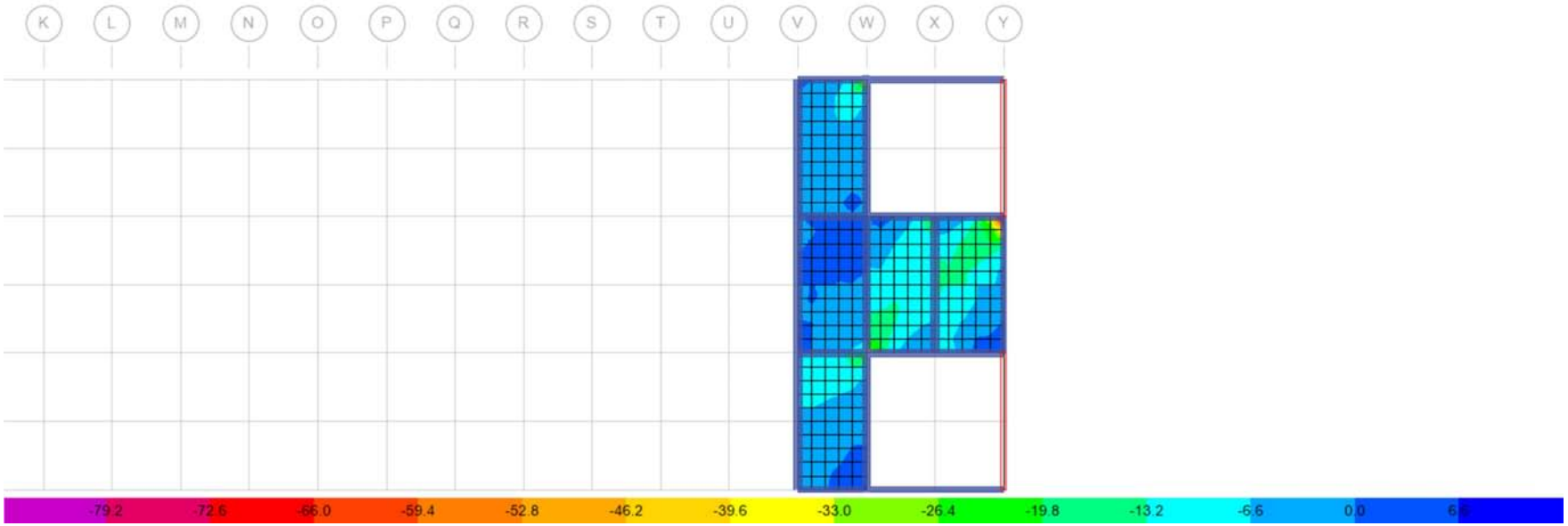

Figure 5-3 Resultant force F12 contour diagram of Diaphragm locations located near diaphragm opening adjacent to shear walls (Model-2, Story 3) from pushover analysis along for orthogonal loading (30%X + 100%Y) (with chord and collector reinforcement in beam near diaphragm opening)

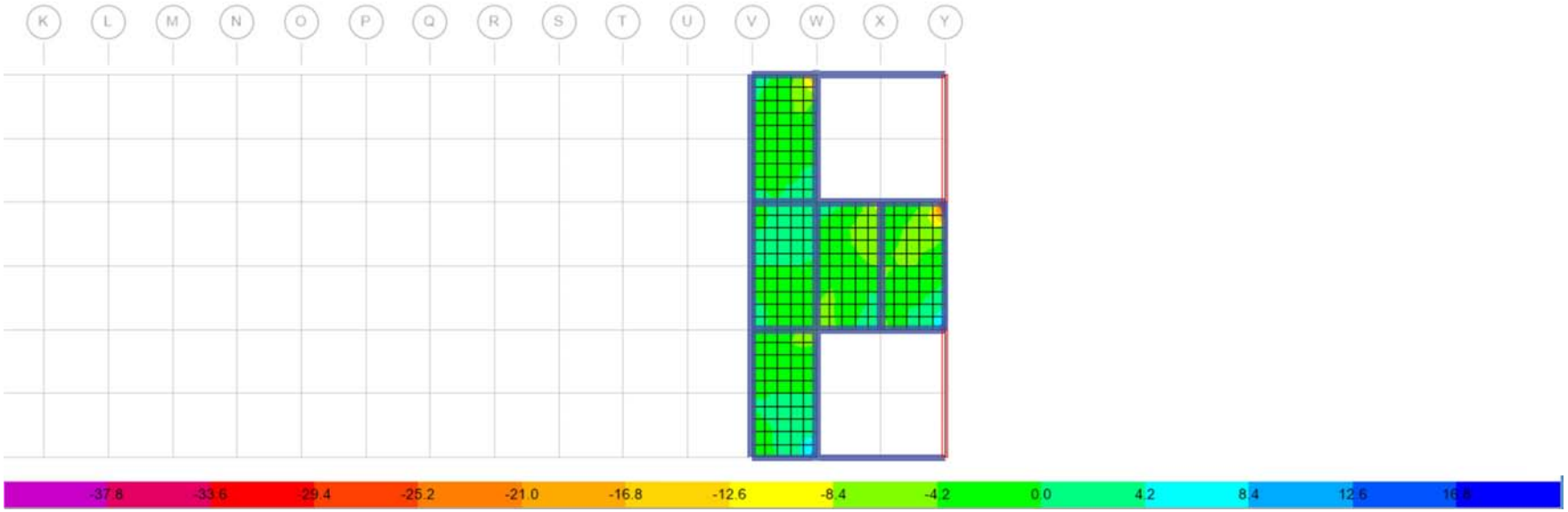

Figure 5-4 Resultant force F12 contour diagram of Diaphragm locations located near diaphragm opening adjacent to shear walls (Model-2, Story 3) from pushover analysis along for orthogonal loading (100%X + 30%Y) (with chord and collector reinforcement in beam near diaphragm opening)

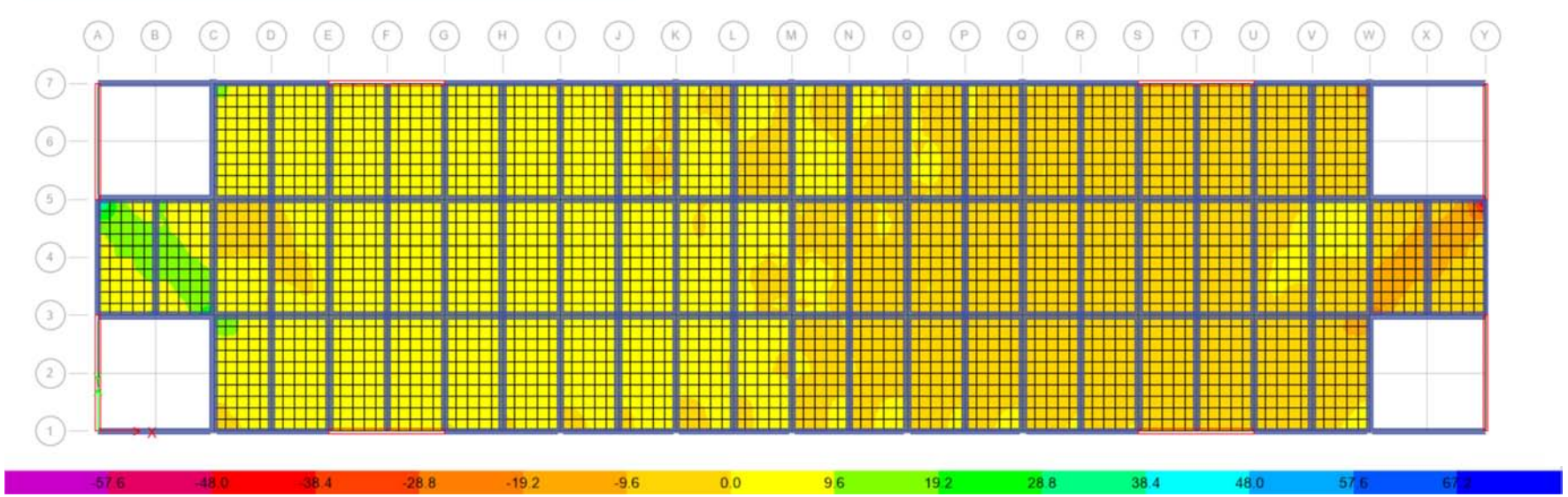

Figure 5-5 Resultant force F12 diaphragm of Diaphragm locations located near diaphragm opening adjacent to shear walls (Model-2, Story 3) from pushover analysis along Y-direction at the target displacement (without chord and collector reinforcement in beam near diaphragm opening)

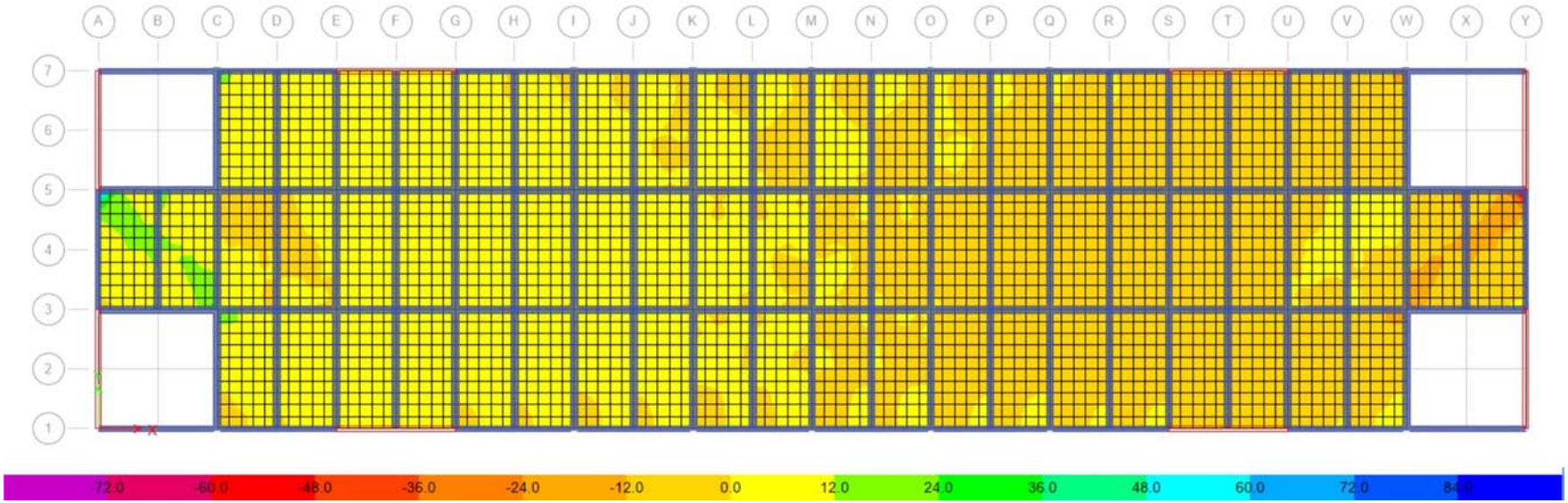

Figure 5-6 Resultant force F12 diaphragm of Diaphragm locations located near diaphragm opening adjacent to shear walls (Model-2, Story 3) from pushover analysis along Y-direction at the target displacement (with chord and collector reinforcement in beam near diaphragm opening)

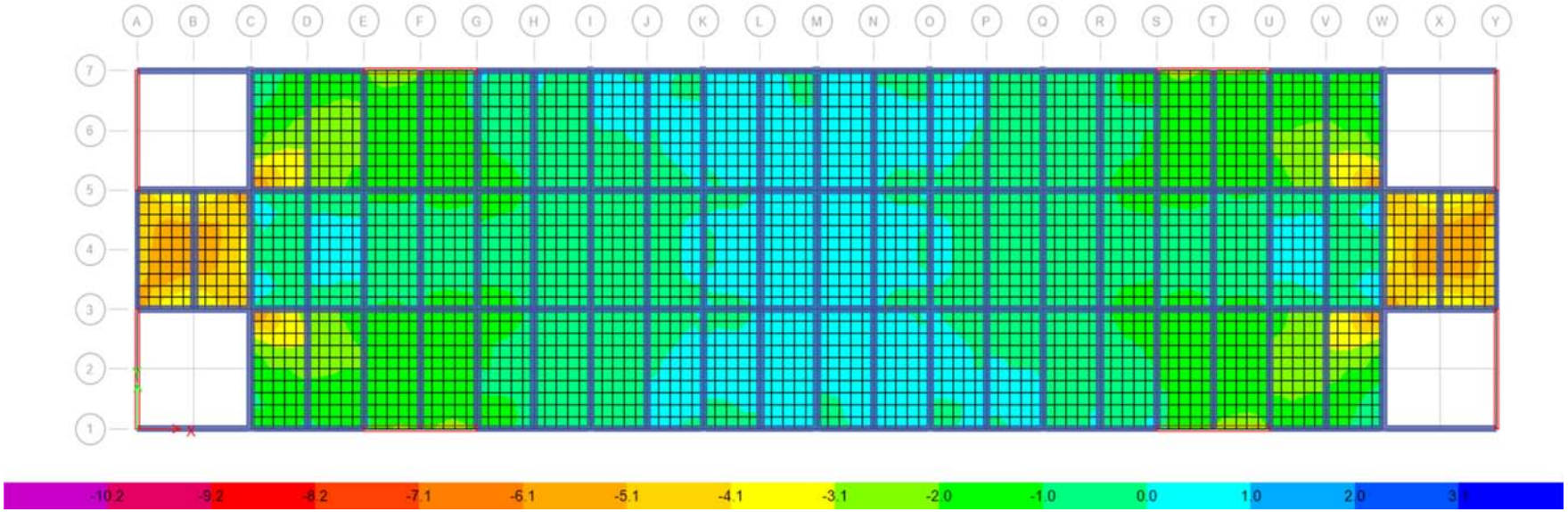

Figure 5-7 Resultant force F12 diaphragm of Diaphragm locations located near diaphragm opening adjacent to shear walls (Model-2, Story 3) from ELFA Method-2 (with chord and collector reinforcement in beam near diaphragm opening)

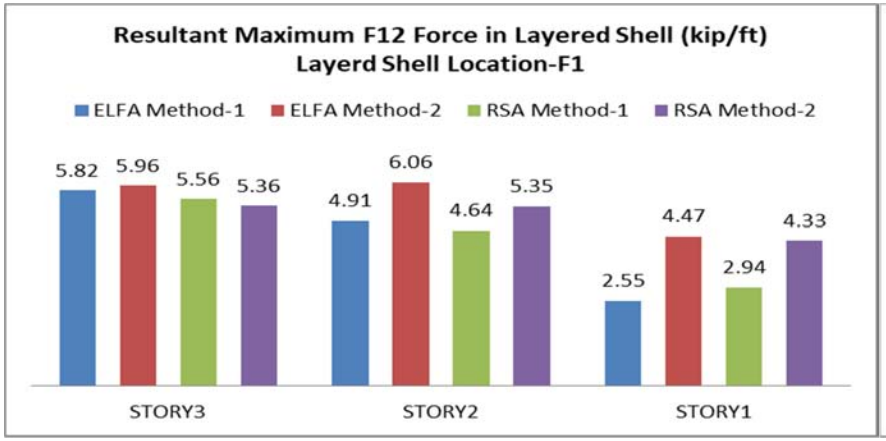

Figure 5-8 Resultant Maximum F12 Force in Layered Shell (kip/ft) for Layerd Shell Location-F1 of Model-2 from Different diaphragm force procedures

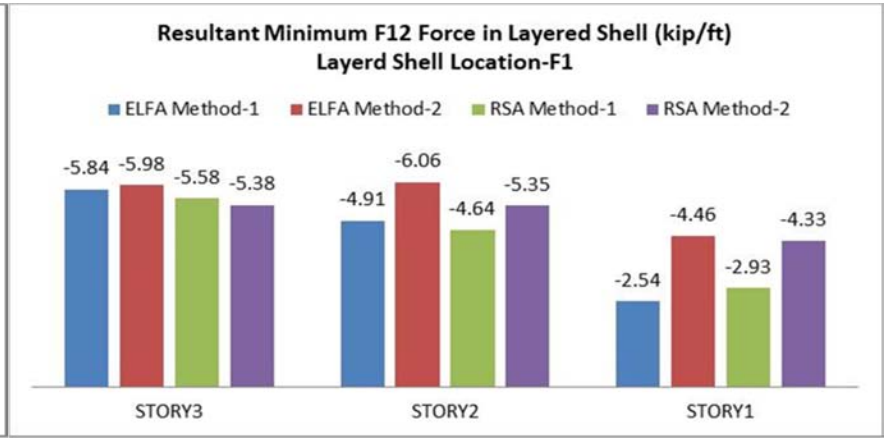

Figure 5-9 Resultant Minimum F12 Force in Layered Shell (kip/ft) for Layerd Shell Location-F1 of Model-2 from Different diaphragm force procedures

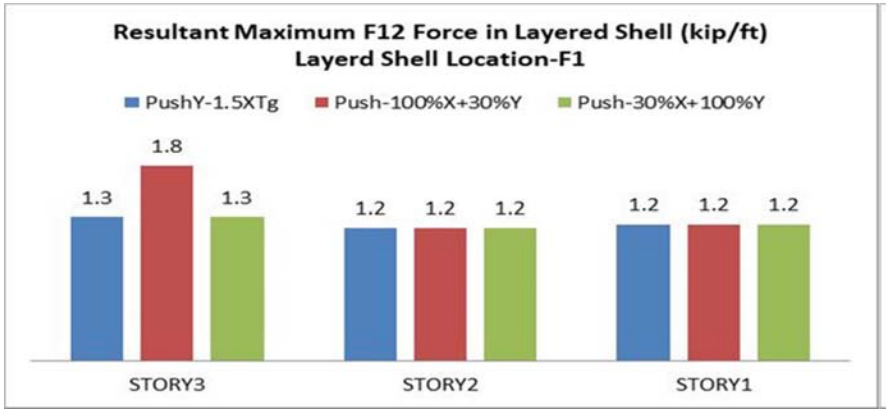

Figure 5-10 Resultant Maximum F12 Force in Layered Shell (kip/ft) for Layerd Shell Location-F1 of Model-2 from Pushover Analyses (with chord and collector reinforcement in beam near diaphragm opening)

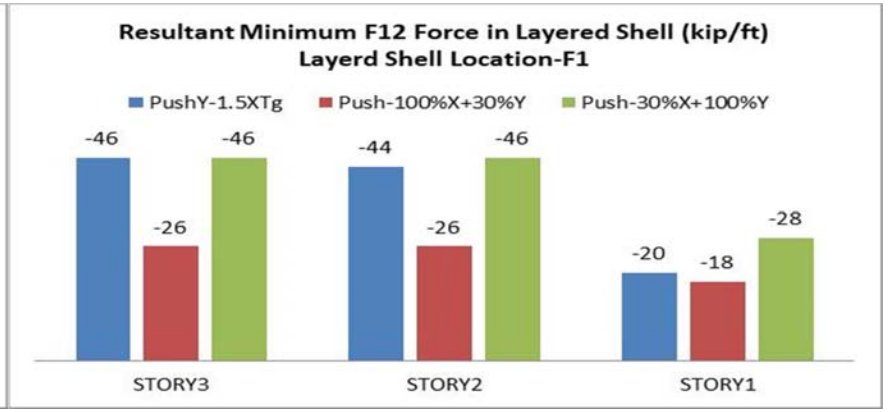

Figure 5-11 Resultant Minimum F12 Force in Layered Shell (kip/ft) for Layerd Shell Location-F1 of Model-2 from Pushover Analyses (with chord and collector reinforcement in beam near diaphragm opening)

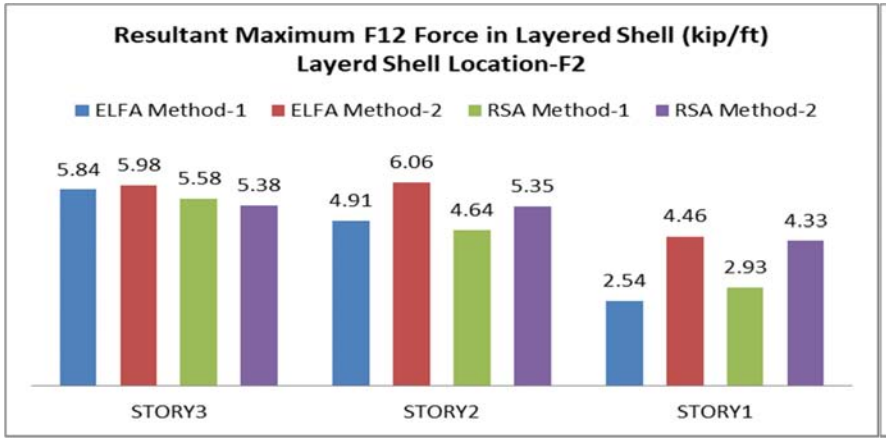

Figure 5-12 Resultant Maximum F12 Force in Layered Shell (kip/ft) for Layerd Shell Location-F2 of Model-2 from Different diaphragm force procedures

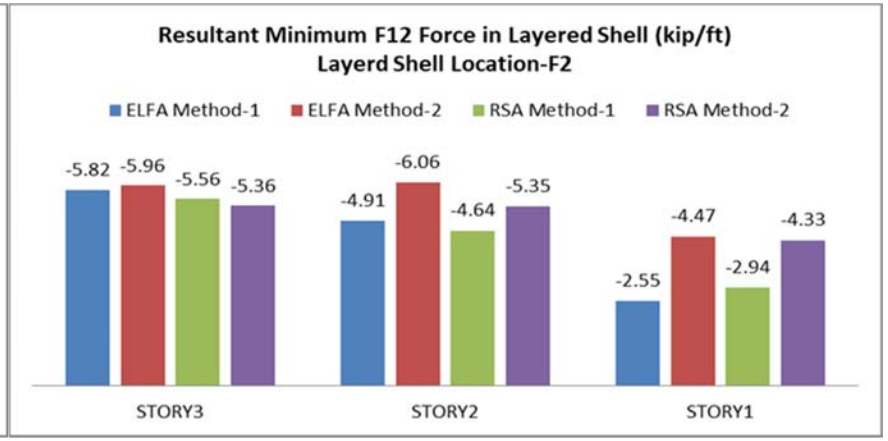

Figure 5-13 Resultant Minimum F12 Force in Layered Shell (kip/ft) for Layerd Shell Location-F2 of Model-2 from Different diaphragm force procedures

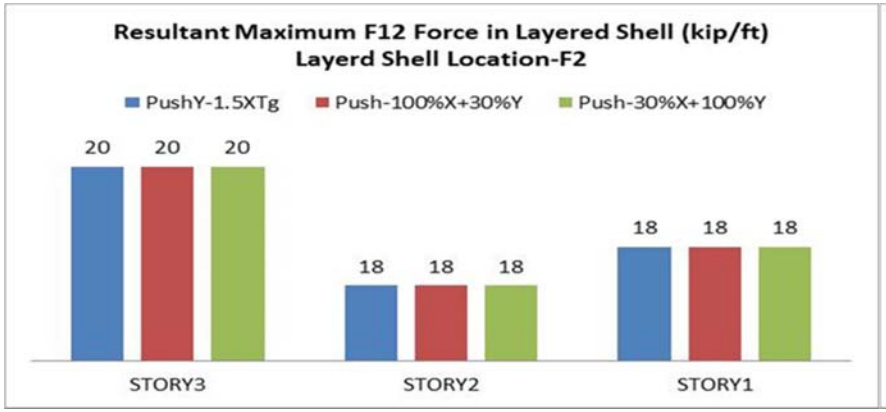

Figure 5-14 Resultant Maximum F12 Force in Layered Shell (kip/ft) for Layerd Shell Location-F2 of Model-2 from Pushover Analyses (with chord and collector reinforcement in beam near diaphragm opening)

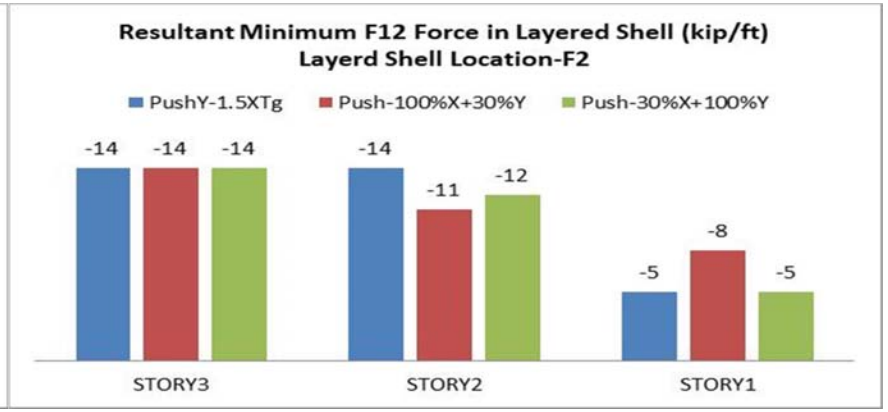

Figure 5-15 Resultant Minimum F12 Force in Layered Shell (kip/ft) for Layerd Shell Location-F2 of Model-2 from Pushover Analyses (with chord and collector reinforcement in beam near diaphragm opening)

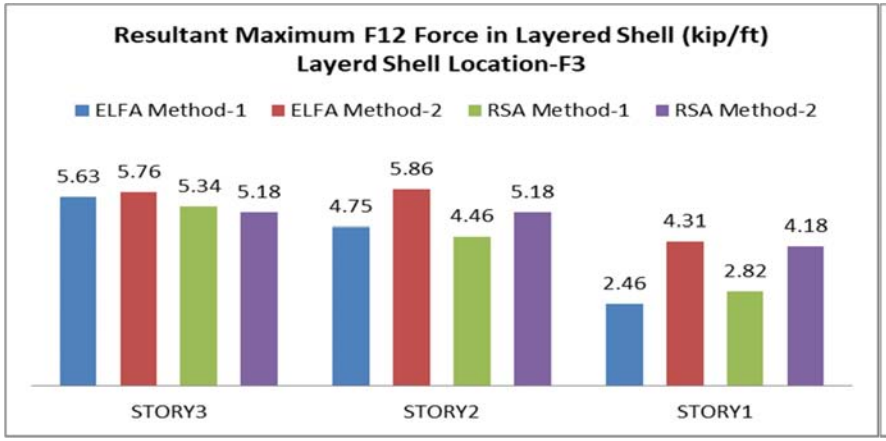

Figure 5-16 Resultant Maximum F12 Force in Layered Shell (kip/ft) for Layerd Shell Location-F3 of Model-2 from Different diaphragm force procedures

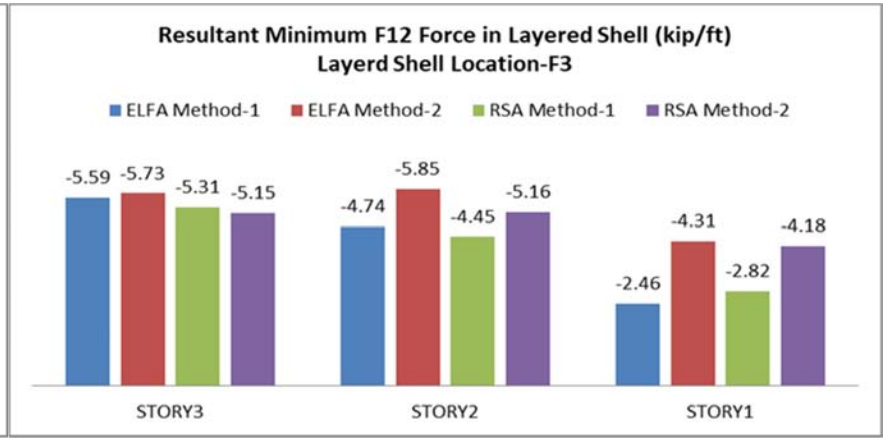

Figure 5-17 Resultant Minimum F12 Force in Layered Shell (kip/ft) for Layerd Shell Location-F3 of Model-2 from Different diaphragm force procedures

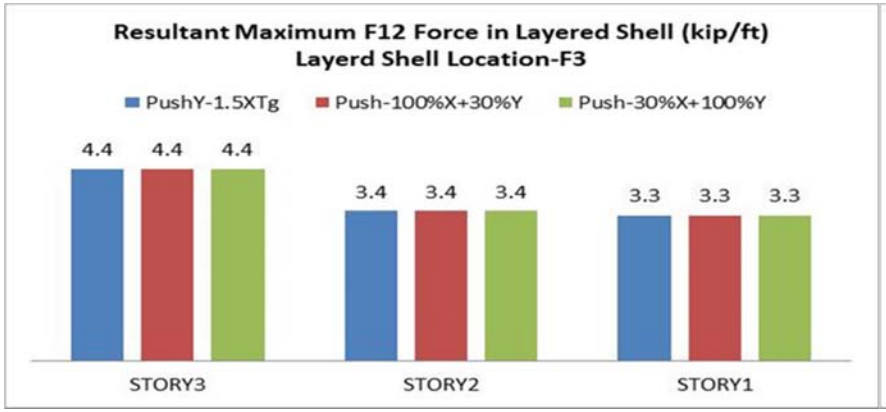

Figure 5-18 Resultant Maximum F12 Force in Layered Shell (kip/ft) for Layerd Shell Location-F3 of Model-2 from Pushover Analyses (with chord and collector reinforcement in beam near diaphragm opening)

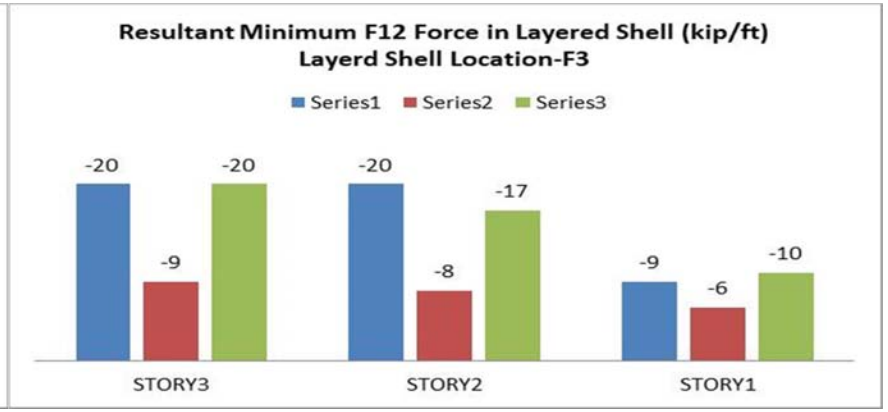

Figure 5-19 Resultant Minimum F12 Force in Layered Shell (kip/ft) for Layerd Shell Location-F3 of Model-2 from Pushover Analyses (with chord and collector reinforcement in beam near diaphragm opening)

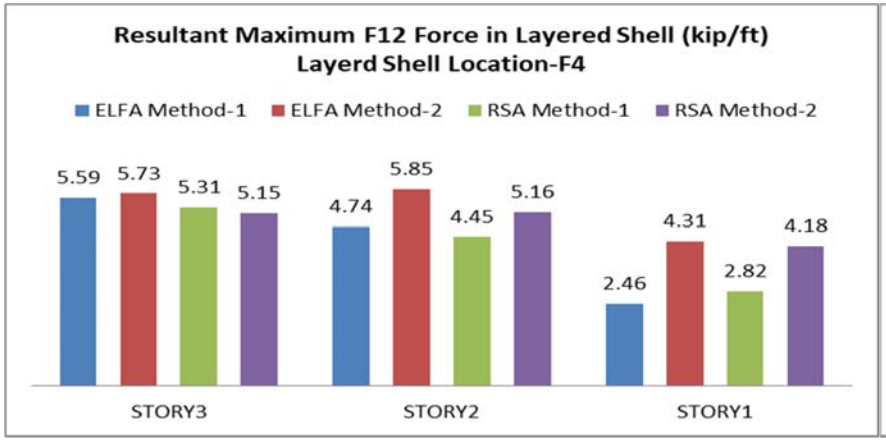

Figure 5-20 Resultant Maximum F12 Force in Layered Shell (kip/ft) for Layerd Shell Location-F4 of Model-2 from Different diaphragm force procedures

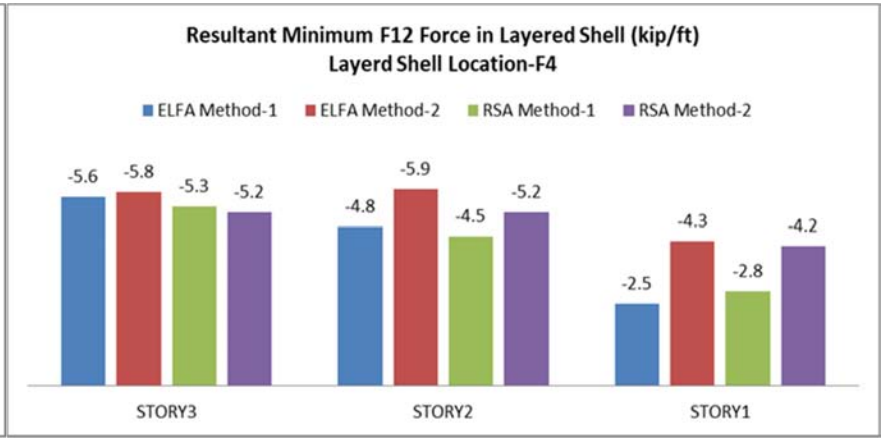

Figure 5-21 Resultant Minimum F12 Force in Layered Shell (kip/ft) for Layerd Shell Location-F4 of Model-2 from Different diaphragm force procedures

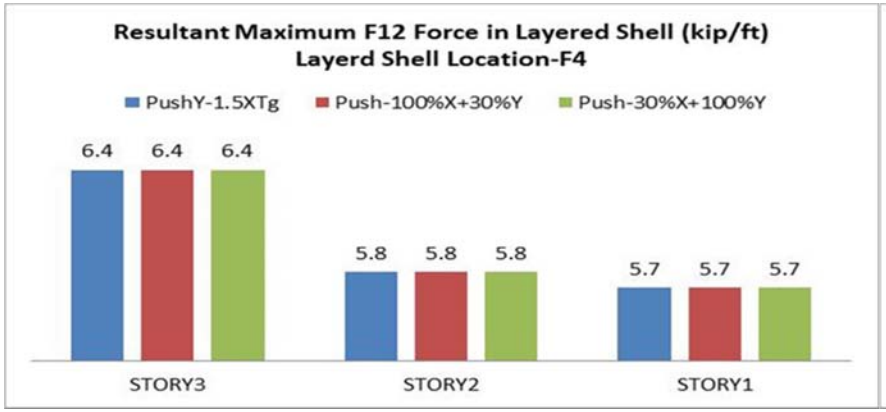

Figure 5-22 Resultant Maximum F12 Force in Layered Shell (kip/ft) for Layerd Shell Location-F4 of Model-2 from Pushover Analyses (with chord and collector reinforcement in beam near diaphragm opening)

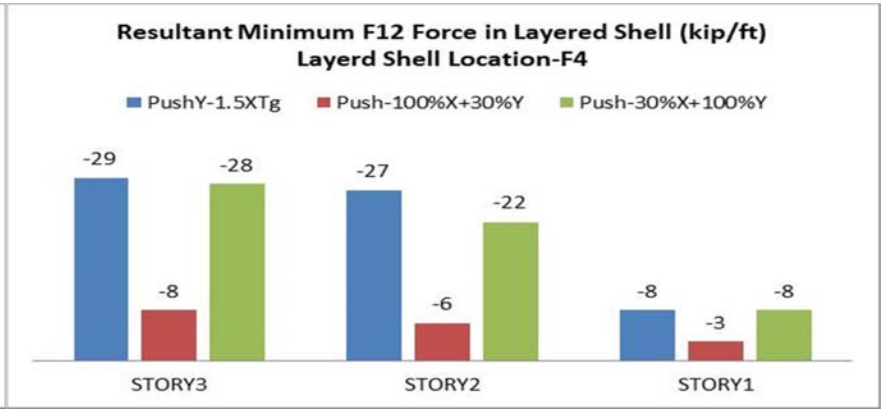

Figure 5-23 Resultant Minimum F12 Force in Layered Shell (kip/ft) for Layerd Shell Location-F4 of Model-2 from Pushover Analyses (with chord and collector reinforcement in beam near diaphragm opening)

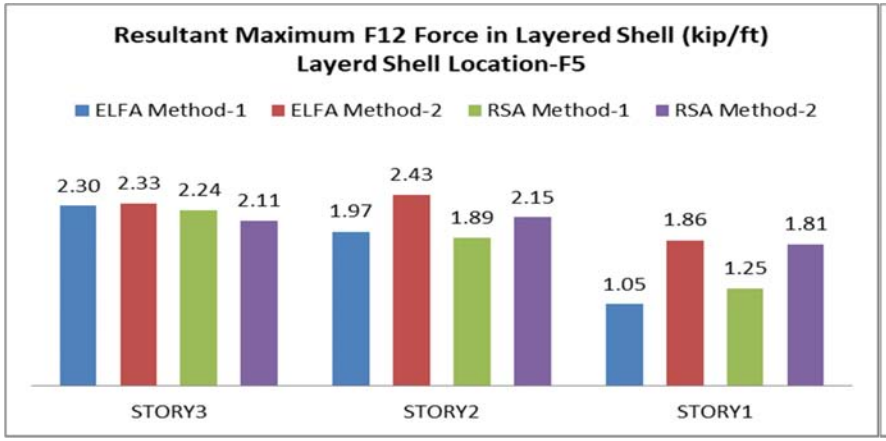

Figure 5-24 Resultant Maximum F12 Force in Layered Shell (kip/ft) for Layerd Shell Location-F5 of Model-2 from Different diaphragm force procedures

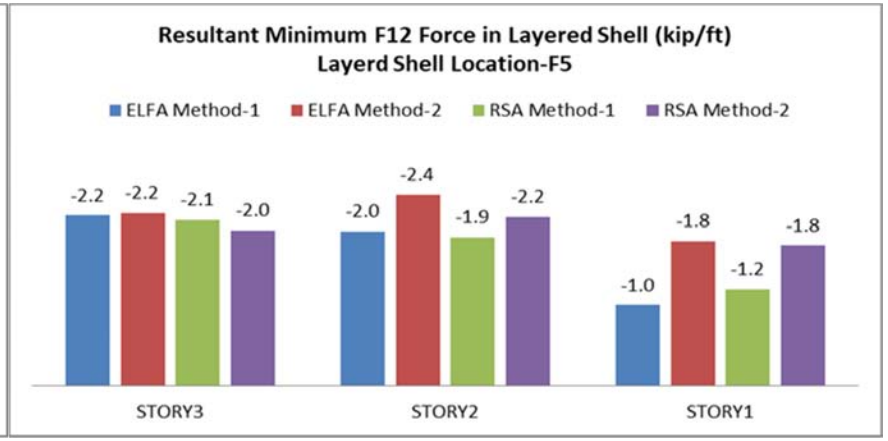

Figure 5-25 Resultant Minimum F12 Force in Layered Shell (kip/ft) for Layerd Shell Location-F5 of Model-2 from Different diaphragm force procedures

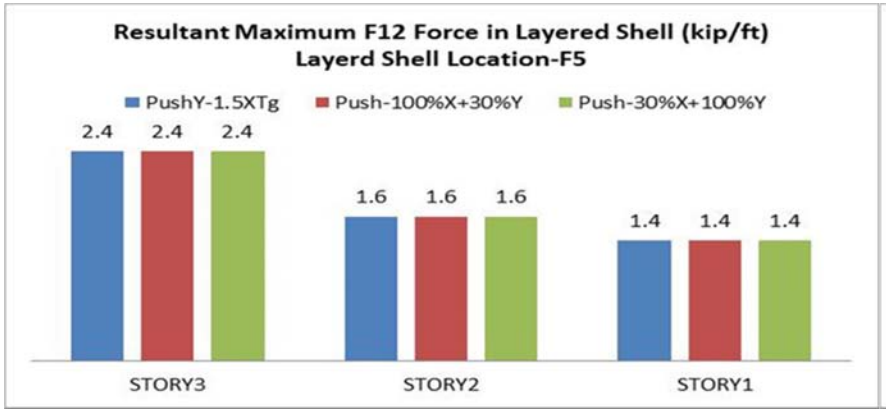

Figure 5-26 Resultant Maximum F12 Force in Layered Shell (kip/ft) for Layerd Shell Location-F5 of Model-2 from Pushover Analyses (with chord and collector reinforcement in beam near diaphragm opening)

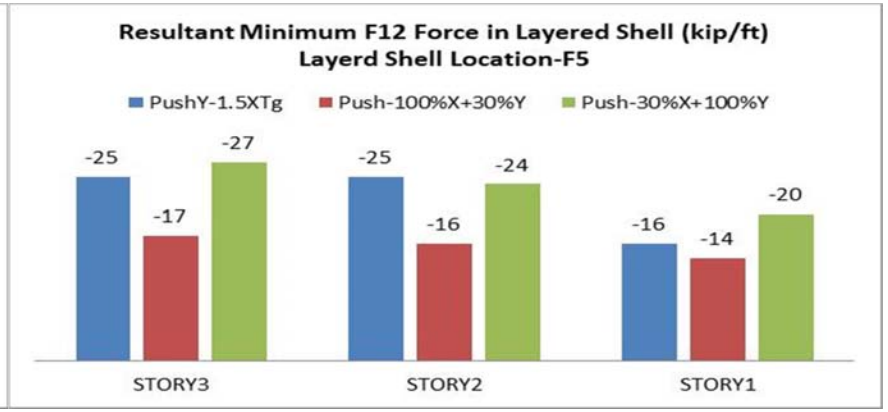

Figure 5-27 Resultant Minimum F12 Force in Layered Shell (kip/ft) for Layerd Shell Location-F5 of Model-2 from Pushover Analyses (with chord and collector reinforcement in beam near diaphragm opening)

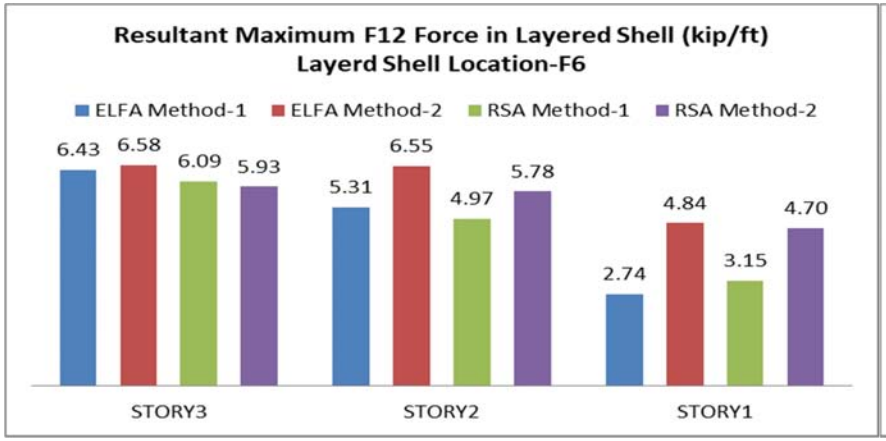

Figure 5-28 Resultant Maximum F12 Force in Layered Shell (kip/ft) for Layerd Shell Location-F6 of Model-2 from Different diaphragm force procedures

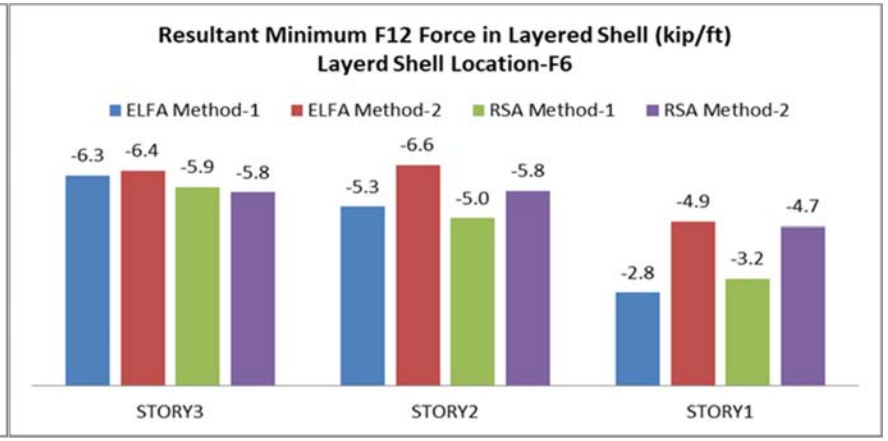

Figure 5-29 Resultant Minimum F12 Force in Layered Shell (kip/ft) for Layerd Shell Location-F6 of Model-2 from Different diaphragm force procedures

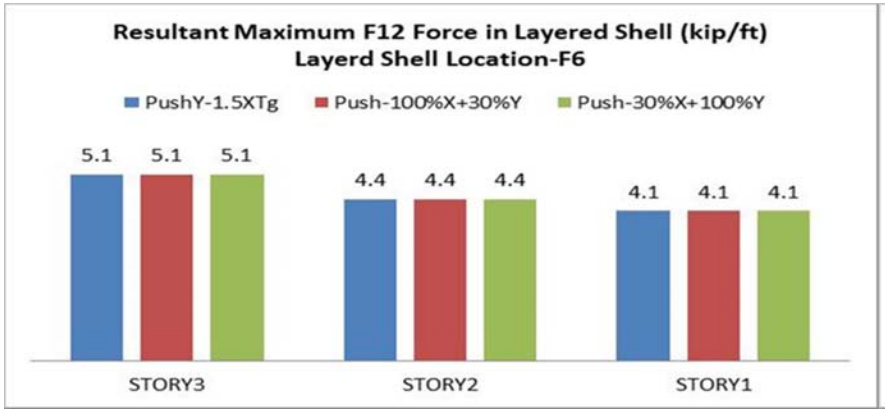

Figure 5-30 Resultant Maximum F12 Force in Layered Shell (kip/ft) for Layerd Shell Location-F6 of Model-2 from Pushover Analyses (with chord and collector reinforcement in beam near diaphragm opening)

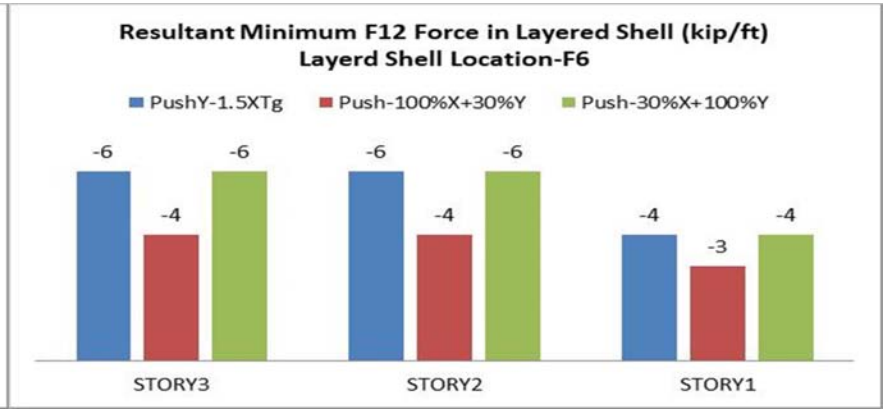

Figure 5-31 Resultant Minimum F12 Force in Layered Shell (kip/ft) for Layerd Shell Location-F6 of Model-2 from Pushover Analyses (with chord and collector reinforcement in beam near diaphragm opening)

In-plane shear force from ELFA Method-2 gives high value compared to ELFA Method-1, RSA Method-1 and RSA Method-2. Hence in-plane shear forces from ELFA Method-2 in diaphragm locations around diaphragm opening adjacent to shear wall are compared with the in-plane shear force value from Pushover analyses.

Diaphragm design shear force from linear elastic procedure (ELFA Method-2) for diaphragm location F1 is 5.98 kips/ft. Diaphragm design shear force from pushover analysis for diaphragm location F1 is 46 kips/ft when chords and collectors are introduced around diaphragm openings. Diaphragm design shear force from pushover analysis for diaphragm location F1 is 7.69 times the diaphragm design force from linear elastic procedure.

Diaphragm design shear force from linear elastic procedure (ELFA Method-2) for diaphragm location F2 is 5.96 kips/ft. Diaphragm design shear force from pushover analysis for diaphragm location F2 is 14 kips/ft when chords and collectors are introduced around diaphragm openings. Diaphragm design shear force from pushover analysis for diaphragm location F2 is 2.34 times the diaphragm design force from linear elastic procedure.

Diaphragm design shear force from linear elastic procedure (ELFA Method-2) for diaphragm location F3 is 5.73 kips/ft. Diaphragm design shear force from pushover analysis for diaphragm location F3 is 20 kips/ft when chords and collectors are introduced around diaphragm openings. Diaphragm design shear force from pushover analysis for diaphragm location F3 is 3.49 times the diaphragm design force from linear elastic procedure.

Diaphragm design shear force from linear elastic procedure (ELFA Method-2) for diaphragm location F4 is 5.8 kips/ft. Diaphragm design shear force from pushover analysis for diaphragm location F4 is 29 kips/ft when chords and collectors are introduced around diaphragm openings. Diaphragm design shear force from pushover analysis for diaphragm location F4 is 5 times the diaphragm design force from linear elastic procedure.

Diaphragm design shear force from linear elastic procedure (ELFA Method-2) for diaphragm location F5 is 2.2 kips/ft. Diaphragm design shear force from pushover analysis for diaphragm location F5 is 27 kips/ft when chords and collectors are introduced around diaphragm openings. Diaphragm design shear force from pushover

analysis for diaphragm location F5 is 12.3 times the diaphragm design force from linear elastic procedure.

Diaphragm design shear force from linear elastic procedure (ELFA Method-2) for diaphragm location F6 is 6.4 kips/ft. Diaphragm design shear force from pushover analysis for diaphragm location F6 is 6 kips/ft when chords and collectors are introduced around diaphragm openings. Diaphragm design shear force from pushover analysis for diaphragm location F6 is 0.94 times the diaphragm design force from linear elastic procedure.

Design of diaphragm location F1 of story 3 of model-2 for in-plane shear is done based on section 2.8.6 and 2.8.7 of this thesis where $\phi = 0.7$. Diaphragm location F1 is design for in-plane shear of 46 kips/ft as per pushover analysis. Thickness required for diaphragm location F1 for safe transfer of in-plane shear to shear wall is 10.5 inch and provide 16m bar @ 4.75 in c/c in both directions. Detailed design calculations are shown in **Appendix-F**.

5.3 Design of Diaphragm for Chord Reinforcements

Locations of chords in plan of model-2 are shown in **Figure 5-32**. Comparative analysis of axial force in chords from different diaphragm force procedures and pushover analyses of diaphragm locations near diaphragm opening of model-2 are shown in **Figures 5-33 to 5-40**.

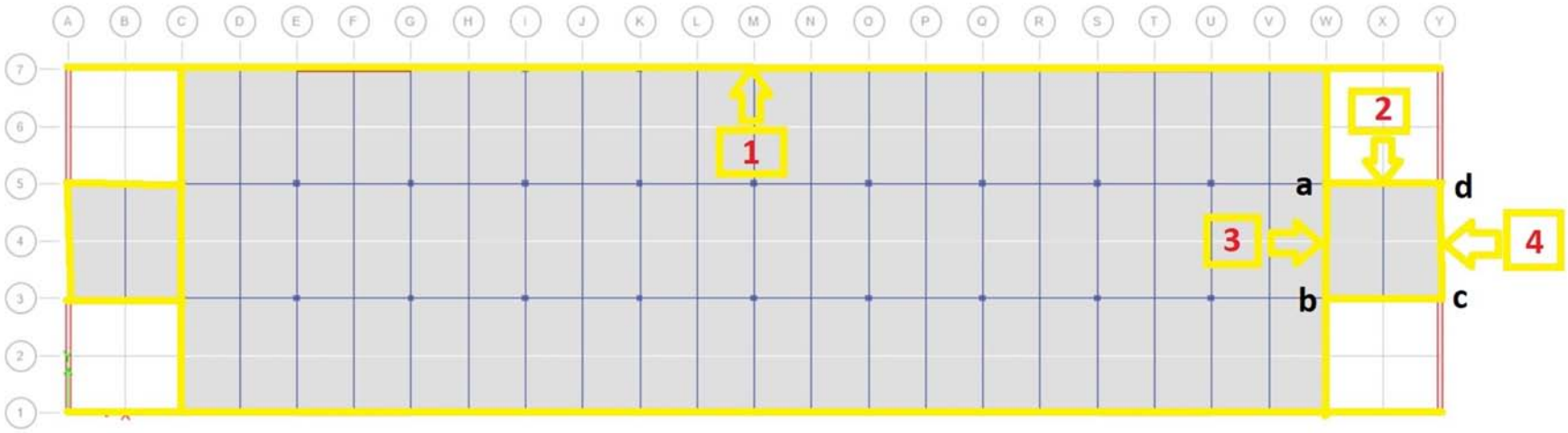

Figure 5-32 Locations of Chord in Story-3 of Model-2

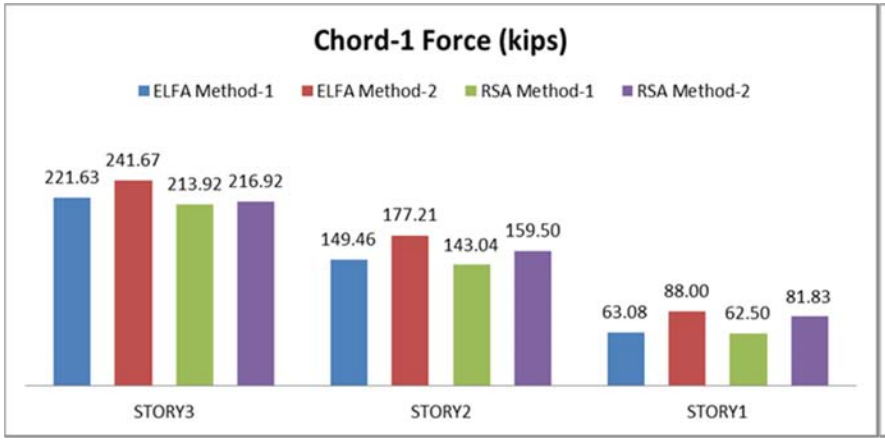

Figure 5-33 Chord-1 force (kips) of Model-2 from Different diaphragm force procedures

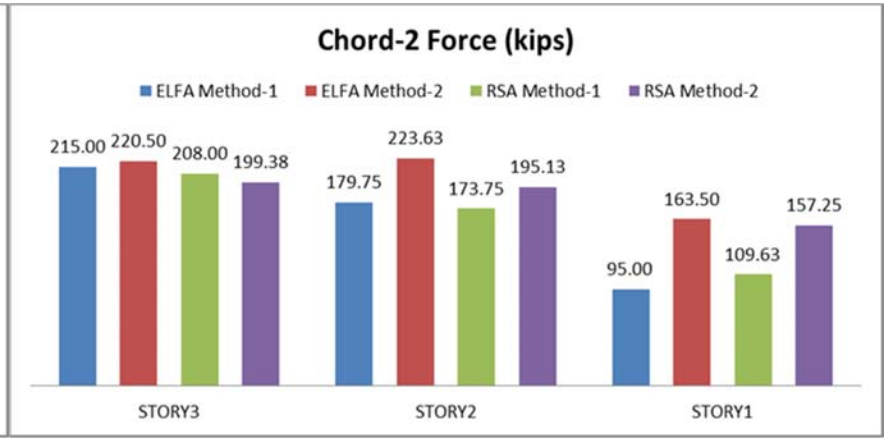

Figure 5-34 Chord-2 force (kips) of Model-2 from Different diaphragm force procedures

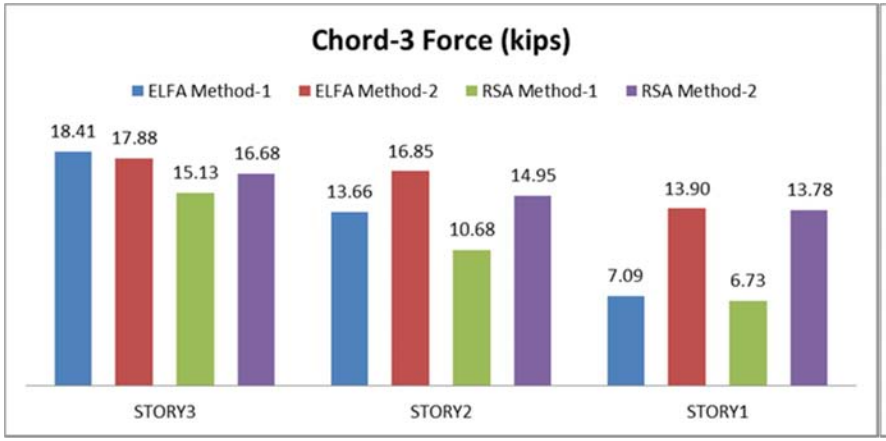

Figure 5-35 Chord-3 force (kips) of Model-2 from Different diaphragm force procedures

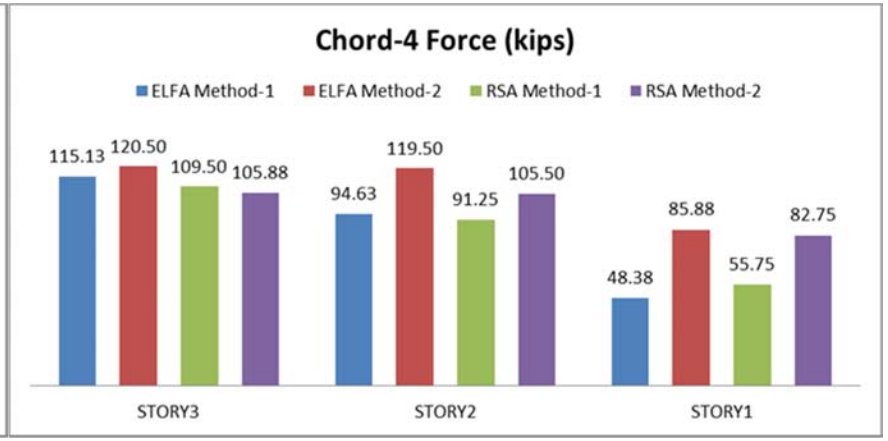

Figure 5-36 Chord-4 force (kips) of Model-2 from Different diaphragm force procedures

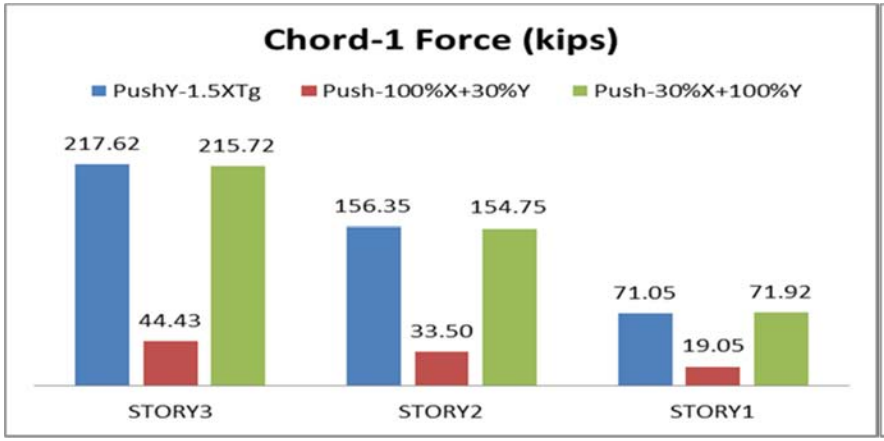

Figure 5-37 Chord-1 force (kips) of Model-2 from Pushover Analyses

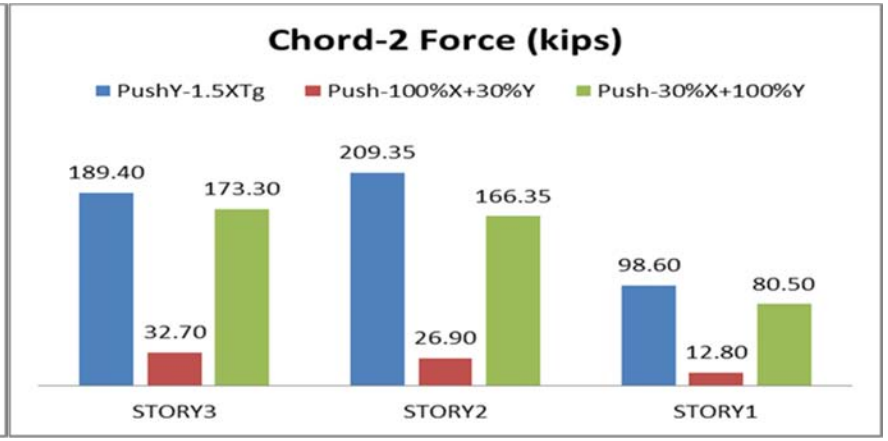

Figure 5-38 Chord-2 force (kips) of Model-2 from Pushover Analyses

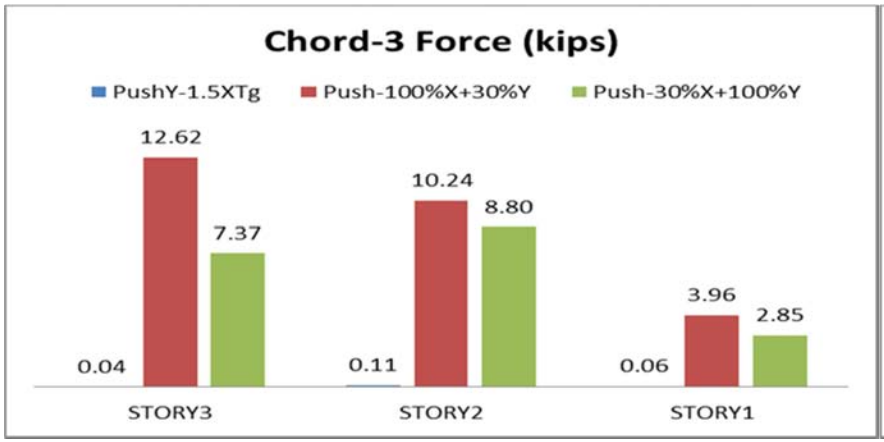

Figure 5-39 Chord-3 force (kips) of Model-2 from Pushover Analyses

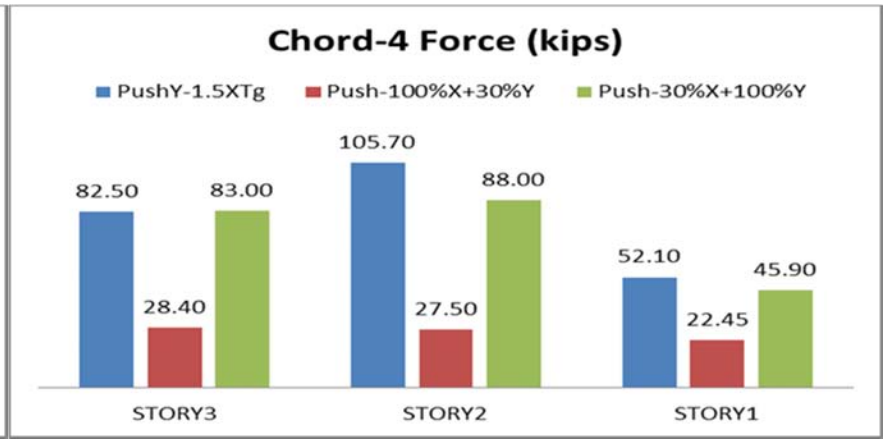

Figure 5-40 Chord-4 force (kips) of Model-2 from Pushover Analyses

Force for design of chord is taken form Pushover analyses. The maximum chord force is 189 kips for chord-2 in story 3 is found form pushover analysis along Y-direction up to 1.5 times of target displacement. Design of chord-2 of diaphragm for model-2 located in story 3 is done based on section 2.8.4 of this thesis paper. Chord reinforcements in beam (B2) are shown in **Figure 5-41**. Detailed design calculations are shown in **Appendix-G**.

Figure 5-41 Reinforcement detailing of Chord-2 reinforcement in Beam (B2)

5.4 Design of Diaphragm for Collector Reinforcements

Locations of collectors in plan of model-2 are shown in **Figure 5-43**. Comparative analysis of axial force in collectors from different diaphragm force procedures and pushover analyses of diaphragm locations near diaphragm opening of model-2 are shown in **Figures 5-44 to 5-55**. Force for design of collector-A is taken form Pushover analyses. The maximum collector force for collector-A in story 3 is found form pushover analysis along Y-direction up to 1.5 times of target displacement. Force from section cut along collector-A from pushover analysis along Y-direction up to 1.5 times of target displacement is 206 kips. Design of collector-A of diaphragm for model-2 located in story 3 is done based on section 2.8.2 of this thesis. Collector-A reinforcements in beam (B3) is shown in **Figure 5-42**. Detailed design calculations are shown in **Appendix-H**.

Figure 5-42 Reinforcement detailing of Collector-A reinforcement in Beam (B3)

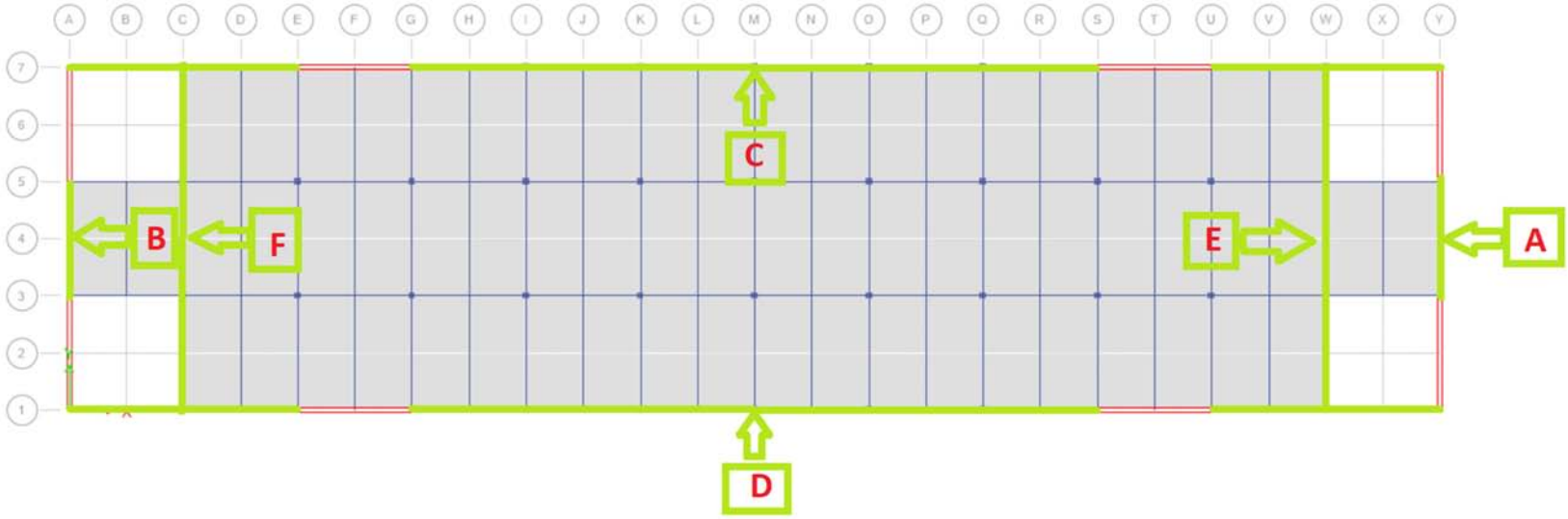

Figure 5-43 Locations of Collector in Story-3 of Model-2

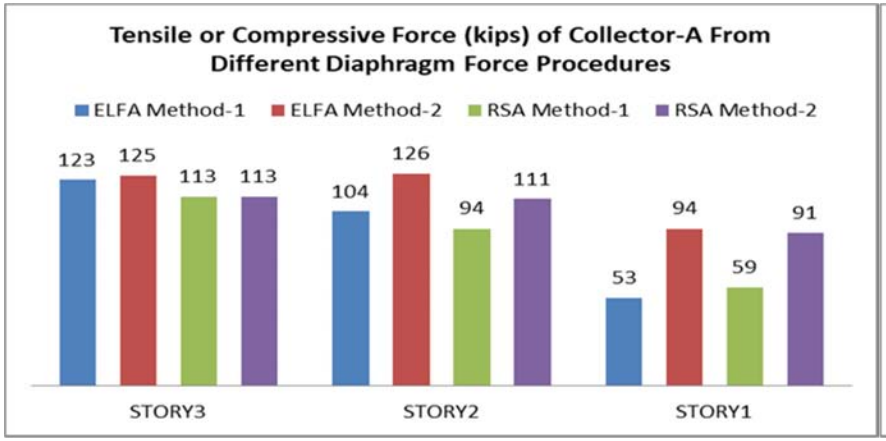

Figure 5-44 Tensile or compressive force of collector-A From Different Diaphragm Force Procedures

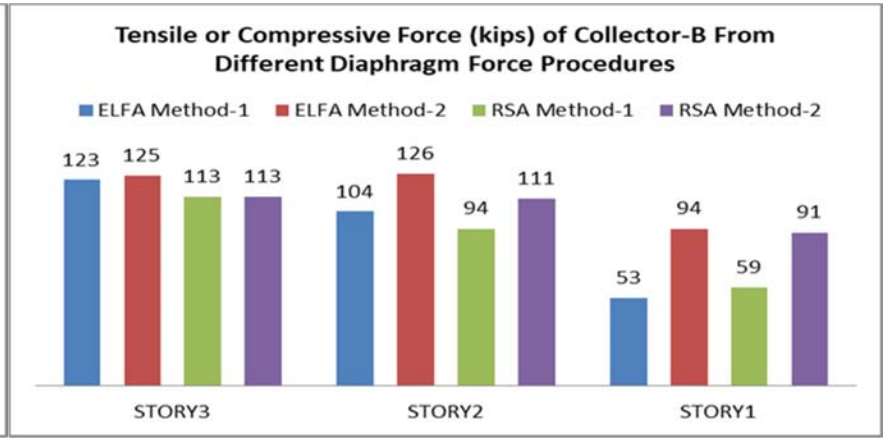

Figure 5-45 Tensile or compressive force of collector-B From Different Diaphragm Force Procedures

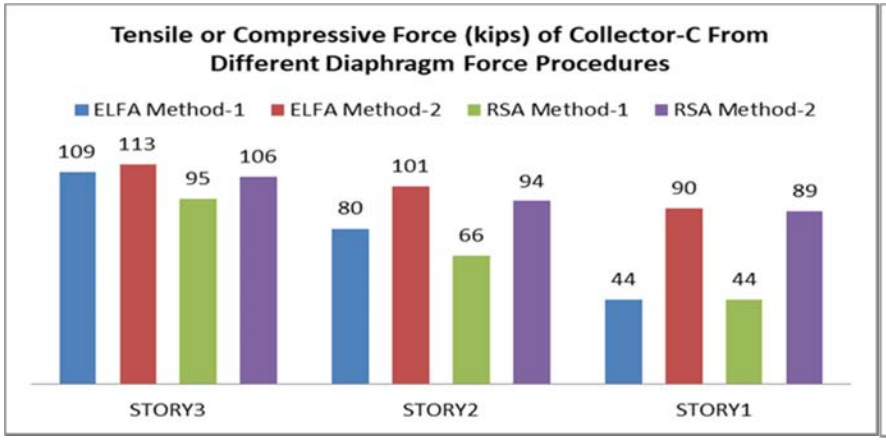

Figure 5-46 Tensile or compressive force of collector-C From Different Diaphragm Force Procedures

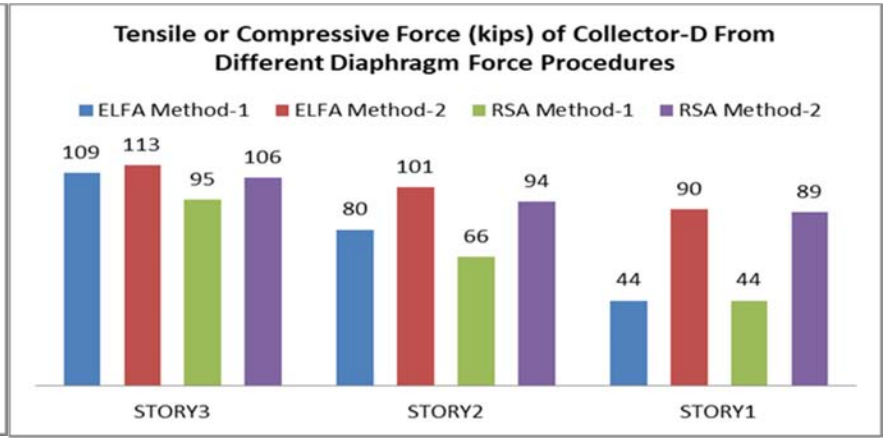

Figure 5-47 Tensile or compressive force of collector-D From Different Diaphragm Force Procedures

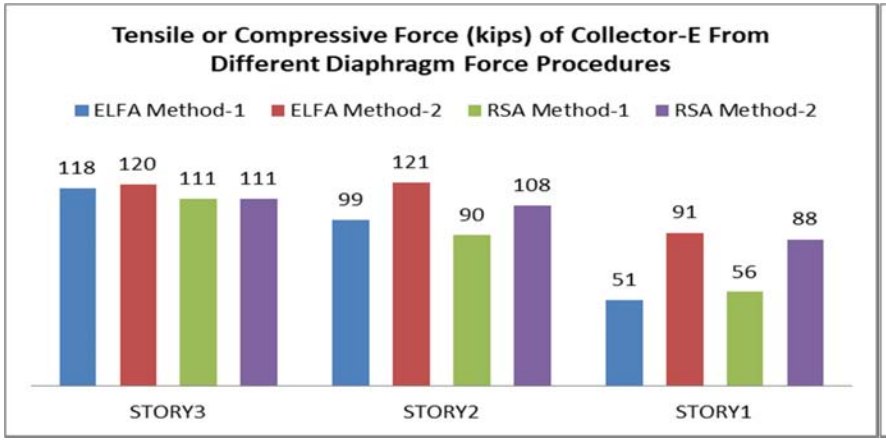

Figure 5-48 Tensile or compressive force of collector-E From Different Diaphragm Force Procedures

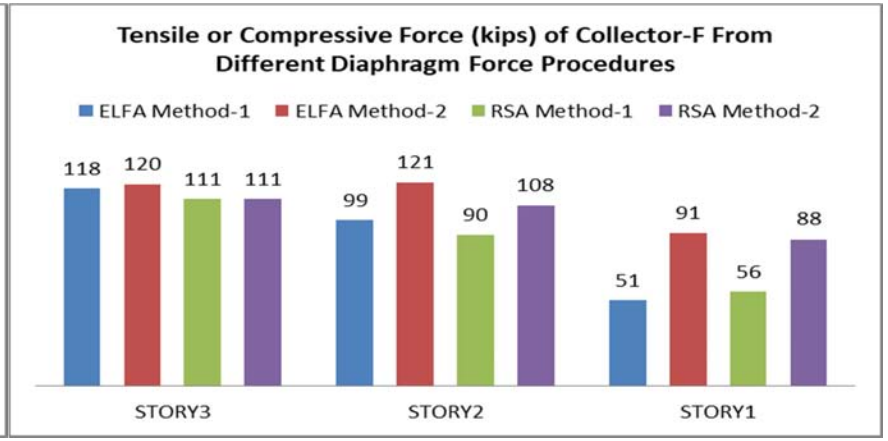

Figure 5-49 Tensile or compressive force of collector-F From Different Diaphragm Force Procedures

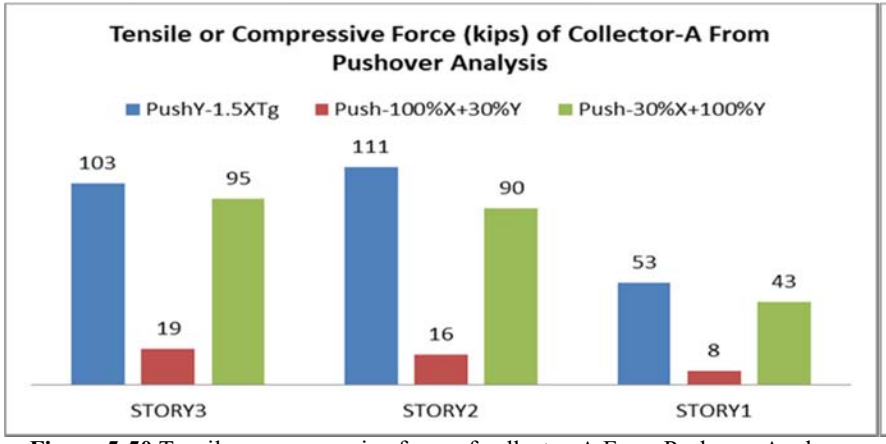

Figure 5-50 Tensile or compressive force of collector-A From Pushover Analyses

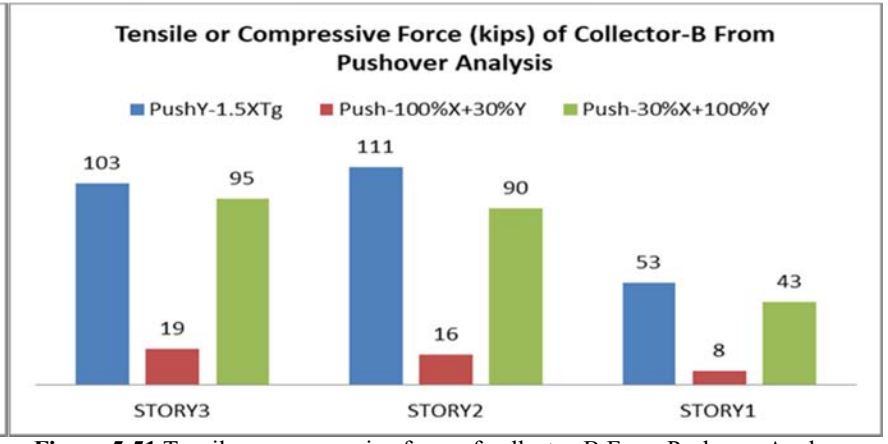

Figure 5-51 Tensile or compressive force of collector-B From Pushover Analyses

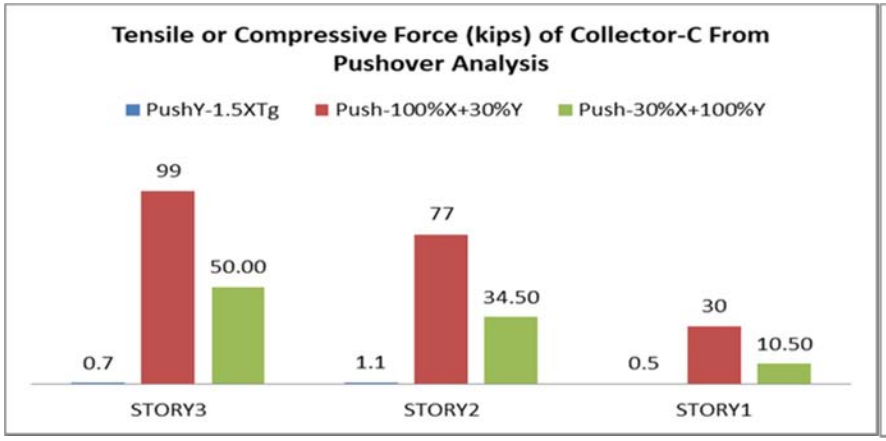

Figure 5-52 Tensile or compressive force of collector-C From Pushover Analyses

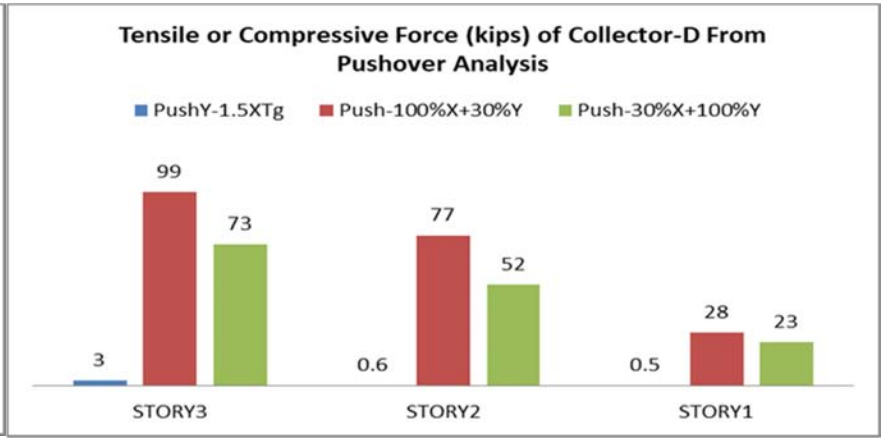

Figure 5-53 Tensile or compressive force of collector-D From Pushover Analyses

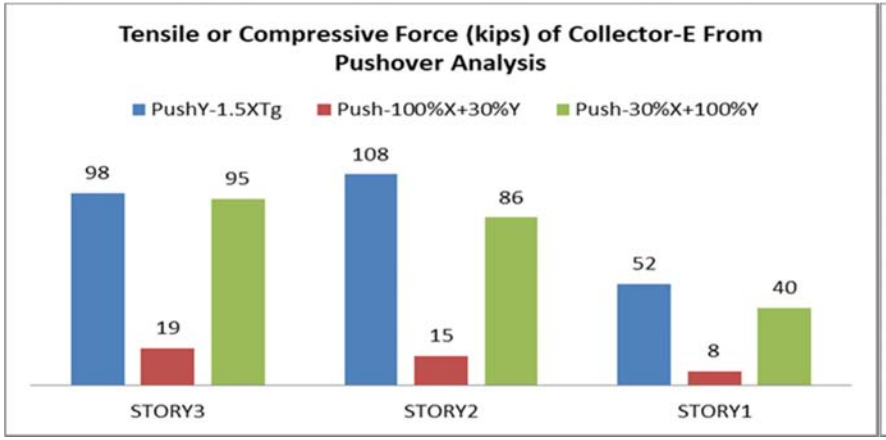

Figure 5-54 Tensile or compressive force of collector-E From Pushover Analyses

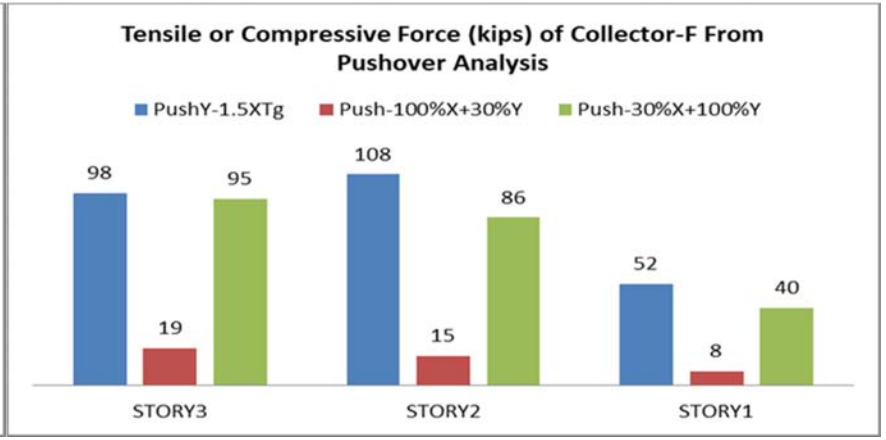

Figure 5-55 Tensile or compressive force of collector-F From Pushover Analyses

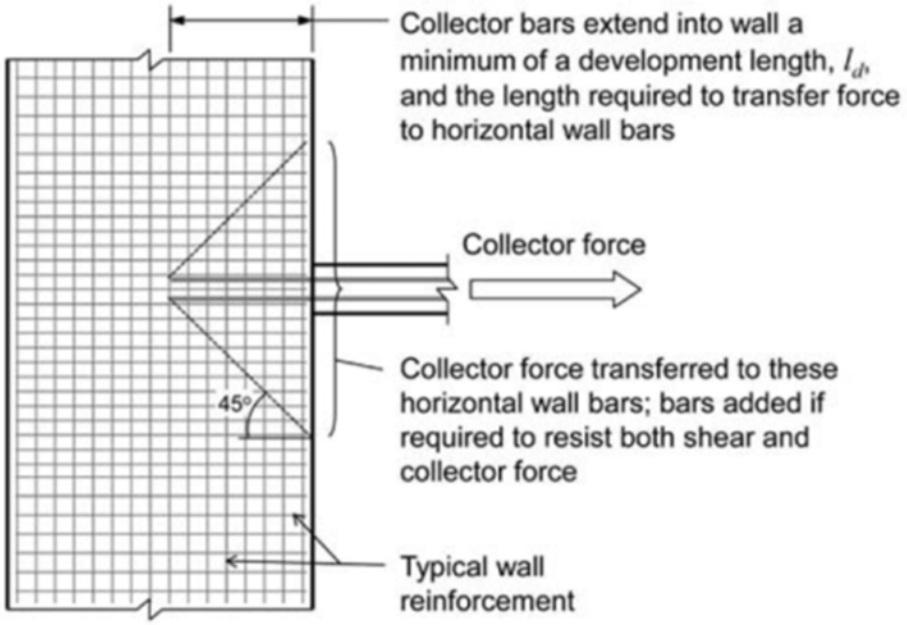

Figure 5-56 Detailing of collector reinforcements in shear wall and horizontal reinforcements of shear wall (Moehle et al., 2010)

5.5 Detailing of connection of collector to shear wall

According to Moehle et al. (2010), Collector bars must extend into the vertical element to transfer the force to bars in the vertical element which are typically much longer than a collector bar development length. Collectors that extend through the entire length of a vertical element ensure that force is safely transferred from the collector to the vertical element without further consideration. The collector force is transferred to horizontal shear wall reinforcement that distributes the collector force to the full length of the wall. This horizontal shear wall reinforcement must not only transfer the collector force but also must resist wall design shear. Therefore the horizontal wall steel is the sum of reinforcement required for the collector force and the reinforcement required for the shear in the wall above the level of the collector (Moehle et al., 2010).

The collector reinforcements of collector-A will extend through entire length of shear walls for safe transfer of collector force to shear wall. Detailing of collector reinforcements in shear wall and horizontal reinforcements of shear wall are shown in **Figure 5-56**.

5.6 Comments on Analysis Results and Design

i. Chord and collector reinforcements can be placed in beam or in the slab. In this thesis chord and collector reinforcements are placed in the beams.

ii. Chords and collector forces form linear elastic procedures considering overstrength factor are very close to chords and collector forces form pushover analyses.

iii. Diaphragm in-plane shear force in diaphragm location F1 from Pushover analyses gives high value compared to other linear elastic diaphragm design force procedures.

iv. In-plane shear forces of diaphragm locations around diaphragm opening adjacent to shear walls of model-2 from pushover analyses are 2.34 to 7.69 times higher than in-plane shear forces from linear elastic diaphragm design force procedures when chords and collectors are introduced around diaphragm openings adjacent to shear walls.

v. In-plane shear forces of diaphragm locations around diaphragm opening adjacent to columns of model-2 from pushover analyses are 3.49 to 12.3 times higher than in-plane shear forces from linear elastic diaphragm design force procedures when chords and collectors are introduced around diaphragm openings adjacent to shear walls.

vi. If the diaphragm moment is resisted by tension and compression chords at the boundaries of the diaphragm, then equilibrium requires that the diaphragm shear be distributed uniformly along the depth of the diaphragm (Moehle et al., 2010). Although chords are placed around diaphragm opening to resist in-plane diaphragm moment, the diaphragm shears are not distributed uniformly in diaphragm around diaphragm opening adjacent to shear wall.

vii. When chords and collectors are not introduced around diaphragm openings adjacent to shear walls, more diaphragm locations around diaphragm openings are subjected to high in-plane shear force. Less diaphragm locations around diaphragm openings are subjected to high in-plane shear force when chords and collectors are introduced around diaphragm openings adjacent to shear walls. Whether chords and collectors are introduced or not introduced near diaphragm openings, in-plane shear forces near columns and shear walls around diaphragm opening adjacent to shear walls remain almost same. These observations are made by analyzing **Figures 5-5 to 5-6**.

viii. We have chosen diaphragm forces from pushover analyses for design of diaphragm as diaphragm forces form pushover analyses are more realistic. Load

combinations with overstrength factor are used to determine chord and collector force, and Load combinations without overstrength factor are used to check in-plane diaphragm shear forces when we are considering diaphragm design force from linear elastic procedures.

ix. Shear reinforcement can be merged with the bottom reinforcement of slab.

x. Openings in diaphragm near shear walls require chords and collectors around it. This often creates situation where chords, collectors and shear walls are intersecting each other. This will create congestion of reinforcements in these locations of intersection. Hence, collector and chord width in beam and shear wall thickness should be increased to reduce congestion of reinforcements in these locations. The author thinks that minimum thickness of shear wall and width of beam (acting as chord or collector element) at intersecting locations should be ten (10) inch for building models used for this research to reduce congestion of reinforcements.

Chapter 6

CONCLUSIONS AND RECOMMENDATIONS FOR FUTURE RESEARCH

The purpose of this study is to provide pertinent insight of the in-plane behavior of cast-in-situ concrete diagram near diaphragm opening adjacent to shear walls. Openings in diaphragm are very common in buildings. The in-plane behavior of cast-in-situ concrete diaphragm near diaphragm opening cannot be fully understood without performing diaphragm in-plane force and stress analyses. There is a knowledge gap in the previously published literature on the subject of seismic analysis of cast-in-situ concrete diaphragm with diaphragm opening subjected to orthogonal seismic loading. All the models are investigated with analytical procedures discussed in chapter two and chapter three. Statistical analyses of the diaphragm in-plane stress data are performed to find out the worst orientation of diaphragm opening adjacent to end shear wall and intermediate shear wall in Dual system buildings. Design of chords, collectors and shear reinforcements around diaphragm opening adjacent to shear wall are done by comparing diaphragm design forces from LEP, LDP and Pushover analyses. Conclusions of this study along with recommendation for future research are presented in this chapter. The limit of diaphragm opening in building plan with respect to diaphragm discontinuity criteria of ASCE 7-10 (ASCE, 2010) for wall-frame structural system are examined by comparing in-plane stresses/forces of diaphragm around diaphragm opening.

6.1 Conclusions

i. Stress concentration around diaphragm opening adjacent shear wall is high for all building models especially near shear wall and columns during earthquake. Hence, diaphragm opening adjacent to shear wall should be avoided.

ii. In-plane stress of diaphragm locations near diaphragm opening adjacent to shear walls from Modal linear response history analysis dominates over other linear elastic procedures.

iii. Linear elastic and linear dynamic diaphragm design force procedures as per ASCE 7-10 (ASCE, 2010) underestimates in-plane stress in diaphragm locations around diaphragm opening adjacent shear wall because in-plane stress form pushover analyses

as per ASCE 41-13 (ASCE, 2014) are higher than linear elastic and linear dynamic diaphragm design force procedures in these diaphragm locations.

iv. Linear elastic diaphragm design force procedure underestimates in-place shear force around diaphragm opening adjacent to shear wall compared to pushover analysis. Hence pushover analysis or nonlinear dynamic analysis should be performed when diaphragm opening is present adjacent to shear wall.

v. Orientation of diaphragm openings adjacent to intermediate shear walls of Model-9 is the worst scenario compared other models. More diaphragm locations near diaphragm opening adjacent to shear wall of Model-9 will experience high in-plane stress in both top and bottom layers of nonlinear layered shell compared to other models.

vi. Although open area in diaphragm (11% and 14% of the diaphragm gross area) is below the diaphragm discontinuity criteria of ASCE 7-10 (ASCE, 2010), linear elastic diaphragm design force procedures as per ASCE 7-10 underestimates in-plane shear forces in diaphragm locations around diaphragm opening adjacent shear wall compared to in-plane shear forces from pushover analyses according to ASCE 41-13 (ASCE, 2014). Therefore, diaphragm discontinuity criteria for wall-frame structural systems (Dual systems) should be reviewed.

vii. ASCE 7-10 (ASCE, 2010) does not provide any guideline or requirements for structure with diaphragm discontinuity assigned to Seismic design category C. The building models analyzed in this thesis are assigned to Seismic design category C and open area in diaphragm does not meet the diaphragm discontinuity criteria of ASCE 7-10 but in-plane shear force form pushover analyses as per ASCE 41-13 (ASCE, 2014) are higher than linear elastic diaphragm design force procedures as per ASCE 7-10 for diaphragm locations around diaphragm opening adjacent to shear wall even though chords and collectors are present around diaphragm openings adjacent to shear walls to resist nonuniform shear stress. Therefore, guidelines and requirements should be developed for structures with diaphragm opening adjacent to shear wall assigned to Seismic Design Category C.

viii. Although open area in diaphragm is less than 50 percent (11% and 14%) of the gross enclosed diaphragm area, diaphragm locations near diaphragm openings adjacent to shear walls experience high in-plane flexural and in-plane shear force/stress which

cannot be overlooked. Sometimes diaphragm locations near diaphragm opening adjacent to shear walls are experiencing high in-plane shear stress that requires shear reinforcements and increase of thickness of diaphragm for safe transfer of in-plane shear stress to seismic force resisting vertical elements. Therefore, diaphragm discontinuity criteria for wall-frame structural systems should be reviewed.

ix. The minimum thickness of shear wall and width of beam (acting as chord or collector element) at intersecting locations near diaphragm opening adjacent to shear wall should be ten inch for building models used for this research to reduce congestion of reinforcements.

6.2 Recommendations for Future Research

Here are some points that demand future investigation in this regard.

i. Future investigation of in-plane behavior (in-plane flexural stress and in-plane shear stress) of diaphragm with diaphragm opening adjacent to shear wall for irregular structures and severe seismic zones.

ii. Future investigation of in-plane behavior (in-plane flexural stress and in-plane shear stress) of diaphragm with diaphragm opening adjacent to shear wall where diaphragm openings are distributed non-symmetrically in the building plan.

iii. Investigation of in-plane behavior (in-plane flexural stress and in-plane shear stress) of diaphragm with diaphragm opening adjacent to shear wall using nonlinear dynamic analysis and soil-structure interaction.

iv. Investigation of in-plane behavior (in-plane flexural stress and in-plane shear stress) of cast-in-situ concrete diaphragm with diaphragm opening adjacent to shear wall using shake table.

v. Investigation of in-plane behavior (in-plane flexural stress and in-plane shear stress) of cast-in-situ concrete diaphragm with diaphragm opening adjacent to shear wall in tall buildings.

vi. Investigation of in-plane behavior (in-plane flexural stress and in-plane shear stress) of cast-in-situ concrete diaphragm under heavy out of plan loadings.

REFERENCES

ACI (2014). *Building code requirements for structural concrete (ACI 318-14) and commentary (ACI 318R-14)*, Farmington Hills, MI: American Concrete Institute.

Ahmed, J. & Reza, S. A. (2014). Seismic vulnerability of RC building by considering plan irregularities using pushover analysis. *International Global Journal for Research Analysis*, *3*(9), 42-47.

ASCE (2010). *Minimum design loads for buildings and other structures (ASCE/SEI 7-10)*, Reston, VA: American Society of Civil Engineers.

ASCE (2014). *Seismic evaluation and retrofit of existing buildings (ASCE/SEI 41-13)*, Reston, VA: American Society of Civil Engineers.

ASCE (2017). *Minimum design loads and associated criteria for buildings and other structures (ASCE/SEI 7-16)*, Reston, VA: American Society of Civil Engineers.

ATC (1996). *Seismic evaluation and retrofit of concrete buildings (ATC-40)*. Redwood City, California: Applied Technology Council, Seismic Safety Commission.

Baratta, A., Corbi, I., Corbi, O., Barros, RC. & Bairrao, R. (2012). Shaking table experimental researches aimed at the protection of structures to dynamic loading. *The Open Construction and Building Technology Journal*, *6*, 355-360.

Baratta, A., Corbi, I., Corbi, O., Barros, RC. & Bairrao, R. (2013). Towards a seismic worst scenario approach for rocking systems: Analytical and experimental set-up for dynamic response. *Acta Mechanica*, *224*, 691-705.

BIS (2002). *Criteria for earthquake resistant design of structures, General provisions and buildings (IS 1893-2002)*. New Delhi, India: Bureau of Indian Standards.

CEN.(2004). *Design of structures for earthquake resistant, Part 1, General rules, seismic actions and rules for buildings (Eurocode 8)*. Brussels, Belgium: Committee European de normalization, European standard.

CSI Analysis Reference Manual [PDF file]. (2016 July). Retrieved March 05, 2019, from http://docs.csiamerica.com/manuals/etabs/Analysis%20Reference.pdf

CSI. (2017). Extended Three-dimensional Analysis of Building Systems, ETABS 2016 (version 16.2.1) [Computer software]. 1646 N. California Blvd, Suite 600, Walnut Creek, CA 94596, USA: Computers and Structures, Inc., Retrieved from https://www.csiamerica.com/products/etabs

FEMA (2012). *2009 NEHRP recommended seismic provisions: Design examples (FEMA P-751).* Washington, D.C: Federal Emergency Management Agency.

FEMA (2015), *NEHRP recommended seismic provisions for new buildings and other structures (FEMA P-1050-1).* Washington, D.C: Federal Emergency Management Agency.

FEMA (2016), *2015 NEHRP recommended seismic provisions: Design examples (FEMA P-1051).* Washington, D.C: Federal Emergency Management Agency.

Frame/Wall Nonlinear Hinge. (n.d). Retrieved March 5, 2019 from http://docs.csiamerica.com/help-files/etabs/Menus/Define/Section_Properties/Frame_Nonlinear_Hinge_Properties/Frame_Nonlinear_Hinge

Gardiner, D.R., Bull, D.K. & Carr, A.J. (2008). Trends of internal forces in concrete floor diaphragms of multi-storey structures during seismic shaking. *The 14th World Conference on Earthquake Engineering.* Retrieved from http://www.iitk.ac.in/nicee/wcee/article/14_05-06-0178.PDF

Guzman, T. (2016 March 04). *Rigid vs. Semi-rigid diaphragm.* Retrieved March 05, 2019 from https://wiki.csiamerica.com/display/etabs/Rigid+vs.+Semi-rigid+diaphragm

Harash, M. T. (2011). *Inelastic seismic response of reinforced concrete buildings with floor diaphragm opening* (Thesis of the degree of Doctor of Science), School of Engineering and Applied Science, Department of Mechanical Engineering and Material Science, Washington University, St. Lousi.

HBRI & BRTC. (2017). *Bangladesh national building code 2017*. Dhaka, Bangladesh: Housing and Building Research Institute and Bureau of Research Testing and Consultancy.

ICC.(2006). *International Building Code (IBC)*. Whittier, California: International Code Council.

Kalny, O. (2014 March 13). *Section cut FAQ.* Retrieved March 05, 2019 from https://wiki.csiamerica.com/display/kb/Section+cut+FAQ

Maniar, O. & John, R. J. (2015). Effect of diaphragm discontinuity on seismic response of multistoried building. *International Journal of Emerging Technology and Advanced Engineering*, *5*(12), 130-135.

Modeling Enhancements Implemented [PDF file]. (2015 July 27). Retrieved March 05, 2019 from http://installs.csiamerica.com/software/ETABS/2015/ReleaseNotesETABS2015v1510.pdf

Moehle, J. P., Hooper, J. D., Kelly, D. J. & Meyer, T. R. (2010). *Seismic design of cast-in-place concrete diaphragms, chords, and collectors: A guide for practicing engineers*. Gaithersburg, MD: NEHRP Consultants Joint Venture, a partnership of the Applied Technology Council and the Consortium of Universities for Research in Earthquake Engineering, for the National Institute of Standards and Technology.

Nilson, A.H., Darwin, D. & Dolan, C. W. (2004). *Design of concrete structures*. 13th edition. Avenue of Americas, NY: McGraw-Hill, The McGraw-Hill Companies, Inc.

NIST (2016). *Seismic design of cast-in-place concrete diaphragms chords, and collectors: A guide for practicing engineers*. Gaithersburg, MD: The Applied Technology Council for the National Institute of Standards and Technology.

Ondrej (2019 March 27). *Layered shells.* Retrieved March 27, 2019 from https://wiki.csiamerica.com/display/kb/Layered+shells

Orakcal, K., Terzioglu, T. & Massone, L.M. (2012). Lateral load behavior of low-rise structural walls. *10th International Congress on Advanced in Civil Engineering*.

Ozturk, T. (2011). A study of the effect of slab gaps in buildings on seismic response according to three different codes. *Scientific Research and Essays*, *6*(19), 3930-3941. doi: 10.5897/SRE10.076.

Ramya, R. (2014). Dynamic analysis of squat shear wall using nonlinear finite element method. *IOSR Journal of Mechanical and Civil Engineering (IOSR-JMCE)*, *11*(2), 06-20.

Ravikumar, C.M., Babu, N. K. S., Sujith, B. V. & Venkat, R. D. (2012). Effect of irregular configurations on seismic vulnerability of RC building. *Architecture Research*, *2*(3), 20-26.

Roper, S. C. & Iding, R. H. (1984). Appropriateness of the rigid floor assumption for buildings with irregular features. *8th World Conference on EQ*, *4*, 751-758.

Saffarini, H. & Qudaimat, M. (1992). In-plane floor deformations in RC structures. *Journal of Structural Engineering*, *118*(11), 3089-3102.

Sahu, R. & Dwivedi, R. (2017). Seismic analysis of RC frame with diaphragm discontinuity. *IOSR Journal of Mechanical and Civil Engineering (IOSR-JMCE)*, *14*(4), 36-41.

SeismoSoft. (2016). SeismoSignal (version 2016) [Computer software]. Piazza Castello, 19, 27100 Pavia (PV), Italy: Seismosoft Ltd. Retrieved from https:// www.seismosoft.com/seismosignal

Shell element internal stresses. (n.d.) Retrieved March 5, 2019 from http://docs.csiamerica.com/help-files/etabs/Output_Conventions/ Shell_Element_Internal_Forces.htm

Slab, Wall Property Layer Definition Data. (n.d). Retrieved March 05, 2019 from http://docs.csiamerica.com/helpfiles/etabs/Menus/Define/Section_Properties/ Slab_Wall_Property_Layer_Definition_Data_Form.htm

Standard deviation. (n.d). Retrieved March 05, 2019 from https://en.wikipedia.org/wiki/ Standard_deviation

Taranath, B.S. (2010). *Reinforced concrete design of tall buildings.* New York, USA, CRC Press: Taylor & Francis Group.

Turkish Ministry of Public Works and Settlement. (2007). *Specification for Structures to be Built in Disaster Areas, TEC-07*.Ankara, Turkey.

Technical note Modified darwin-pecknold 2-d reinforced concrete Material model [PDF File]. (2015 July). Retrieved March 05, 2019 from http://docs.csiamerica.com/manuals/etabs/Technical%20Notes/ S-TN-MAT 002.pdf

Vinod, V. & Pramod, K. H. V. (2017). Influence of stiffness discontinuous diaphragm characteristics on the seismic behavior of RC structure. *International Journal of Emerging Technology and Advanced Engineering*, 2(6), 366-381.

Appendix-A

LOAD COMBINATIONS FOR ELFA METHOD-1, ELFA METHOD-2 AND RSA METHOD-2

The basic load combinations for strength design as per section 12.4.2.3 of ASCE 7-10 (ASCE, 2010) with orthogonal seismic loading and accidental torsion to determine diaphragm forces.

1. $(1.2 + 0.2\ S_{DS})D+0.5L+\rho$ [1]
2. $(1.2 + 0.2\ S_{DS})D+0.5L+\rho$ [2]
3. $(1.2 + 0.2\ S_{DS})D+0.5L+\rho$ [3]
4. $(1.2 + 0.2\ S_{DS})D+0.5L+\rho$ [4]
5. $(1.2 + 0.2\ S_{DS})D+0.5L+\rho$ [5]
6. $(1.2 + 0.2\ S_{DS})D+0.5L+\rho$ [6]
7. $(1.2 + 0.2\ S_{DS})D+0.5L+\rho$ [7]
8. $(1.2 + 0.2\ S_{DS})D+0.5L+\rho$ [8]
9. $(1.2 + 0.2\ S_{DS})D+0.5L+\rho$ [9]
10. $(1.2 + 0.2\ S_{DS})D+0.5L+\rho$ [10]
11. $(1.2 + 0.2\ S_{DS})D+0.5L+\rho$ [11]
12. $(1.2 + 0.2\ S_{DS})D+0.5L+\rho$ [12]
13. $(1.2 + 0.2\ S_{DS})D+0.5L+\rho$ [13]
14. $(1.2 + 0.2\ S_{DS})D+0.5L+\rho$ [14]
15. $(1.2 + 0.2\ S_{DS})D+0.5L+\rho$ [15]
16. $(1.2 + 0.2\ S_{DS})D+0.5L+\rho$ [16]
17. $(1.2 + 0.2\ S_{DS})D+0.5L+\rho$ [17]
18. $(1.2 + 0.2\ S_{DS})D+0.5L+\rho$ [18]
19. $(1.2 + 0.2\ S_{DS})D+0.5L+\rho$ [19]
20. $(1.2 + 0.2\ S_{DS})D+0.5L+\rho$ [20]
21. $(1.2 + 0.2\ S_{DS})D+0.5L+\rho$ [21]
22. $(1.2 + 0.2\ S_{DS})D+0.5L+\rho$ [22]
23. $(1.2 + 0.2\ S_{DS})D+0.5L+\rho$ [23]
24. $(1.2 + 0.2\ S_{DS})D+0.5L+\rho$ [24]
25. $(0.9 - 0.2\ S_{DS})D+\rho$ [1]
26. $(0.9 - 0.2\ S_{DS})D+\rho$ [2]
27. $(0.9 - 0.2\ S_{DS})D+\rho$ [3]
28. $(0.9 - 0.2\ S_{DS})D+\rho$ [4]
29. $(0.9 - 0.2\ S_{DS})D+\rho$ [5]
30. $(0.9 - 0.2\ S_{DS})D+\rho$ [6]
31. $(0.9 - 0.2\ S_{DS})D+\rho$ [7]
32. $(0.9 - 0.2\ S_{DS})D+\rho$ [8]
33. $(0.9 - 0.2\ S_{DS})D+\rho$ [9]
34. $(0.9 - 0.2\ S_{DS})D+\rho$ [10]
35. $(0.9 - 0.2\ S_{DS})D+\rho$ [11]
36. $(0.9 - 0.2\ S_{DS})D+\rho$ [12]
37. $(0.9 - 0.2\ S_{DS})D+\rho$ [13]
38. $(0.9 - 0.2\ S_{DS})D+\rho$ [14]
39. $(0.9 - 0.2\ S_{DS})D+\rho$ [15]
40. $(0.9 - 0.2\ S_{DS})D+\rho$ [16]
41. $(0.9 - 0.2\ S_{DS})D+\rho$ [17]
42. $(0.9 - 0.2\ S_{DS})D+\rho$ [18]
43. $(0.9 - 0.2\ S_{DS})D+\rho$ [19]
44. $(0.9 - 0.2\ S_{DS})D+\rho$ [20]
45. $(0.9 - 0.2\ S_{DS})D+\rho$ [21]
46. $(0.9 - 0.2\ S_{DS})D+\rho$ [22]
47. $(0.9 - 0.2\ S_{DS})D+\rho$ [23]
48. $(0.9 - 0.2\ S_{DS})D+\rho$ [24]

The basic load combinations with overstrength factor for strength design as per section 12.4.3.2 of ASCE 7-10 (ASCE, 2010) with orthogonal seismic loading and accidental torsion to determine collector forces and chord forces in diaphragm.

1. $(1.2 + 0.2\ S_{DS})D+0.5L+\Omega$ [1]
2. $(1.2 + 0.2\ S_{DS})D+0.5L+\Omega$ [2]
3. $(1.2 + 0.2\ S_{DS})D+0.5L+\Omega$ [3]
4. $(1.2 + 0.2\ S_{DS})D+0.5L+\Omega$ [4]
5. $(1.2 + 0.2\ S_{DS})D+0.5L+\Omega$ [5]
6. $(1.2 + 0.2\ S_{DS})D+0.5L+\Omega$ [6]
7. $(1.2 + 0.2\ S_{DS})D+0.5L+\Omega$ [7]
8. $(1.2 + 0.2\ S_{DS})D+0.5L+\Omega$ [8]
9. $(1.2 + 0.2\ S_{DS})D+0.5L+\Omega$ [9]
10. $(1.2 + 0.2\ S_{DS})D+0.5L+\Omega$ [10]
11. $(1.2 + 0.2\ S_{DS})D+0.5L+\Omega$ [11]
12. $(1.2 + 0.2\ S_{DS})D+0.5L+\Omega$ [12]
13. $(1.2 + 0.2\ S_{DS})D+0.5L+\Omega$ [13]
14. $(1.2 + 0.2\ S_{DS})D+0.5L+\Omega$[14]
15. $(1.2 + 0.2\ S_{DS})D+0.5L+\Omega$ [15]
16. $(1.2 + 0.2\ S_{DS})D+0.5L+\Omega$ [16]
17. $(1.2 + 0.2\ S_{DS})D+0.5L+\Omega$ [17]
18. $(1.2 + 0.2\ S_{DS})D+0.5L+\Omega$ [18]
19. $(1.2 + 0.2\ S_{DS})D+0.5L+\Omega$ [19]
20. $(1.2 + 0.2\ S_{DS})D+0.5L+\Omega$ [20]
21. $(1.2 + 0.2\ S_{DS})D+0.5L+\Omega$ [21]
22. $(1.2 + 0.2\ S_{DS})D+0.5L+\Omega$ [22]
23. $(1.2 + 0.2\ S_{DS})D+0.5L+\Omega$ [23]
24. $(1.2 + 0.2\ S_{DS})D+0.5L+\Omega$ [24]
25. $(0.9 - 0.2\ S_{DS})D+\Omega$ [1]
26. $(0.9 - 0.2\ S_{DS})D+\Omega$ [2]
27. $(0.9 - 0.2\ S_{DS})D+\Omega$ [3]
28. $(0.9 - 0.2\ S_{DS})D+\Omega$ [4]
29. $(0.9 - 0.2\ S_{DS})D+\Omega$[5]
30. $(0.9 - 0.2\ S_{DS})D+\Omega$ [6]
31. $(0.9 - 0.2\ S_{DS})D+\Omega$ [7]
32. $(0.9 - 0.2\ S_{DS})D+\Omega$ [8]
33. $(0.9 - 0.2\ S_{DS})D+\Omega$ [9]
34. $(0.9 - 0.2\ S_{DS})D+\Omega$ [10]
35. $(0.9 - 0.2\ S_{DS})D+\Omega$ [11]
36. $(0.9 - 0.2\ S_{DS})D+\Omega$ [12]
37. $(0.9 - 0.2\ S_{DS})D+\Omega$ [13]
38. $(0.9 - 0.2\ S_{DS})D+\Omega$ [14]
39. $(0.9 - 0.2\ S_{DS})D+\Omega$ [15]
40. $(0.9 - 0.2\ S_{DS})D+\Omega$ [16]
41. $(0.9 - 0.2\ S_{DS})D+\Omega$ [17]
42. $(0.9 - 0.2\ S_{DS})D+\Omega$ [18]
43. $(0.9 - 0.2\ S_{DS})D+\Omega$ [19]
44. $(0.9 - 0.2\ S_{DS})D+\Omega$ [20]
45. $(0.9 - 0.2\ S_{DS})D+\Omega$ [21]
46. $(0.9 - 0.2\ S_{DS})D+\Omega$ [22]
47. $(0.9 - 0.2\ S_{DS})D+\Omega$ [23]
48. $(0.9 - 0.2\ S_{DS})D+\Omega$ [24]

Appendix-B

LOAD COMBINATIONS FOR RSA METHOD-1

The basic load combinations for strength design as per section 12.4.2.3 of ASCE 7-10 (ASCE, 2010) with orthogonal seismic loading and accidental torsion to determine diaphragm forces.

1. $(1.2 + 0.2\ S_{DS})D+0.5L+\rho$ [1]
2. $(1.2 + 0.2\ S_{DS})D+0.5L+\rho$ [2]
3. $(1.2 + 0.2\ S_{DS})D+0.5L+\rho$ [3]
4. $(1.2 + 0.2\ S_{DS})D+0.5L+\rho$ [4]
5. $(1.2 + 0.2\ S_{DS})D+0.5L+\rho$ [5]
6. $(1.2 + 0.2\ S_{DS})D+0.5L+\rho$ [6]
7. $(0.9 - 0.2\ S_{DS})D+\rho$ [1]
8. $(0.9 - 0.2\ S_{DS})D+\rho$ [2]
9. $(0.9 - 0.2\ S_{DS})D+\rho$ [3]
10. $(0.9 - 0.2\ S_{DS})D+\rho$ [4]
11. $(0.9 - 0.2\ S_{DS})D+\rho$ [5]
12. $(0.9 - 0.2\ S_{DS})D+\rho$ [6]

The basic load combinations with overstrength factor for strength design as per section 12.4.3.2 of ASCE 7-10 (ASCE, 2010) with orthogonal seismic loading and accidental torsion to determine collector forces and chord forces in diaphragm.

1. $(1.2 + 0.2\ S_{DS})D+0.5L+\Omega$ [1]
2. $(1.2 + 0.2\ S_{DS})D+0.5L+\Omega$ [2]
3. $(1.2 + 0.2\ S_{DS})D+0.5L+\Omega$ [3]
4. $(1.2 + 0.2\ S_{DS})D+0.5L+\Omega$ [4]
5. $(1.2 + 0.2\ S_{DS})D+0.5L+\Omega$ [5]
6. $(1.2 + 0.2\ S_{DS})D+0.5L+\Omega$ [6]
7. $(0.9 - 0.2\ S_{DS})D+\Omega$ [1]
8. $(0.9 - 0.2\ S_{DS})D+\Omega$ [2]
9. $(0.9 - 0.2\ S_{DS})D+\Omega$ [3]
10. $(0.9 - 0.2\ S_{DS})D+\Omega$ [4]
11. $(0.9 - 0.2\ S_{DS})D+\Omega$[5]
12. $(0.9 - 0.2\ S_{DS})D+\Omega$ [6]

Appendix-C

LOAD COMBINATIONS FOR MRHA

The basic load combinations for strength design as per section 12.4.2.3 of ASCE 7-10 (ASCE, 2010) with orthogonal seismic loading and accidental torsion to determine diaphragm forces.

1. $(1.2 + 0.2\ S_{DS})D+0.5L+\rho$ [1]
2. $(1.2 + 0.2\ S_{DS})D+0.5L+\rho$ [2]
3. $(1.2 + 0.2\ S_{DS})D+0.5L+\rho$ [3]
4. $(1.2 + 0.2\ S_{DS})D+0.5L+\rho$ [4]
5. $(1.2 + 0.2\ S_{DS})D+0.5L+\rho$ [5]
6. $(1.2 + 0.2\ S_{DS})D+0.5L+\rho$ [6]
7. $(1.2 + 0.2\ S_{DS})D+0.5L+\rho$ [7]
8. $(1.2 + 0.2\ S_{DS})D+0.5L+\rho$ [8]
9. $(1.2 + 0.2\ S_{DS})D+0.5L+\rho$ [9]
10. $(1.2 + 0.2\ S_{DS})D+0.5L+\rho$ [10]
11. $(1.2 + 0.2\ S_{DS})D+0.5L+\rho$ [11]
12. $(1.2 + 0.2\ S_{DS})D+0.5L+\rho$ [12]
13. $(1.2 + 0.2\ S_{DS})D+0.5L+\rho$ [13]
14. $(1.2 + 0.2\ S_{DS})D+0.5L+\rho$ [14]
15. $(1.2 + 0.2\ S_{DS})D+0.5L+\rho$ [15]
16. $(1.2 + 0.2\ S_{DS})D+0.5L+\rho$ [16]
17. $(1.2 + 0.2\ S_{DS})D+0.5L+\rho$ [17]
18. $(1.2 + 0.2\ S_{DS})D+0.5L+\rho$ [18]
19. $(1.2 + 0.2\ S_{DS})D+0.5L+\rho$ [19]
20. $(1.2 + 0.2\ S_{DS})D+0.5L+\rho$ [20]
21. $(0.9 - 0.2\ S_{DS})D+\rho$ [1]
22. $(0.9 - 0.2\ S_{DS})D+\rho$ [2]
23. $(0.9 - 0.2\ S_{DS})D+\rho$ [3]
24. $(0.9 - 0.2\ S_{DS})D+\rho$ [4]
25. $(0.9 - 0.2\ S_{DS})D+\rho$ [5]
26. $(0.9 - 0.2\ S_{DS})D+\rho$ [6]
27. $(0.9 - 0.2\ S_{DS})D+\rho$ [7]
28. $(0.9 - 0.2\ S_{DS})D+\rho$ [8]
29. $(0.9 - 0.2\ S_{DS})D+\rho$ [9]
30. $(0.9 - 0.2\ S_{DS})D+\rho$ [10]
31. $(0.9 - 0.2\ S_{DS})D+\rho$ [11]
32. $(0.9 - 0.2\ S_{DS})D+\rho$ [12]
33. $(0.9 - 0.2\ S_{DS})D+\rho$ [13]
34. $(0.9 - 0.2\ S_{DS})D+\rho$ [14]
35. $(0.9 - 0.2\ S_{DS})D+\rho$ [15]
36. $(0.9 - 0.2\ S_{DS})D+\rho$ [16]
37. $(0.9 - 0.2\ S_{DS})D+\rho$ [17]
38. $(0.9 - 0.2\ S_{DS})D+\rho$ [18]
39. $(0.9 - 0.2\ S_{DS})D+\rho$ [19]
40. $(0.9 - 0.2\ S_{DS})D+\rho$ [20]

The basic load combinations with overstrength factor for strength design as per section 12.4.3.2 of ASCE 7-10 (ASCE, 2010) with orthogonal seismic loading and accidental torsion to determine collector forces and chord forces in diaphragm.

1. $(1.2 + 0.2\ S_{DS})D+0.5L+\Omega$ [1]
2. $(1.2 + 0.2\ S_{DS})D+0.5L+\Omega$ [2]
3. $(1.2 + 0.2\ S_{DS})D+0.5L+\Omega$ [3]
4. $(1.2 + 0.2\ S_{DS})D+0.5L+\Omega$ [4]
5. $(1.2 + 0.2\ S_{DS})D+0.5L+\Omega$ [5]
6. $(1.2 + 0.2\ S_{DS})D+0.5L+\Omega$ [6]
7. $(1.2 + 0.2\ S_{DS})D+0.5L+\Omega$ [7]
8. $(1.2 + 0.2\ S_{DS})D+0.5L+\Omega$ [8]
9. $(1.2 + 0.2\ S_{DS})D+0.5L+\Omega$ [9]
10. $(1.2 + 0.2\ S_{DS})D+0.5L+\Omega$ [10]
11. $(1.2 + 0.2\ S_{DS})D+0.5L+\Omega$ [11]
12. $(1.2 + 0.2\ S_{DS})D+0.5L+\Omega$ [12]
13. $(1.2 + 0.2\ S_{DS})D+0.5L+\Omega$ [13]
14. $(1.2 + 0.2\ S_{DS})D+0.5L+\Omega$[14]
15. $(1.2 + 0.2\ S_{DS})D+0.5L+\Omega$ [15]
16. $(1.2 + 0.2\ S_{DS})D+0.5L+\Omega$ [16]
17. $(1.2 + 0.2\ S_{DS})D+0.5L+\Omega$ [17]
18. $(1.2 + 0.2\ S_{DS})D+0.5L+\Omega$ [18]
19. $(1.2 + 0.2\ S_{DS})D+0.5L+\Omega$ [19]
20. $(1.2 + 0.2\ S_{DS})D+0.5L+\Omega$ [20]
21. $(0.9 - 0.2\ S_{DS})D+\Omega$ [1]
22. $(0.9 - 0.2\ S_{DS})D+\Omega$ [2]
23. $(0.9 - 0.2\ S_{DS})D+\Omega$ [3]
24. $(0.9 - 0.2\ S_{DS})D+\Omega$ [4]
25. $(0.9 - 0.2\ S_{DS})D+\Omega$[5]
26. $(0.9 - 0.2\ S_{DS})D+\Omega$ [6]
27. $(0.9 - 0.2\ S_{DS})D+\Omega$ [7]
28. $(0.9 - 0.2\ S_{DS})D+\Omega$ [8]
29. $(0.9 - 0.2\ S_{DS})D+\Omega$ [9]
30. $(0.9 - 0.2\ S_{DS})D+\Omega$ [10]
31. $(0.9 - 0.2\ S_{DS})D+\Omega$ [11]
32. $(0.9 - 0.2\ S_{DS})D+\Omega$ [12]
33. $(0.9 - 0.2\ S_{DS})D+\Omega$ [13]
34. $(0.9 - 0.2\ S_{DS})D+\Omega$ [14]
35. $(0.9 - 0.2\ S_{DS})D+\Omega$ [15]
36. $(0.9 - 0.2\ S_{DS})D+\Omega$ [16]
37. $(0.9 - 0.2\ S_{DS})D+\Omega$ [17]
38. $(0.9 - 0.2\ S_{DS})D+\Omega$ [18]
39. $(0.9 - 0.2\ S_{DS})D+\Omega$ [19]
40. $(0.9 - 0.2\ S_{DS})D+\Omega$ [20]

Appendix-D

STATISTICAL ANALYSES OF SHELL LAYER STRESSES OF IN-PLANE STRESS COMPONENTS FROM LEP, LDP & NSP

Table 4-4 Maximum S11 in-plane flexural stress at the top of layered shells from different diaphragm force procedures at stories of models

S11-Top-Max-Story 3-LEP and LDP μ = 421 psi σ = 167 psi

Model Number-Diaphragm Location-Diaphragm Design Force Procedures	Stress at Story 3 (psi)	Stress value over Modulus of Rupture	Location	Data points Location in Normal distribution curve/Bell curve/Gaussian distribution	Z-Score	Reference figure
M8-F34-LRHA	789	Yes	Near Shear wall	Value between μ +3σ and μ +2σ	2.21	Figure 4-20
M8-F33-LRHA	788	Yes	Near Shear wall	Value between μ +3σ and μ +2σ	2.21	Figure 4-21
M8-F39-ELFA Method-2	675	Yes	Near Shear wall	Value between μ +2σ and μ +σ	1.53	Figure 4-22
M8-F40-ELFA Method-2	666	Yes	Near Shear wall	Value between μ +2σ and μ +σ	1.47	Figure 4-23
M9-F33-ELFA Method-2	640	Yes	Near Shear wall	Value between μ +2σ and μ +σ	1.32	Figure 4-21
M9-F34-LRHA	634	Yes	Near Shear wall	Value between μ +2σ and μ +σ	1.28	Figure 4-20
M2-F3-LRHA	609	Yes	Near Column	Value between μ +2σ and μ +σ	1.13	Figure 4-24

S11-Top-Max-Story 2-LEP and LDP μ =437 psi σ = 157 psi

Model Number-Diaphragm Location-Diaphragm Design Force Procedures	Stress at Story 2 (psi)	Stress value over Modulus of Rupture	Location	Data points Location in Normal distribution curve/Bell curve/Gaussian distribution	Z-Score	Reference figure
M8-F33-LRHA	792	Yes	Near Shear wall	Value between μ +3σ and μ +2σ	2.25	Figure 4-21
M8-F34-LRHA	790	Yes	Near Shear wall	Value between μ +3σ and μ +2σ	2.25	Figure 4-20
M8-F39-ELFA Method-2	678	Yes	Near Shear wall	Value between μ +2σ and μ +σ	1.53	Figure 4-22
M8-F40-ELFA Method-2	667	Yes	Near Shear wall	Value between μ +2σ and μ +σ	1.46	Figure 4-23
M9-F33-LRHA	645	Yes	Near Shear wall	Value between μ +2σ and μ +σ	1.32	Figure 4-21
M9-F34-ELFA Method-2	639	Yes	Near Shear wall	Value between μ +2σ and μ +σ	1.29	Figure 4-20

S11-Top-Max-Story 1-LEP and LDP μ = 411 psi σ = 154 psi

Model Number-Diaphragm Location-Diaphragm Design Force Procedures	Stress at Story 1 (psi)	Stress value over Modulus of Rupture	Location	Data points Location in Normal distribution curve/Bell curve/Gaussian distribution	Z-Score	Reference figure
M8-F33-ELFA Method-2	747	Yes	Near Shear wall	Value between μ +3σ and μ +2σ	2.19	Figure 4-21
M8-F34-ELFA Method-2	746	Yes	Near Shear wall	Value between μ +3σ and μ +2σ	2.18	Figure 4-20
M8-F39-ELFA Method-2	655	Yes	Near Shear wall	Value between μ +2σ and μ +σ	1.59	Figure 4-22
M8-F40-ELFA Method-2	649	Yes	Near Shear wall	Value between μ +2σ and μ +σ	1.55	Figure 4-23
M9-F33-ELFA Method-2	615	Yes	Near Shear wall	Value between μ +2σ and μ +σ	1.33	Figure 4-21
M9-F34-ELFA Method-2	614	Yes	Near Shear wall	Value between μ +2σ and μ +σ	1.32	Figure 4-20

Table 4-5 Maximum S11 in-plane flexural stress at the bottom of layered shells from different diaphragm force procedures at stories of Models

S11-Bottom-Max-Story 3-LEP and LDP μ = 350 psi σ = 52 psi

Model Number-Diaphragm Location-Diaphragm Design Force Procedures	Stress at Story 3 (psi)	Stress value over Modulus of Rupture	Location	Data points Location in Normal distribution curve/Bell curve/Gaussian distribution	Z-Score	Reference figure
M8-F36-LRHA	423	No	Near Shear wall	Value between μ +2σ and μ +σ	1.39	Figure 4-26
M8-F35-LRHA	418	No	Near Shear wall	Value between μ +2σ and μ +σ	1.29	Figure 4-25
M9-F42-LRHA	446	No	Near Shear wall	Value between μ +2σ and μ +σ	1.82	Figure 4-28
M9-F41-LRHA	440	No	Near Shear wall	Value between μ +2σ and μ +σ	1.71	Figure 4-27
M2-F2-LRHA	428	No	Near Shear wall	Value between μ +2σ and μ +σ	1.48	Figure 4-29
M2-F5-LRHA	411	No	Near Column	Value between μ +2σ and μ +σ	1.16	
M2-F6-LRHA	404	No	Near Column	Value between μ +2σ and μ +σ	1.02	Figure 4-30
M3-F11-LRHA	413	No	Near Shear wall	Value between μ +2σ and μ +σ	1.19	Figure 4-31
M3-F12-LRHA	406	No	Near Column	Value between μ +2σ and μ +σ	1.05	Figure 4-32

S11-Bottom-Max-Story 2-LEP and LDP μ = 346 psi σ = 43 psi

Model Number-Diaphragm Location-Diaphragm Design Force Procedures	Stress at Story 2 (psi)	Stress value over Modulus of Rupture	Location	Data points Location in Normal distribution curve/Bell curve/Gaussian distribution	Z-Score	Reference figure
M2-F2-LRHA	427	No	Near Shear wall	Value between μ +2σ and μ +σ	1.87	Figure 4-29
M2-F3-LRHA	397	No	Near Column	Value between μ +2σ and μ +σ	1.18	Figure 4-33
M9-F42-LRHA	425	No	Near Shear wall	Value between μ +2σ and μ +σ	1.83	Figure 4-28
M9-F41-LRHA	420	No	Near Shear wall	Value between μ +2σ and μ +σ	1.72	Figure 4-27
M8-F36-LRHA	409	No	Near Shear wall	Value between μ +2σ and μ +σ	1.46	Figure 4-26
M8-F35-LRHA	405	No	Near Shear wall	Value between μ +2σ and μ +σ	1.35	Figure 4-25

S11-Bottom-Max-Story 1-LEP and LDP μ = 338 psi σ = 42 psi

Model Number-Diaphragm Location-Diaphragm Design Force Procedures	Stress at Story 1 (psi)	Stress value over Modulus of Rupture	Location	Data points Location in Normal distribution curve/Bell curve/Gaussian distribution	Z-Score	Reference figure
M2-F2-ELFA Method-2	422	No	Near Shear wall	Value between μ +2σ and μ +σ	1.99	Figure 4-29
M2-F3-LRHA	382	No	Near Column	Value between μ +2σ and μ +σ	1.05	Figure 4-33
M2-F5-ELFA Method-2	381	No	Near Column	Value between μ +2σ and μ +σ	1.03	N/A
M9-F42-LRHA	416	No	Near Shear wall	Value between μ +2σ and μ +σ	1.86	Figure 4-28
M9-F41-LRHA	411	No	Near Shear wall	Value between μ +2σ and μ +σ	1.74	Figure 4-27
M9-F25-LRHA	382	No	Near Column	Value between μ +2σ and μ +σ	1.04	N/A
M9-F28-LRHA	381	No	Near Column	Value between μ +2σ and μ +σ	1.01	N/A
M8-F36-LRHA	407	No	Near Shear wall	Value between μ +2σ and μ +σ	1.64	N/A
M8-F35-LRHA	402	No	Near Shear wall	Value between μ +2σ and μ +σ	1.55	N/A

Table 4-6 Minimum S11 in-plane flexural stress at the top of layered shells from different diaphragm force procedures at stories of models

S11-Top-Min-Story 3-LEP and LDP μ = -361 psi σ = 59 psi

Model Number-Diaphragm Location-Diaphragm Design Force Procedures	Stress at Story 3 (psi)	Location	Data points Location in Normal distribution curve/Bell curve/Gaussian distribution	Z-Score	Reference figure
M9-F42-LRHA	-463	Near Shear wall	Value is between μ - σ and μ -2σ	-1.74	Figure 4-24
M9-F41-LRHA	-457	Near Shear wall	Value is between μ - σ and μ -2σ	-1.64	Figure 4-35
M9-F37-LRHA	-420	Near Column	Value is between μ - σ and μ -2σ	-1.01	N/A
M2-F2-LRHA	-440	Near Shear wall	Value is between μ - σ and μ -2σ	-1.35	Figure 4-36
M8-F36-LRHA	-442	Near Shear wall	Value is between μ - σ and μ -2σ	-1.38	Figure 4-37
M8-F35-LRHA	-436	Near Shear wall	Value is between μ - σ and μ -2σ	-1.28	Figure 4-38
M5-F14-LRHA	-440	Near Shear wall	Value is between μ - σ and μ -2σ	-1.35	N/A

S11-Top-Min-Story 2-LEP and LDP μ = -353 psi σ = 47 psi

Model Number-Diaphragm Location-Diaphragm Design Force Procedures	Stress at Story 2 (psi)	Location	Data points Location in Normal distribution curve/Bell curve/Gaussian distribution	Z-Score	Reference figure
M9-F42-LRHA	-432	Near Shear wall	Value is between μ - σ and μ -2σ	-1.69	Figure 4-34
M9-F41-LRHA	-427	Near Shear wall	Value is between μ - σ and μ -2σ	-1.58	Figure 4-35
M9-F37-LRHA	-400	Near Column	Value is between μ - σ and μ -2σ	-1.01	N/A
M2-F2-LRHA	-428	Near Shear wall	Value is between μ - σ and μ -2σ	-1.60	Figure 4-36
M8-F36-LRHA	-418	Near Shear wall	Value is between μ - σ and μ -2σ	-1.38	Figure 4-37
M8-F35-LRHA	-413	Near Shear wall	Value is between μ - σ and μ -2σ	-1.28	Figure 4-38

S11-Top-Min-Story 1-LEP and LDP μ = -343 psi σ = 45 psi

Model Number-Diaphragm Location-Diaphragm Design Force Procedures	Stress at Story 1 (psi)	Location	Data points Location in Normal distribution curve/Bell curve/Gaussian distribution	Z-Score	Reference figure
M2-F2-LRHA	-425	Near Shear wall	Value is between μ - σ and μ -2σ	-1.82	Figure 4-36
M9-F42-LRHA	-421	Near Shear wall	Value is between μ - σ and μ -2σ	-1.72	Figure 4-34
M9-F41-LRHA	-416	Near Shear wall	Value is between μ - σ and μ -2σ	-1.60	Figure 4-35
M9-F25-LRHA	-389	Near Column	Value is between μ - σ and μ -2σ	-1.03	N/A
M8-F36-LRHA	-413	Near Shear wall	Value is between μ - σ and μ -2σ	-1.53	Figure 4-37
M8-F35-LRHA	-407	Near Shear wall	Value is between μ - σ and μ -2σ	-1.42	Figure 4-38

Table 4-7 Minimum S11 in-plane flexural stress at the bottom of layered shells from different diaphragm force procedures at stories of models

S11-Bottom-Min-Story 3-LEP and LDP μ = -429 psi σ = 158 psi

Model Number-Diaphragm Location-Diaphragm Design Force Procedures	Stress at Story 3 (psi)	Location	Data points Location in Normal distribution curve/Bell curve/Gaussian distribution	Z-Score	Reference figure
M8-F34-LRHA	-770	Near Shear wall	Value between μ -2σ and μ -3σ	-2.16	Figure 4-40
M8-F33-LRHA	-769	Near Shear wall	Value between μ -2σ and μ -3σ	-2.15	Figure 4-39
M8-F40-ELFA Method-2	-672	Near Shear wall	Value is between μ - σ and μ -2σ	-1.54	Figure 4-42
M8-F39-ELFA Method-2	-667	Near Shear wall	Value is between μ - σ and μ -2σ	-1.50	Figure 4-41
M9-F34-ELFA Method-2	-630	Near Shear wall	Value is between μ - σ and μ -2σ	-1.27	N/A
M9-F33-ELFA Method-2	-623	Near Shear wall	Value is between μ - σ and μ -2σ	-1.23	N/A

S11-Bottom-Min-Story 2-LEP and LDP μ = -435 psi σ = 152 psi

Model Number-Diaphragm Location-Diaphragm Design Force Procedures	Stress at Story 2 (psi)	Location	Data points Location in Normal distribution curve/Bell curve/Gaussian distribution	Z-Score	Reference figure
M8-F33-LRHA	-765	Near Shear wall	Value between μ -2σ and μ -3σ	-2.18	Figure 4-39
M8-F34-LRHA	-765	Near Shear wall	Value between μ -2σ and μ -3σ	-2.18	Figure 4-40
M8-F40-ELFA Method-2	-662	Near Shear wall	Value is between μ - σ and μ -2σ	-1.50	Figure 4-42
M8-F39-ELFA Method-2	-656	Near Shear wall	Value is between μ - σ and μ -2σ	-1.46	Figure 4-41
M9-F34-ELFA Method-2	-627	Near Shear wall	Value is between μ - σ and μ -2σ	-1.27	N/A
M9-F33-ELFA Method-2	-619	Near Shear wall	Value is between μ - σ and μ -2σ	-1.21	N/A

S11-Bottom-Min-Story 1-LEP and LDP μ = -407 psi σ = 147 psi

Model Number-Diaphragm Location-Diaphragm Design Force Procedures	Stress at Story 1 (psi)	Location	Data points Location in Normal distribution curve/Bell curve/Gaussian distribution	Z-Score	Reference figure
M8-F34-LRHA	-728	Near Shear wall	Value between μ -2σ and μ -3σ	-2.19	Figure 4-40
M8-F33-LRHA	-728	Near Shear wall	Value between μ -2σ and μ -3σ	-2.19	Figure 4-39
M8-F40-ELFA Method-2	-639	Near Shear wall	Value is between μ - σ and μ -2σ	-1.58	Figure 4-42
M8-F39-ELFA Method-2	-639	Near Shear wall	Value is between μ - σ and μ -2σ	-1.58	Figure 4-41
M9-F34-ELFA Method-2	-599	Near Shear wall	Value is between μ - σ and μ -2σ	-1.31	N/A
M9-F33-RSA Method-2	-596	Near Shear wall	Value is between μ - σ and μ -2σ	-1.29	N/A

Table 4-8 Maximum S11 in-plane flexural stress at the top of layered shells from Pushover analyses at stories of models

S11-Top-Max-Story 3-NSP μ = 64 psi σ = 49 psi

Model Number-Diaphragm Location-Diaphragm Design Force Procedures	Stress at Story 3 (psi)	Stress value over Modulus of Rupture	Location	Data points Location in Normal distribution curve/Bell curve/Gaussian distribution	Z-Score	Reference figure
M8-F31-Push-30%X+100%Y	392	No	Near Column	Value Greater than μ +3σ	6.68	Figure 4-44
M8-F33-PushY-1.5XTg	116	No	Near Shear wall	Value between μ +2σ and μ +σ	1.07	Figure 4-43
M9-F38-PushY-1.5XTg	262	No	Near Shear wall	Value Greater than μ +3σ	4.03	Figure 4-47
M9-F25-Push-30%X+100%Y	247	No	Near Column	Value Greater than μ +3σ	3.73	Figure 4-45
M9-F33-Push-30%X+100%Y	208	No	Near Shear wall	Value between μ +3σ and μ +2σ	2.94	
M9-F37-PushY-1.5XTg	203	No	Near Column	Value between μ +3σ and μ +2σ	2.84	Figure 4-46
M9-F30-Push-30%X+100%Y	145	No	Near Column	Value between μ +2σ and μ +σ	1.66	Figure 4-51
M2-F1-PushY-1.5XTg	199	No	Near Shear wall	Value between μ +3σ and μ +2σ	2.75	Figure 4-48
M2-F4-PushY-1.5XTg	122	No	Near Column	Value between μ +2σ and μ +σ	1.20	N/A
M5-F13-PushY-1.5XTg	183	No	Near Shear wall	Value between μ +3σ and μ +2σ	2.43	Figure 4-49
M5-F16-PushY-1.5XTg	130	No	Near Column	Value between μ +2σ and μ +σ	1.35	N/A
M3-F9-PushY-1.5XTg	118	No	Near Column	Value between μ +2σ and μ +σ	1.11	N/A

S11-Top-Max-Story 2-NSP μ = 57 psi σ = 44 psi

Model Number-Diaphragm Location-Diaphragm Design Force Procedures	Stress at Story 2 (psi)	Stress value over Modulus of Rupture	Location	Data points Location in Normal distribution curve/Bell curve/Gaussian distribution	Z-Score	Reference figure
M2-F1-Push-30%X+100%Y	326	No	Near Shear wall	Value Greater than μ +3σ	6.14	Figure 4-48
M2-F4-Push-30%X+100%Y	110	No	Near Column	Value between μ +2σ and μ +σ	1.20	N/A
M5-F13-PushY-1.5XTg	283	No	Near Shear wall	Value Greater than μ +3σ	5.16	Figure 4-49
M8-F31-Push-30%X+100%Y	207	No	Near Column	Value Greater than μ +3σ	3.43	Figure 4-44
M8-F36-Push-30%X+100%Y	103	No	Near Shear wall	Value between μ +2σ and μ +σ	1.06	Figure 4-50
M9-F33-Push-30%X+100%Y	189	No	Near Shear wall	Value Greater than μ +3σ	3.00	Figure 4-43
M9-F25-Push-30%X+100%Y	181	No	Near Column	Value between μ +3σ and μ +2σ	2.84	Figure 4-45
M9-F30-Push-30%X+100%Y	140	No	Near Column	Value between μ +2σ and μ +σ	1.90	Figure 4-51
M9-F38-Push-30%X+100%Y	128	No	Near Shear wall	Value between μ +2σ and μ +σ	1.63	Figure 4-47
M9-F42-Push-100%X+30%Y	103	No	Near Shear wall	Value between μ +2σ and μ +σ	1.05	Figure 4-52
M9-F37-Push-30%X+100%Y	101	No	Near Column	Value between μ +2σ and μ +σ	1.01	Figure 4-46
M3-F9-PushY-1.5XTg	108	No	Near Column	Value between μ +2σ and μ +σ	1.16	N/A

S11-Top-Max-Story 1-NSP μ = 46 psi σ = 24 psi

Model Number-Diaphragm Location-Diaphragm Design Force Procedures	Stress at Story 1 (psi)	Stress value over Modulus of Rupture	Location	Data points Location in Normal distribution curve/Bell curve/Gaussian distribution	Z-Score	Reference figure
M2-F1-PushY-1.5XTg	153	No	Near Shear wall	Value Greater than μ +3σ	4.50	Figure 4-48
M2-F5-PushY-1.5XTg	72	No	Near Column	Value between μ +2σ and μ +σ	1.11	N/A
M5-F13-PushY-1.5XTg	136	No	Near Shear wall	Value Greater than μ +3σ	3.77	Figure 4-49
M5-F17-PushY-1.5XTg	74	No	Near Column	Value between μ +2σ and μ +σ	1.16	N/A
M8-F31-Push-30%X+100%Y	113	No	Near Column	Value between μ +3σ and μ +2σ	2.83	Figure 4-44
M8-F36-PushY-1.5XTg	105	No	Near Shear wall	Value between μ +3σ and μ +2σ	2.46	Figure 4-50
M9-F33-PushY-1.5XTg	112	No	Near Shear wall	Value between μ +3σ and μ +2σ	2.77	Figure 4-43
M9-F42-Push-100%X+30%Y	108	No	Near Shear wall	Value between μ +3σ and μ +2σ	2.61	Figure 4-52
M9-F30-PushY-1.5XTg	97	No	Near Column	Value between μ +3σ and μ +2σ	2.15	Figure 4-51
M9-F41-Push-100%X+30%Y	83	No	Near Shear wall	Value between μ +2σ and μ +σ	1.53	N/A
M9-F28-Push-100%X+30%Y	73	No	Near Column	Value between μ +2σ and μ +σ	1.15	N/A
M9-F25-Push-100%X+30%Y	73	No	Near Column	Value between μ +2σ and μ +σ	1.13	Figure 4-45
M3-F7-Push-30%X+100%Y	74	No	Near Shear wall	Value between μ +2σ and μ +σ	1.18	N/A
M6-F19-Push-30%X+100%Y	71	No	Near Column	Value between μ +2σ and μ +σ	1.05	N/A

Table 4-9 Maximum S11 in-plane flexural stress at the bottom of layered shells from Pushover analyses at stories of models

S11-Bottom-Max-Story 3-NSP μ = 35 psi σ = 21 psi

Model Number-Diaphragm Location-Diaphragm Design Force Procedures	Stress at Story 3 (psi)	Stress value over Modulus of Rupture	Location	Data points Location in Normal distribution curve/Bell curve/Gaussian distribution	Z-Score	Reference figure
M8-F40-PushY-1.5XTg	96	No	Near Shear wall	Value between μ +3σ and μ +2σ	2.95	N/A
M8-F31-Push-30%X+100%Y	77	No	Near Column	Value between μ +3σ and μ +2σ	2.04	N/A
M8-F36-Push-30%X+100%Y	66	No	Near Shear wall	Value between μ +2σ and μ +σ	1.50	N/A
M9-F30-PushY-1.5XTg	82	No	Near Column	Value between μ +3σ and μ +2σ	2.31	N/A
M9-F37-Push-30%X+100%Y	80	No	Near Column	Value between μ +3σ and μ +2σ	2.17	N/A
M9-F42-Push-100%X+30%Y	73	No	Near Shear wall	Value between μ +2σ and μ +σ	1.87	N/A
M9-F25-PushY-1.5XTg	65	No	Near Column	Value between μ +2σ and μ +σ	1.44	N/A
M6-F22-Push-30%X+100%Y	71	No	Near Column	Value between μ +2σ and μ +σ	1.77	N/A
M3-F10-Push-30%X+100%Y	67	No	Near Column	Value between μ +2σ and μ +σ	1.56	N/A
M2-F1-Push-30%X+100%Y	63	No	Near Shear wall	Value between μ +2σ and μ +σ	1.35	N/A
M5-F13-PushY-1.5XTg	62	No	Near Shear wall	Value between μ +2σ and μ +σ	1.30	N/A

S11-Bottom-Max-Story 2-NSP μ = 35 psi σ = 22 psi

Model Number-Diaphragm Location-Diaphragm Design Force Procedures	Stress at Story 2 (psi)	Stress value over Modulus of Rupture	Location	Data points Location in Normal distribution curve/Bell curve/Gaussian distribution	Z-Score	Reference figure
M8-F40-PushY-1.5XTg	86	No	Near Shear wall	Value between μ +3σ and μ +2σ	2.27	N/A
M8-F31-Push-30%X+100%Y	74	No	Near Column	Value between μ +2σ and μ +σ	1.72	N/A
M8-F36-PushY-1.5XTg	59	No	Near Shear wall	Value between μ +2σ and μ +σ	1.07	N/A
M3-F11-Push-30%X+100%Y	78	No	Near Shear wall	Value between μ +2σ and μ +σ	1.90	N/A
M9-F37-Push-30%X+100%Y	74	No	Near Column	Value between μ +2σ and μ +σ	1.74	N/A
M9-F42-Push-30%X+100%Y	69	No	Near Shear wall	Value between μ +2σ and μ +σ	1.54	N/A
M9-F30-PushY-1.5XTg	69	No	Near Column	Value between μ +2σ and μ +σ	1.51	N/A
M9-F41-Push-100%X+30%Y	64	No	Near Shear wall	Value between μ +2σ and μ +σ	1.31	N/A
M9-F25-PushY-1.5XTg	58	No	Near Column	Value between μ +2σ and μ +σ	1.04	N/A
M6-F23-Push-30%X+100%Y	66	No	Near Shear wall	Value between μ +2σ and μ +σ	1.40	N/A
M2-F5-Push-100%X+30%Y	63	No	Near Column	Value between μ +2σ and μ +σ	1.23	N/A
M2-F4-PushY-1.5XTg	62	No	Near Column	Value between μ +2σ and μ +σ	1.18	N/A

S11-Bottom-Max-Story 1-NSP μ = 25 psi σ = 18 psi

Model Number-Diaphragm Location-Diaphragm Design Force Procedures	Stress at Story 1 (psi)	Stress value over Modulus of Rupture	Location	Data points Location in Normal distribution curve/Bell curve/Gaussian distribution	Z-Score	Reference figure
M9-F42-PushY-1.5XTg	70	No	Near Shear wall	Value between μ +3σ and μ +2σ	2.50	N/A
M9-F37-Push-100%X+30%Y	56	No	Near Column	Value between μ +2σ and μ +σ	1.70	N/A
M9-F25-PushY-1.5XTg	47	No	Near Column	Value between μ +2σ and μ +σ	1.19	N/A
M9-F28-PushY-1.5XTg	45	No	Near Column	Value between μ +2σ and μ +σ	1.10	N/A
M3-F11-Push-30%X+100%Y	66	No	Near Shear wall	Value between μ +3σ and μ +2σ	2.25	N/A
M3-F7-PushY-1.5XTg	50	No	Near Shear wall	Value between μ +2σ and μ +σ	1.37	N/A
M2-F5-Push-100%X+30%Y	59	No	Near Column	Value between μ +2σ and μ +σ	1.87	N/A
M2-F6-Push-30%X+100%Y	44	No	Near Column	Value between μ +2σ and μ +σ	1.05	N/A
M8-F36-Push-30%X+100%Y	57	No	Near Shear wall	Value between μ +2σ and μ +σ	1.75	N/A
M8-F31-PushY-1.5XTg	53	No	Near Column	Value between μ +2σ and μ +σ	1.53	N/A
M5-F17-Push-100%X+30%Y	51	No	Near Column	Value between μ +2σ and μ +σ	1.44	N/A
M5-F14-Push-30%X+100%Y	45	No	Near Shear wall	Value between μ +2σ and μ +σ	1.11	N/A
M5-F18-Push-30%X+100%Y	45	No	Near Column	Value between μ +2σ and μ +σ	1.08	N/A
M6-F23-Push-100%X+30%Y	51	No	Near Shear wall	Value between μ +2σ and μ +σ	1.41	N/A
M6-F19-PushY-1.5XTg	50	No	Near Shear wall	Value between μ +2σ and μ +σ	1.38	N/A

Table 4-10 Minimum S11 in-plane flexural stress at the top of layered shells from Pushover analyses at Stories of Models

S11-Top-Min-Story 3-NSP **μ = -454 psi** **σ = 125 psi**

Model Number-Diaphragm Location-Diaphragm Design Force Procedures	Stress at Story 3 (psi)	Location	Data points Location in Normal distribution curve/Bell curve/Gaussian distribution	Z-Score	Reference figure
M2-F1-PushY-1.5XTg	-1096	Near Shear wall	Value is less than μ -3σ	-5.15	Figure 4-53
M5-F13-PushY-1.5XTg	-1091	Near Shear wall	Value is less than μ -3σ	-5.11	Figure 4-54
M8-F31-PushY-1.5XTg	-1071	Near Column	Value is less than μ -3σ	-4.95	Figure 4-57
M9-F33-PushY-1.5XTg	-1040	Near Shear wall	Value is less than μ -3σ	-4.70	Figure 4-55
M9-F25-Push-30%X+100%Y	-856	Near Column	Value is less than μ -3σ	-3.23	Figure 4-56
M9-F30-PushY-1.5XTg	-780	Near Column	Value between μ -2σ and μ -3σ	-2.62	N/A
M9-F37-Push-30%X+100%Y	-748	Near Column	Value between μ -2σ and μ -3σ	-2.36	N/A
M9-F38-PushY-1.5XTg	-607	Near Shear wall	Value is between μ - σ and μ -2σ	-1.23	N/A
M9-F29-PushY-1.5XTg	-591	Near Column	Value is between μ - σ and μ -2σ	-1.10	N/A

S11-Top-Min-Story 2-NSP **μ = -432 psi** **σ = 75 psi**

Model Number-Diaphragm Location-Diaphragm Design Force Procedures	Stress at Story 2 (psi)	Location	Data points Location in Normal distribution curve/Bell curve/Gaussian distribution	Z-Score	Reference figure
M2-F1-PushY-1.5XTg	-1011	Near Shear wall	Value is less than μ -3σ	-7.74	Figure 4-53
M9-F33-PushY-1.5XTg	-787	Near Shear wall	Value is less than μ -3σ	-4.74	Figure 4-55
M9-F30-PushY-1.5XTg	-617	Near Column	Value between μ -2σ and μ -3σ	-2.47	N/A
M9-F25-Push-30%X+100%Y	-545	Near Column	Value is between μ - σ and μ -2σ	-1.51	Figure 4-56
M9-F37-Push-30%X+100%Y	-526	Near Column	Value is between μ - σ and μ -2σ	-1.26	N/A
M5-F13-Push-30%X+100%Y	-773	Near Shear wall	Value is less than μ -3σ	-4.55	Figure 4-54
M8-F31-Push-30%X+100%Y	-727	Near Column	Value is less than μ -3σ	-3.94	Figure 4-57

S11-Top-Min-Story 1-NSP **μ = -416 psi** **σ = 29 psi**

Model Number-Diaphragm Location-Diaphragm Design Force Procedures	Stress at Story 1 (psi)	Location	Data points Location in Normal distribution curve/Bell curve/Gaussian distribution	Z-Score	Reference figure
M2-F1-PushY-1.5XTg	-470	Near Shear wall	Value is between μ - σ and μ -2σ	-1.91	Figure 4-53
M2-F2-Push-100%X+30%Y	-463	Near Shear wall	Value is between μ - σ and μ -2σ	-1.63	N/A
M9-F28-Push-100%X+30%Y	-463	Near Column	Value is between μ - σ and μ -2σ	-1.65	N/A
M9-F25-Push-100%X+30%Y	-456	Near Column	Value is between μ - σ and μ -2σ	-1.40	Figure 4-56
M9-F37-PushY-1.5XTg	-455	Near Column	Value is between μ - σ and μ -2σ	-1.37	N/A
M9-F41-Push-100%X+30%Y	-452	Near Shear wall	Value is between μ - σ and μ -2σ	-1.26	N/A
M9-F42-Push-100%X+30%Y	-447	Near Shear wall	Value is between μ - σ and μ -2σ	-1.08	N/A
M8-F44-Push-100%X+30%Y	-458	Near Column	Value is between μ - σ and μ -2σ	-1.46	N/A
M8-F43-Push-100%X+30%Y	-458	Near Column	Value is between μ - σ and μ -2σ	-1.46	N/A
M8-F36-Push-30%X+100%Y	-455	Near Shear wall	Value is between μ - σ and μ -2σ	-1.37	N/A
M5-F14-PushY-1.5XTg	-457	Near Shear wall	Value is between μ - σ and μ -2σ	-1.45	N/A
M5-F13-PushY-1.5XTg	-457	Near Shear wall	Value is between μ - σ and μ -2σ	-1.42	N/A

Table 4-11 Minimum S11 in-plane flexural stress at the bottom of layered shells from Pushover analyses at Stories of models

S11-Bottom-Min-Story 3-NSP μ = -543 psi σ = 227 psi

Model Number-Diaphragm Location-Diaphragm Design Force Procedures	Stress at Story 3 (psi)	Location	Data points Location in Normal distribution curve/Bell curve/Gaussian distribution	Z-Score	Reference figure
M8-F31-PushY-1.5XTg	-1573	Near Column	Value is less than μ -3σ	-4.53	Figure 4-58
M8-F39-Push-100%X+30%Y	-804	Near Shear wall	Value is between μ - σ and μ -2σ	-1.15	Figure 4-62
M8-F40-Push-100%X+30%Y	-804	Near Shear wall	Value is between μ - σ and μ -2σ	-1.15	Figure 4-63
M8-F33-PushY-1.5XTg	-788	Near Shear wall	Value is between μ - σ and μ -2σ	-1.08	Figure 4-59
M9-F33-PushY-1.5XTg	-1463	Near Shear wall	Value is less than μ -3σ	-4.05	Figure 4-59
M9-F25-PushY-1.5XTg	-1302	Near Column	Value is less than μ -3σ	-3.34	Figure 4-60
M9-F37-Push-30%X+100%Y	-1213	Near Column	Value between μ -2σ and μ -3σ	-2.95	N/A
M9-F30-PushY-1.5XTg	-1030	Near Column	Value between μ -2σ and μ -3σ	-2.14	N/A
M9-F38-PushY-1.5XTg	-918	Near Shear wall	Value is between μ - σ and μ -2σ	-1.65	N/A
M5-F13-PushY-1.5XTg	-1129	Near Shear wall	Value between μ -2σ and μ -3σ	-2.58	N/A
M5-F16-PushY-1.5XTg	-996	Near Column	Value is between μ - σ and μ -2σ	-1.99	N/A
M5-F17-Push-30%X+100%Y	-809	Near Column	Value is between μ - σ and μ -2σ	-1.17	N/A
M2-F1-PushY-1.5XTg	-1117	Near Shear wall	Value between μ -2σ and μ -3σ	-2.53	Figure 4-61
M2-F4-PushY-1.5XTg	-980	Near Column	Value is between μ - σ and μ -2σ	-1.93	N/A
M2-F5-PushY-1.5XTg	-830	Near Column	Value is between μ - σ and μ -2σ	-1.26	N/A

S11-Bottom-Min-Story 2-NSP μ = -537 psi σ = 187 psi

Model Number-Diaphragm Location-Diaphragm Design Force Procedures	Stress at Story 2 (psi)	Location	Data points Location in Normal distribution curve/Bell curve/Gaussian distribution	Z-Score	Reference figure
M2-F1-PushY-1.5XTg	-1436	Near Shear wall	Value is less than μ -3σ	-4.80	Figure 4-61
M2-F4-PushY-1.5XTg	-951	Near Column	Value between μ -2σ and μ -3σ	-2.21	N/A
M2-F5-PushY-1.5XTg	-942	Near Column	Value between μ -2σ and μ -3σ	-2.16	N/A
M8-F31-PushY-1.5XTg	-1279	Near Column	Value is less than μ -3σ	-3.96	Figure 4-58
M8-F40-Push-100%X+30%Y	-837	Near Shear wall	Value is between μ - σ and μ -2σ	-1.60	Figure 4-63
M8-F39-Push-100%X+30%Y	-837	Near Shear wall	Value is between μ - σ and μ -2σ	-1.60	Figure 4-62
M9-F33-PushY-1.5XTg	-1210	Near Shear wall	Value is less than μ -3σ	-3.59	Figure 4-59
M9-F25-PushY-1.5XTg	-1083	Near Column	Value between μ -2σ and μ -3σ	-2.91	Figure 4-60
M9-F37-Push-30%X+100%Y	-1003	Near Column	Value between μ -2σ and μ -3σ	-2.48	N/A
M9-F30-PushY-1.5XTg	-860	Near Column	Value is between μ - σ and μ -2σ	-1.72	N/A
M9-F38-Push-30%X+100%Y	-755	Near Shear wall	Value is between μ - σ and μ -2σ	-1.16	N/A
M5-F13-Push-30%X+100%Y	-982	Near Shear wall	Value between μ -2σ and μ -3σ	-2.37	N/A
M5-F16-PushY-1.5XTg	-802	Near Column	Value is between μ - σ and μ -2σ	-1.42	N/A
M5-F17-Push-30%X+100%Y	-802	Near Column	Value is between μ - σ and μ -2σ	-1.41	N/A
M3-F11-Push-100%X+30%Y	-724.53	Near Shear wall	Value is between μ - σ and μ -2σ	-1.00	N/A

S11-Bottom-Min-Story 1-NSP μ = -499 psi σ = 133 psi

Model Number-Diaphragm Location-Diaphragm Design Force Procedures	Stress at Story 1 (psi)	Location	Data points Location in Normal distribution curve/Bell curve/Gaussian distribution	Z-Score	Reference figure
M8-F39-Push-100%X+30%Y	-828	Near Shear wall	Value between μ -2σ and μ -3σ	-2.49	Figure 4-62
M8-F40-Push-100%X+30%Y	-828	Near Shear wall	Value between μ -2σ and μ -3σ	-2.49	Figure 4-63
M8-F31-PushY-1.5XTg	-780	Near Column	Value between μ -2σ and μ -3σ	-2.12	Figure 4-58
M2-F1-PushY-1.5XTg	-800	Near Shear wall	Value between μ -2σ and μ -3σ	-2.27	Figure 4-61
M2-F5-PushY-1.5XTg	-761	Near Column	Value is between μ - σ and μ -2σ	-1.98	N/A
M9-F33-PushY-1.5XTg	-741	Near Shear wall	Value is between μ - σ and μ -2σ	-1.83	Figure 4-59
M9-F25-PushY-1.5XTg	-731	Near Column	Value is between μ - σ and μ -2σ	-1.75	Figure 4-60
M9-F37-Push-30%X+100%Y	-701	Near Column	Value is between μ - σ and μ -2σ	-1.53	N/A
M3-F11-Push-100%X+30%Y	-672	Near Shear wall	Value is between μ - σ and μ -2σ	-1.31	N/A
M5-F17-Push-30%X+100%Y	-650	Near Column	Value is between μ - σ and μ -2σ	-1.14	N/A

Table 4-12 Maximum S22 in-plane flexural stress at the top of layered shells from diaphragm design force procedures at Stories of Models

S22-Top-Max-Story 3-LEP and LDP **μ = 268 psi** **σ = 127 psi**

Model Number-Diaphragm Location-Diaphragm Design Force Procedures	Stress at Story 3 (psi)	Stress value over Modulus of Rupture	Location	Data points Location in Normal distribution curve/Bell curve/Gaussian distribution	Z-Score	Reference figure
M2-F3-LRHA	456	No	Near column	Value between μ +2σ and μ +σ	1.49	N/A
M2-F6-LRHA	449	No	Near column	Value between μ +2σ and μ +σ	1.43	N/A
M5-F18-LRHA	426	No	Near column	Value between μ +2σ and μ +σ	1.25	N/A
M5-F15-LRHA	406	No	Near column	Value between μ +2σ and μ +σ	1.09	N/A
M3-F8-ELFA Method-1	420	No	Near column	Value between μ +2σ and μ +σ	1.20	N/A
M3-F12-ELFA Method-2	416	No	Near column	Value between μ +2σ and μ +σ	1.17	N/A
M3-F10-LRHA	405	No	Near column	Value between μ +2σ and μ +σ	1.08	N/A
M9-F26-LRHA	405	No	Near column	Value between μ +2σ and μ +σ	1.08	N/A
M9-F27-LRHA	405	No	Near column	Value between μ +2σ and μ +σ	1.08	N/A
M6-F20-ELFA Method-1	410	No	Near column	Value between μ +2σ and μ +σ	1.12	N/A
M6-F24-ELFA Method-2	409	No	Near column	Value between μ +2σ and μ +σ	1.12	N/A

S22-Top-Max-Story 2-LEP and LDP **μ = 285 psi** **σ = 111 psi**

Model Number-Diaphragm Location-Diaphragm Design Force Procedures	Stress at Story 2 (psi)	Stress value over Modulus of Rupture	Location	Data points Location in Normal distribution curve/Bell curve/Gaussian distribution	Z-Score	Reference figure
M2-F3-LRHA	446	No	Near column	Value between μ +2σ and μ +σ	1.45	N/A
M2-F6-ELFA Method-2	424	No	Near column	Value between μ +2σ and μ +σ	1.25	N/A
M3-F8-ELFA Method-2	434	No	Near column	Value between μ +2σ and μ +σ	1.35	N/A
M3-F12-ELFA Method-2	408	No	Near column	Value between μ +2σ and μ +σ	1.11	N/A
M3-F10-LRHA	405	No	Near column	Value between μ +2σ and μ +σ	1.08	N/A
M6-F20-RSA Method-2	418	No	Near column	Value between μ +2σ and μ +σ	1.20	N/A
M6-F24-RSA Method-2	402	No	Near column	Value between μ +2σ and μ +σ	1.05	N/A
M5-F18-ELFA Method-2	414	No	Near column	Value between μ +2σ and μ +σ	1.16	N/A
M5-F15-LRHA	411	No	Near column	Value between μ +2σ and μ +σ	1.14	N/A
M9-F27-LRHA	405	No	Near column	Value between μ +2σ and μ +σ	1.08	N/A
M9-F26-LRHA	402	No	Near column	Value between μ +2σ and μ +σ	1.06	N/A

S22-Top-Max-Story 1-LEP and LDP **μ = 278 psi** **σ = 118 psi**

Model Number-Diaphragm Location-Diaphragm Design Force Procedures	Stress at Story 1 (psi)	Stress value over Modulus of Rupture	Location	Data points Location in Normal distribution curve/Bell curve/Gaussian distribution	Z-Score	Reference figure
M3-F8-ELFA Method-2	429	No	Near column	Value between μ +2σ and μ +σ	1.28	N/A
M3-F12-LRHA	409	No	Near column	Value between μ +2σ and μ +σ	1.11	N/A
M2-F6-RSA Method-2	421	No	Near column	Value between μ +2σ and μ +σ	1.22	N/A
M2-F3-ELFA Method-2	419	No	Near column	Value between μ +2σ and μ +σ	1.20	N/A
M6-F20-RSA Method-2	419	No	Near column	Value between μ +2σ and μ +σ	1.20	N/A
M6-F24-RSA Method-2	407	No	Near column	Value between μ +2σ and μ +σ	1.09	N/A
M5-F18-RSA Method-2	416	No	Near column	Value between μ +2σ and μ +σ	1.17	N/A
M9-F27-RSA Method-2	400	No	Near column	Value between μ +2σ and μ +σ	1.04	N/A
M9-F26-RSA Method-2	398	No	Near column	Value between μ +2σ and μ +σ	1.02	N/A

Table 4-13 Maximum S22 in-plane flexural stress at the bottom of layered shells from diaphragm design force procedures at stories of models

S22-Bottom-Max-Story 3-LEP and LDP μ = 323 psi σ = 61 psi

Model Number-Diaphragm Location-Diaphragm Design Force Procedures	Stress at Story 3 (psi)	Stress value over Modulus of Rupture	Location	Data points Location in Normal distribution curve/Bell curve/Gaussian distribution	Z-Score	Reference figure
M9-F37-LRHA	400	No	Near column	Value between μ +2σ and μ +σ	1.29	N/A
M9-F25-LRHA	387	No	Near column	Value between μ +2σ and μ +σ	1.07	N/A
M9-F28-LRHA	387	No	Near column	Value between μ +2σ and μ +σ	1.06	N/A
M8-F31-LRHA	397	No	Near column	Value between μ +2σ and μ +σ	1.23	N/A
M5-F14-LRHA	392	No	Near shear wall	Value between μ +2σ and μ +σ	1.15	N/A
M5-F15-LRHA	383	No	Near column	Value between μ +2σ and μ +σ	1.00	N/A
M2-F2-LRHA	393	No	Near shear wall	Value between μ +2σ and μ +σ	1.17	N/A
M2-F3-LRHA	384	No	Near column	Value between μ +2σ and μ +σ	1.02	N/A
M3-F11-LRHA	386	No	Near shear wall	Value between μ +2σ and μ +σ	1.05	N/A

S22-Bottom-Max-Story 2-LEP and LDP μ = 312 psi σ = 50 psi

Model Number-Diaphragm Location-Diaphragm Design Force Procedures	Stress at Story 2 (psi)	Stress value over Modulus of Rupture	Location	Data points Location in Normal distribution curve/Bell curve/Gaussian distribution	Z-Score	Reference figure
M2-F2-LRHA	379	No	Near shear wall	Value between μ +2σ and μ +σ	1.33	N/A
M2-F5-LRHA	371	No	Near column	Value between μ +2σ and μ +σ	1.17	N/A
M2-F3-LRHA	370	No	Near column	Value between μ +2σ and μ +σ	1.15	N/A
M5-F14-LRHA	378	No	Near shear wall	Value between μ +2σ and μ +σ	1.31	N/A
M5-F15-LRHA	369	No	Near column	Value between μ +2σ and μ +σ	1.13	N/A
M5-F17-LRHA	369	No	Near column	Value between μ +2σ and μ +σ	1.13	N/A
M9-F37-LRHA	372	No	Near column	Value between μ +2σ and μ +σ	1.19	N/A
M9-F25-LRHA	370	No	Near column	Value between μ +2σ and μ +σ	1.16	N/A
M9-F28-LRHA	370	No	Near column	Value between μ +2σ and μ +σ	1.16	N/A
M8-F31-LRHA	370	No	Near column	Value between μ +2σ and μ +σ	1.16	N/A
M3-F11-LRHA	365	No	Near shear wall	Value between μ +2σ and μ +σ	1.07	N/A

S22-Bottom-Max-Story 1-LEP and LDP μ = 312 psi σ = 53 psi

Model Number-Diaphragm Location-Diaphragm Design Force Procedures	Stress at Story 1 (psi)	Stress value over Modulus of Rupture	Location	Data points Location in Normal distribution curve/Bell curve/Gaussian distribution	Z-Score	Reference figure
M9-F37-LRHA	376	No	Near column	Value between μ +2σ and μ +σ	1.20	N/A
M9-F25-LRHA	373	No	Near column	Value between μ +2σ and μ +σ	1.15	N/A
M9-F28-LRHA	373	No	Near column	Value between μ +2σ and μ +σ	1.15	N/A
M8-F31-LRHA	376	No	Near column	Value between μ +2σ and μ +σ	1.20	N/A
M2-F2-LRHA	375	No	Near shear wall	Value between μ +2σ and μ +σ	1.19	N/A
M2-F5-LRHA	372	No	Near column	Value between μ +2σ and μ +σ	1.12	N/A
M2-F3-LRHA	365	No	Near column	Value between μ +2σ and μ +σ	1.00	N/A
M5-F14-LRHA	374	No	Near shear wall	Value between μ +2σ and μ +σ	1.17	N/A
M5-F17-LRHA	371	No	Near column	Value between μ +2σ and μ +σ	1.11	N/A

Table 4-14 Minimum S22 in-plane flexural stress at the top of layered shells from diaphragm design force procedures at stories of models

S22-Top-Min-Story 3-LEP and LDP μ = -328 psi σ = 66 psi

Model Number-Diaphragm Location-Diaphragm Design Force Procedures	Stress at Story 3 (psi)	Location	Data points Location in Normal distribution curve/Bell curve/Gaussian distribution	Z-Score	Reference figure
M9-F37-LRHA	-405	Near column	Value is between μ - σ and μ -2σ	-1.17	N/A
M9-F25-LRHA	-397	Near column	Value is between μ - σ and μ -2σ	-1.05	N/A
M9-F28-LRHA	-397	Near column	Value is between μ - σ and μ -2σ	-1.05	N/A
M8-F31-LRHA	-401	Near column	Value is between μ - σ and μ -2σ	-1.12	N/A
M2-F2-LRHA	-398	Near shear wall	Value is between μ - σ and μ -2σ	-1.07	N/A
M2-F5-LRHA	-396	Near column	Value is between μ - σ and μ -2σ	-1.04	N/A
M5-F14-LRHA	-396	Near shear wall	Value is between μ - σ and μ -2σ	-1.04	N/A

S22-Top-Min-Story 2-LEP and LDP μ = -313 psi σ = 54 psi

Model Number-Diaphragm Location-Diaphragm Design Force Procedures	Stress at Story 2 (psi)	Location	Data points Location in Normal distribution curve/Bell curve/Gaussian distribution	Z-Score	Reference figure
M2-F2-LRHA	-380	Near shear wall	Value is between μ - σ and μ -2σ	-1.22	N/A
M2-F5-LRHA	-377	Near column	Value is between μ - σ and μ -2σ	-1.19	N/A
M2-F3-LRHA	-371	Near column	Value is between μ - σ and μ -2σ	-1.07	N/A
M5-F14-LRHA	-379	Near shear wall	Value is between μ - σ and μ -2σ	-1.21	N/A
M5-F17-LRHA	-373	Near column	Value is between μ - σ and μ -2σ	-1.11	N/A
M5-F15-LRHA	-370	Near column	Value is between μ - σ and μ -2σ	-1.05	N/A
M9-F25-LRHA	-375	Near column	Value is between μ - σ and μ -2σ	-1.14	N/A
M9-F28-LRHA	-375	Near column	Value is between μ - σ and μ -2σ	-1.13	N/A
M9-F37-LRHA	-371	Near column	Value is between μ - σ and μ -2σ	-1.06	N/A
M3-F11-LRHA	-368	Near shear wall	Value is between μ - σ and μ -2σ	-1.02	N/A

S22-Top-Min-Story 1-LEP and LDP μ = -313 psi σ = 58 psi

Model Number-Diaphragm Location-Diaphragm Design Force Procedures	Stress at Story 1 (psi)	Location	Data points Location in Normal distribution curve/Bell curve/Gaussian distribution	Z-Score	Reference figure
M9-F25-LRHA	-378	Near column	Value is between μ - σ and μ -2σ	-1.14	N/A
M9-F28-LRHA	-377	Near column	Value is between μ - σ and μ -2σ	-1.12	N/A
M9-F37-LRHA	-373	Near column	Value is between μ - σ and μ -2σ	-1.05	N/A
M2-F5-LRHA	-376	Near column	Value is between μ - σ and μ -2σ	-1.10	N/A
M2-F2-LRHA	-376	Near shear wall	Value is between μ - σ and μ -2σ	-1.09	N/A
M5-F14-LRHA	-375	Near shear wall	Value is between μ - σ and μ -2σ	-1.08	N/A
M8-F31-LRHA	-374	Near column	Value is between μ - σ and μ -2σ	-1.07	N/A

Table 4-15 Minimum S22 in-plane flexural stress at the bottom of layered shells from diaphragm design force procedures at stories of models

S22-Bottom-Min-Story 3-LEP and LDP μ = -283 psi σ = 135 psi

Model Number-Diaphragm Location-Diaphragm Design Force Procedures	Stress at Story 3 (psi)	Location	Data points Location in Normal distribution curve/Bell curve/Gaussian distribution	Z-Score	Reference figure
M2-F6-LRHA	-511	Near column	Value is between μ - σ and μ -2σ	-1.69	N/A
M2-F2-LRHA	-501	Near shear wall	Value is between μ - σ and μ -2σ	-1.61	N/A
M2-F3-LRHA	-443	Near column	Value is between μ - σ and μ -2σ	-1.19	N/A
M5-F18-ELFA Method-2	-454	Near column	Value is between μ - σ and μ -2σ	-1.27	N/A
M3-F12-LRHA	-430	Near column	Value is between μ - σ and μ -2σ	-1.09	N/A
M8-F32-ELFA Method-2	-428	Near shear wall	Value is between μ - σ and μ -2σ	-1.07	N/A

S22-Bottom-Min-Story 2-LEP and LDP μ = -290 psi σ = 121 psi

Model Number-Diaphragm Location-Diaphragm Design Force Procedures	Stress at Story 2 (psi)	Location	Data points Location in Normal distribution curve/Bell curve/Gaussian distribution	Z-Score	Reference figure
M2-F6-ELFA Method-2	-457	Near column	Value is between μ - σ and μ -2σ	-1.39	N/A
M2-F2-LRHA	-414	Near shear wall	Value is between μ - σ and μ -2σ	-1.03	N/A
M5-F18-ELFA Method-2	-439	Near column	Value is between μ - σ and μ -2σ	-1.24	N/A
M3-F12-ELFA Method-2	-437	Near column	Value is between μ - σ and μ -2σ	-1.22	N/A
M3-F8-ELFA Method-2	-412	Near column	Value is between μ - σ and μ -2σ	-1.02	N/A
M6-F24-RSA Method-2	-418	Near column	Value is between μ - σ and μ -2σ	-1.06	N/A

S22-Bottom-Min-Story 1-LEP and LDP μ = -277 psi σ = 124 psi

Model Number-Diaphragm Location-Diaphragm Design Force Procedures	Stress at Story 1 (psi)	Location	Data points Location in Normal distribution curve/Bell curve/Gaussian distribution	Z-Score	Reference figure
M2-F6-ELFA Method-2	-458	Near column	Value is between μ - σ and μ -2σ	-1.46	N/A
M5-F18-ELFA Method-2	-443	Near column	Value is between μ - σ and μ -2σ	-1.34	N/A
M3-F12-ELFA Method-2	-433	Near column	Value is between μ - σ and μ -2σ	-1.26	N/A
M3-F8-RSA Method-2	-405	Near column	Value is between μ - σ and μ -2σ	-1.04	N/A
M6-F24-RSA Method-2	-422	Near column	Value is between μ - σ and μ -2σ	-1.17	N/A
M6-F20-RSA Method-2	-401	Near column	Value is between μ - σ and μ -2σ	-1.00	N/A
M9-F27-LRHA	-410	Near column	Value is between μ - σ and μ -2σ	-1.07	N/A
M9-F26-ELFA Method-2	-405	Near column	Value is between μ - σ and μ -2σ	-1.04	N/A

Table 4-16 Maximum S22 in-plane flexural stress at the top of layered shells from Pushover analyses at stories of models

S22-Top-Max-Story 3-NSP μ = 47 psi σ = 39 psi

Model Number-Diaphragm Location-Diaphragm Design Force Procedures	Stress at Story 3 (psi)	Stress value over Modulus of Rupture	Location	Data points Location in Normal distribution curve/Bell curve/Gaussian distribution	Z-Score	Reference figure
M2-F1-PushY-1.5XTg	219	No	Near shear wall	Value Greater than μ +3σ	4.40	N/A
M2-F4-PushY-1.5XTg	186	No	Near column	Value Greater than μ +3σ	3.56	N/A
M2-F5-Push-30%X+100%Y	151	No	Near column	Value between μ +3σ and μ +2σ	2.66	N/A
M5-F13-Push-30%X+100%Y	208	No	Near shear wall	Value Greater than μ +3σ	4.11	N/A
M5-F16-PushY-1.5XTg	190	No	Near column	Value Greater than μ +3σ	3.66	N/A
M5-F17-Push-30%X+100%Y	154	No	Near column	Value between μ +3σ and μ +2σ	2.73	N/A
M8-F31-PushY-1.5XTg	153	No	Near column	Value between μ +3σ and μ +2σ	2.72	N/A
M9-F30-Push-30%X+100%Y	152	No	Near column	Value between μ +3σ and μ +2σ	2.68	N/A
M9-F33-PushY-1.5XTg	151	No	Near shear wall	Value between μ +3σ and μ +2σ	2.65	N/A
M9-F25-PushY-1.5XTg	137	No	Near column	Value between μ +3σ and μ +2σ	2.29	N/A
M9-F27-PushY-1.5XTg	130	No	Near column	Value between μ +3σ and μ +2σ	2.13	N/A
M9-F38-PushY-1.5XTg	127	No	Near shear wall	Value between μ +3σ and μ +2σ	2.03	N/A
M9-F37-Push-30%X+100%Y	90	No	Near column	Value between μ +2σ and μ +σ	1.09	N/A
M3-F9-PushY-1.5XTg	100	No	Near column	Value between μ +2σ and μ +σ	1.36	N/A

S22-Top-Max-Story 2-NSP μ = 45 psi σ = 41 psi

Model Number-Diaphragm Location-Diaphragm Design Force Procedures	Stress at Story 2 (psi)	Stress value over Modulus of Rupture	Location	Data points Location in Normal distribution curve/Bell curve/Gaussian distribution	Z-Score	Reference figure
M2-F1-Push-30%X+100%Y	315	No	Near shear wall	Value Greater than μ +3σ	6.56	N/A
M2-F4-PushY-1.5XTg	176	No	Near column	Value Greater than μ +3σ	3.19	N/A
M5-F13-Push-30%X+100%Y	288	No	Near shear wall	Value Greater than μ +3σ	5.92	N/A
M5-F16-Push-30%X+100%Y	100	No	Near column	Value between μ +2σ and μ +σ	1.34	N/A
M9-F33-PushY-1.5XTg	157	No	Near shear wall	Value between μ +3σ and μ +2σ	2.72	N/A
M9-F25-PushY-1.5XTg	147	No	Near column	Value between μ +3σ and μ +2σ	2.49	N/A
M9-F30-Push-30%X+100%Y	145	No	Near column	Value between μ +3σ and μ +2σ	2.44	N/A
M9-F27-PushY-1.5XTg	106	No	Near column	Value between μ +2σ and μ +σ	1.49	N/A
M9-F38-PushY-1.5XTg	95	No	Near shear wall	Value between μ +2σ and μ +σ	1.23	N/A
M8-F31-PushY-1.5XTg	155	No	Near column	Value between μ +3σ and μ +2σ	2.68	N/A
M3-F9-PushY-1.5XTg	109	No	Near column	Value between μ +2σ and μ +σ	1.56	N/A

S22-Top-Max-Story 1-NSP μ = 33 psi σ = 19 psi

Model Number-Diaphragm Location-Diaphragm Design Force Procedures	Stress at Story 1 (psi)	Stress value over Modulus of Rupture	Location	Data points Location in Normal distribution curve/Bell curve/Gaussian distribution	Z-Score	Reference figure
M5-F13-Push-30%X+100%Y	139	No	Near shear wall	Value Greater than μ +3σ	5.68	N/A
M5-F18-Push-30%X+100%Y	64	No	Near column	Value between μ +2σ and μ +σ	1.68	N/A
M5-F14-Push-30%X+100%Y	54	No	Near shear wall	Value between μ +2σ and μ +σ	1.13	N/A
M2-F1-PushY-1.5XTg	135	No	Near shear wall	Value Greater than μ +3σ	5.46	N/A
M2-F2-PushY-1.5XTg	98	No	Near shear wall	Value Greater than μ +3σ	3.50	N/A
M2-F4-PushY-1.5XTg	89	No	Near column	Value Greater than μ +3σ	3.01	N/A
M2-F5-PushY-1.5XTg	71	No	Near column	Value between μ +3σ and μ +2σ	2.03	N/A
M2-F6-Push-30%X+100%Y	66	No	Near column	Value between μ +2σ and μ +σ	1.77	N/A
M9-F33-PushY-1.5XTg	88	No	Near shear wall	Value between μ +3σ and μ +2σ	2.94	N/A
M9-F30-Push-30%X+100%Y	81	No	Near column	Value between μ +3σ and μ +2σ	2.56	N/A
M9-F26-PushY-1.5XTg	53	No	Near column	Value between μ +2σ and μ +σ	1.05	N/A

Table 4-17 Maximum S22 in-plane flexural stress at the bottom of layered shells from Pushover analyses at stories of models

S22-Bottom-Max-Story 3-NSP μ = 39 psi σ = 24 psi

Model Number-Diaphragm Location-Diaphragm Design Force Procedures	Stress at Story 3 (psi)	Stress value over Modulus of Rupture	Location	Data points Location in Normal distribution curve/Bell curve/Gaussian distribution	Z-Score	Reference figure
M9-F41-Push-30%X+100%Y	102	No	Near shear wall	Value between μ +3σ and μ +2σ	2.66	N/A
M9-F42-Push-100%X+30%Y	97	No	Near shear wall	Value between μ +3σ and μ +2σ	2.46	N/A
M9-F26-PushY-1.5XTg	85	No	Near column	Value between μ +2σ and μ +σ	1.95	N/A
M9-F25-PushY-1.5XTg	79	No	Near column	Value between μ +2σ and μ +σ	1.69	N/A
M9-F28-PushY-1.5XTg	69	No	Near column	Value between μ +2σ and μ +σ	1.25	N/A
M9-F37-PushY-1.5XTg	68	No	Near column	Value between μ +2σ and μ +σ	1.24	N/A
M9-F27-PushY-1.5XTg	65	No	Near column	Value between μ +2σ and μ +σ	1.09	N/A
M6-F24-PushY-1.5XTg	97	No	Near column	Value between μ +3σ and μ +2σ	2.47	N/A
M6-F23-Push-30%X+100%Y	82	No	Near shear wall	Value between μ +2σ and μ +σ	1.84	N/A
M3-F12-PushY-1.5XTg	94	No	Near column	Value between μ +3σ and μ +2σ	2.33	N/A
M3-F11-Push-30%X+100%Y	80	No	Near shear wall	Value between μ +2σ and μ +σ	1.74	N/A
M8-F36-Push-30%X+100%Y	85	No	Near shear wall	Value between μ +2σ and μ +σ	1.96	N/A
M8-F31-PushY-1.5XTg	78	No	Near column	Value between μ +2σ and μ +σ	1.63	N/A
M8-F40-PushY-1.5XTg	70	No	Near shear wall	Value between μ +2σ and μ +σ	1.31	N/A
M8-F32-PushY-1.5XTg	67	No	Near shear wall	Value between μ +2σ and μ +σ	1.19	N/A
M5-F18-PushY-1.5XTg	80	No	Near column	Value between μ +2σ and μ +σ	1.75	N/A
M5-F13-PushY-1.5XTg	70	No	Near shear wall	Value between μ +2σ and μ +σ	1.31	N/A

S22-Bottom-Max-Story 2-NSP μ = 38 psi σ = 24 psi

Model Number-Diaphragm Location-Diaphragm Design Force Procedures	Stress at Story 2 (psi)	Stress value over Modulus of Rupture	Location	Data points Location in Normal distribution curve/Bell curve/Gaussian distribution	Z-Score	Reference figure
M3-F11-Push-30%X+100%Y	96	No	Near shear wall	Value between μ +3σ and μ +2σ	2.50	N/A
M3-F12-PushY-1.5XTg	82	No	Near column	Value between μ +2σ and μ +σ	1.91	N/A
M3-F10-PushY-1.5XTg	82	No	Near column	Value between μ +2σ and μ +σ	1.91	N/A
M3-F7-PushY-1.5XTg	66	No	Near shear wall	Value between μ +2σ and μ +σ	1.22	N/A
M6-F23-Push-30%X+100%Y	96	No	Near shear wall	Value between μ +3σ and μ +2σ	2.49	N/A
M6-F24-Push-30%X+100%Y	74	No	Near column	Value between μ +2σ and μ +σ	1.56	N/A
M6-F19-PushY-1.5XTg	67	No	Near shear wall	Value between μ +2σ and μ +σ	1.28	N/A
M6-F22-PushY-1.5XTg	64	No	Near column	Value between μ +2σ and μ +σ	1.16	N/A
M9-F42-Push-30%X+100%Y	93	No	Near shear wall	Value between μ +3σ and μ +2σ	2.37	N/A
M9-F26-PushY-1.5XTg	87	No	Near column	Value between μ +3σ and μ +2σ	2.15	N/A
M9-F41-Push-30%X+100%Y	77	No	Near shear wall	Value between μ +2σ and μ +σ	1.71	N/A
M9-F37-PushY-1.5XTg	71	No	Near column	Value between μ +2σ and μ +σ	1.46	N/A
M9-F28-PushY-1.5XTg	71	No	Near column	Value between μ +2σ and μ +σ	1.43	N/A
M8-F36-PushY-1.5XTg	80	No	Near shear wall	Value between μ +2σ and μ +σ	1.84	N/A
M8-F31-PushY-1.5XTg	72	No	Near column	Value between μ +2σ and μ +σ	1.49	N/A
M8-F32-Push-30%X+100%Y	71	No	Near shear wall	Value between μ +2σ and μ +σ	1.45	N/A
M5-F13-PushY-1.5XTg	76	No	Near shear wall	Value between μ +2σ and μ +σ	1.66	N/A
M5-F18-PushY-1.5XTg	71	No	Near column	Value between μ +2σ and μ +σ	1.44	N/A
M2-F1-Push-30%X+100%Y	77	No	Near shear wall	Value between μ +2σ and μ +σ	1.72	N/A
M2-F6-Push-30%X+100%Y	68	No	Near column	Value between μ +2σ and μ +σ	1.29	N/A
M2-F2-Push-100%X+30%Y	66	No	Near shear wall	Value between μ +2σ and μ +σ	1.25	N/A
M2-F5-Push-100%X+30%Y	63	No	Near column	Value between μ +2σ and μ +σ	1.10	N/A

S22-Bottom-Max-Story 1-NSP μ = 29 psi σ = 19 psi

Model Number-Diaphragm Location-Diaphragm Design Force Procedures	Stress at Story 1 (psi)	Stress value over Modulus of Rupture	Location	Data points Location in Normal distribution curve/Bell curve/Gaussian distribution	Z-Score	Reference figure
M9-F42-PushY-1.5XTg	92	No	Near shear wall	Value Greater than μ +3σ	3.25	N/A
M9-F37-PushY-1.5XTg	64	No	Near column	Value between μ +2σ and μ +σ	1.80	N/A
M9-F28-PushY-1.5XTg	60	No	Near column	Value between μ +2σ and μ +σ	1.62	N/A
M9-F26-PushY-1.5XTg	53	No	Near column	Value between μ +2σ and μ +σ	1.24	N/A
M8-F36-Push-30%X+100%Y	76	No	Near shear wall	Value between μ +3σ and μ +2σ	2.46	N/A
M8-F31-PushY-1.5XTg	64	No	Near column	Value between μ +2σ and μ +σ	1.83	N/A
M8-F33-Push-30%X+100%Y	57	No	Near shear wall	Value between μ +2σ and μ +σ	1.45	N/A
M2-F1-PushY-1.5XTg	72	No	Near shear wall	Value between μ +3σ and μ +2σ	2.25	N/A
M2-F5-PushY-1.5XTg	67	No	Near column	Value between μ +2σ and μ +σ	1.99	N/A
M2-F6-Push-30%X+100%Y	67	No	Near column	Value between μ +2σ and μ +σ	1.97	N/A
M2-F3-PushY-1.5XTg	56	No	Near column	Value between μ +2σ and μ +σ	1.41	N/A
M3-F11-Push-30%X+100%Y	70	No	Near shear wall	Value between μ +3σ and μ +2σ	2.15	N/A
M3-F7-PushY-1.5XTg	66	No	Near shear wall	Value between μ +2σ and μ +σ	1.90	N/A
M3-F10-PushY-1.5XTg	52	No	Near column	Value between μ +2σ and μ +σ	1.19	N/A
M5-F18-Push-30%X+100%Y	69	No	Near column	Value between μ +3σ and μ +2σ	2.08	N/A
M5-F13-Push-30%X+100%Y	64	No	Near shear wall	Value between μ +2σ and μ +σ	1.81	N/A
M5-F17-Push-100%X+30%Y	59	No	Near column	Value between μ +2σ and μ +σ	1.58	N/A
M6-F19-PushY-1.5XTg	67	No	Near shear wall	Value between μ +2σ and μ +σ	1.98	N/A
M6-F23-PushY-1.5XTg	61	No	Near shear wall	Value between μ +2σ and μ +σ	1.68	N/A

Table 4-18 Minimum S22 in-plane flexural stress at the top of layered shells from Pushover analyses at stories of models

S22-Top-Min-Story 3-NSP μ = -386 psi σ = 141 psi

Model Number-Diaphragm Location-Diaphragm Design Force Procedures	Stress at Story 3 (psi)	Location	Data points Location in Normal distribution curve/Bell curve/Gaussian distribution	Z-Score	Reference figure
M5-F13-PushY-1.5XTg	-1236	Near shear wall	Value is less than μ -3σ	-6.01	Figure 4-65
M5-F14-Push-30%X+100%Y	-640	Near shear wall	Value is between μ - σ and μ -2σ	-1.79	N/A
M2-F1-PushY-1.5XTg	-1222	Near shear wall	Value is less than μ -3σ	-5.91	Figure 4-64
M2-F2-PushY-1.5XTg	-710	Near shear wall	Value between μ -2σ and μ -3σ	-2.29	Figure 4-66
M2-F3-PushY-1.5XTg	-543	Near column	Value is between μ - σ and μ -2σ	-1.11	N/A
M9-F30-PushY-1.5XTg	-880	Near column	Value is less than μ -3σ	-3.49	Figure 4-67
M9-F33-PushY-1.5XTg	-742	Near shear wall	Value between μ -2σ and μ -3σ	-2.52	Figure 4-68
M9-F34-PushY-1.5XTg	-610	Near shear wall	Value is between μ - σ and μ -2σ	-1.58	N/A
M9-F29-PushY-1.5XTg	-562	Near column	Value is between μ - σ and μ -2σ	-1.24	N/A

S22-Top-Min-Story 2 -NSP μ = -363 psi σ = 95 psi

Model Number-Diaphragm Location-Diaphragm Design Force Procedures	Stress at Story 2 (psi)	Location	Data points Location in Normal distribution curve/Bell curve/Gaussian distribution	Z-Score	Reference figure
M2-F1-Push-30%X+100%Y	-848	Near shear wall	Value is less than μ -3σ	-5.11	Figure 4-64
M2-F2-PushY-1.5XTg	-741	Near shear wall	Value is less than μ -3σ	-3.98	Figure 4-66
M2-F4-PushY-1.5XTg	-581	Near column	Value between μ -2σ and μ -3σ	-2.30	N/A
M2-F3-PushY-1.5XTg	-520	Near column	Value is between μ - σ and μ -2σ	-1.65	N/A
M5-F13-Push-30%X+100%Y	-767	Near shear wall	Value is less than μ -3σ	-4.26	Figure 4-65
M5-F14-Push-30%X+100%Y	-541	Near shear wall	Value is between μ - σ and μ -2σ	-1.88	N/A
M9-F30-PushY-1.5XTg	-674	Near column	Value is less than μ -3σ	-3.28	Figure 4-67
M9-F33-PushY-1.5XTg	-649	Near shear wall	Value is less than μ -3σ	-3.02	Figure 4-68
M9-F34-PushY-1.5XTg	-469	Near shear wall	Value is between μ - σ and μ -2σ	-1.13	N/A
M9-F29-PushY-1.5XTg	-465	Near column	Value is between μ - σ and μ -2σ	-1.08	N/A
M9-F37-Push-30%X+100%Y	-459	Near column	Value is between μ - σ and μ -2σ	-1.02	N/A

S22-Top-Min-Story 1-NSP μ = -344 psi σ = 66 psi

Model Number-Diaphragm Location-Diaphragm Design Force Procedures	Stress at Story 1 (psi)	Location	Data points Location in Normal distribution curve/Bell curve/Gaussian distribution	Z-Score	Reference figure
M2-F2-PushY-1.5XTg	-646	Near shear wall	Value is less than μ -3σ	-4.61	Figure 4-66
M2-F1-PushY-1.5XTg	-466	Near shear wall	Value is between μ - σ and μ -2σ	-1.87	Figure 4-64
M9-F37-PushY-1.5XTg	-448	Near column	Value is between μ - σ and μ -2σ	-1.60	N/A
M9-F28-Push-100%X+30%Y	-433	Near column	Value is between μ - σ and μ -2σ	-1.36	N/A
M9-F25-Push-100%X+30%Y	-430	Near column	Value is between μ - σ and μ -2σ	-1.31	N/A
M5-F14-Push-100%X+30%Y	-431	Near shear wall	Value is between μ - σ and μ -2σ	-1.33	N/A
M8-F31-Push-100%X+30%Y	-424	Near column	Value is between μ - σ and μ -2σ	-1.22	N/A
M3-F7-PushY-1.5XTg	-420	Near shear wall	Value is between μ - σ and μ -2σ	-1.16	N/A
M3-F11-PushY-1.5XTg	-418	Near shear wall	Value is between μ - σ and μ -2σ	-1.13	N/A
M6-F23-PushY-1.5XTg	-420	Near shear wall	Value is between μ - σ and μ -2σ	-1.16	N/A
M6-F19-PushY-1.5XTg	-420	Near shear wall	Value is between μ - σ and μ -2σ	-1.16	N/A

Table 4-19 Minimum S22 in-plane flexural stress at the bottom of layered shells from Pushover analyses at stories of models

S22-Bottom-Min-Story 3-NSP μ = -431 psi σ = 189 psi

Model Number-Diaphragm Location-Diaphragm Design Force Procedures	Stress at Story 3 (psi)	Location	Data points Location in Normal distribution curve/Bell curve/Gaussian distribution	Z-Score	Reference figure
M5-F13-PushY-1.5XTg	-1239	Near shear wall	Value is less than μ -3σ	-4.29	Figure 4-70
M5-F16-PushY-1.5XTg	-668	Near column	Value is between μ - σ and μ -2σ	-1.26	N/A
M5-F17-Push-30%X+100%Y	-653	Near column	Value is between μ - σ and μ -2σ	-1.18	N/A
M2-F1-PushY-1.5XTg	-1221	Near shear wall	Value is less than μ -3σ	-4.19	Figure 4-71
M2-F5-PushY-1.5XTg	-744	Near column	Value is between μ - σ and μ -2σ	-1.66	Figure 4-74
M2-F4-PushY-1.5XTg	-653	Near column	Value is between μ - σ and μ -2σ	-1.18	N/A
M9-F30-PushY-1.5XTg	-1159	Near column	Value is less than μ -3σ	-3.86	Figure 4-72
M9-F33-PushY-1.5XTg	-856	Near shear wall	Value between μ -2σ and μ -3σ	-2.26	Figure 4-73
M9-F25-PushY-1.5XTg	-740	Near column	Value is between μ - σ and μ -2σ	-1.64	N/A
M9-F34-PushY-1.5XTg	-734	Near shear wall	Value is between μ - σ and μ -2σ	-1.61	N/A
M9-F27-PushY-1.5XTg	-725	Near column	Value is between μ - σ and μ -2σ	-1.56	N/A
M9-F38-PushY-1.5XTg	-699	Near shear wall	Value is between μ - σ and μ -2σ	-1.43	N/A
M9-F41-PushY-1.5XTg	-660	Near shear wall	Value is between μ - σ and μ -2σ	-1.21	N/A
M8-F31-PushY-1.5XTg	-845	Near column	Value between μ -2σ and μ -3σ	-2.20	N/A
M8-F35-PushY-1.5XTg	-704	Near shear wall	Value is between μ - σ and μ -2σ	-1.45	N/A
M3-F9-PushY-1.5XTg	-720	Near column	Value is between μ - σ and μ -2σ	-1.54	N/A

S22-Bottom-Min-Story 2 -NSP μ = -426 psi σ = 198 psi

Model Number-Diaphragm Location-Diaphragm Design Force Procedures	Stress at Story 2 (psi)	Location	Data points Location in Normal distribution curve/Bell curve/Gaussian distribution	Z-Score	Reference figure
M2-F1-PushY-1.5XTg	-1896	Near shear wall	Value is less than μ -3σ	-7.43	Figure 4-71
M2-F5-PushY-1.5XTg	-934	Near column	Value between μ -2σ and μ -3σ	-2.57	Figure 4-74
M5-F13-PushY-1.5XTg	-1265	Near shear wall	Value is less than μ -3σ	-4.24	Figure 4-70
M5-F17-Push-30%X+100%Y	-682	Near column	Value is between μ - σ and μ -2σ	-1.30	N/A
M9-F30-PushY-1.5XTg	-917	Near column	Value between μ -2σ and μ -3σ	-2.48	Figure 4-72
M9-F33-PushY-1.5XTg	-804	Near shear wall	Value is between μ - σ and μ -2σ	-1.91	Figure 4-73
M9-F25-PushY-1.5XTg	-692	Near column	Value is between μ - σ and μ -2σ	-1.35	N/A
M9-F27-PushY-1.5XTg	-649	Near column	Value is between μ - σ and μ -2σ	-1.13	N/A
M8-F31-PushY-1.5XTg	-793	Near column	Value is between μ - σ and μ -2σ	-1.85	N/A
M3-F9-PushY-1.5XTg	-768	Near column	Value is between μ - σ and μ -2σ	-1.73	N/A

S22-Bottom-Min-Story 1-NSP μ = -373 psi σ = 143 psi

Model Number-Diaphragm Location-Diaphragm Design Force Procedures	Stress at Story 1 (psi)	Location	Data points Location in Normal distribution curve/Bell curve/Gaussian distribution	Z-Score	Reference figure
M2-F1-PushY-1.5XTg	-1419	Near shear wall	Value is less than μ -3σ	-7.30	Figure 4-71
M2-F5-PushY-1.5XTg	-762	Near column	Value between μ -2σ and μ -3σ	-2.72	Figure 4-74
M5-F13-PushY-1.5XTg	-801	Near shear wall	Value between μ -2σ and μ -3σ	-2.99	Figure 4-70
M5-F17-Push-30%X+100%Y	-535	Near column	Value is between μ - σ and μ -2σ	-1.13	N/A
M9-F27-PushY-1.5XTg	-559	Near column	Value is between μ - σ and μ -2σ	-1.30	N/A
M8-F35-PushY-1.5XTg	-538	Near shear wall	Value is between μ - σ and μ -2σ	-1.15	N/A
M8-F31-PushY-1.5XTg	-535	Near column	Value is between μ - σ and μ -2σ	-1.13	N/A

Table 4-20 Maximum S12 in-plane shear stress at the top of layered shells from Diaphragm force procedures at Stories of models

S12-Top-Max-Story 3-LEP and LDP μ = 90 psi σ = 79 psi

Model Number-Diaphragm Location-Diaphragm Design Force Procedures	Stress at Story 3 (psi)	Shear reinforcement required or not	Change of Diaphragm section required or not	Location	Data points Location in Normal distribution curve/Bell curve/Gaussian distribution	Z-Score	Reference figure
M9-F41-LRHA	440	Yes	Yes	Near shear wall	Value Greater than μ +3σ	4.45	Figure 4-75
M9-F42-ELFA Method-2	412	Yes	Yes	Near shear wall	Value Greater than μ +3σ	4.09	Figure 4-76
M9-F34-LRHA	263	Yes	No	Near shear wall	Value between μ +3σ and μ +2σ	2.20	Figure 4-77
M9-F37-LRHA	246	Yes	No	Near column	Value between μ +2σ and μ +σ	1.99	N/A
M9-F28-LRHA	221	Yes	No	Near column	Value between μ +2σ and μ +σ	1.66	N/A
M9-F29-LRHA	190	Yes	No	Near column	Value between μ +2σ and μ +σ	1.27	N/A
M8-F36-LRHA	281	Yes	No	Near shear wall	Value between μ +3σ and μ +2σ	2.43	N/A
M8-F39-ELFA Method-2	211	Yes	No	Near shear wall	Value between μ +2σ and μ +σ	1.53	N/A
M8-F32-LRHA	197	Yes	No	Near shear wall	Value between μ +2σ and μ +σ	1.36	N/A
M3-F9-LRHA	188	Yes	No	Near column	Value between μ +2σ and μ +σ	1.25	N/A
M3-F11-LRHA	179	Yes	No	Near shear wall	Value between μ +2σ and μ +σ	1.13	N/A

S12-Top-Max-Story 2-LEP and LDP μ = 94 psi σ = 96 psi

Model Number-Diaphragm Location-Diaphragm Design Force Procedures	Stress at Story 2 (psi)	Shear reinforcement required or not	Change of Diaphragm section required or not	Location	Data points Location in Normal distribution curve/Bell curve/Gaussian distribution	Z-Score	Reference figure
M9-F42-ELFA Method-2	585	Yes	Yes	Near shear wall	Value Greater than μ +3σ	5.10	Figure 4-76
M9-F41-LRHA	555	Yes	Yes	Near shear wall	Value Greater than μ +3σ	4.80	Figure 4-75
M9-F37-LRHA	257	Yes	No	Near column	Value between μ +2σ and μ +σ	1.70	N/A
M9-F34-LRHA	240	Yes	No	Near shear wall	Value between μ +2σ and μ +σ	1.52	Figure 4-77
M9-F28-LRHA	220	Yes	No	Near column	Value between μ +2σ and μ +σ	1.31	N/A
M8-F36-LRHA	223	Yes	No	Near shear wall	Value between μ +2σ and μ +σ	1.35	N/A
M2-F5-LRHA	193	Yes	No	Near column	Value between μ +2σ and μ +σ	1.03	N/A

S12-Top-Max-Story 1-LEP and LDP μ = 80 psi σ = 87 psi

Model Number-Diaphragm Location-Diaphragm Design Force Procedures	Stress at Story 1 (psi)	Shear reinforcement required or not	Change of Diaphragm section required or not	Location	Data points Location in Normal distribution curve/Bell curve/Gaussian distribution	Z-Score	Reference figure
M9-F42-ELFA Method-2	509	Yes	Yes	Near shear wall	Value Greater than μ +3σ	4.96	Figure 4-76
M9-F41-ELFA Method-2	477	Yes	Yes	Near shear wall	Value Greater than μ +3σ	4.59	Figure 4-75
M9-F34-LRHA	220	Yes	No	Near shear wall	Value between μ +2σ and μ +σ	1.62	Figure 4-77
M9-F37-LRHA	215	Yes	No	Near column	Value between μ +2σ and μ +σ	1.57	N/A
M9-F28-RSA Method-2	183	Yes	No	Near column	Value between μ +2σ and μ +σ	1.19	N/A
M9-F26-LRHA	170	Yes	No	Near column	Value between μ +2σ and μ +σ	1.04	N/A
M9-F29-LRHA	168	Yes	No	Near column	Value between μ +2σ and μ +σ	1.02	N/A
M8-F36-ELFA Method-2	207	Yes	No	Near shear wall	Value between μ +2σ and μ +σ	1.47	N/A
M8-F39-RSA Method-2	184	Yes	No	Near shear wall	Value between μ +2σ and μ +σ	1.20	N/A
M8-F32-LRHA	169	Yes	No	Near shear wall	Value between μ +2σ and μ +σ	1.03	N/A
M2-F5-ELFA Method-2	179	Yes	No	Near column	Value between μ +2σ and μ +σ	1.15	N/A
M5-F17-ELFA Method-2	176	Yes	No	Near column	Value between μ +2σ and μ +σ	1.12	N/A

Table 4-21 Minimum S12 in-plane shear stress at the top of layered shells from Diaphragm force procedures at stories of models

S12-Top-Min-Story 3-LEP and LDP **μ = -99 psi** **σ = 91 psi**

Model Number-Diaphragm Location-Diaphragm Design Force Procedures	Stress at Story 3 (psi)	Shear reinforcement required or not	Change of Diaphragm section required or not	Location	Data points Location in Normal distribution curve/Bell curve/Gaussian distribution	Z-Score	Reference figure
M9-F42-LRHA	-463	Yes	Yes	Near shear wall	Value is less than μ -3σ	-3.99	Figure 4-83
M9-F41-LRHA	-457	Yes	Yes	Near shear wall	Value is less than μ -3σ	-3.93	Figure 4-82
M9-F33-LRHA	-258	Yes	No	Near shear wall	Value is between μ - σ and μ -2σ	-1.75	N/A
M9-F38-LRHA	-249	Yes	No	Near shear wall	Value is between μ - σ and μ -2σ	-1.65	N/A
M9-F25-LRHA	-223	Yes	No	Near column	Value is between μ - σ and μ -2σ	-1.37	N/A
M9-F30-LRHA	-192	Yes	No	Near column	Value is between μ - σ and μ -2σ	-1.02	N/A
M2-F6-LRHA	-287	Yes	No	Near column	Value between μ -2σ and μ -3σ	-2.06	Figure 4-84
M2-F3-LRHA	-261	Yes	No	Near column	Value is between μ - σ and μ -2σ	-1.78	N/A
M2-F2-LRHA	-217	Yes	No	Near shear wall	Value is between μ - σ and μ -2σ	-1.30	N/A
M8-F31-LRHA	-268	Yes	No	Near column	Value is between μ - σ and μ -2σ	-1.85	N/A
M8-F40-ELFA Method-2	-211	Yes	No	Near shear wall	Value is between μ - σ and μ -2σ	-1.23	N/A
M5-F18-LRHA	-242	Yes	No	Near column	Value is between μ - σ and μ -2σ	-1.57	N/A
M5-F15-LRHA	-222	Yes	No	Near column	Value is between μ - σ and μ -2σ	-1.35	N/A
M3-F12-LRHA	-218	Yes	No	Near column	Value is between μ - σ and μ -2σ	-1.31	N/A
M3-F10-LRHA	-211	Yes	No	Near column	Value is between μ - σ and μ -2σ	-1.23	N/A
M3-F7-LRHA	-194	Yes	No	Near shear wall	Value is between μ - σ and μ -2σ	-1.04	N/A

S12-Top-Min-Story 2 -LEP and LDP **μ = -98 psi** **σ = 88 psi**

Model Number-Diaphragm Location-Diaphragm Design Force Procedures	Stress at Story 2 (psi)	Shear reinforcement required or not	Change of Diaphragm section required or not	Location	Data points Location in Normal distribution curve/Bell curve/Gaussian distribution	Z-Score	Reference figure
M9-F42-LRHA	-432	Yes	Yes	Near shear wall	Value is less than μ -3σ	-3.83	Figure 4-83
M9-F41-LRHA	-427	Yes	Yes	Near shear wall	Value is less than μ -3σ	-3.78	Figure 4-82
M9-F33-LRHA	-233	Yes	No	Near shear wall	Value is between μ - σ and μ -2σ	-1.55	N/A
M9-F38-LRHA	-229	Yes	No	Near shear wall	Value is between μ - σ and μ -2σ	-1.50	N/A
M9-F25-LRHA	-222	Yes	No	Near column	Value is between μ - σ and μ -2σ	-1.42	N/A
M8-F31-LRHA	-269	Yes	No	Near column	Value is between μ - σ and μ -2σ	-1.96	N/A
M8-F40-ELFA Method-2	-190	Yes	No	Near shear wall	Value is between μ - σ and μ -2σ	-1.06	N/A
M2-F6-LRHA	-254	Yes	No	Near column	Value is between μ - σ and μ -2σ	-1.79	Figure 4-84
M2-F3-LRHA	-233	Yes	No	Near column	Value is between μ - σ and μ -2σ	-1.55	N/A
M2-F6-ELFA Method-1	-228	Yes	No	Near column	Value is between μ - σ and μ -2σ	-1.50	N/A
M2-F2-LRHA	-211	Yes	No	Near shear wall	Value is between μ - σ and μ -2σ	-1.30	N/A
M5-F18-LRHA	-224	Yes	No	Near column	Value is between μ - σ and μ -2σ	-1.45	N/A
M5-F15-LRHA	-207	Yes	No	Near column	Value is between μ - σ and μ -2σ	-1.26	N/A
M5-F14-LRHA	-190	Yes	No	Near shear wall	Value is between μ - σ and μ -2σ	-1.06	N/A
M3-F7-LRHA	-205	Yes	No	Near shear wall	Value is between μ - σ and μ -2σ	-1.23	N/A
M3-F10-LRHA	-194	Yes	No	Near column	Value is between μ - σ and μ -2σ	-1.10	N/A

S12-Top-Min-Story 1-LEP and LDP **μ = -86 psi** **σ = 83 psi**

Model Number-Diaphragm Location-Diaphragm Design Force Procedures	Stress at Story 1 (psi)	Shear reinforcement required or not	Change of Diaphragm section required or not	Location	Data points Location in Normal distribution curve/Bell curve/Gaussian distribution	Z-Score	Reference figure
M9-F42-LRHA	-421	Yes	Yes	Near shear wall	Value is less than μ -3σ	-4.03	Figure 4-83
M9-F41-LRHA	-416	Yes	Yes	Near shear wall	Value is less than μ -3σ	-3.96	Figure 4-82
M9-F33-LRHA	-215	Yes	No	Near shear wall	Value is between μ - σ and μ -2σ	-1.55	N/A
M9-F38-LRHA	-194	Yes	No	Near shear wall	Value is between μ - σ and μ -2σ	-1.30	N/A
M9-F25-ELFA Method-2	-184	Yes	No	Near column	Value is between μ - σ and μ -2σ	-1.18	N/A
M9-F27-LRHA	-170	Yes	No	Near column	Value is between μ - σ and μ -2σ	-1.02	N/A
M8-F31-LRHA	-226	Yes	No	Near column	Value is between μ - σ and μ -2σ	-1.68	N/A
M8-F40-ELFA Method-2	-186	Yes	No	Near shear wall	Value is between μ - σ and μ -2σ	-1.20	N/A
M2-F6-ELFA Method-2	-223	Yes	No	Near column	Value is between μ - σ and μ -2σ	-1.65	Figure 4-84
M2-F3-ELFA Method-2	-209	Yes	No	Near column	Value is between μ - σ and μ -2σ	-1.48	N/A
M2-F2-ELFA Method-2	-189	Yes	No	Near shear wall	Value is between μ - σ and μ -2σ	-1.24	N/A
M5-F18-LRHA	-208	Yes	No	Near column	Value is between μ - σ and μ -2σ	-1.48	N/A
M5-F15-LRHA	-193	Yes	No	Near column	Value is between μ - σ and μ -2σ	-1.28	N/A
M5-F14-LRHA	-180	Yes	No	Near shear wall	Value is between μ - σ and μ -2σ	-1.14	N/A
M3-F7-ELFA Method-2	-185	Yes	No	Near shear wall	Value is between μ - σ and μ -2σ	-1.20	N/A
M3-F10-ELFA Method-2	-182	Yes	No	Near column	Value is between μ - σ and μ -2σ	-1.15	N/A
M6-F19-LRHA	-177	Yes	No	Near shear wall	Value is between μ - σ and μ -2σ	-1.10	N/A

Table 4-22 Minimum S12 in-plane shear stress at the bottom of layered shells from Diaphragm force procedures at stories of models

S12-Bottom-Min-Story 3-LEP and LDP $\mu = 93$ psi $\sigma = 81$ psi

Model Number-Diaphragm Location-Diaphragm Design Force Procedures	Stress at Story 3 (psi)	Shear reinforcement required or not	Change of Diaphragm section required or not	Location	Data points Location in Normal distribution curve/Bell curve/Gaussian distribution	Z-Score	Reference figure
M9-F41-LRHA	-441	Yes	Yes	Near shear wall	Value is less than μ -3σ	-4.30	Figure 4-86
M9-F42-ELFA Method-2	-418	Yes	Yes	Near shear wall	Value is less than μ -3σ	-4.02	Figure 4-85
M9-F37-LRHA	-268	Yes	No	Near column	Value between μ -2σ and μ -3σ	-2.17	Figure 4-87
M9-F34-LRHA	-257	Yes	No	Near shear wall	Value between μ -2σ and μ -3σ	-2.02	N/A
M9-F28-LRHA	-246	Yes	No	Near column	Value is between μ - σ and μ -2σ	-1.89	N/A
M9-F29-LRHA	-200	Yes	No	Near column	Value is between μ - σ and μ -2σ	-1.32	N/A
M8-F36-LRHA	-271	Yes	No	Near shear wall	Value between μ -2σ and μ -3σ	-2.19	Figure 4-88
M8-F32-LRHA	-214	Yes	No	Near shear wall	Value is between μ - σ and μ -2σ	-1.49	N/A
M8-F39-ELFA Method-2	-196	Yes	No	Near shear wall	Value is between μ - σ and μ -2σ	-1.27	N/A
M3-F11-LRHA	-232	Yes	No	Near shear wall	Value is between μ - σ and μ -2σ	-1.72	N/A
M3-F9-LRHA	-196	Yes	No	Near column	Value is between μ - σ and μ -2σ	-1.27	N/A
M6--F23-LRHA	-203	Yes	No	Near shear wall	Value is between μ - σ and μ -2σ	-1.36	N/A

S12-Bottom-Min-Story 2 -LEP and LDP $\mu = -94$ psi $\sigma = 95$ psi

Model Number-Diaphragm Location-Diaphragm Design Force Procedures	Stress at Story 2 (psi)	Shear reinforcement required or not	Change of Diaphragm section required or not	Location	Data points Location in Normal distribution curve/Bell curve/Gaussian distribution	Z-Score	Reference figure
M9-F42-ELFA Method-2	-561	Yes	Yes	Near shear wall	Value is less than μ -3σ	-4.90	Figure 4-85
M9-F41-ELFA Method-2	-547	Yes	Yes	Near shear wall	Value is less than μ -3σ	-4.76	Figure 4-86
M9-F37-LRHA	-266	Yes	No	Near column	Value is between μ - σ and μ -2σ	-1.81	Figure 4-87
M9-F34-LRHA	-234	Yes	No	Near shear wall	Value is between μ - σ and μ -2σ	-1.48	N/A
M9-F28-LRHA	-232	Yes	No	Near column	Value is between μ - σ and μ -2σ	-1.45	N/A
M8-F36-ELFA Method-2	-218	Yes	No	Near shear wall	Value is between μ - σ and μ -2σ	-1.31	Figure 4-88
M3-F11-LRHA	-206	Yes	No	Near shear wall	Value is between μ - σ and μ -2σ	-1.18	N/A
M3-F9-LRHA	-191	Yes	No	Near column	Value is between μ - σ and μ -2σ	-1.02	N/A
M2-F5-LRHA	-196	Yes	No	Near column	Value is between μ - σ and μ -2σ	-1.08	N/A
M5-F17-ELFA Method-2	-189	Yes	No	Near column	Value is between μ - σ and μ -2σ	-1.01	N/A

S12-Bottom-Min-Story 1-LEP and LDP $\mu = -80$ psi $\sigma = 85$ psi

Model Number-Diaphragm Location-Diaphragm Design Force Procedures	Stress at Story 1 (psi)	Shear reinforcement required or not	Change of Diaphragm section required or not	Location	Data points Location in Normal distribution curve/Bell curve/Gaussian distribution	Z-Score	Reference figure
M9-F42-ELFA Method-2	-488	Yes	Yes	Near shear wall	Value is less than μ -3σ	-4.81	Figure 4-85
M9-F41-ELFA Method-2	-472	Yes	Yes	Near shear wall	Value is less than μ -3σ	-4.62	Figure 4-86
M9-F37-LRHA	-216	Yes	No	Near column	Value is between μ - σ and μ -2σ	-1.61	Figure 4-87
M9-F34-LRHA	-209	Yes	No	Near shear wall	Value is between μ - σ and μ -2σ	-1.53	N/A
M9-F28-LRHA	-188	Yes	No	Near column	Value is between μ - σ and μ -2σ	-1.27	N/A
M9-F29-LRHA	-166	Yes	No	Near column	Value is between μ - σ and μ -2σ	-1.02	N/A
M8-F36-ELFA Method-2	-199	Yes	No	Near shear wall	Value is between μ - σ and μ -2σ	-1.41	Figure 4-88
M8-F32-LRHA	-176	Yes	No	Near shear wall	Value is between μ - σ and μ -2σ	-1.13	N/A
M8-F39-ELFA Method-2	-171	Yes	No	Near shear wall	Value is between μ - σ and μ -2σ	-1.08	N/A
M2-F5-ELFA Method-2	-183	Yes	No	Near column	Value is between μ - σ and μ -2σ	-1.21	N/A
M5-F17-ELFA Method-2	-176	Yes	No	Near column	Value is between μ - σ and μ -2σ	-1.13	N/A
M3-F9-ELFA Method-2	-175	Yes	No	Near column	Value is between μ - σ and μ -2σ	-1.13	N/A
M3-F11-LRHA	-174	Yes	No	Near shear wall	Value is between μ - σ and μ -2σ	-1.11	N/A

Table 4-23 Maximum S12 in-plane shear stress at the top of layered shells from Pushover analyses at stories of models

S12-Top-Max-Story 3-NSP μ = 174 psi σ = 141 psi

Model Number-Diaphragm Location-Diaphragm Design Force Procedures	Stress at Story 3 (psi)	Shear reinforcement required or not	Change of Diaphragm section required or not	Location	Data points Location in Normal distribution curve/Bell curve/Gaussian distribution	Z-Score	Reference figure
M9-F33-PushY-1.5XTg	890	Yes	Yes	Near shear wall	Value Greater than μ +3σ	5.07	Figure 4-89
M9-F30-PushY-1.5XTg	837	Yes	Yes	Near column	Value Greater than μ +3σ	4.70	Figure 4-90
M9-F25-PushY-1.5XTg	636	Yes	Yes	Near column	Value Greater than μ +3σ	3.27	Figure 4-91
M9-F34-PushY-1.5XTg	593	Yes	Yes	Near shear wall	Value between μ +3σ and μ +2σ	2.97	Figure 4-92
M9-F29-PushY-1.5XTg	553	Yes	Yes	Near column	Value between μ +3σ and μ +2σ	2.69	Figure 4-93
M9-F38-PushY-1.5XTg	516	Yes	Yes	Near shear wall	Value between μ +3σ and μ +2σ	2.43	Figure 4-94
M9-F28-Push-30%X+100%Y	388	Yes	Yes	Near column	Value between μ +2σ and μ +σ	1.52	Figure 4-96
M9-F27-Push-30%X+100%Y	356	Yes	Yes	Near column	Value between μ +2σ and μ +σ	1.30	N/A
M9-F26-PushY-1.5XTg	317	Yes	Yes	Near column	Value between μ +2σ and μ +σ	1.02	N/A
M8-F31-PushY-1.5XTg	759	Yes	Yes	Near column	Value Greater than μ +3σ	4.15	Figure 4-95
M8-F36-PushY-1.5XTg	366	Yes	Yes	Near shear wall	Value between μ +2σ and μ +σ	1.36	N/A

S12-Top-Max-Story 2-NSP μ = 162 psi σ = 113 psi

Model Number-Diaphragm Location-Diaphragm Design Force Procedures	Stress at Story 2 (psi)	Shear reinforcement required or not	Change of Diaphragm section required or not	Location	Data points Location in Normal distribution curve/Bell curve/Gaussian distribution	Z-Score	Reference figure
M9-F33-PushY-1.5XTg	726	Yes	Yes	Near shear wall	Value Greater than μ +3σ	5.00	Figure 4-89
M9-F30-PushY-1.5XTg	652	Yes	Yes	Near column	Value Greater than μ +3σ	4.34	Figure 4-90
M9-F29-PushY-1.5XTg	476	Yes	Yes	Near column	Value between μ +3σ and μ +2σ	2.78	Figure 4-93
M9-F34-PushY-1.5XTg	466	Yes	Yes	Near shear wall	Value between μ +3σ and μ +2σ	2.69	Figure 4-92
M9-F25-Push-30%X+100%Y	403	Yes	Yes	Near column	Value between μ +3σ and μ +2σ	2.14	Figure 4-91
M9-F28-Push-30%X+100%Y	342	Yes	Yes	Near column	Value between μ +2σ and μ +σ	1.60	Figure 4-96
M9-F27-Push-30%X+100%Y	339	Yes	Yes	Near column	Value between μ +2σ and μ +σ	1.57	N/A
M9-F38-PushY-1.5XTg	336	Yes	Yes	Near shear wall	Value between μ +2σ and μ +σ	1.54	Figure 4-94
M9-F26-PushY-1.5XTg	302	Yes	No	Near column	Value between μ +2σ and μ +σ	1.24	N/A
M8-F31-PushY-1.5XTg	541	Yes	Yes	Near column	Value Greater than μ +3σ	3.36	Figure 4-95
M8-F36-PushY-1.5XTg	325	Yes	Yes	Near shear wall	Value between μ +2σ and μ +σ	1.45	N/A
M8-F32-PushY-1.5XTg	285	Yes	No	Near shear wall	Value between μ +2σ and μ +σ	1.09	N/A
M2-F1-Push-30%X+100%Y	305	Yes	Yes	Near shear wall	Value between μ +2σ and μ +σ	1.27	N/A

S12-Top-Max-Story 1-NSP μ = 130 psi σ = 72 psi

Model Number-Diaphragm Location-Diaphragm Design Force Procedures	Stress at Story 1 (psi)	Shear reinforcement required or not	Change of Diaphragm section required or not	Location	Data points Location in Normal distribution curve/Bell curve/Gaussian distribution	Z-Score	Reference figure
M9-F28-Push-30%X+100%Y	302	Yes	No	Near column	Value between μ +3σ and μ +2σ	2.38	Figure 4-96
M9-F34-PushY-1.5XTg	302	Yes	No	Near shear wall	Value between μ +3σ and μ +2σ	2.38	Figure 4-92
M9-F29-PushY-1.5XTg	292	Yes	No	Near column	Value between μ +3σ and μ +2σ	2.25	Figure 4-93
M9-F30-PushY-1.5XTg	291	Yes	No	Near column	Value between μ +3σ and μ +2σ	2.22	Figure 4-90
M9-F33-PushY-1.5XTg	284	Yes	No	Near shear wall	Value between μ +3σ and μ +2σ	2.13	Figure 4-89
M9-F27-Push-30%X+100%Y	252	Yes	No	Near column	Value between μ +2σ and μ +σ	1.68	N/A
M9-F25-PushY-1.5XTg	239	Yes	No	Near column	Value between μ +2σ and μ +σ	1.50	Figure 4-91
M9-F41-PushY-1.5XTg	227	Yes	No	Near shear wall	Value between μ +2σ and μ +σ	1.34	N/A
M9-F37-Push-100%X+30%Y	223	Yes	No	Near column	Value between μ +2σ and μ +σ	1.28	N/A
M9-F26-PushY-1.5XTg	218	Yes	No	Near column	Value between μ +2σ and μ +σ	1.21	N/A
M8-F36-Push-30%X+100%Y	272	Yes	No	Near shear wall	Value between μ +2σ and μ +σ	1.97	N/A
M8-F31-PushY-1.5XTg	236	Yes	No	Near column	Value between μ +2σ and μ +σ	1.47	Figure 4-95
M8-F32-Push-100%X+30%Y	225	Yes	No	Near shear wall	Value between μ +2σ and μ +σ	1.31	N/A
M8-F39-Push-100%X+30%Y	205	Yes	No	Near shear wall	Value between μ +2σ and μ +σ	1.04	N/A
M5-F17-PushY-1.5XTg	228	Yes	No	Near column	Value between μ +2σ and μ +σ	1.35	N/A
M5-F16-PushY-1.5XTg	211	Yes	No	Near column	Value between μ +2σ and μ +σ	1.11	N/A
M2-F5-PushY-1.5XTg	227	Yes	No	Near column	Value between μ +2σ and μ +σ	1.33	N/A
M2-F4-Push-30%X+100%Y	211	Yes	No	Near column	Value between μ +2σ and μ +σ	1.12	N/A
M6-F20-PushY-1.5XTg	219	Yes	No	Near column	Value between μ +2σ and μ +σ	1.23	N/A
M3-F8-PushY-1.5XTg	215	Yes	No	Near column	Value between μ +2σ and μ +σ	1.18	N/A

Table 4-24 Minimum S12 in-plane shear stress at the top of layered shells from Pushover analyses at stories of models

S12-Top-Min-Story 3-NSP μ = -207 psi σ = 160 psi

Model Number-Diaphragm Location-Diaphragm Design Force Procedures	Stress at Story 3 (psi)	Shear reinforcement required or not	Change of Diaphragm section required or not	Location	Data points Location in Normal distribution curve/Bell curve/Gaussian distribution	Z-Score	Reference figure
M5-F13-PushY-1.5XTg	-1183	Yes	Yes	Near shear wall	Value is less than μ -3σ	-6.11	Figure 4-105
M5-F14-PushY-1.5XTg	-470	Yes	Yes	Near shear wall	Value is between μ - σ and μ -2σ	-1.65	N/A
M5-F15-PushY-1.5XTg	-438	Yes	Yes	Near column	Value is between μ - σ and μ -2σ	-1.45	N/A
M5-F16-PushY-1.5XTg	-421	Yes	Yes	Near column	Value is between μ - σ and μ -2σ	-1.34	N/A
M2-F1-PushY-1.5XTg	-1177	Yes	Yes	Near shear wall	Value is less than μ -3σ	-6.08	Figure 4-106
M2-F2-PushY-1.5XTg	-527	Yes	Yes	Near shear wall	Value between μ -2σ and μ -3σ	-2.01	Figure 4-107
M2-F3-PushY-1.5XTg	-487	Yes	Yes	Near column	Value is between μ - σ and μ -2σ	-1.75	Figure 4-109
M2-F4-PushY-1.5XTg	-472	Yes	Yes	Near column	Value is between μ - σ and μ -2σ	-1.66	Figure 4-108
M2-F6-Push-100%X+30%Y	-391	Yes	Yes	Near column	Value is between μ - σ and μ -2σ	-1.16	Figure 4-110
M9-F37-Push-30%X+100%Y	-414	Yes	Yes	Near column	Value is between μ - σ and μ -2σ	-1.30	N/A

S12-Top-Min-Story 2-NSP μ = -189 psi σ = 129 psi

Model Number-Diaphragm Location-Diaphragm Design Force Procedures	Stress at Story 2 (psi)	Shear reinforcement required or not	Change of Diaphragm section required or not	Location	Data points Location in Normal distribution curve/Bell curve/Gaussian distribution	Z-Score	Reference figure
M2-F1-PushY-1.5XTg	-886	Yes	Yes	Near shear wall	Value is less than μ -3σ	-5.40	Figure 4-106
M2-F2-PushY-1.5XTg	-551	Yes	Yes	Near shear wall	Value between μ -2σ and μ -3σ	-2.80	Figure 4-107
M2-F4-PushY-1.5XTg	-538	Yes	Yes	Near column	Value between μ -2σ and μ -3σ	-2.70	Figure 4-108
M2-F3-PushY-1.5XTg	-482	Yes	Yes	Near column	Value between μ -2σ and μ -3σ	-2.27	Figure 4-109
M2-F6-Push-100%X+30%Y	-385	Yes	Yes	Near column	Value is between μ - σ and μ -2σ	-1.52	Figure 4-110
M2-F5-PushY-1.5XTg	-321	Yes	Yes	Near column	Value is between μ - σ and μ -2σ	-1.02	N/A
M5-F13-Push-30%X+100%Y	-784	Yes	Yes	Near shear wall	Value is less than μ -3σ	-4.61	Figure 4-105
M5-F14-PushY-1.5XTg	-425	Yes	Yes	Near shear wall	Value is between μ - σ and μ -2σ	-1.83	N/A
M5-F16-Push-30%X+100%Y	-369	Yes	Yes	Near column	Value is between μ - σ and μ -2σ	-1.40	N/A
M5-F15-Push-30%X+100%Y	-364	Yes	Yes	Near column	Value is between μ - σ and μ -2σ	-1.35	N/A
M3-F7-Push-30%X+100%Y	-336	Yes	Yes	Near shear wall	Value is between μ - σ and μ -2σ	-1.14	N/A
M3-F9-PushY-1.5XTg	-325	Yes	Yes	Near column	Value is between μ - σ and μ -2σ	-1.05	N/A
M6-F19-Push-30%X+100%Y	-325	Yes	Yes	Near shear wall	Value is between μ - σ and μ -2σ	-1.06	N/A

S12-Top-Min-Story 1-NSP μ = -149 psi σ = 87 psi

Model Number-Diaphragm Location-Diaphragm Design Force Procedures	Stress at Story 1 (psi)	Shear reinforcement required or not	Change of Diaphragm section required or not	Location	Data points Location in Normal distribution curve/Bell curve/Gaussian distribution	Z-Score	Reference figure
M2-F2-PushY-1.5XTg	-442	Yes	Yes	Near shear wall	Value is less than μ -3σ	-3.39	Figure 4-107
M2-F1-PushY-1.5XTg	-422	Yes	Yes	Near shear wall	Value is less than μ -3σ	-3.15	Figure 4-106
M2-F6-Push-100%X+30%Y	-381	Yes	Yes	Near column	Value between μ -2σ and μ -3σ	-2.68	Figure 4-110
M2-F4-PushY-1.5XTg	-371	Yes	Yes	Near column	Value between μ -2σ and μ -3σ	-2.56	Figure 4-108
M2-F3-PushY-1.5XTg	-354	Yes	Yes	Near column	Value between μ -2σ and μ -3σ	-2.37	Figure 4-109
M2-F5-PushY-1.5XTg	-289	Yes	No	Near column	Value is between μ - σ and μ -2σ	-1.63	N/A
M5-F13-Push-30%X+100%Y	-341	Yes	Yes	Near shear wall	Value between μ -2σ and μ -3σ	-2.22	Figure 4-105
M5-F14-PushY-1.5XTg	-340	Yes	Yes	Near shear wall	Value between μ -2σ and μ -3σ	-2.21	N/A
M5-F15-Push-30%X+100%Y	-282	Yes	No	Near column	Value is between μ - σ and μ -2σ	-1.54	N/A
M5-F18-Push-30%X+100%Y	-271	Yes	No	Near column	Value is between μ - σ and μ -2σ	-1.41	N/A
M5-F17-Push-30%X+100%Y	-268	Yes	No	Near column	Value is between μ - σ and μ -2σ	-1.37	N/A
M5-F16-Push-30%X+100%Y	-257	Yes	No	Near column	Value is between μ - σ and μ -2σ	-1.26	N/A
M3-F7-PushY-1.5XTg	-266	Yes	No	Near shear wall	Value is between μ - σ and μ -2σ	-1.36	N/A
M9-F42-Push-100%X+30%Y	-246	Yes	No	Near shear wall	Value is between μ - σ and μ -2σ	-1.13	N/A
M8-F35-Push-30%X+100%Y	-244	Yes	No	Near shear wall	Value is between μ - σ and μ -2σ	-1.10	N/A

Table 4-25 Minimum S12 in-plane shear stress at the bottom of layered shells from Pushover analyses at stories of models

S12-Bottom-Min-Story 3-NSP μ = -232 psi σ = 192 psi

Model Number-Diaphragm Location-Diaphragm Design Force Procedures	Stress at Story 3 (psi)	Shear reinforcement required or not	Change of Diaphragm section required or not	Location	Data points Location in Normal distribution curve/Bell curve/Gaussian distribution	Z-Score	Reference figure
M5-F13-PushY-1.5XTg	-1197	Yes	Yes	Near shear wall	Value is less than μ -3σ	-5.03	Figure 4-111
M5-F16-PushY-1.5XTg	-744	Yes	Yes	Near column	Value between μ -2σ and μ -3σ	-2.67	Figure 4-112
M5-F17-Push-30%X+100%Y	-659	Yes	Yes	Near column	Value between μ -2σ and μ -3σ	-2.23	Figure 4-113
M2-F1-PushY-1.5XTg	-1182	Yes	Yes	Near shear wall	Value is less than μ -3σ	-4.95	Figure 4-114
M2-F4-PushY-1.5XTg	-729	Yes	Yes	Near column	Value between μ -2σ and μ -3σ	-2.59	Figure 4-115
M2-F5-PushY-1.5XTg	-695	Yes	Yes	Near column	Value between μ -2σ and μ -3σ	-2.42	Figure 4-116
M2-F6-Push-100%X+30%Y	-503	Yes	Yes	Near column	Value is between μ - σ and μ -2σ	-1.42	Figure 4-119
M9-F37-Push-30%X+100%Y	-705	Yes	Yes	Near column	Value between μ -2σ and μ -3σ	-2.47	Figure 4-117
M3-F9-PushY-1.5XTg	-647	Yes	Yes	Near column	Value between μ -2σ and μ -3σ	-2.17	Figure 4-118
M3-F8-PushY-1.5XTg	-432	Yes	Yes	Near column	Value is between μ - σ and μ -2σ	-1.05	N/A
M6-F21-Push-30%X+100%Y	-526	Yes	Yes	Near column	Value is between μ - σ and μ -2σ	-1.53	N/A

S12-Bottom-Min-Story 2-NSP μ = -224 psi σ = 194 psi

Model Number-Diaphragm Location-Diaphragm Design Force Procedures	Stress at Story 2 (psi)	Shear reinforcement required or not	Change of Diaphragm section required or not	Location	Data points Location in Normal distribution curve/Bell curve/Gaussian distribution	Z-Score	Reference figure
M2-F1-PushY-1.5XTg	-1272	Yes	Yes	Near shear wall	Value is less than μ -3σ	-5.41	Figure 4-114
M2-F5-PushY-1.5XTg	-832	Yes	Yes	Near column	Value is less than μ -3σ	-3.14	Figure 4-116
M2-F4-PushY-1.5XTg	-671	Yes	Yes	Near column	Value between μ -2σ and μ -3σ	-2.31	Figure 4-115
M2-F6-Push-100%X+30%Y	-484	Yes	Yes	Near column	Value is between μ - σ and μ -2σ	-1.34	Figure 4-119
M5-F13-Push-30%X+100%Y	-1080	Yes	Yes	Near shear wall	Value is less than μ -3σ	-4.42	Figure 4-111
M5-F17-Push-30%X+100%Y	-646	Yes	Yes	Near column	Value between μ -2σ and μ -3σ	-2.18	Figure 4-113
M5-F16-PushY-1.5XTg	-602	Yes	Yes	Near column	Value is between μ - σ and μ -2σ	-1.95	Figure 4-112
M3-F9-PushY-1.5XTg	-680	Yes	Yes	Near column	Value between μ -2σ and μ -3σ	-2.36	Figure 4-118
M3-F11-Push-100%X+30%Y	-497	Yes	Yes	Near shear wall	Value is between μ - σ and μ -2σ	-1.41	N/A
M3-F8-PushY-1.5XTg	-421	Yes	Yes	Near column	Value is between μ - σ and μ -2σ	-1.02	N/A
M9-F37-Push-30%X+100%Y	-622	Yes	Yes	Near column	Value between μ -2σ and μ -3σ	-2.06	Figure 4-117
M6-F21-PushY-1.5XTg	-493	Yes	Yes	Near column	Value is between μ - σ and μ -2σ	-1.39	N/A
M6-F23-Push-100%X+30%Y	-453	Yes	Yes	Near shear wall	Value is between μ - σ and μ -2σ	-1.18	N/A

S12-Bottom-Min-Story 1-NSP μ = -178 psi σ = 144 psi

Model Number-Diaphragm Location-Diaphragm Design Force Procedures	Stress at Story 1 (psi)	Shear reinforcement required or not	Change of Diaphragm section required or not	Location	Data points Location in Normal distribution curve/Bell curve/Gaussian distribution	Z-Score	Reference figure
M2-F1-PushY-1.5XTg	-969	Yes	Yes	Near shear wall	Value is less than μ -3σ	-5.52	Figure 4-114
M2-F5-PushY-1.5XTg	-625	Yes	Yes	Near column	Value is less than μ -3σ	-3.12	Figure 4-116
M2-F6-Push-100%X+30%Y	-487	Yes	Yes	Near column	Value between μ -2σ and μ -3σ	-2.16	Figure 4-119
M2-F4-PushY-1.5XTg	-409	Yes	Yes	Near column	Value is between μ - σ and μ -2σ	-1.61	Figure 4-115
M5-F13-PushY-1.5XTg	-602	Yes	Yes	Near shear wall	Value between μ -2σ and μ -3σ	-2.96	Figure 4-111
M5-F17-Push-30%X+100%Y	-523	Yes	Yes	Near column	Value between μ -2σ and μ -3σ	-2.41	Figure 4-113
M5-F16-Push-30%X+100%Y	-386	Yes	Yes	Near column	Value is between μ - σ and μ -2σ	-1.45	Figure 4-112
M9-F37-Push-30%X+100%Y	-473	Yes	Yes	Near column	Value between μ -2σ and μ -3σ	-2.06	Figure 4-117
M9-F41-Push-100%X+30%Y	-361	Yes	Yes	Near shear wall	Value is between μ - σ and μ -2σ	-1.28	N/A
M9-F28-PushY-1.5XTg	-342	Yes	Yes	Near column	Value is between μ - σ and μ -2σ	-1.14	N/A
M3-F11-Push-100%X+30%Y	-461	Yes	Yes	Near shear wall	Value is between μ - σ and μ -2σ	-1.97	N/A
M3-F9-PushY-1.5XTg	-452	Yes	Yes	Near column	Value is between μ - σ and μ -2σ	-1.91	Figure 4-118
M3-F8-PushY-1.5XTg	-348	Yes	Yes	Near column	Value is between μ - σ and μ -2σ	-1.19	N/A
M8-F36-PushY-1.5XTg	-409	Yes	Yes	Near shear wall	Value is between μ - σ and μ -2σ	-1.61	N/A
M6-F23-Push-100%X+30%Y	-414	Yes	Yes	Near shear wall	Value is between μ - σ and μ -2σ	-1.65	N/A
M6-F21-Push-30%X+100%Y	-337	Yes	Yes	Near column	Value is between μ - σ and μ -2σ	-1.11	N/A
M6-F20-Push-30%X+100%Y	-326	Yes	Yes	Near column	Value is between μ - σ and μ -2σ	-1.03	N/A

Appendix-E

COMPARISON OF SHELL LAYER STRESSES OF IN-PLANE STRESS COMPONENTS USING LEP, LDP AND NSP

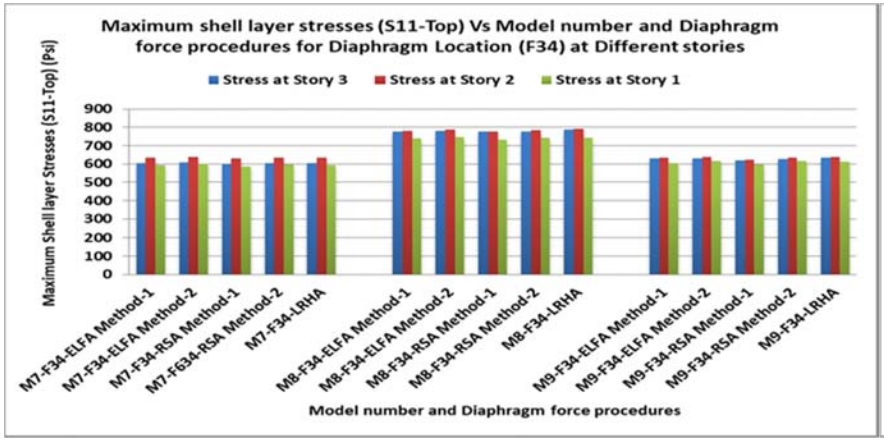

Figure 4-23 Maximum shell layer stresses (S11-Top) Vs Model number and Diaphragm force procedures for Diaphragm Location (F34) at Different stories

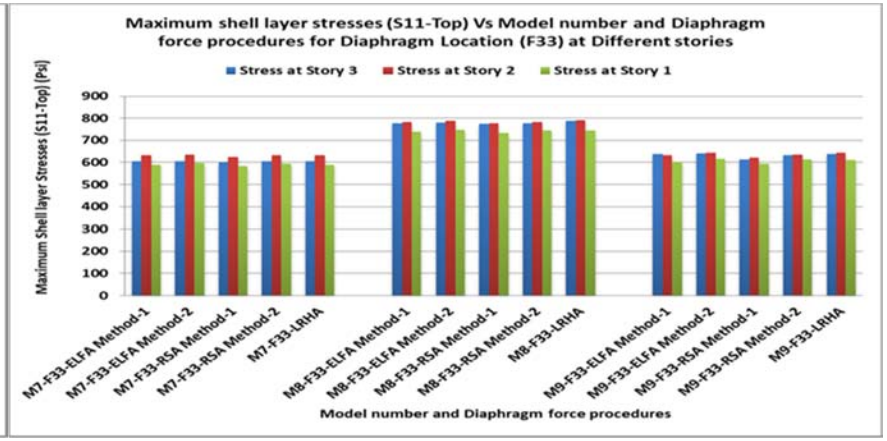

Figure 4-24 Maximum shell layer stresses (S11-Top) Vs Model number and Diaphragm force procedures for Diaphragm Location (F33) at Different stories

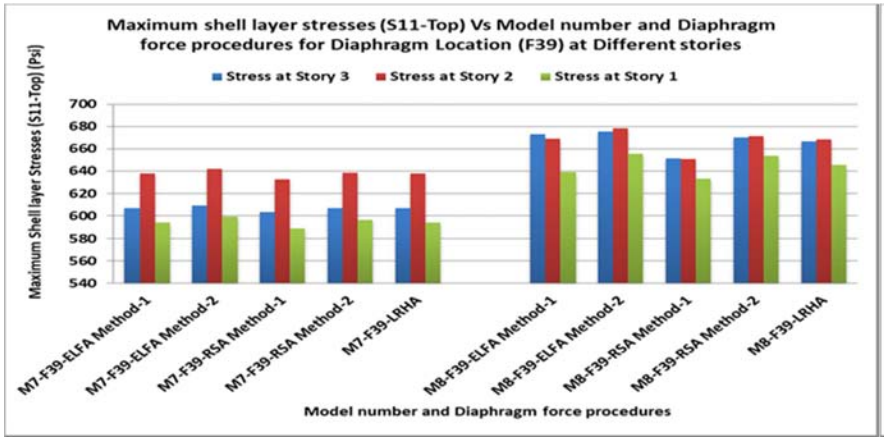

Figure 4-25 Maximum shell layer stresses (S11-Top) Vs Model number and Diaphragm force procedures for Diaphragm Location (F39) at Different stories

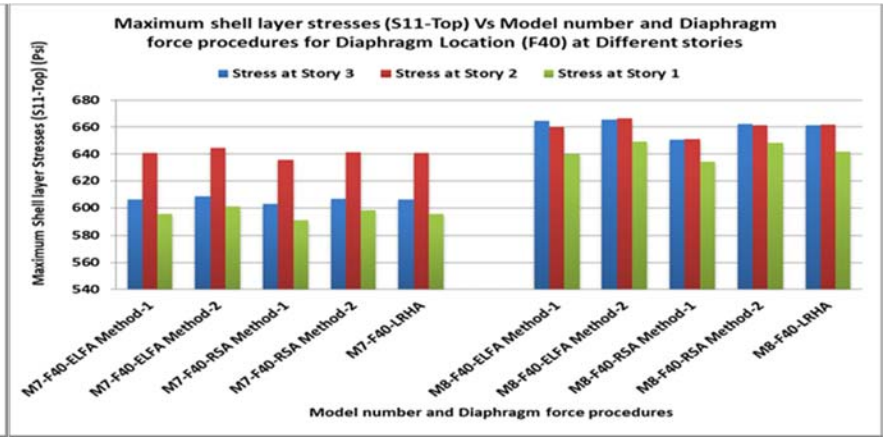

Figure 4-26 Maximum shell layer stresses (S11-Top) Vs Model number and Diaphragm force procedures for Diaphragm Location (F40) at Different stories

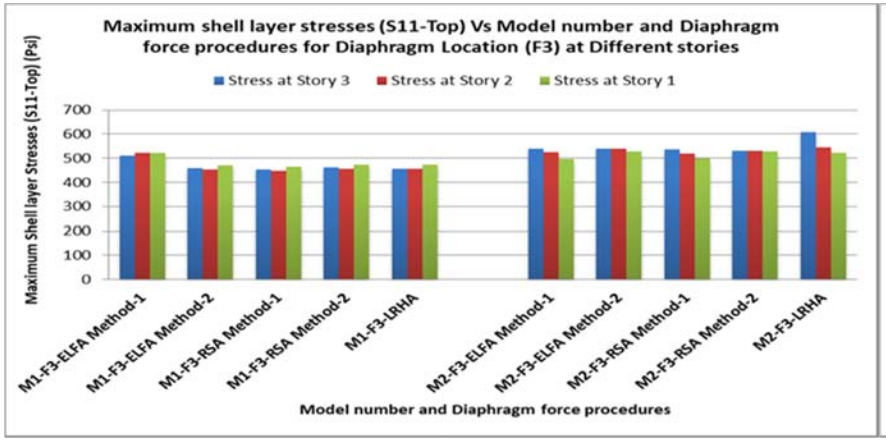

Figure 4-27 Maximum shell layer stresses (S11-Top) Vs Model number and Diaphragm force procedures for Diaphragm Location (F3) at Different stories

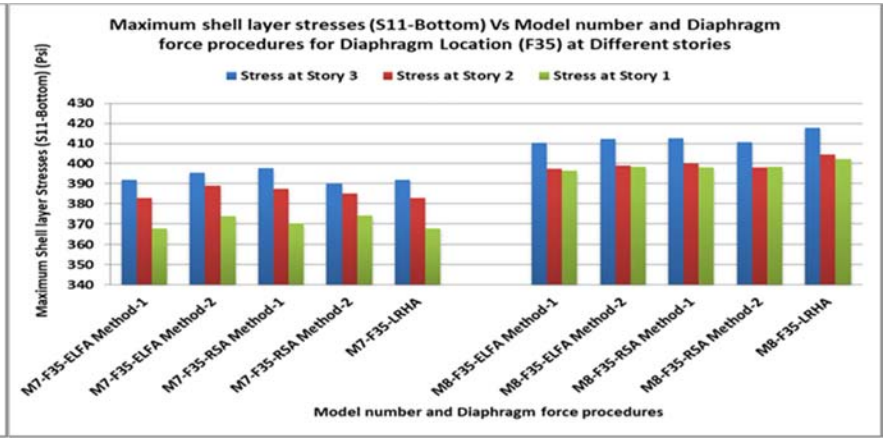

Figure 4-28 Maximum shell layer stresses (S11-Bottom) Vs Model number and Diaphragm force procedures for Diaphragm Location (F35) at Different stories

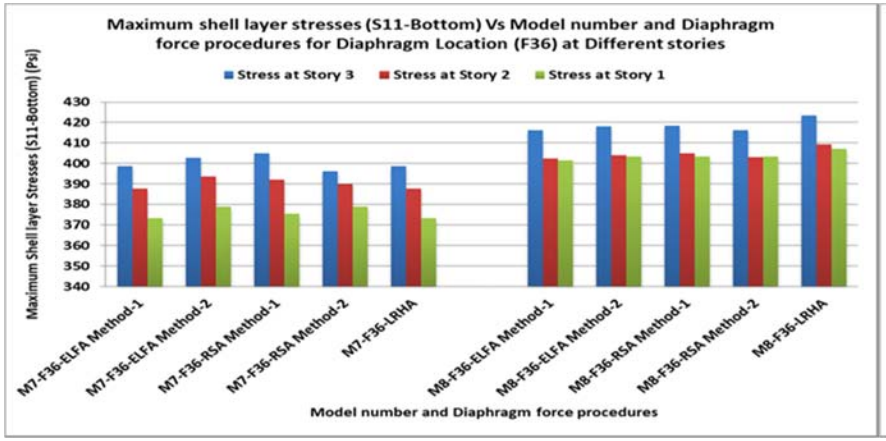

Figure 4-29 Maximum shell layer stresses (S11-Bottom) Vs Model number and Diaphragm force procedures for Diaphragm Location (F36) at Different stories

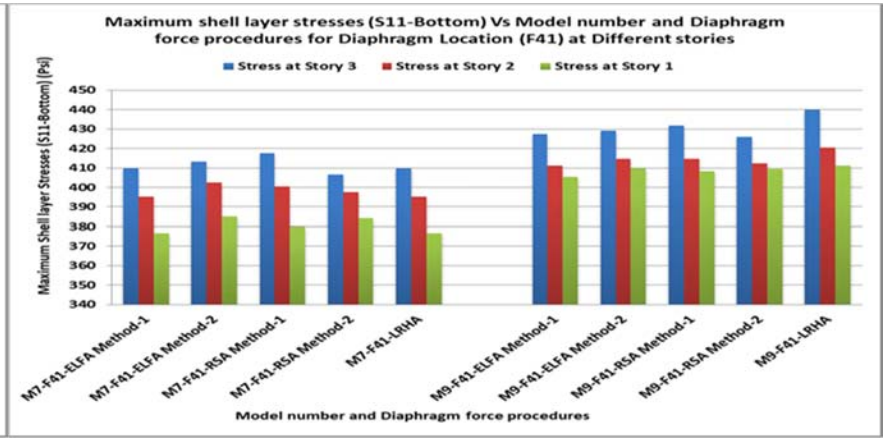

Figure 4-30 Maximum shell layer stresses (S11-Bottom) Vs Model number and Diaphragm force procedures for Diaphragm Location (F41) at Different stories

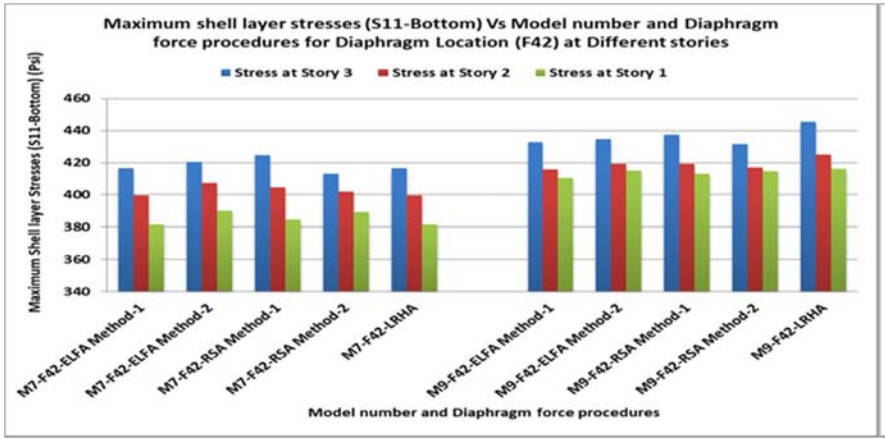

Figure 4-31 Maximum shell layer stresses (S11-Bottom) Vs Model number and Diaphragm force procedures for Diaphragm Location (F42) at Different stories

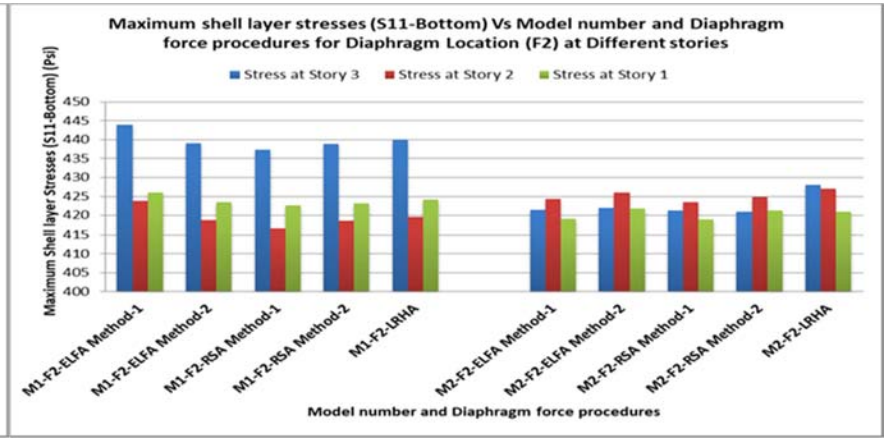

Figure 4-32 Maximum shell layer stresses (S11-Bottom) Vs Model number and Diaphragm force procedures for Diaphragm Location (F2) at Different stories

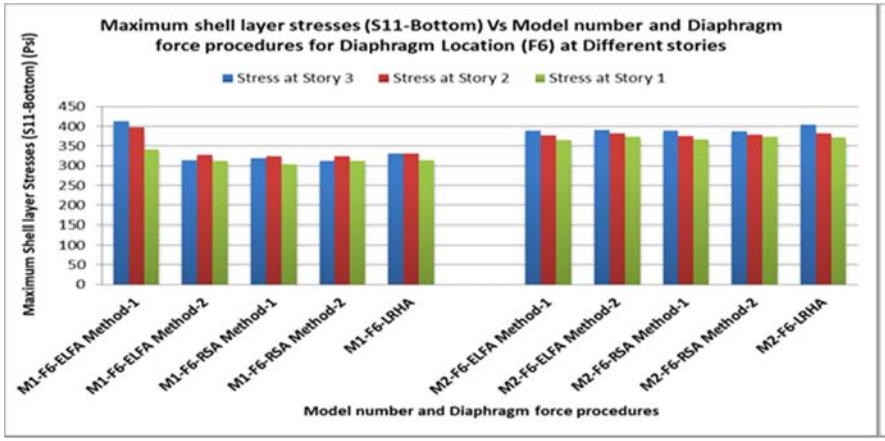

Figure 4-33 Maximum shell layer stresses (S11-Bottom) Vs Model number and Diaphragm force procedures for Diaphragm Location (F6) at Different stories

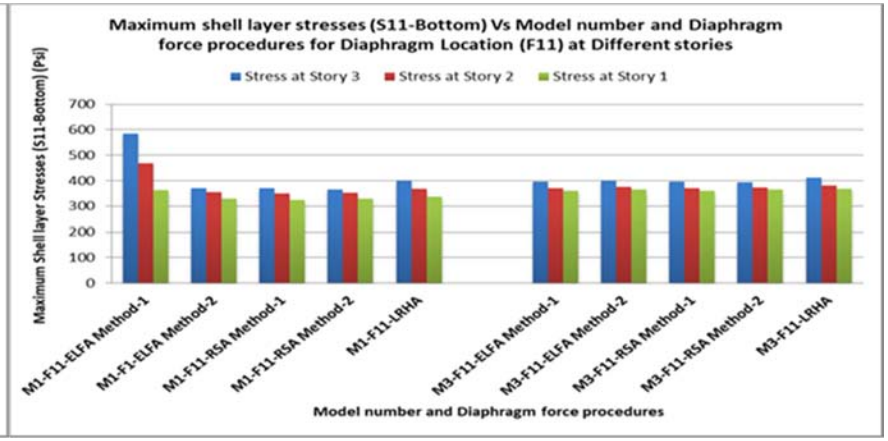

Figure 4-34 Maximum shell layer stresses (S11-Bottom) Vs Model number and Diaphragm force procedures for Diaphragm Location (F11) at Different stories

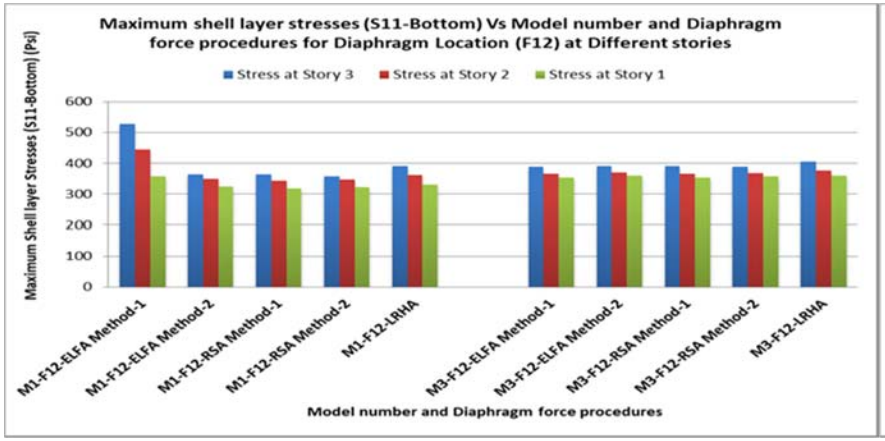

Figure 4-35 Maximum shell layer stresses (S11-Bottom) Vs Model number and Diaphragm force procedures for Diaphragm Location (F12) at Different stories

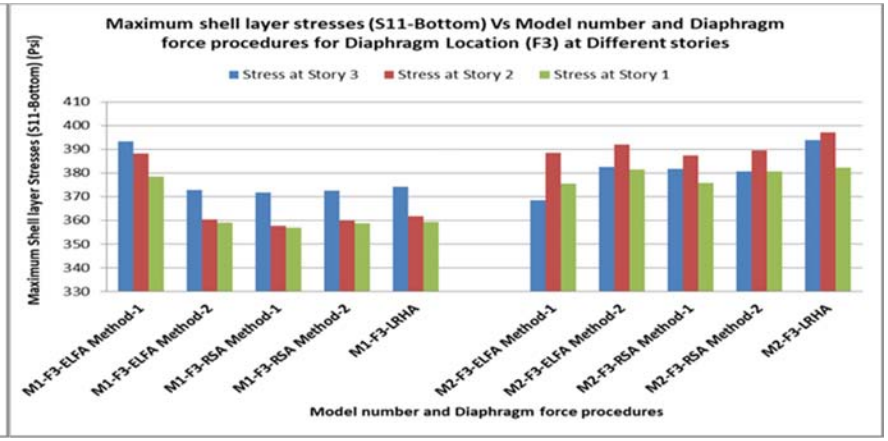

Figure 4-36 Maximum shell layer stresses (S11-Bottom) Vs Model number and Diaphragm force procedures for Diaphragm Location (F3) at Different stories

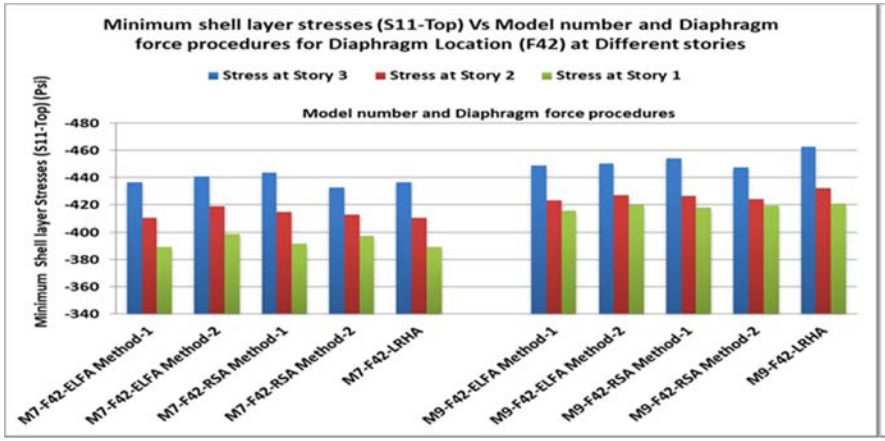

Figure 4-37 Minimum shell layer stresses (S11-Top) Vs Model number and Diaphragm force procedures for Diaphragm Location (F42) at Different stories

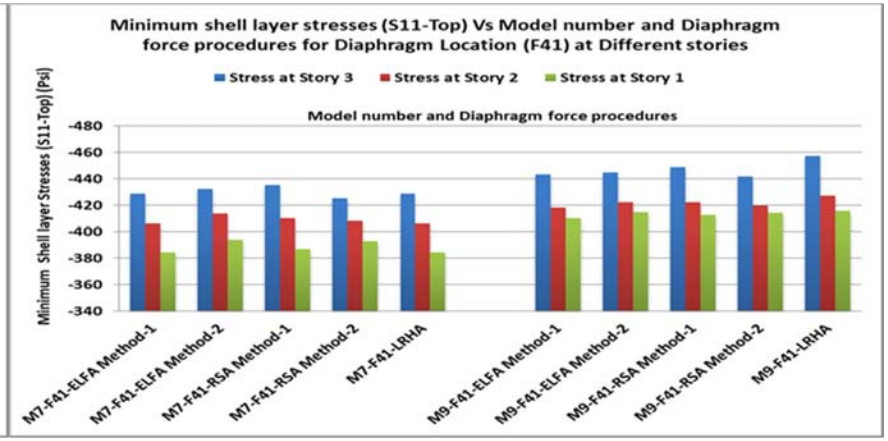

Figure 4-38 Minimum shell layer stresses (S11-Top) Vs Model number and Diaphragm force procedures for Diaphragm Location (F41) at Different stories

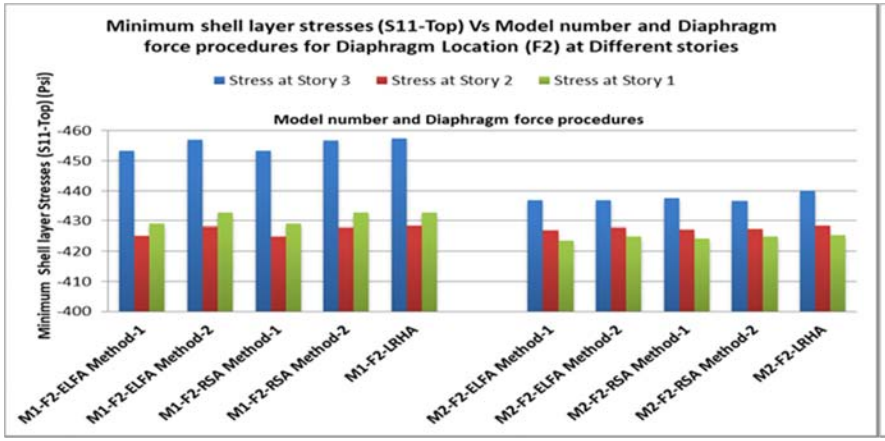

Figure 4-39 Minimum shell layer stresses (S11-Top) Vs Model number and Diaphragm force procedures for Diaphragm Location (F2) at Different stories

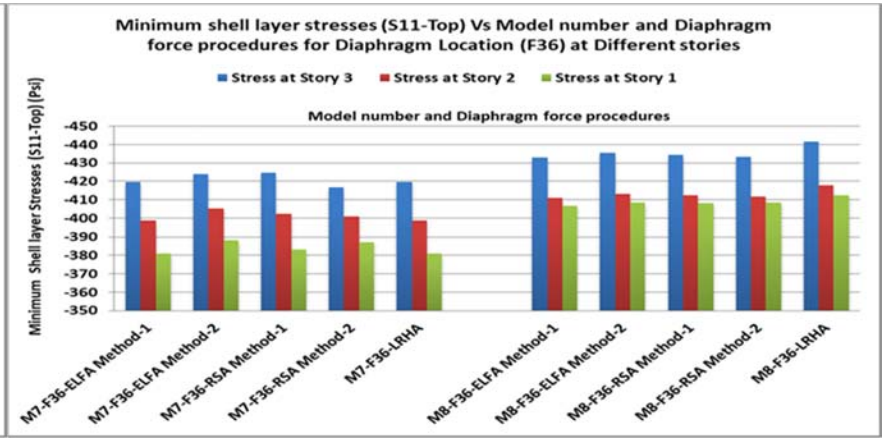

Figure 4-40 Minimum shell layer stresses (S11-Top) Vs Model number and Diaphragm force procedures for Diaphragm Location (F36) at Different stories

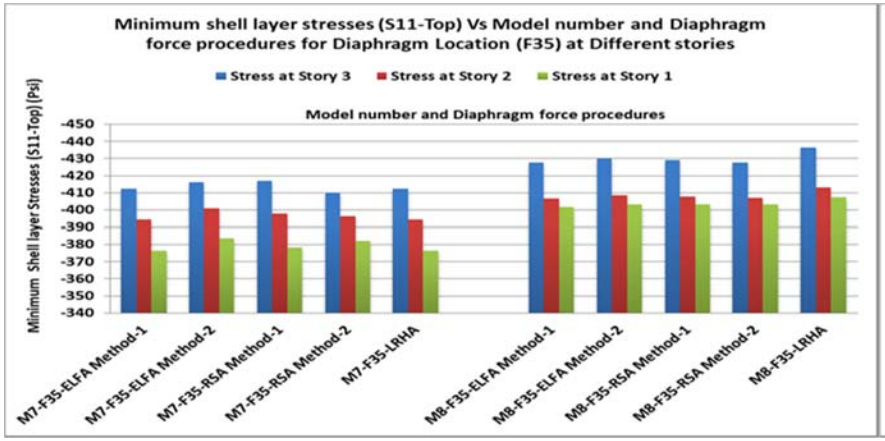

Figure 4-41 Minimum shell layer stresses (S11-Top) Vs Model number and Diaphragm force procedures for Diaphragm Location (F35) at Different stories

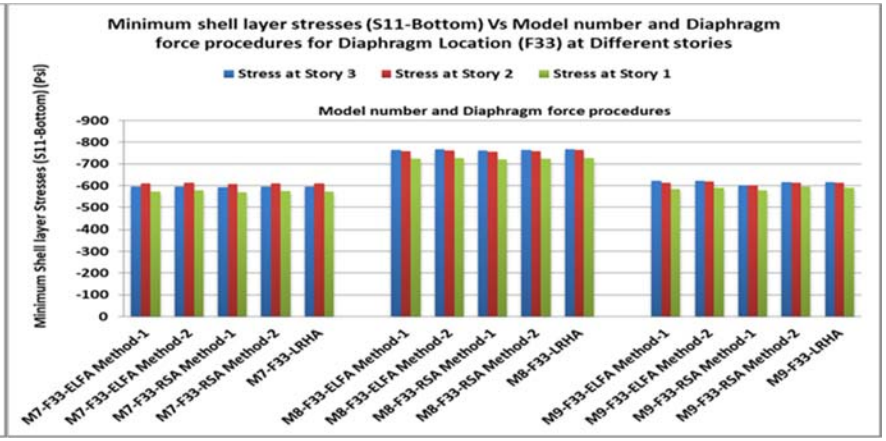

Figure 4-42 Minimum shell layer stresses (S11-Bottom) Vs Model number and Diaphragm force procedures for Diaphragm Location (F33) at Different stories

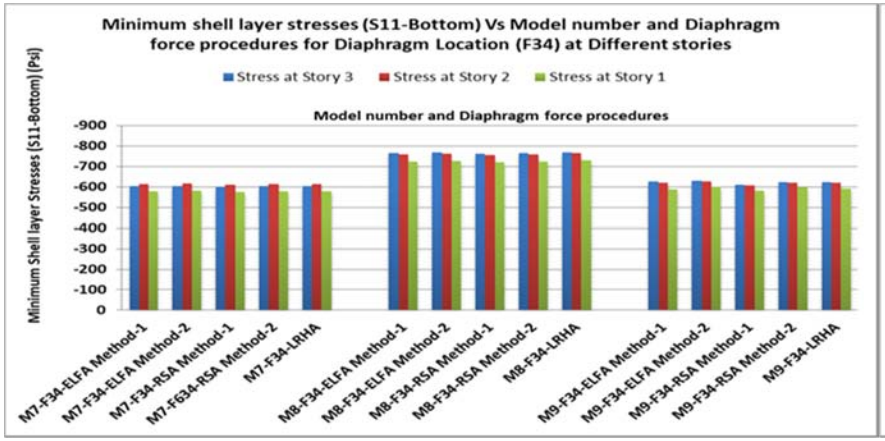

Figure 4-43 Minimum shell layer stresses (S11-Bottom) Vs Model number and Diaphragm force procedures for Diaphragm Location (F34) at Different stories

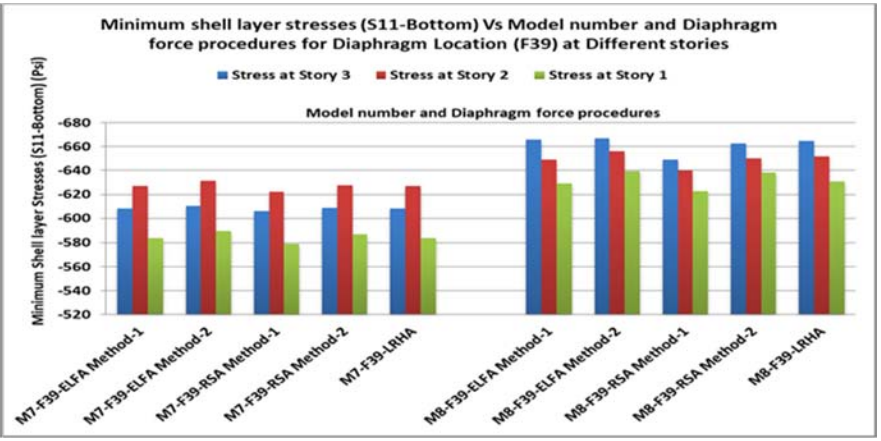

Figure 4-44 Minimum shell layer stresses (S11-Bottom) Vs Model number and Diaphragm force procedures for Diaphragm Location (F39) at Different stories

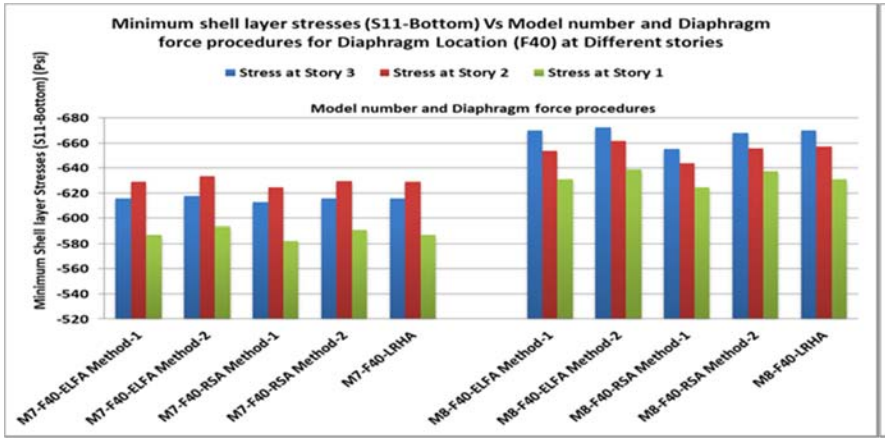

Figure 4-45 Minimum shell layer stresses (S11-Bottom) Vs Model number and Diaphragm force procedures for Diaphragm Location (F40) at Different stories

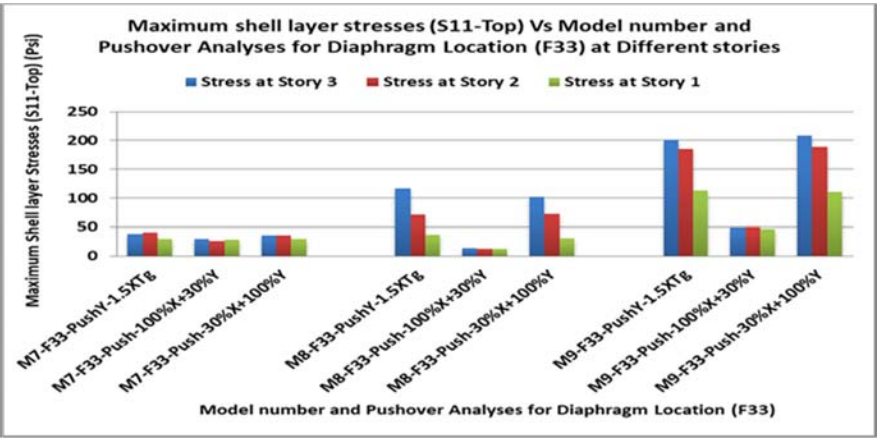

Figure 4-46 Maximum shell layer stresses (S11-Top) Vs Model number and Pushover Analyses for Diaphragm Location (F33) at Different stories

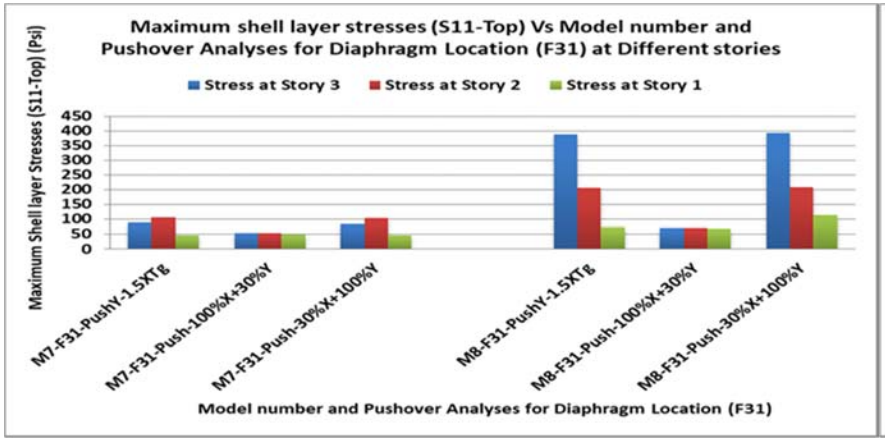

Figure 4-47 Maximum shell layer stresses (S11-Top) Vs Model number and Pushover Analyses for Diaphragm Location (F31) at Different stories

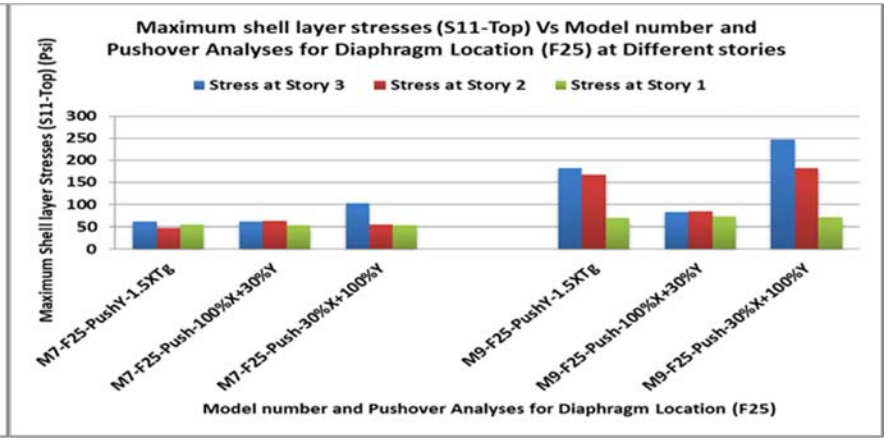

Figure 4-48 Maximum shell layer stresses (S11-Top) Vs Model number and Pushover Analyses for Diaphragm Location (F25) at Different stories

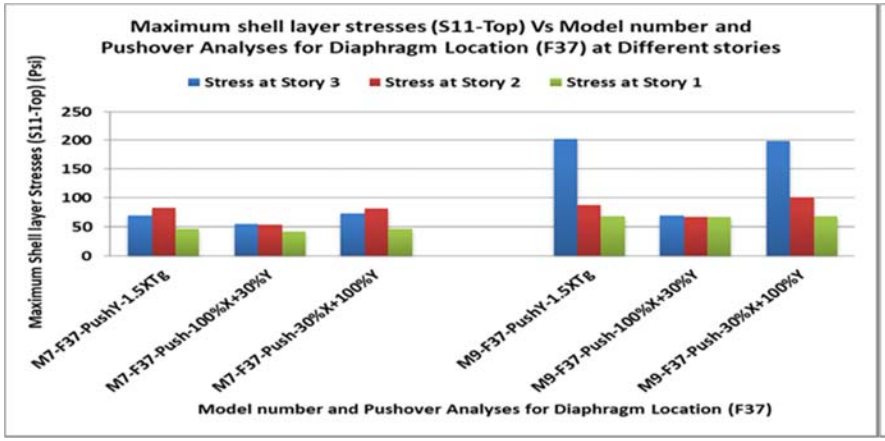

Figure 4-49 Maximum shell layer stresses (S11-Top) Vs Model number and Pushover Analyses for Diaphragm Location (F37) at Different stories

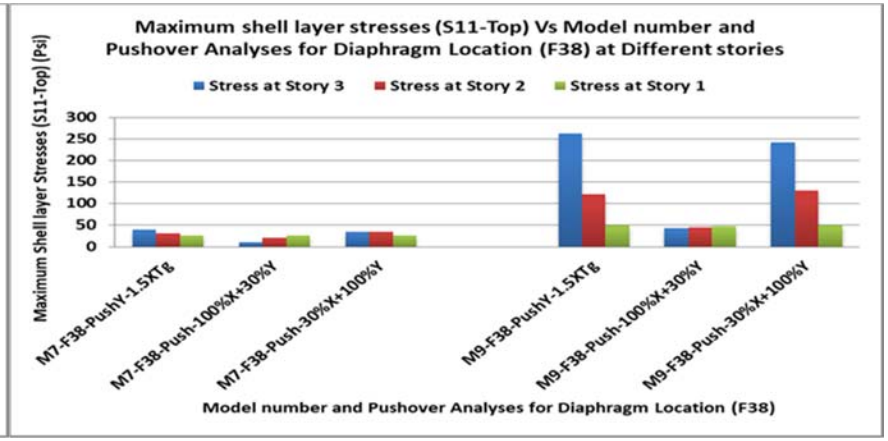

Figure 4-50 Maximum shell layer stresses (S11-Top) Vs Model number and Pushover Analyses for Diaphragm Location (F38) at Different stories

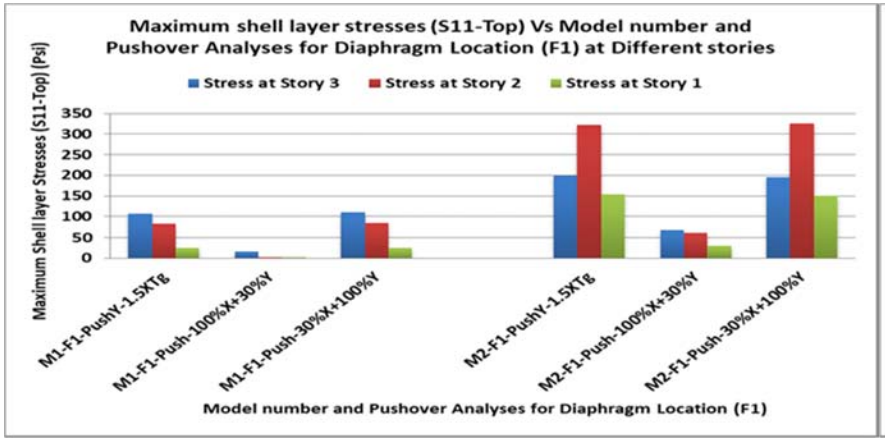

Figure 4-51 Maximum shell layer stresses (S11-Top) Vs Model number and Pushover Analyses for Diaphragm Location (F1) at Different stories

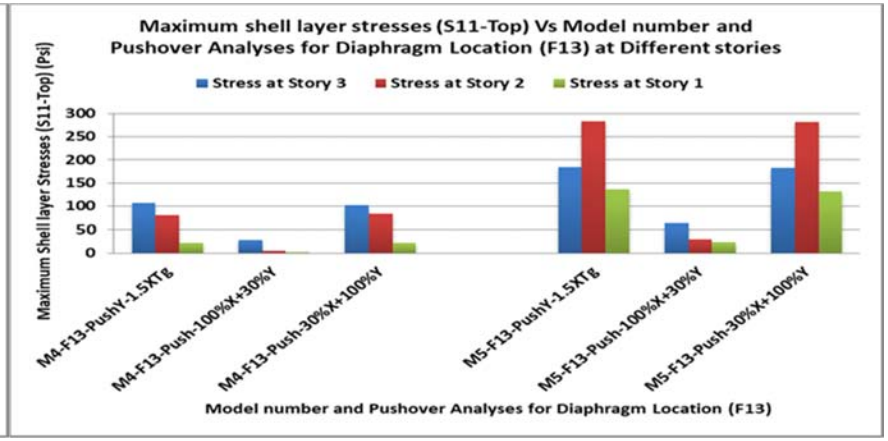

Figure 4-52 Maximum shell layer stresses (S11-Top) Vs Model number and Pushover Analyses for Diaphragm Location (F13) at Different stories

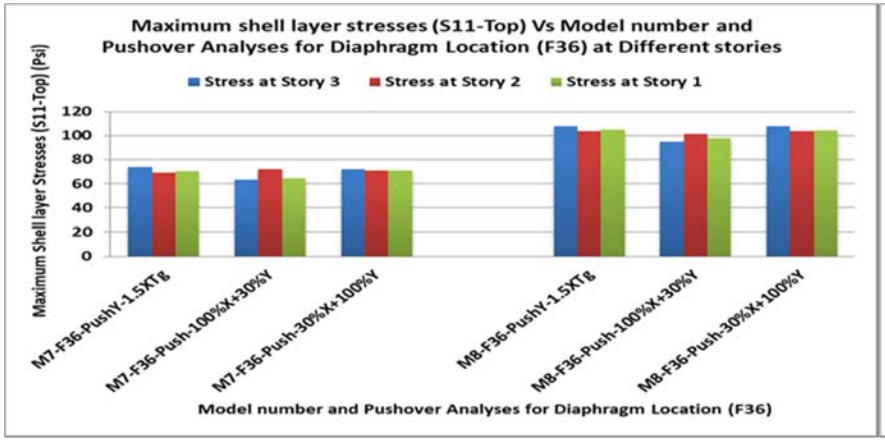

Figure 4-53 Maximum shell layer stresses (S11-Top) Vs Model number and Pushover Analyses for Diaphragm Location (F36) at Different stories

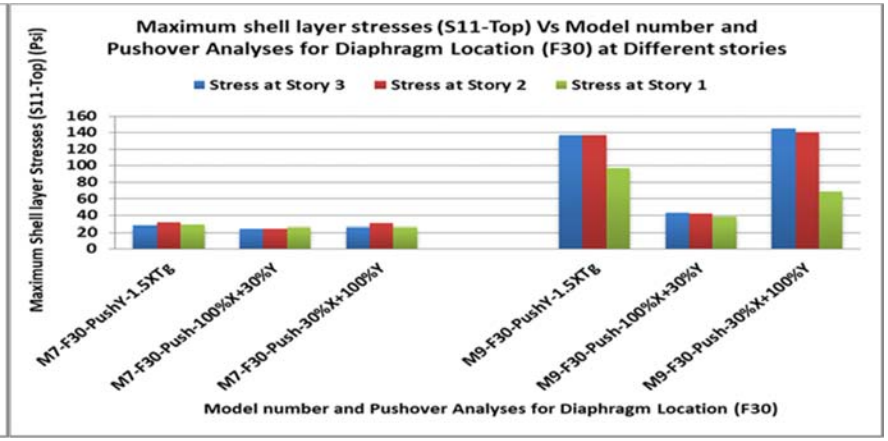

Figure 4-54 Maximum shell layer stresses (S11-Top) Vs Model number and Pushover Analyses for Diaphragm Location (F30) at Different stories

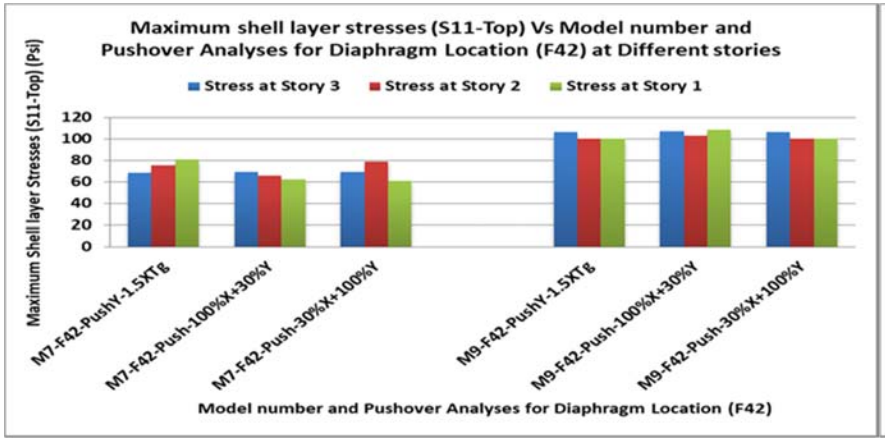

Figure 4-55 Maximum shell layer stresses (S11-Top) Vs Model number and Pushover Analyses for Diaphragm Location (F42) at Different stories

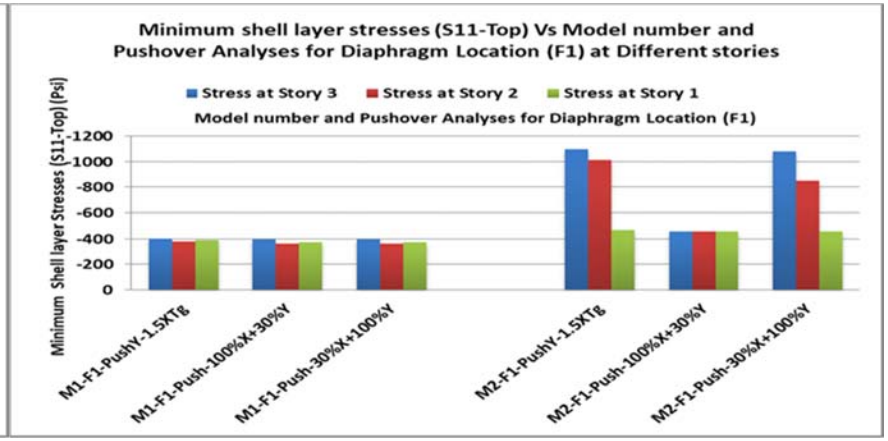

Figure 4-56 Minimum shell layer stresses (S11-Top) Vs Model number and Pushover Analyses for Diaphragm Location (F1) at Different stories

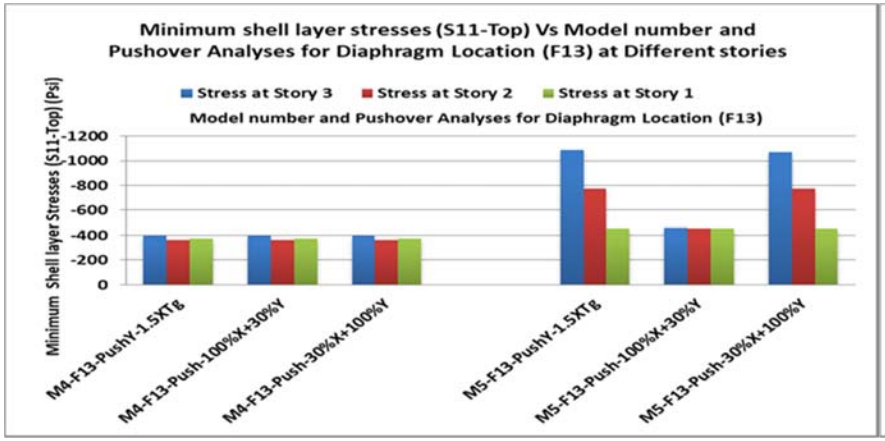

Figure 4-57 Minimum shell layer stresses (S11-Top) Vs Model number and Pushover Analyses for Diaphragm Location (F13) at Different stories

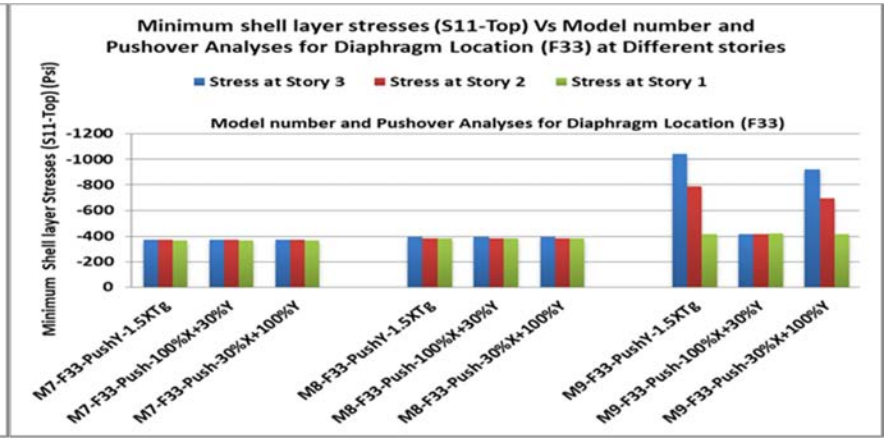

Figure 4-58 Minimum shell layer stresses (S11-Top) Vs Model number and Pushover Analyses for Diaphragm Location (F33) at Different stories

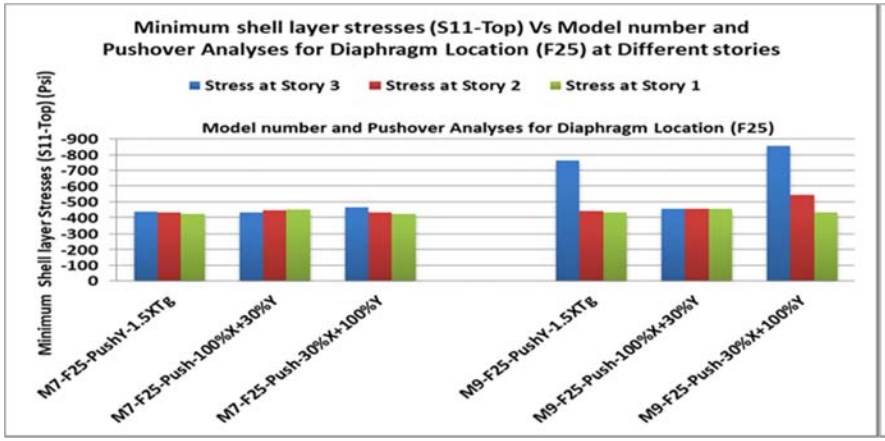

Figure 4-59 Minimum shell layer stresses (S11-Top) Vs Model number and Pushover Analyses for Diaphragm Location (F25) at Different stories

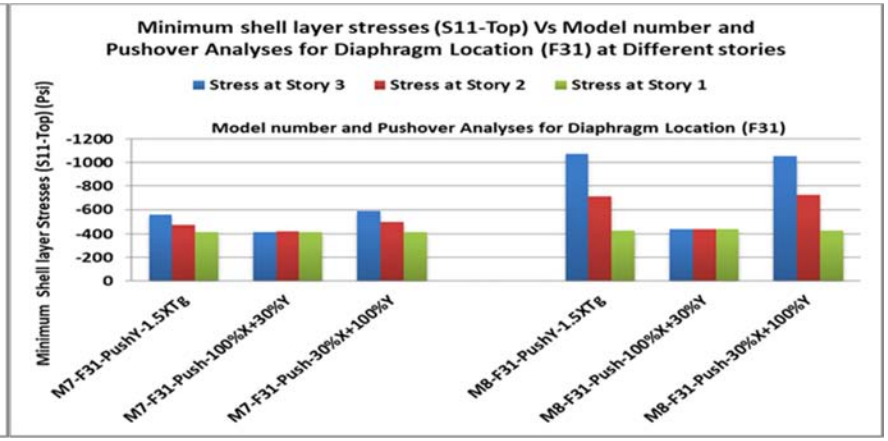

Figure 4-60 Minimum shell layer stresses (S11-Top) Vs Model number and Pushover Analyses for Diaphragm Location (F31) at Different stories

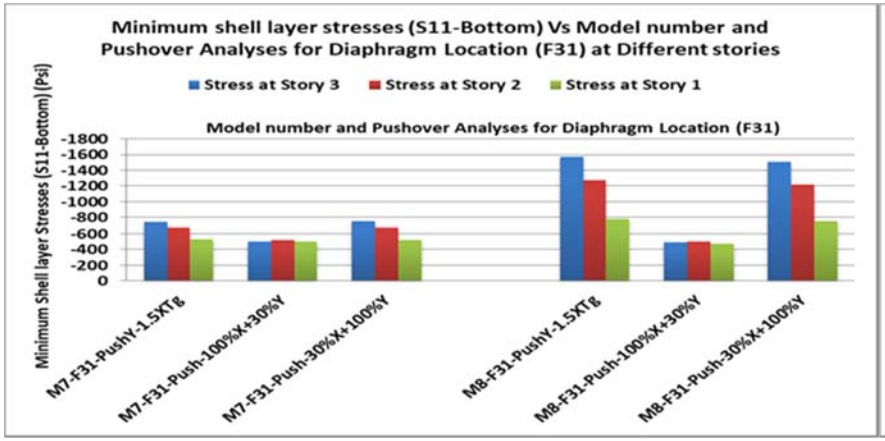

Figure 4-61 Minimum shell layer stresses (S11-Bottom) Vs Model number and Pushover Analyses for Diaphragm Location (F31) at Different stories

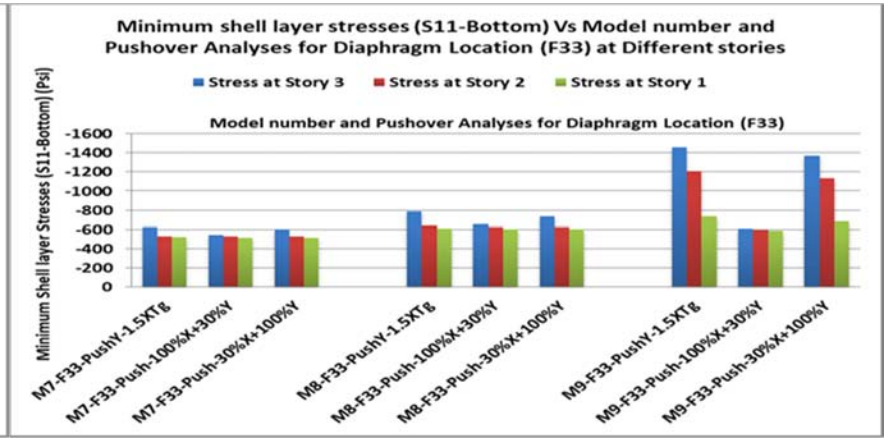

Figure 4-62 Minimum shell layer stresses (S11-Bottom) Vs Model number and Pushover Analyses for Diaphragm Location (F33) at Different stories

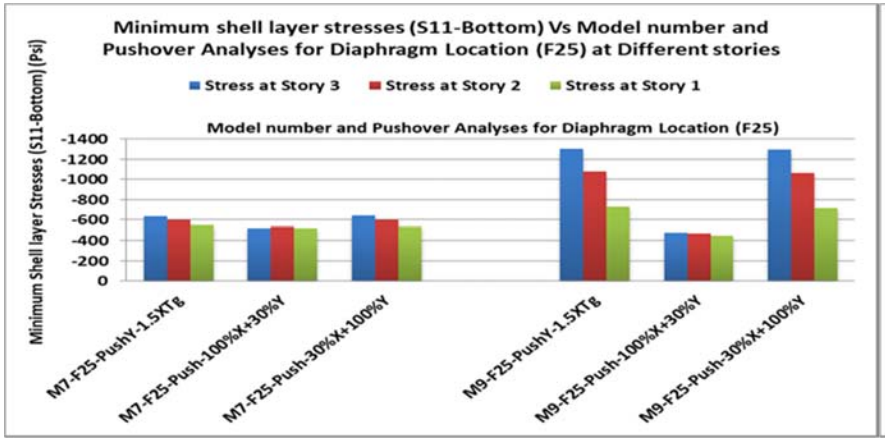

Figure 4-63 Minimum shell layer stresses (S11-Bottom) Vs Model number and Pushover Analyses for Diaphragm Location (F25) at Different stories

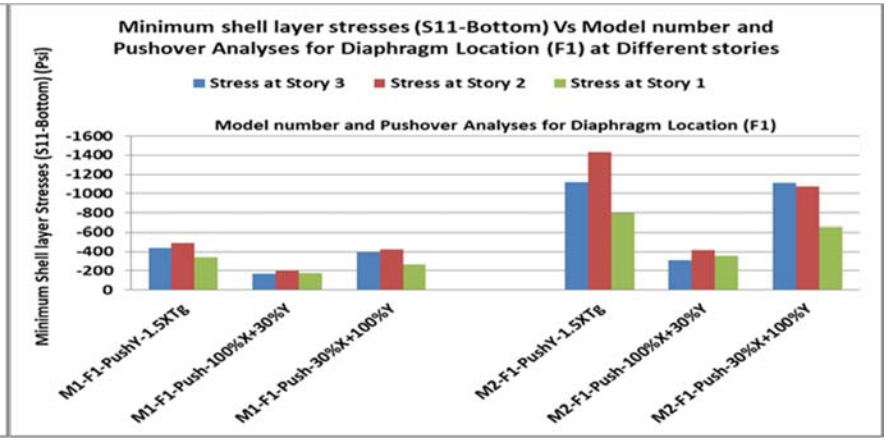

Figure 4-64 Minimum shell layer stresses (S11-Bottom) Vs Model number and Pushover Analyses for Diaphragm Location (F1) at Different stories

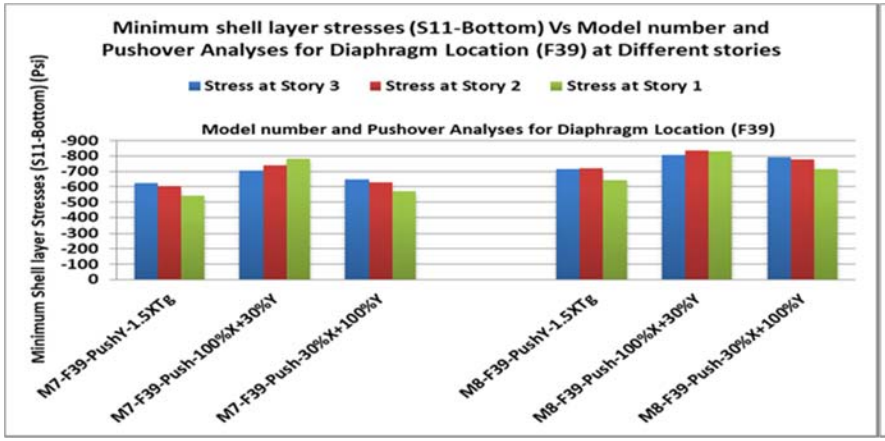

Figure 4-65 Minimum shell layer stresses (S11-Bottom) Vs Model number and Pushover Analyses for Diaphragm Location (F39) at Different stories

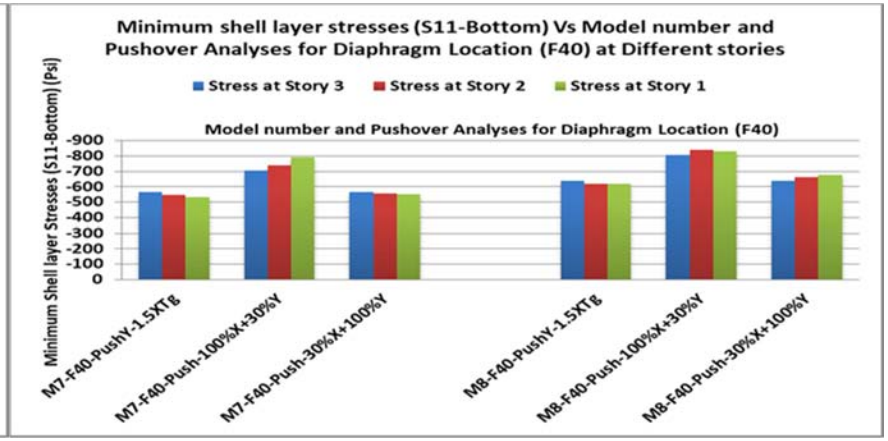

Figure 4-66 Minimum shell layer stresses (S11-Bottom) Vs Model number and Pushover Analyses for Diaphragm Location (F40) at Different stories

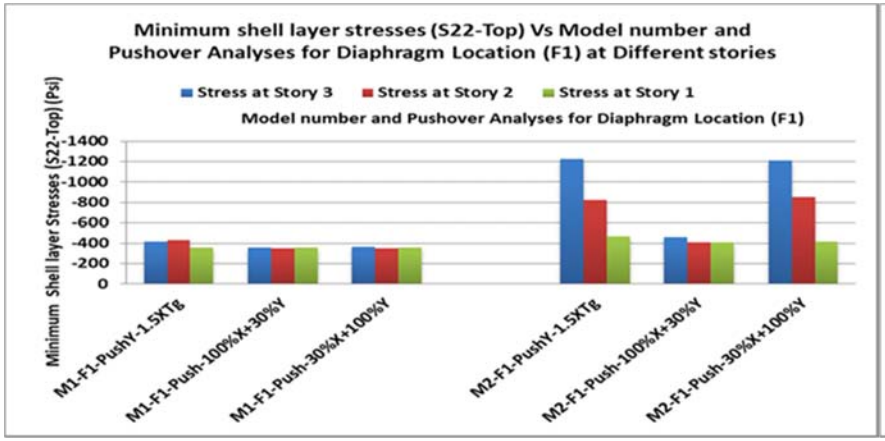

Figure 4-67 Minimum shell layer stresses (S22-Top) Vs Model number and Pushover Analyses for Diaphragm Location (F1) at Different stories

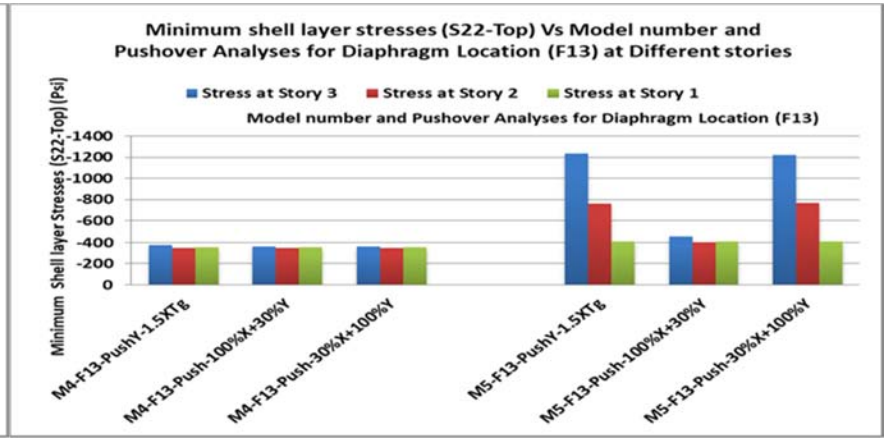

Figure 4-68 Minimum shell layer stresses (S22-Top) Vs Model number and Pushover Analyses for Diaphragm Location (F13) at Different stories

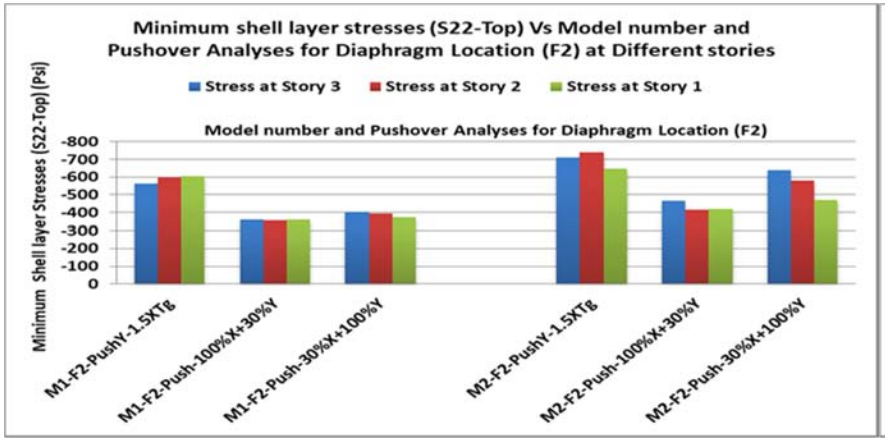

Figure 4-69 Minimum shell layer stresses (S22-Top) Vs Model number and Pushover Analyses for Diaphragm Location (F2) at Different stories

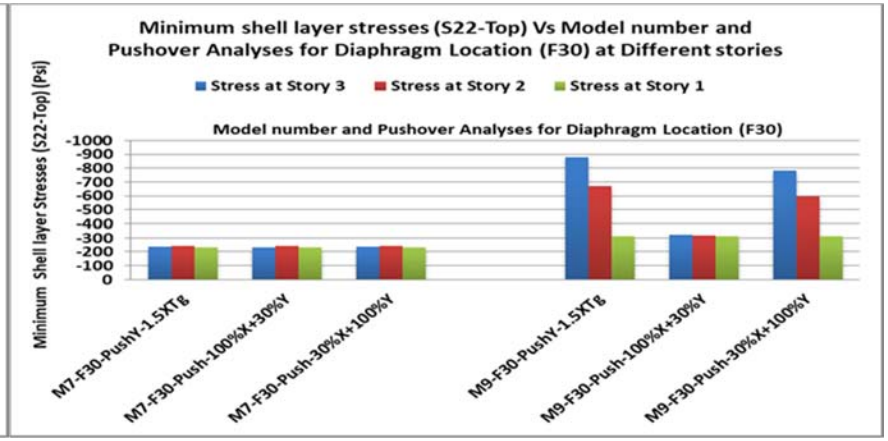

Figure 4-70 Minimum shell layer stresses (S22-Top) Vs Model number and Pushover Analyses for Diaphragm Location (F30) at Different stories

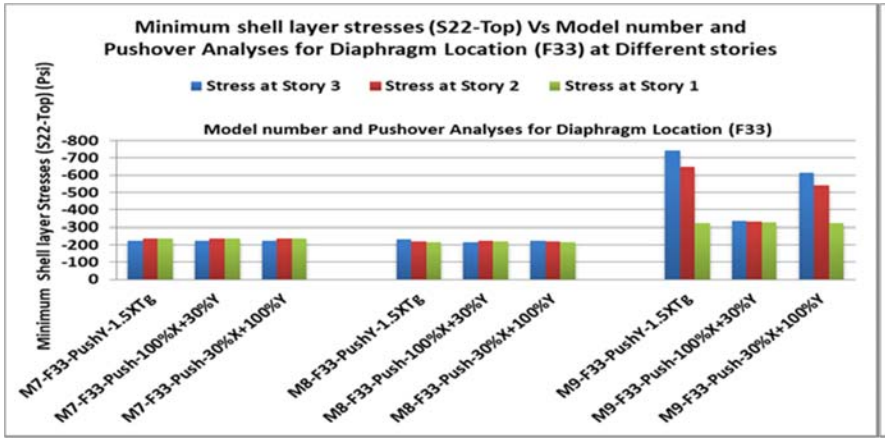

Figure 4-71 Minimum shell layer stresses (S22-Top) Vs Model number and Pushover Analyses for Diaphragm Location (F33) at Different stories

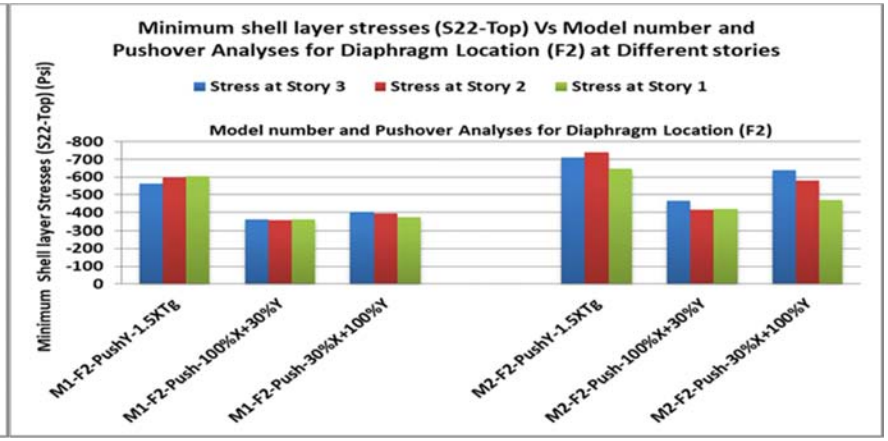

Figure 4-72 Minimum shell layer stresses (S22-Top) Vs Model number and Pushover Analyses for Diaphragm Location (F2) at Different stories

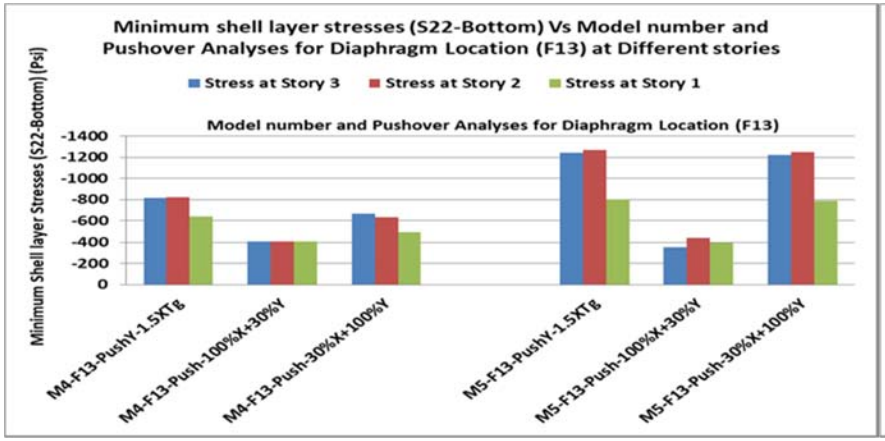

Figure 4-73 Minimum shell layer stresses (S22-Bottom) Vs Model number and Pushover Analyses for Diaphragm Location (F13) at Different stories

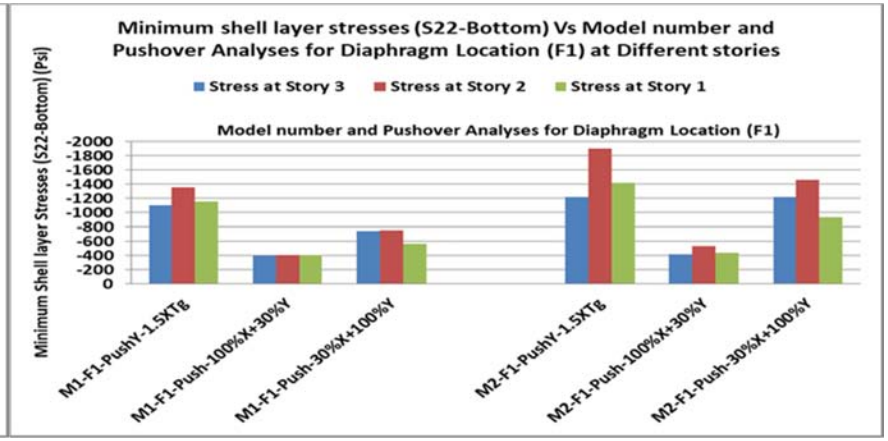

Figure 4-74 Minimum shell layer stresses (S22-Bottom) Vs Model number and Pushover Analyses for Diaphragm Location (F1) at Different stories

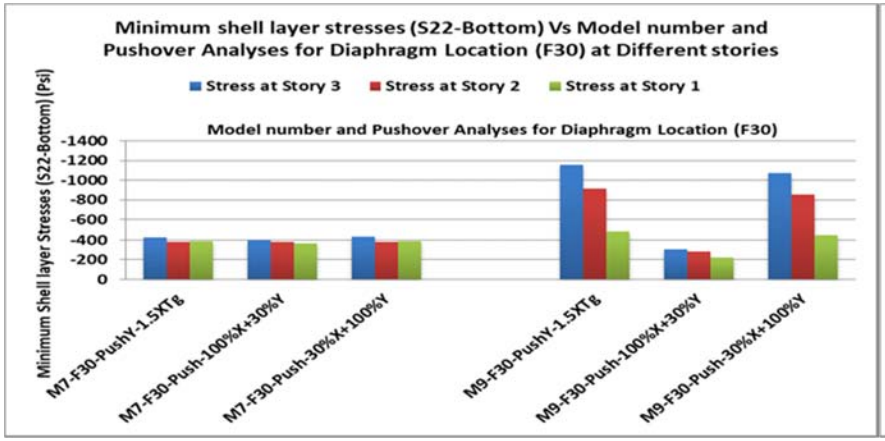

Figure 4-75 Minimum shell layer stresses (S22-Bottom) Vs Model number and Pushover Analyses for Diaphragm Location (F30) at Different stories

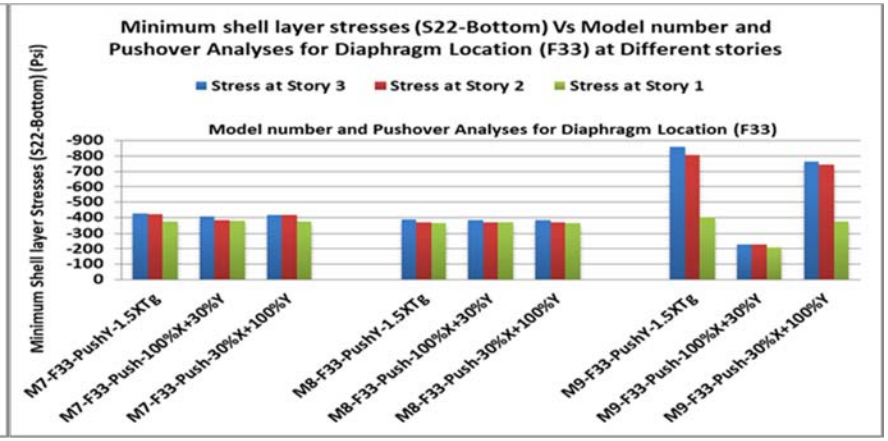

Figure 4-76 Minimum shell layer stresses (S22-Bottom) Vs Model number and Pushover Analyses for Diaphragm Location (F33) at Different stories

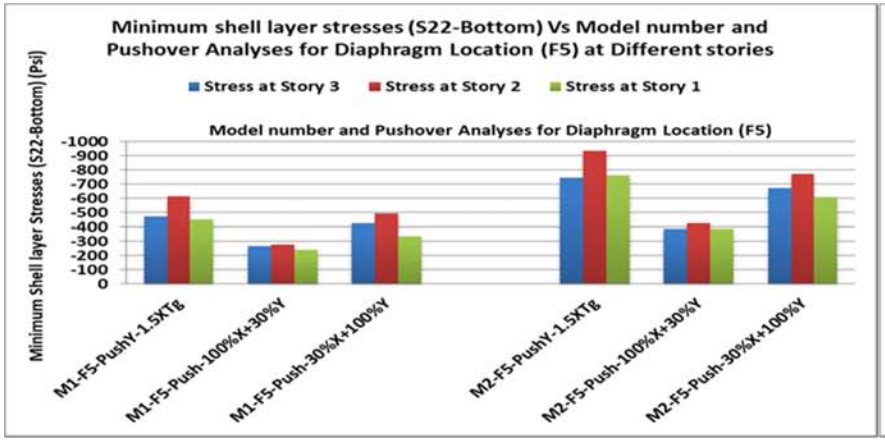

Figure 4-77 Minimum shell layer stresses (S22-Bottom) Vs Model number and Pushover Analyses for Diaphragm Location (F5) at Different stories

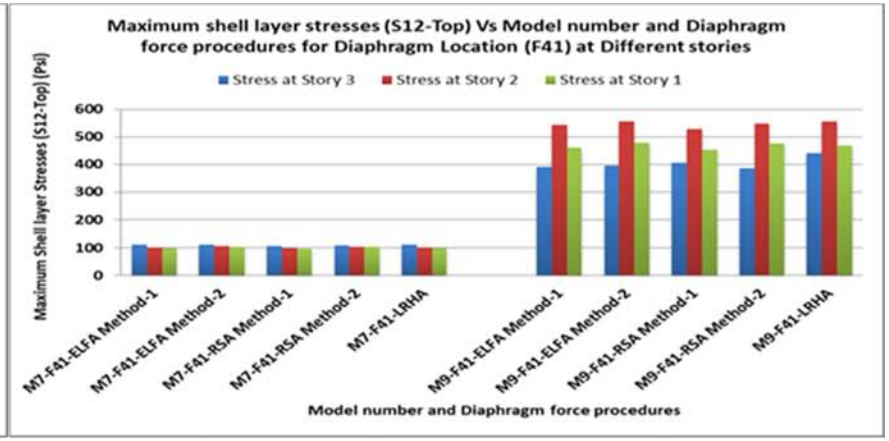

Figure 4-78 Maximum shell layer stresses (S12-Top) Vs Model number and Diaphragm force procedures for Diaphragm Location (F41) at Different stories

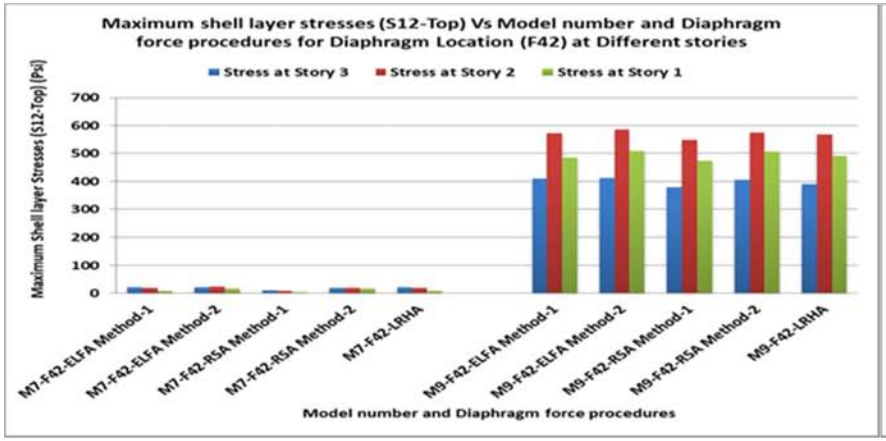

Figure 4-79 Maximum shell layer stresses (S12-Top) Vs Model number and Diaphragm force procedures for Diaphragm Location (F42) at Different stories

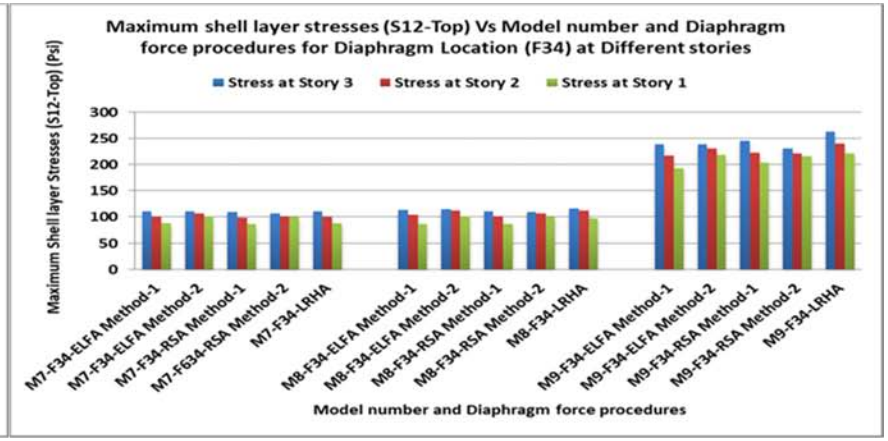

Figure 4-80 Maximum shell layer stresses (S12-Top) Vs Model number and Diaphragm force procedures for Diaphragm Location (F34) at Different stories

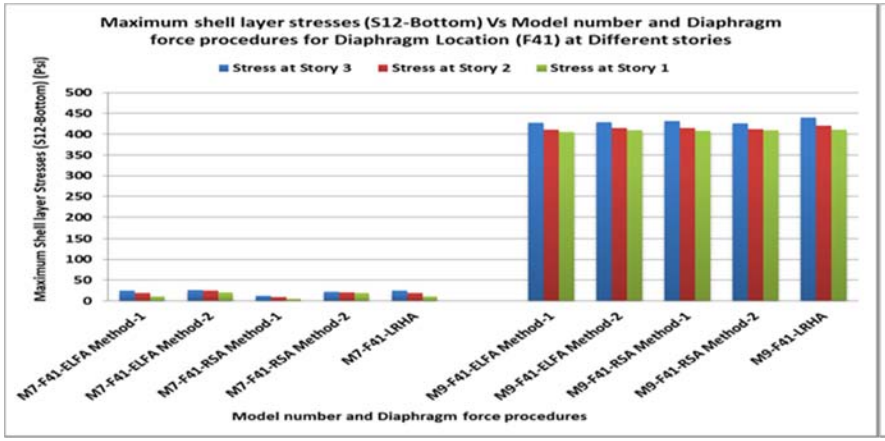

Figure 4-81 Maximum shell layer stresses (S12-Bottom) Vs Model number and Diaphragm force procedures for Diaphragm Location (F41) at Different stories

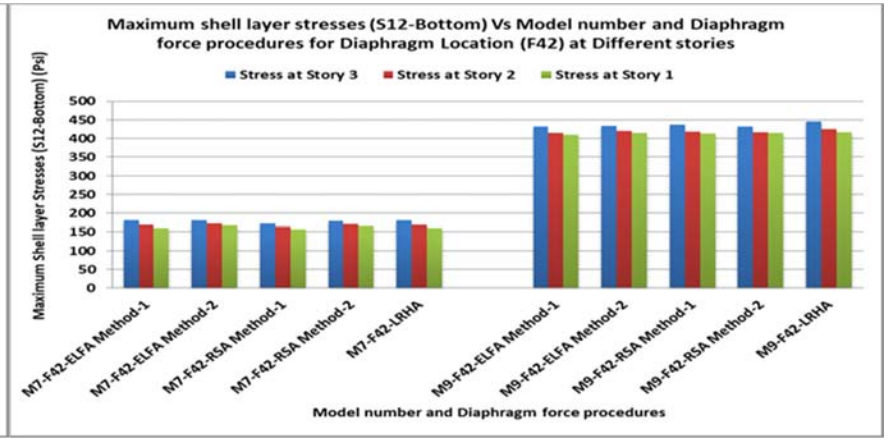

Figure 4-82 Maximum shell layer stresses (S12-Bottom) Vs Model number and Diaphragm force procedures for Diaphragm Location (F42) at Different stories

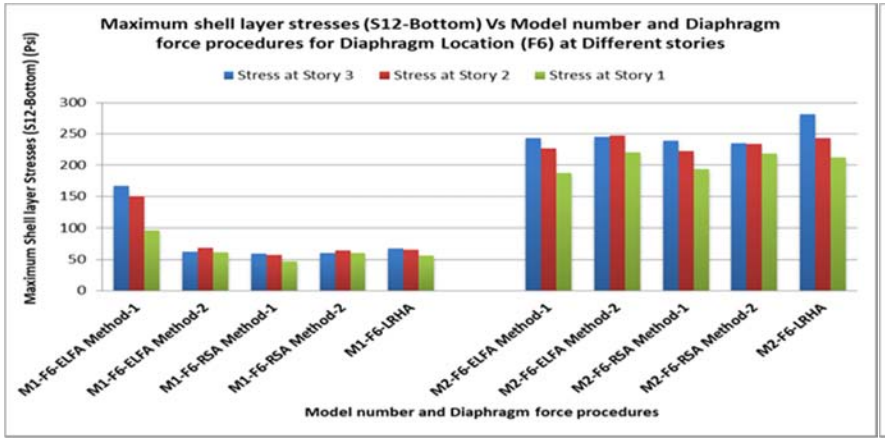

Figure 4-83 Maximum shell layer stresses (S12-Bottom) Vs Model number and Diaphragm force procedures for Diaphragm Location (F6) at Different stories

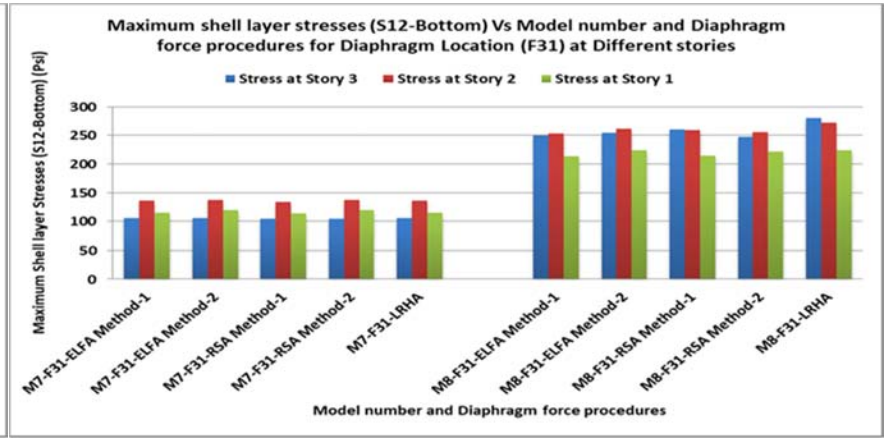

Figure 4-84 Maximum shell layer stresses (S12-Bottom) Vs Model number and Diaphragm force procedures for Diaphragm Location (F31) at Different stories

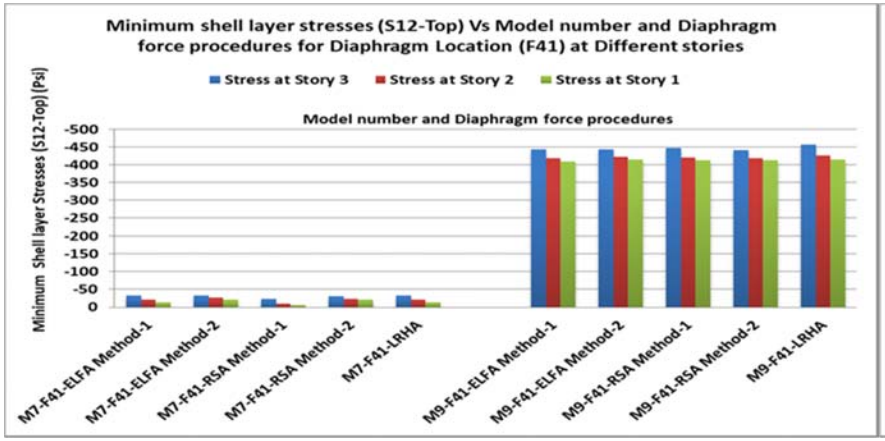

Figure 4-85 Minimum shell layer stresses (S12-Top) Vs Model number and Diaphragm force procedures for Diaphragm Location (F41) at Different stories

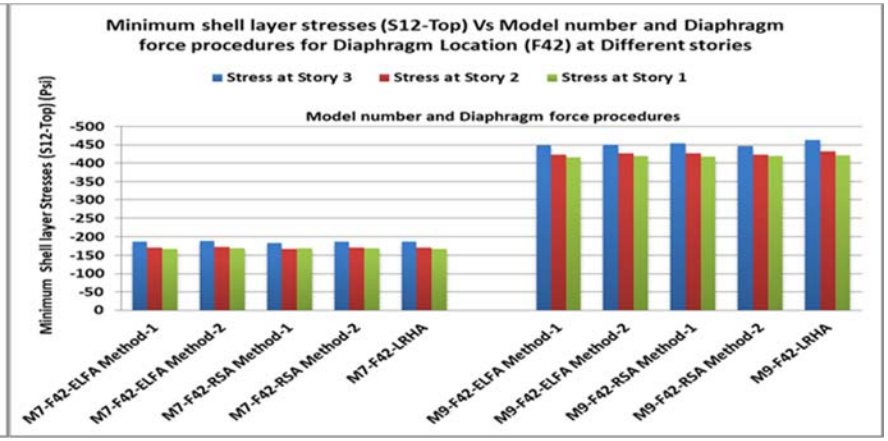

Figure 4-86 Minimum shell layer stresses (S12-Top) Vs Model number and Diaphragm force procedures for Diaphragm Location (F42) at Different stories

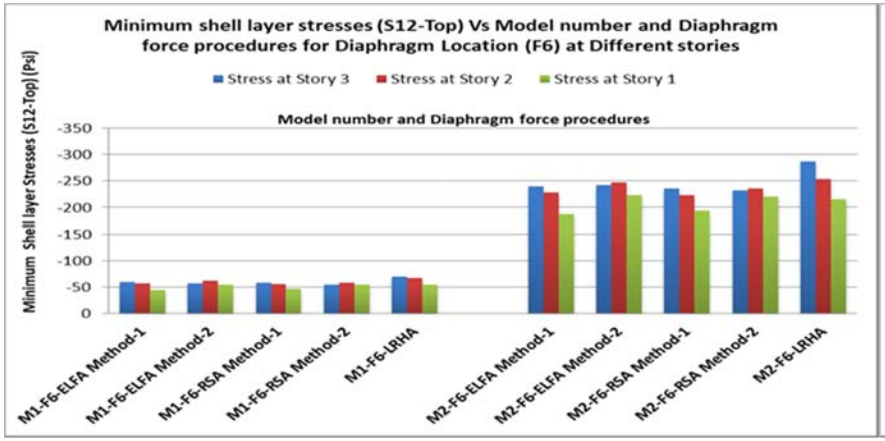

Figure 4-87 Minimum shell layer stresses (S12-Top) Vs Model number and Diaphragm force procedures for Diaphragm Location (F6) at Different stories

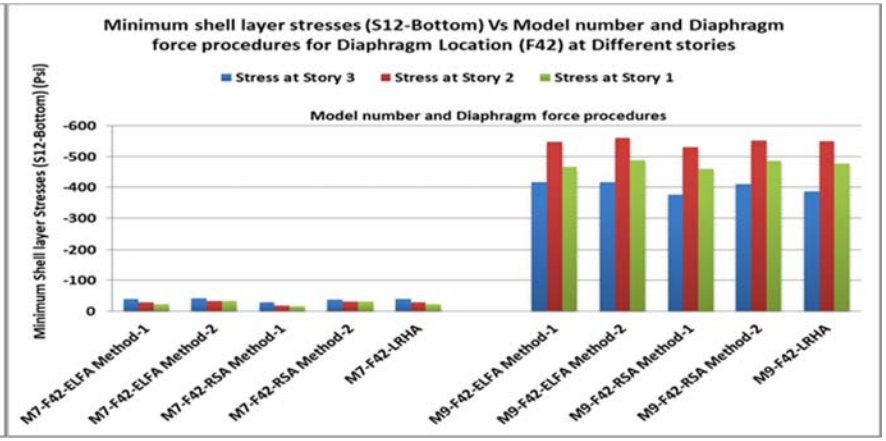

Figure 4-88 Minimum shell layer stresses (S12-Bottom) Vs Model number and Diaphragm force procedures for Diaphragm Location (F42) at Different stories

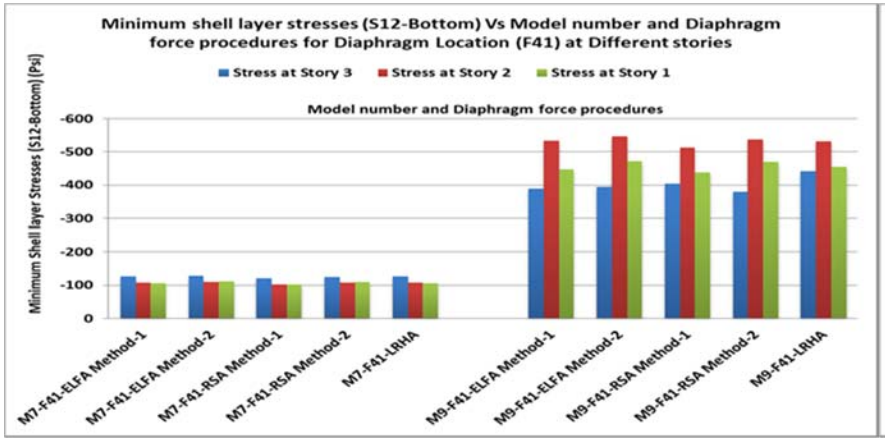

Figure 4-89 Minimum shell layer stresses (S12-Bottom) Vs Model number and Diaphragm force procedures for Diaphragm Location (F41) at Different stories

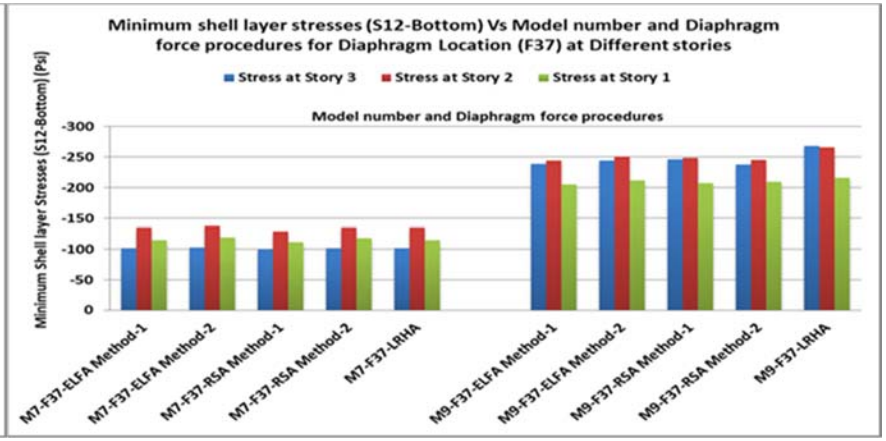

Figure 4-90 Minimum shell layer stresses (S12-Bottom) Vs Model number and Diaphragm force procedures for Diaphragm Location (F37) at Different stories

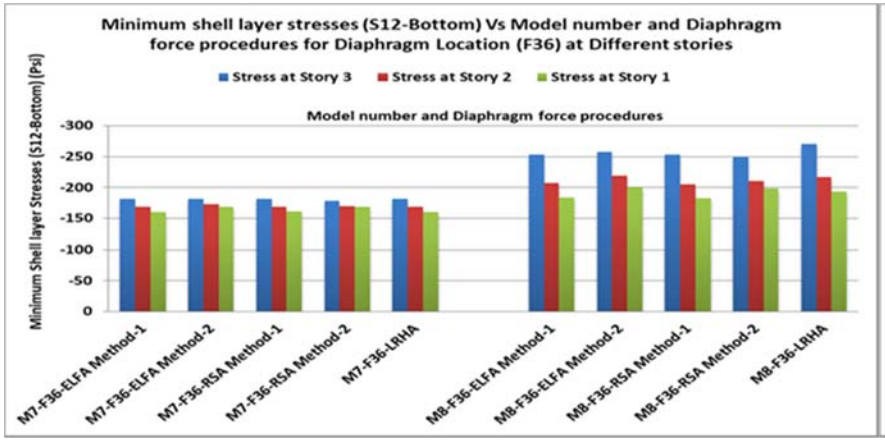

Figure 4-91 Minimum shell layer stresses (S12-Bottom) Vs Model number and Diaphragm force procedures for Diaphragm Location (F36) at Different stories

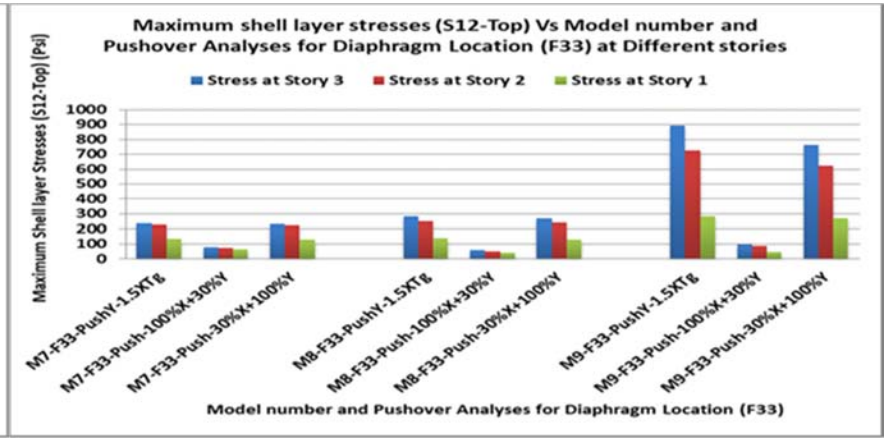

Figure 4-92 Maximum shell layer stresses (S12-Top) Vs Model number and Pushover Analyses for Diaphragm Location (F33) at Different stories

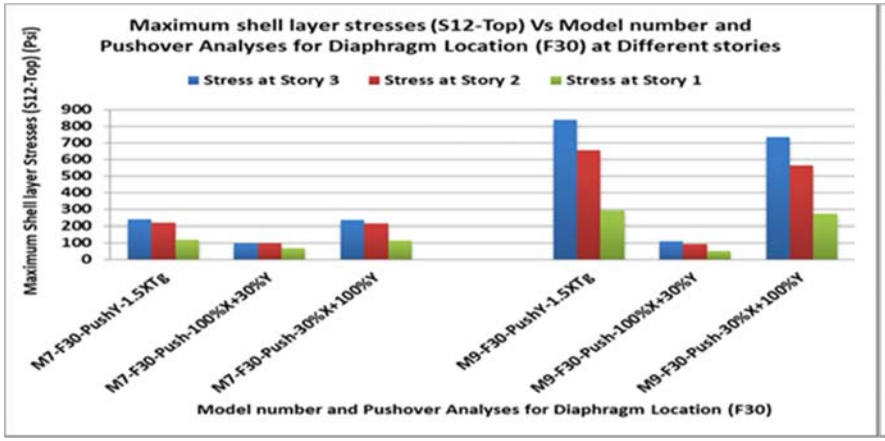

Figure 4-93 Maximum shell layer stresses (S12-Top) Vs Model number and Pushover Analyses for Diaphragm Location (F30) at Different stories

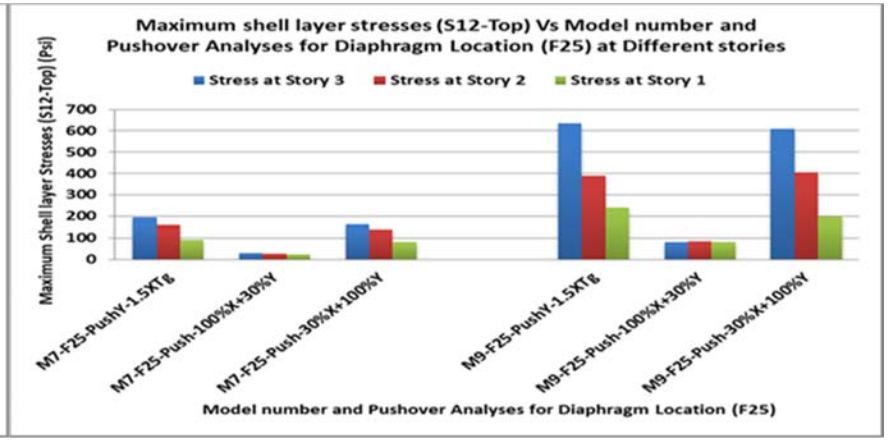

Figure 4-94 Maximum shell layer stresses (S12-Top) Vs Model number and Pushover Analyses for Diaphragm Location (F25) at Different stories

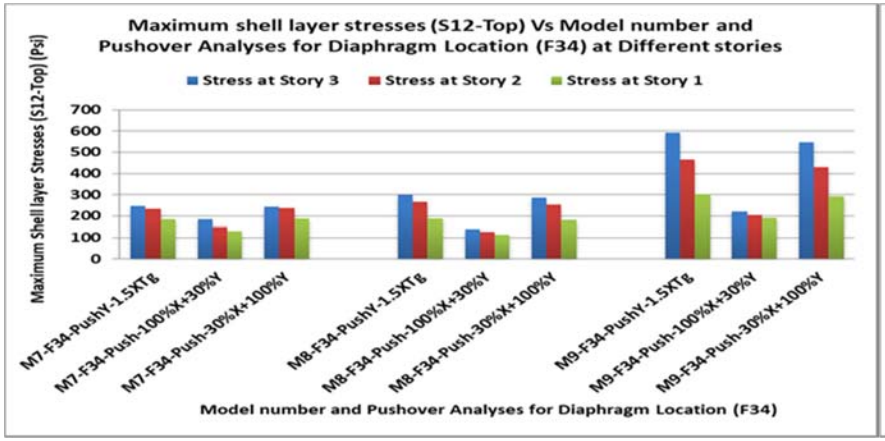

Figure 4-95 Maximum shell layer stresses (S12-Top) Vs Model number and Pushover Analyses for Diaphragm Location (F34) at Different stories

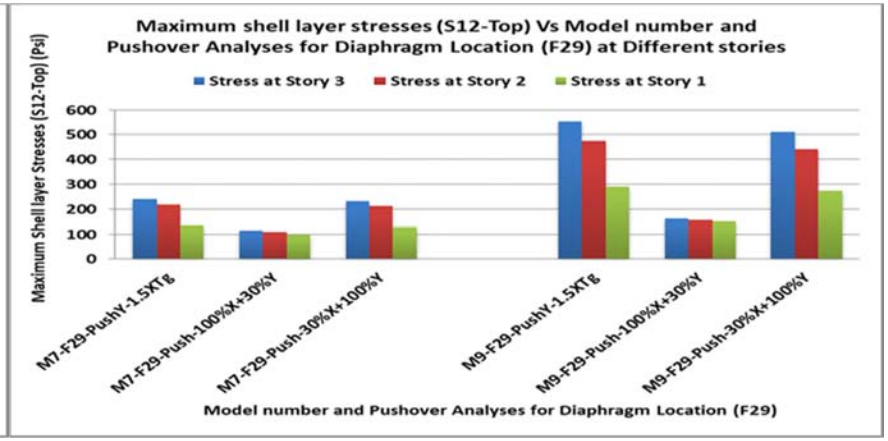

Figure 4-96 Maximum shell layer stresses (S12-Top) Vs Model number and Pushover Analyses for Diaphragm Location (F29) at Different stories

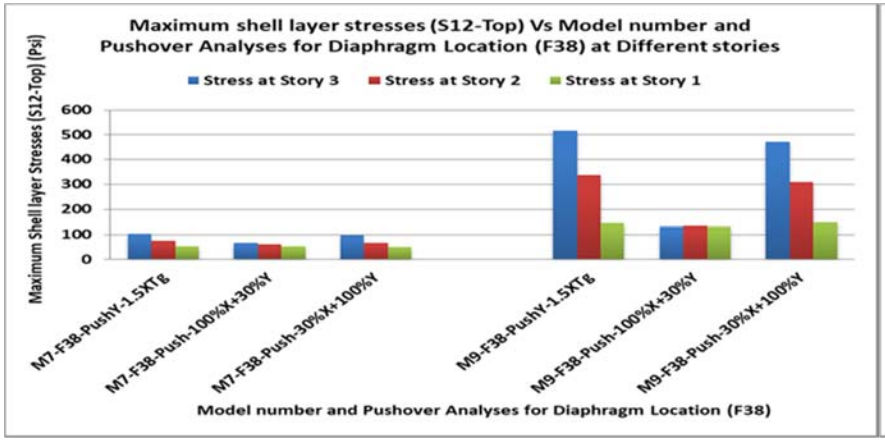

Figure 4-97 Maximum shell layer stresses (S12-Top) Vs Model number and Pushover Analyses for Diaphragm Location (F38) at Different stories

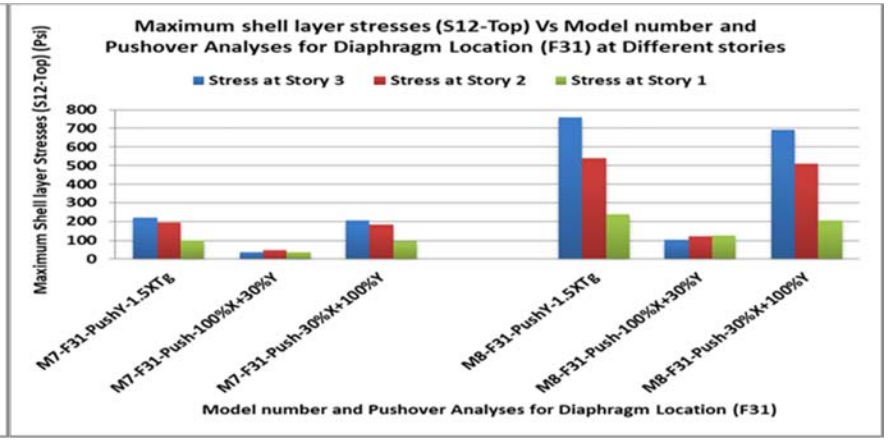

Figure 4-98 Maximum shell layer stresses (S12-Top) Vs Model number and Pushover Analyses for Diaphragm Location (F31) at Different stories

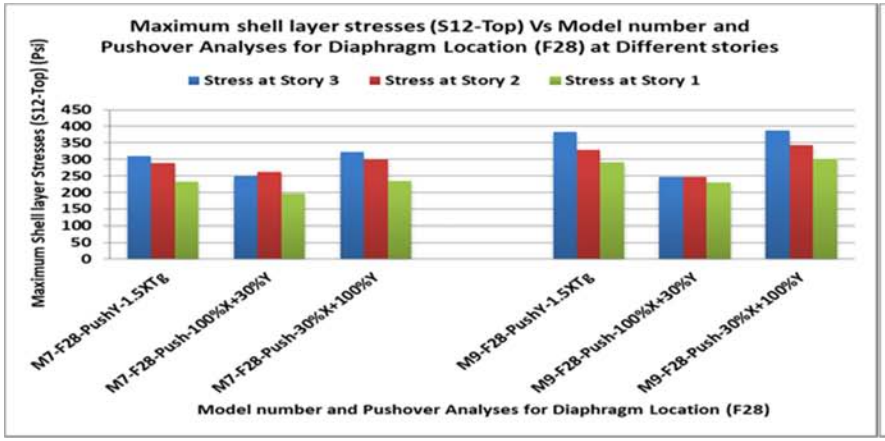

Figure 4-99 Maximum shell layer stresses (S12-Top) Vs Model number and Pushover Analyses for Diaphragm Location (F28) at Different stories

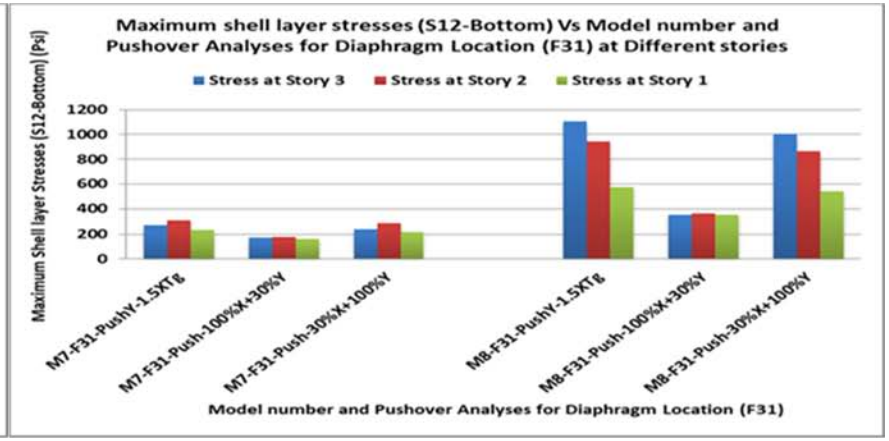

Figure 4-100 Maximum shell layer stresses (S12-Bottom) Vs Model number and Pushover Analyses for Diaphragm Location (F31) at Different stories

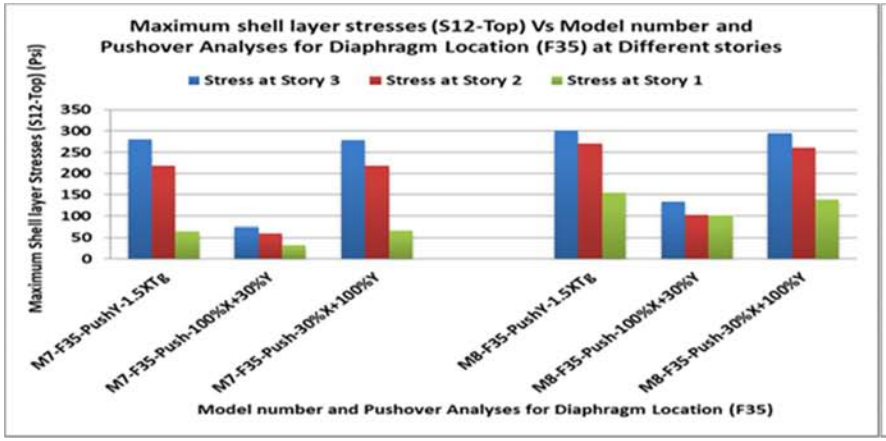

Figure 4-101 Maximum shell layer stresses (S12-Top) Vs Model number and Pushover Analyses for Diaphragm Location (F35) at Different stories

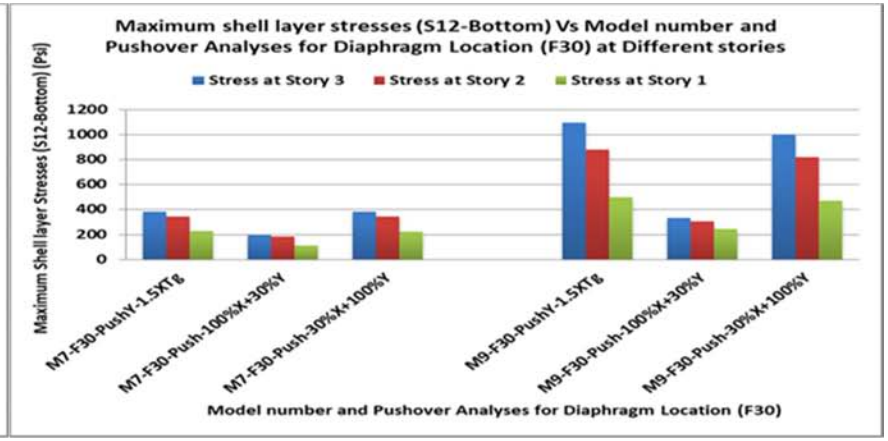

Figure 4-102 Maximum shell layer stresses (S12-Bottom) Vs Model number and Pushover Analyses for Diaphragm Location (F30) at Different stories

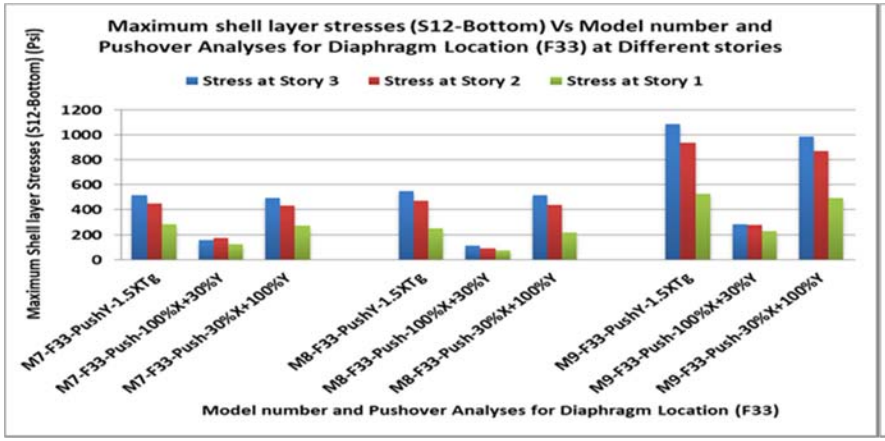

Figure 4-103 Maximum shell layer stresses (S12-Bottom) Vs Model number and Pushover Analyses for Diaphragm Location (F33) at Different stories

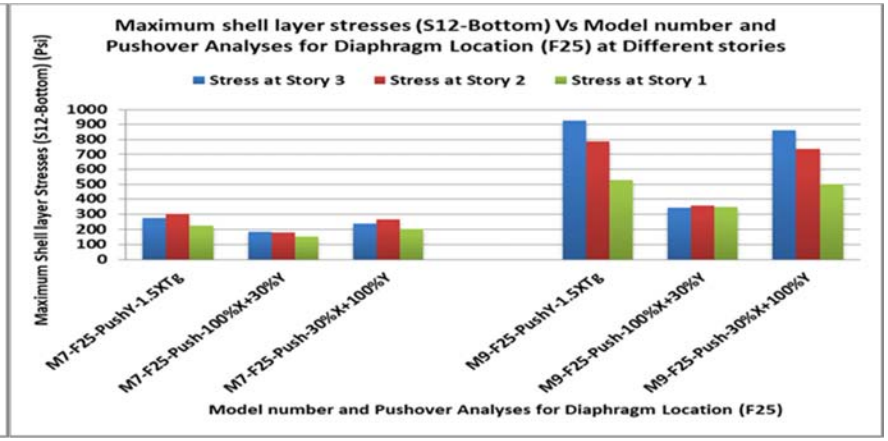

Figure 4-104 Maximum shell layer stresses (S12-Bottom) Vs Model number and Pushover Analyses for Diaphragm Location (F25) at Different stories

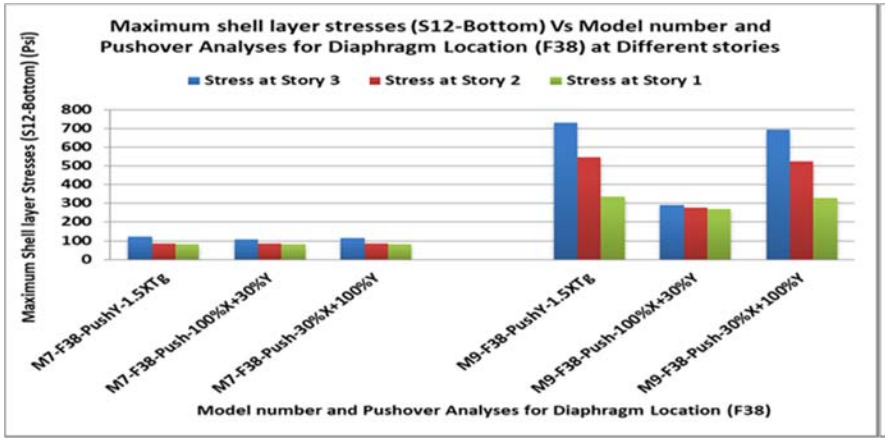

Figure 4-105 Maximum shell layer stresses (S12-Bottom) Vs Model number and Pushover Analyses for Diaphragm Location (F38) at Different stories

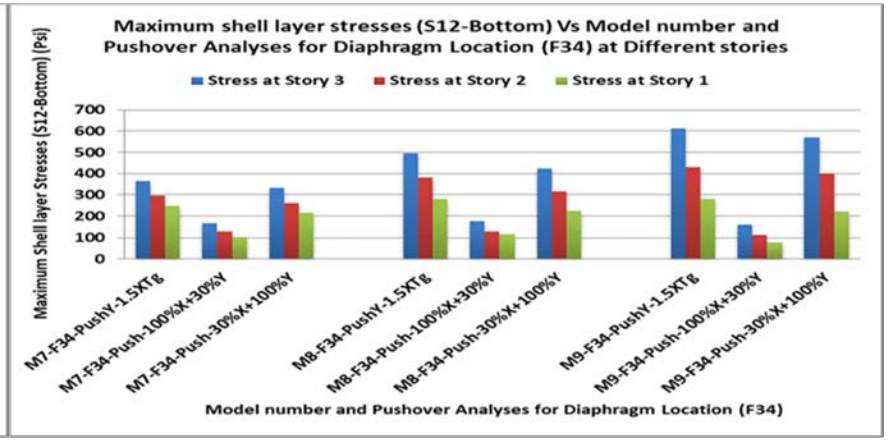

Figure 4-106 Maximum shell layer stresses (S12-Bottom) Vs Model number and Pushover Analyses for Diaphragm Location (F34) at Different stories

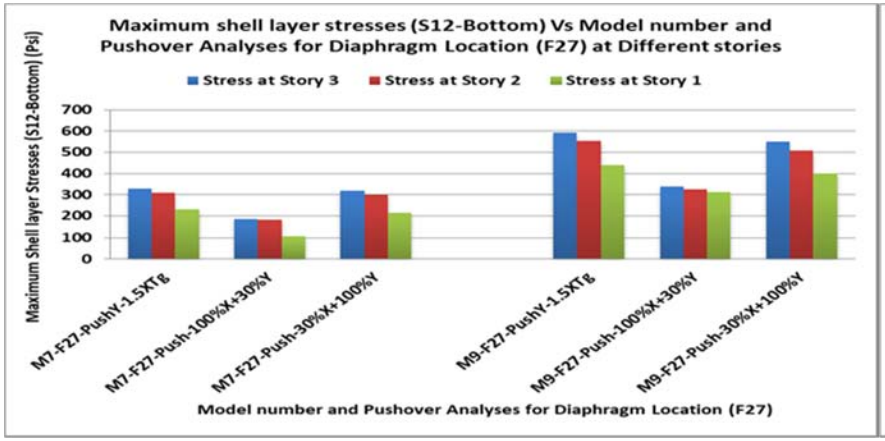

Figure 4-107 Maximum shell layer stresses (S12-Bottom) Vs Model number and Pushover Analyses for Diaphragm Location (F27) at Different stories

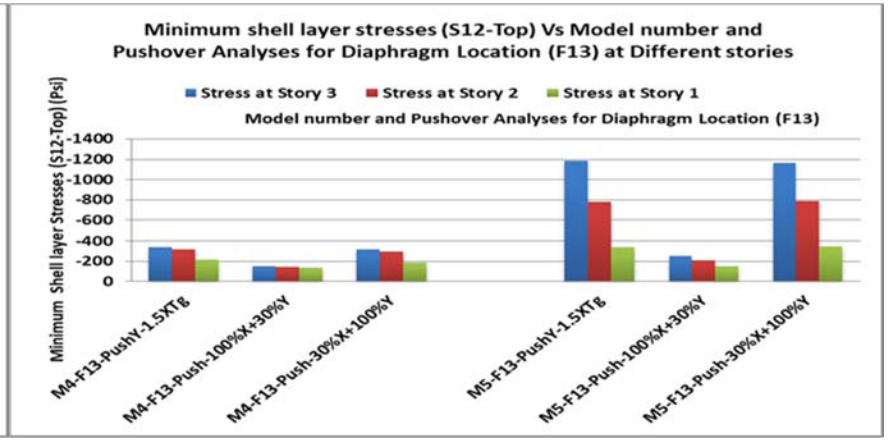

Figure 4-108 Minimum shell layer stresses (S12-Top) Vs Model number and Pushover Analyses for Diaphragm Location (F13) at Different stories

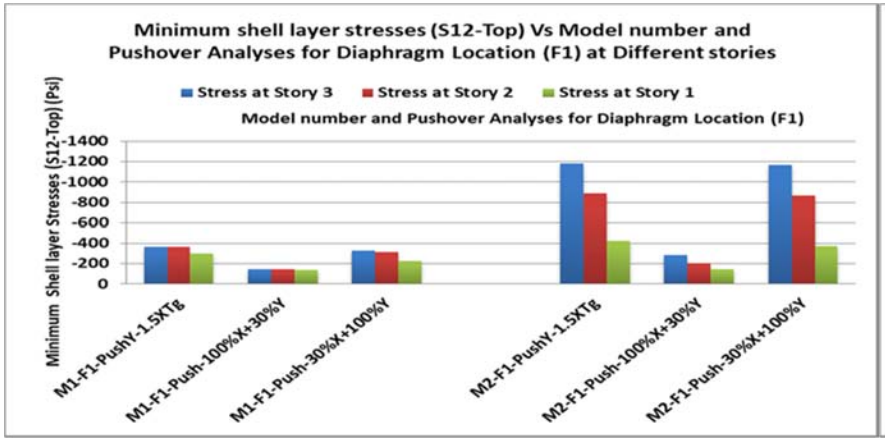

Figure 4-109 Minimum shell layer stresses (S12-Top) Vs Model number and Pushover Analyses for Diaphragm Location (F1) at Different stories

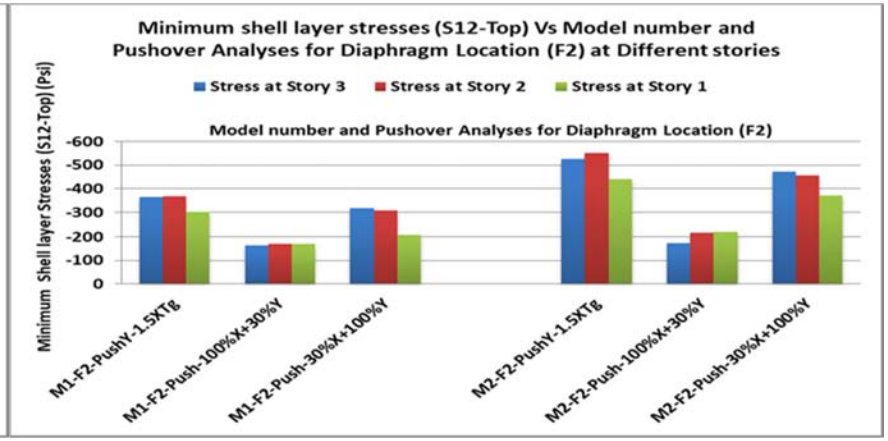

Figure 4-110 Minimum shell layer stresses (S12-Top) Vs Model number and Pushover Analyses for Diaphragm Location (F2) at Different stories

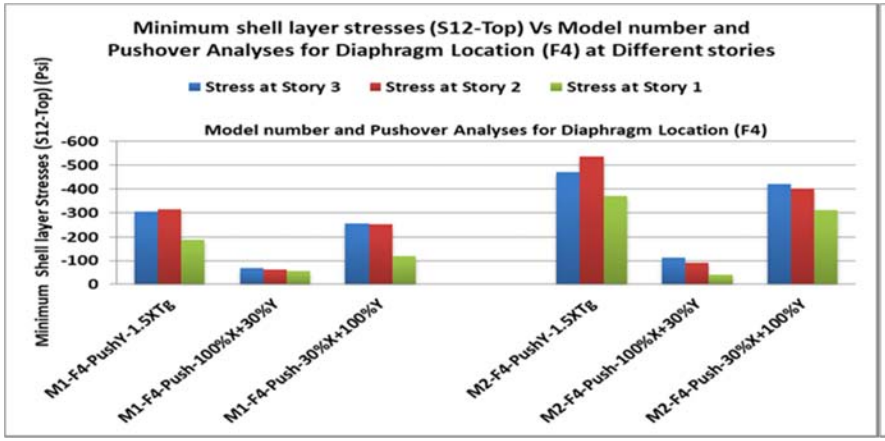

Figure 4-111 Minimum shell layer stresses (S12-Top) Vs Model number and Pushover Analyses for Diaphragm Location (F4) at Different stories

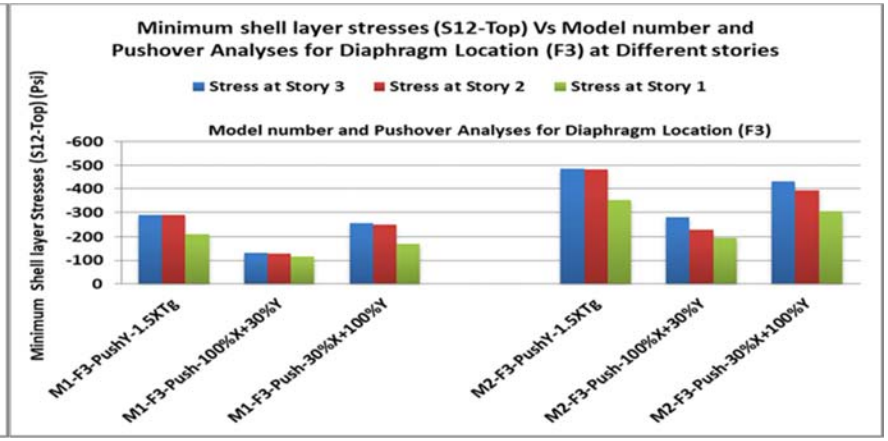

Figure 4-112 Minimum shell layer stresses (S12-Top) Vs Model number and Pushover Analyses for Diaphragm Location (F3) at Different stories

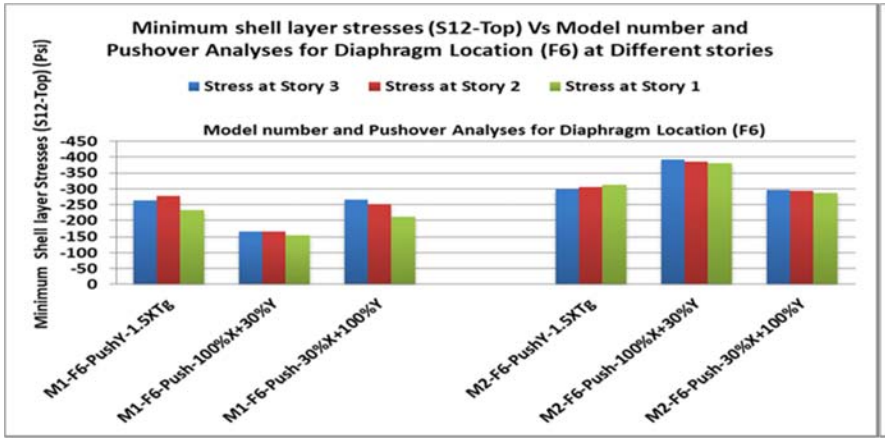

Figure 4-113 Minimum shell layer stresses (S12-Top) Vs Model number and Pushover Analyses for Diaphragm Location (F6) at Different stories

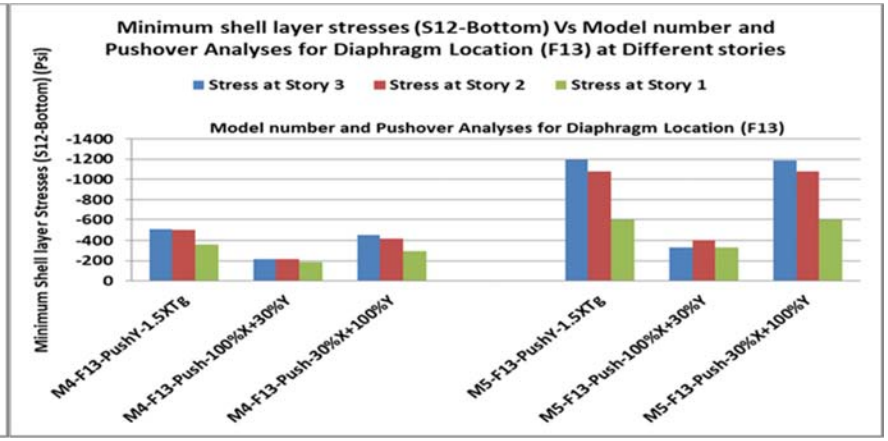

Figure 4-114 Minimum shell layer stresses (S12-Bottom) Vs Model number and Pushover Analyses for Diaphragm Location (F13) at Different stories

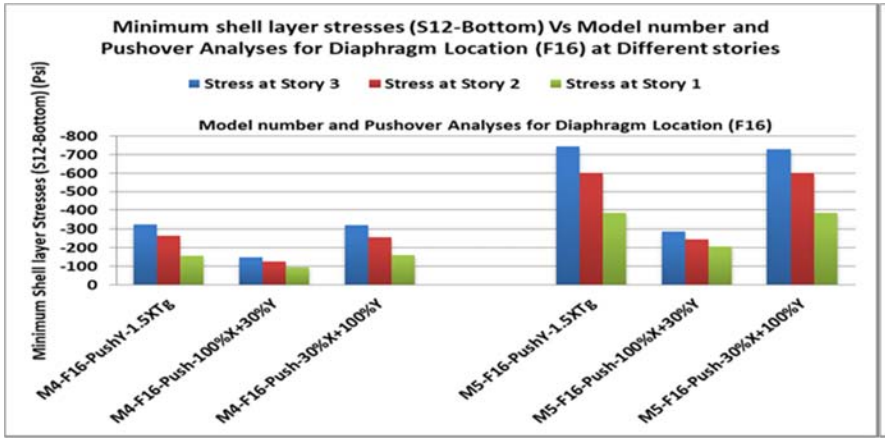

Figure 4-115 Minimum shell layer stresses (S12-Bottom) Vs Model number and Pushover Analyses for Diaphragm Location (F16) at Different stories

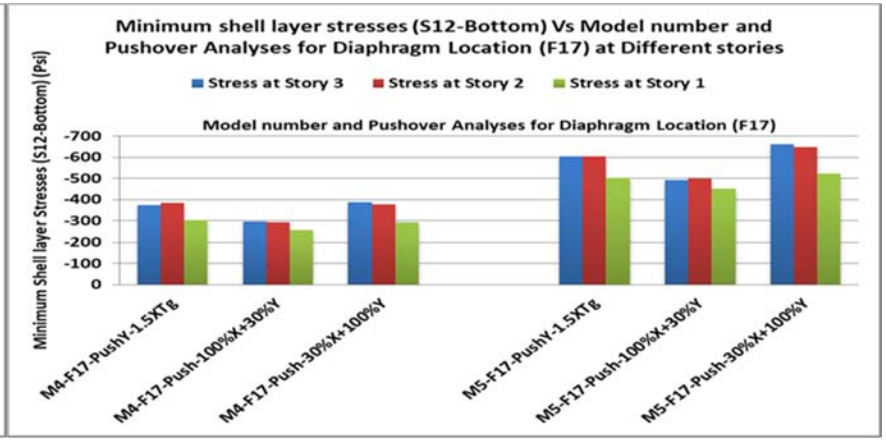

Figure 4-116 Minimum shell layer stresses (S12-Bottom) Vs Model number and Pushover Analyses for Diaphragm Location (F17) at Different stories

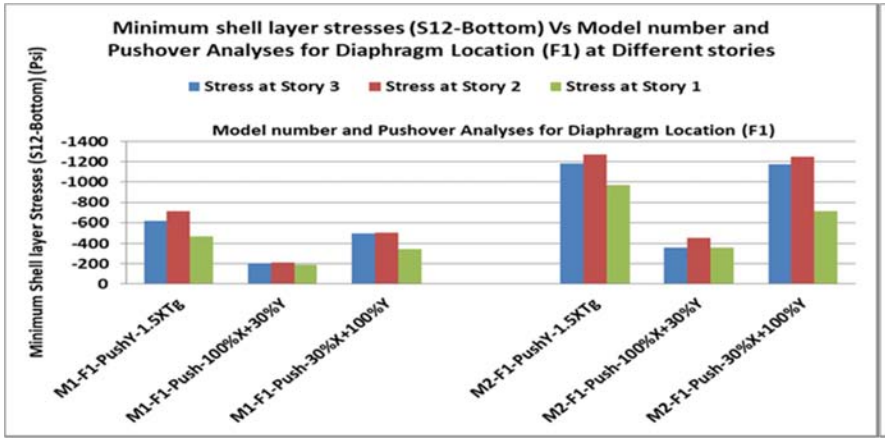

Figure 4-117 Minimum shell layer stresses (S12-Top) Vs Model number and Pushover Analyses for Diaphragm Location (F1) at Different stories

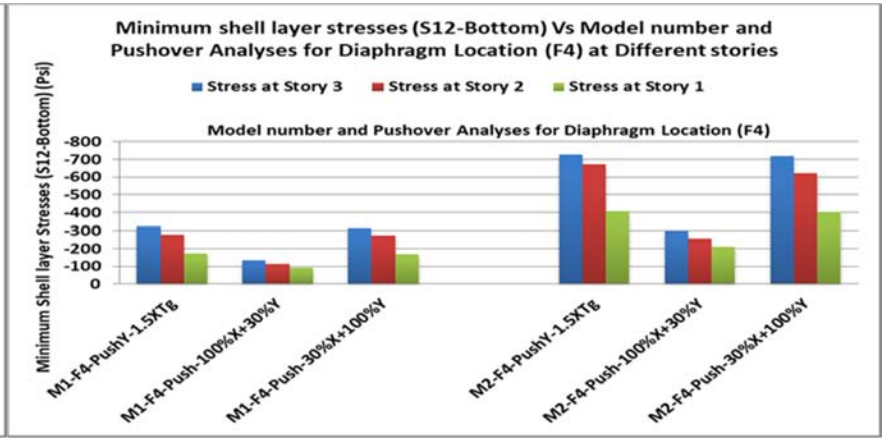

Figure 4-118 Minimum shell layer stresses (S12-Bottom) Vs Model number and Pushover Analyses for Diaphragm Location (F4) at Different stories

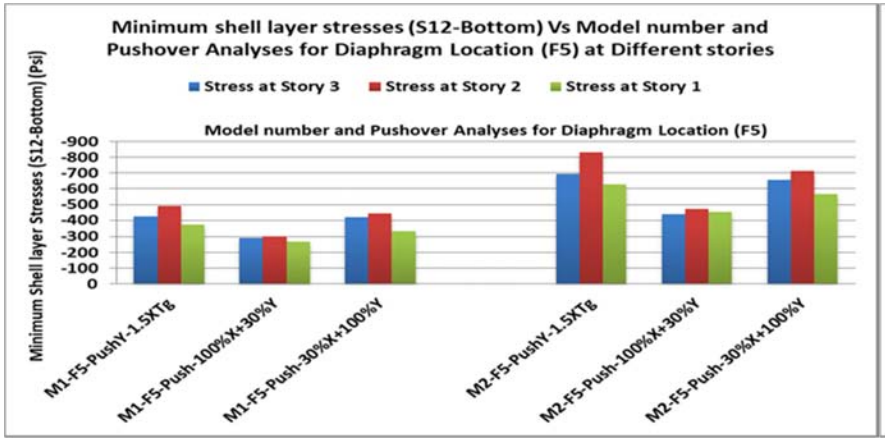

Figure 4-119 Minimum shell layer stresses (S12-Bottom) Vs Model number and Pushover Analyses for Diaphragm Location (F5) at Different stories

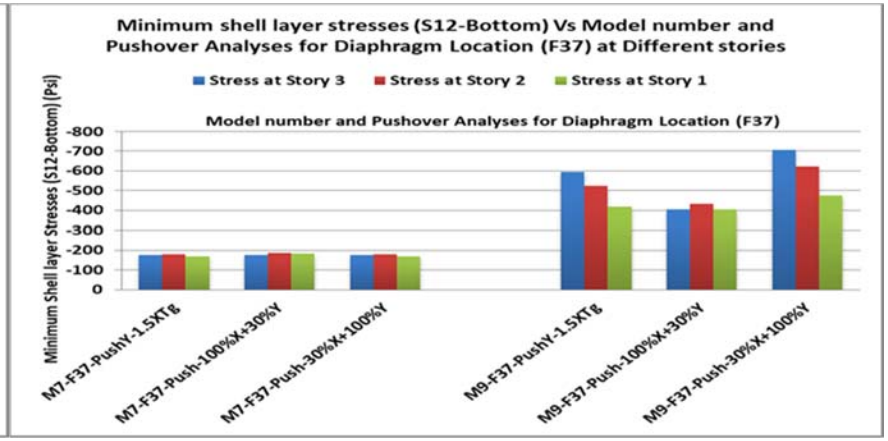

Figure 4-120 Minimum shell layer stresses (S12-Bottom) Vs Model number and Pushover Analyses for Diaphragm Location (F37) at Different stories

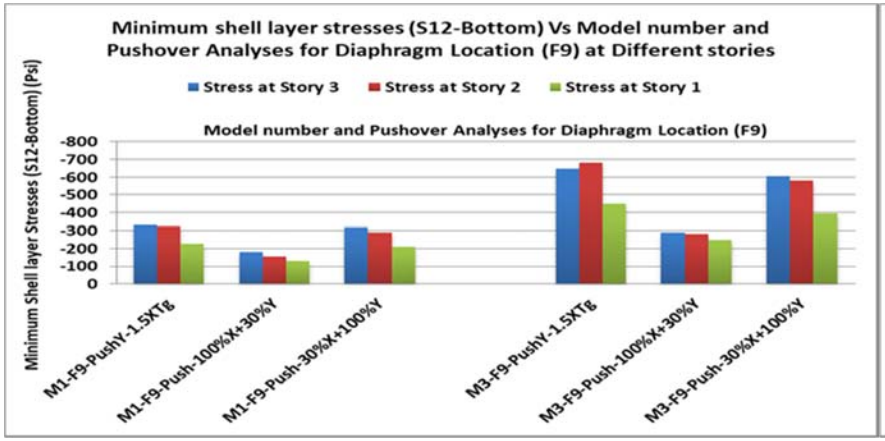

Figure 4-121 Minimum shell layer stresses (S12-Bottom) Vs Model number and Pushover Analyses for Diaphragm Location (F9) at Different stories

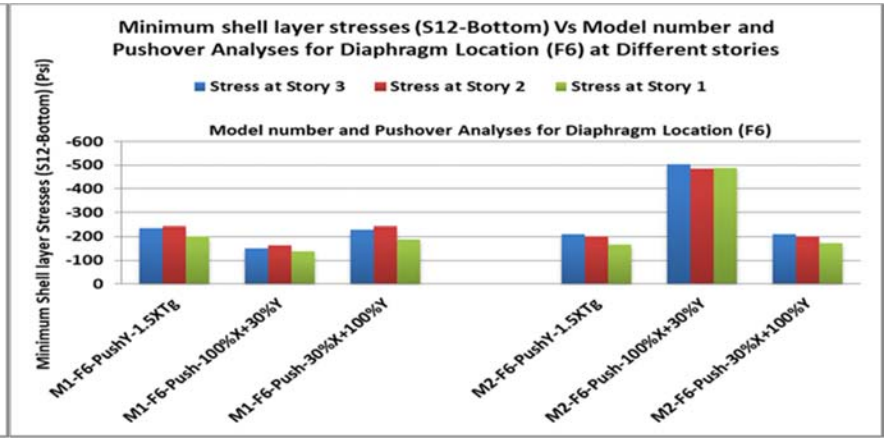

Figure 4-122 Minimum shell layer stresses (S12-Bottom) Vs Model number and Pushover Analyses for Diaphragm Location (F6) at Different stories

Appendix-F

DESIGN OF DIAPHRAGM FOR IN-PLANE SHEAR

Design of diaphragm for in-plane shear (diaphragm location F1 of story 3 of model-2)

φ= 0.75

λ= 1

fc′= 4000 psi , fy= 60000 psi

t(thickness)= 10.5 inch

Length of section, b = 12 inch

Vu= 46.62 kips/ft (From Pushover analyses)

φ Vc = φ x2x√fc‘bt

= (0.75 * 2 * √4000 * 12 * 10.5)/1000

= 11.95 kips/ft

Vu > φ Vc. So shear reinforcement required.

Vu = ϕ Vn

Vn = Vu / ϕ

= 46.62 / 0.75

= 62.16 kips/ft

Vn < $8A_{cv}\sqrt{f_c'}$

< (8 * √4000 * 12 * 10.5)/1000

< 63.75 kips/ft. So thickness of Diaphragm need not to be changed.

$V_n = A_{cv}\left(2\lambda\sqrt{f_c'} + \rho_t f_y\right)$

V_n = 10.5*12*(2*1*√4000 + ρ_t * 60000)

ρ_t = 0.00611

As (required) = ρ_t *b*t

= 0.00611 *12*10.5

= 0.770 in^2/ft

Provide 16 mm bar @ 4.75 in c/c

As (provided) = (Area of bar provided * b)/ Spacing

= (.31*12)/4.75 = 0.783 in^2/ft So ok

Provide 16 mm bar @ 4.75 in c/c in both directions.

Appendix-G

DESIGN OF CHORD OF DIAPHRAGM

Design of chord-2 of diaphragm for model-2 located in story 3

Force for design of chord is taken form Pushover analyses. The maximum chord force for chord-2 in story 3 is found form pushover analysis along Y-direction up to 1.5 times of target displacement.

Tu = Cu = Mu/Slab width

Mu = in-plane bending moment, kip-ft

In-plane bending moment of diaphragm (Mu) of locations a-b-c-d = 3788 kips-ft

Slab width = 20 ft

Tu = 3788/20 = 189.40 kips

$$A_s = \frac{T_u}{\varphi f_y}$$

Where

$A_s =$ Tension reinforcement of Chord (in^2)

Cu = Flexural compressive force of Chord, kips

T_u = Flexural Tension force for Chord (kips)

f_y = yield strength of Reinforcing bar (ksi)

φ = Strength reduction factor for tension member ($\varphi = 0.9$)

Tu = 189.40 kips

fy = 60 ksi

φ = 0.9

$$A_s = \frac{T_u}{\varphi f_y}$$

As = 189.40/ (0.9x60) = 3.50 in^2

The confinement reinforcement is required for flexural compressive zone of chord where flexural compressive stress exceeds $0.2f_c'$ or $0.5f_c'$ where design flexural compressive forces have been amplified to account for overstrength of the vertical elements of the seismic force-resisting system.

If Chord reinforcement is placed in Girder B1 beam (10 inx24 in) then

The compressive stress in girder due to chord action

$$= \frac{C_u}{\text{Area of Beam where chord reinforcements are placed}}$$

=189.40*10^3/(10x24)= 789.17 psi < 0.5fc' =0.5*4000 =2000 psi

Therefore no additional transverse reinforcement is required in the chord beam.

Appendix-H

DESIGN OF COLLECTOR OF DIAPHRAGM

Design of collector-A of diaphragm for model-2 located in story 3

Force for design of collector-A is taken form Pushover analyses. The maximum collector force for collector-A in story 3 is found form pushover analysis along Y-direction up to 1.5 times of target displacement.

Force from section cut along collector-A from pushover analysis along Y-direction up to 1.5 times of target displacement = 206 kips.

Cu + Tu = 206 kips

Where,

Cu = axial compressive force in collector A, kips

Tu = axial tensile force in collector A, kips

From section cut we found that Cu = Tu

So,

Cu + Tu = 206 kips

Tu + Tu = 206 kips

2 Tu = 206 kips

Tu = 103 kips

$$A_s = \frac{T_u}{\varphi f_y}$$

Where

$A_s =$ Tension reinforcement of Collector (in^2)

T_u = Flexural Tension force for Collector (kips)

f_y = yield strength of Reinforcing bar (ksi)

φ = Strength reduction factor for tension member ($\varphi = 0.9$)

Tu = 103 kips

fy = 60 ksi

φ = 0.9

$$A_s = \frac{T_u}{\varphi f_y}$$

As = 103/ (0.9x60) = 1.90 in^2

The confinement reinforcement is required for flexural compressive zone of collector where flexural compressive stress exceeds $0.2f_c'$ or $0.5f_c'$ where design flexural compressive forces have been amplified to account for overstrength of the vertical elements of the seismic force-resisting system.

If Collector reinforcement is placed in Girder B3 beam (10 inx24 in) then

The compressive stress in girder due to collector action

$$= \frac{C_u}{\text{Area of Beam where collector reinforcements are placed}}$$

=103*10^3/(10x24)= 429.17 psi < 0.5fc' =0.5*4000 =2000 psi

Therefore no additional transverse reinforcement is required in the collector beam.

For the case of compression, the factored compressive force must not exceed the design compressive strength of the chord eleemnt, defined by

$$\varphi P_0 = \varphi\left[0.85f_c'\left(A_g - A_s\right) + f_y A_s\right] \geq C_u$$

φP_0= [.80 x [{ .85 x 4000 x (10 x 24-1.90)}+(60000x1.90)]]/1000

= 738.88 kips > 103 kips , so ok